

***IN VITRO* PROCESSING OF HUMAN BONE MARROW DERIVED  
MESENCHYMAL STEM CELLS TO ENHANCE DELIVERY IN LIVER  
DISEASE**

**by**

**ABHILOK GARG**

A thesis submitted to the University of Birmingham for the degree of  
**DOCTOR OF PHILOSOPHY**

Centre for Liver Research  
Institute of Biomedical Research  
School of Immunity and Infection  
College of Medical and Dental Sciences  
University of Birmingham  
September 2012

UNIVERSITY OF  
BIRMINGHAM

**University of Birmingham Research Archive**

**e-theses repository**

This unpublished thesis/dissertation is copyright of the author and/or third parties. The intellectual property rights of the author or third parties in respect of this work are as defined by The Copyright Designs and Patents Act 1988 or as modified by any successor legislation.

Any use made of information contained in this thesis/dissertation must be in accordance with that legislation and must be properly acknowledged. Further distribution or reproduction in any format is prohibited without the permission of the copyright holder.

## ABSTRACT

Currently the only effective treatment for end stage liver disease is transplantation together with immune-modulating drugs. Human bone marrow derived mesenchymal stem cells (MSC) have been shown to suppress inflammation, potentiate regeneration and act as vectors for gene therapy. Thus, MSC infusions offer an attractive potential therapy for treating liver disease. However a number of obstacles exist in MSC delivery before they can be used therapeutically. Although MSC can migrate to sites of injury after *in vivo* administration, their engraftment within the liver is often poor, potentially limiting their therapeutic action. I have shown that detaching MSC from culture using non-enzymatic methods is superior in retaining surface chemokine receptor expression. Furthermore, I have shown that these receptors are functional in migration and attachment assays both *in vitro* and *in vivo* in carbon-tetrachloride induced liver injury. TGF $\beta$ 1 stimulated MSC were able to further enhance engraftment via up-regulation of surface CXCR3. Additionally the potent immunosuppressive properties of MSC, mediated via Prostaglandin E2, were enhanced after TGF $\beta$ 1 stimulation. Thus my studies demonstrate that manipulation of MSC through careful choice of detachment methods and exogenous cytokine stimulation can improve their engraftment in injured liver and their immunosuppressive properties with implications for improving the efficacy of MSC therapy.

कर् मण् ये वधि करस् थे मा फले षु कदाचना ।

मा कर् मफल हे तुर भु रमा, ते सं घस् त् व अकर् मणि ॥

Karmanye Vadhi Karasthe Maa Phaleshu Kadachana,  
Maa Karmaphal Hetur Bhurma, Te Sanghastva Akarmani

“Do your duty and don't worry, think about or expect the desired result, it will follow”

- Srimad Bhagavad Gita

Thank you to my father, Mr Kapil Dev Garga, who gave me this advice.

I could not have completed this work without it.

## **DEDICATION**

I would like to dedicate this thesis to my family who are the source of my motivation, without their love and support I would never have made it this far.

My parents: Mr Kapil Dev Garga and Mrs Naresh Garga

My Brother and Sister in law: Mr Sidharath Garg and Mrs Narinder Garg

My Nieces: Miss Shivanghi Garg and Miss Sakshi Garg

I would also like to dedicate this work to Dr Tasneem Rahman, my best friend, who was a constant source of support and encouragement and a pillar of unwavering belief in me especially during difficult times.

In loving memory of my Grandparents:

Mr Chanak Dev Garg and Mrs Humesh Kumari Garg,

Dr Lekh Raj Sharma and Mrs Rampyari Sharma

## **ACKNOWLEDGEMENTS**

I would like to thank my supervisors, Dr Philip Newsome and Dr Patricia Lalor, for their support and guidance throughout this PhD project.

In addition I would like to thank everyone in the Centre for Liver Research, both past and present, for technical assistance, encouragement and for making my time here so enjoyable.

In particular I would like to thank my colleagues and friends, Mr Rupesh Sutaria and Mr John Pravin for their invaluable help, encouragement and advice during my project and thesis writing which were critical in helping me finish.

Thank you also to Dr Evaggalia Liaskou for always taking time out to help me and for her always useful scientific advice which has been instrumental in allowing me to move this project forward. I am grateful to Dr Andy King, Dr Nick Davies and Mrs Janine Youster for their assistance with *in vivo* experiments. Thank you to Dr Chris Weston, Dr Diarmaid Houlihan, Dr Victoria Aldridge and Dr Sophie Hidden for day to day support and input throughout my project. Thank you also to Mrs Laura Vass for all her help.

Last but not least, thank you to my friends and family for their continued and unquestioning support and invaluable guidance. I am sincerely humbled by the efforts and the lengths that people have gone to help me in completing this project, I will never forget all that everyone has done for me in these past years and I will remain eternally grateful.

## PUBLICATIONS

Aldridge, V., Garg, A., Davies, N., *et al.* (2012) **Human mesenchymal stem cells are recruited to injured liver in a beta1-integrin and CD44 dependent manner.** *Hepatology*, 56: (3): 1063-1073.

Faint, J.M., Tuncer, C., Garg, A., *et al.* (2011) **Functional consequences of human lymphocyte cryopreservation: implications for subsequent interactions of cells with endothelium.** *Journal of Immunotherapy*, 34: (8): 588-596.





# TABLE OF CONTENTS

CHAPTER 1: INTRODUCTION.....	1
1.1 The Liver.....	2
1.1.1 Liver function .....	2
1.1.2 Liver Disease .....	3
1.1.3 Liver Inflammation.....	6
1.2 Human Bone Marrow derived Mesenchymal Stem Cells (MSC) .....	10
1.2.1 MSC Markers .....	10
1.1.1 Function in Niche .....	14
1.3 Therapeutic uses of MSC in disease .....	15
1.3.1 MSC as a vector to deliver cellular treatment .....	15
1.3.2 MSC administration to pre-clinical models of liver disease.....	16
1.3.3 Therapeutic effect of MSC through transdifferentiation into hepatocytes .....	18
1.3.4 Paracrine anti-fibrotic effects of MSC in liver disease.....	19
1.3.5 Immunomodulatory effects of MSC.....	22
1.3.6 Effects of cytokines on immunomodulatory properties of MSC.....	23
1.3.7 MSC Immunotherapy in liver specific models.....	24
1.3.8 The effects of MSC in Cancer .....	25
1.3.9 MSC contribution to fibrosis .....	26
1.3.10 Bone marrow derived stromal cells contributing to hepatic fibrosis: HSC derived fibrocytes .....	28
1.3.11 The mechanism of MSC engraftment.....	30
1.4 Aims of the thesis .....	43
CHAPTER 2: MATERIALS AND METHODS .....	47
2.1 Human Tissue .....	48
2.2 Isolation of Human Hepatic Sinusoidal Endothelial Cells (HSEC), Biliary Epithelial cells (BEC) and hepatic myofibroblasts (MF) and peripheral Blood Mononuclear Cells (PBMC). .....	48
2.3 Cell culture and viability measurement .....	51
2.4 Attachment of cells onto microscope slides using Cytospin .....	54
2.5 Immunohistochemistry .....	54
2.6 Flow Cytometric analysis of cells.....	58

2.7	Quantification of autophagy and cell stress .....	60
2.8	Polymerase Chain Reaction (PCR).....	63
2.8.1	RNA extraction and cDNA preparation from cytokine stimulated MSC.....	63
2.8.2	Use of quantitative PCR (QPCR) to assess expression of CCR by MSC .....	65
2.8.3	Measurement of Collagen-1 (Col1a1) and alpha smooth muscle actin ( $\alpha$ SMA) mRNA levels in injured mouse livers by QPCR.....	68
2.9	Measurement of MSC tri-lineage differentiation capacity .....	69
2.10	Quantification of TGF $\beta$ 1 in MSC Supernatants by ELISA .....	72
2.11	Quantification of adhesion molecule levels of Human (HSEC) Stimulated with Cytokine stimulated MSC conditioned media by cell based ELISA.....	73
2.11.1	Quantification of Cytokine and Pro-Angiogenic mediators in MSC Supernatants.....	74
2.12	Use of an immunosuppression assay to assess ability of MSC to inhibit T effector cell proliferation .....	75
2.13	Use of a modified Boyden chamber migration assay to assess MSC migration towards chemokines .....	76
2.14	Use of murine liver injury models to assess the hepatic trafficking of infused MSC.....	79
2.14.1	The CCl <sub>4</sub> injury model.....	79
2.14.2	Measuring injury in C57 BL/6 and carbon tetrachloride injured mice.....	79
2.15	Quantification of MSC adhesion and recruitment into injured tissue.....	81
2.15.1	Use of Modified Stamper Woodruff Assays to assess adhesion of MSC to Injured Human Liver sections .....	81
2.15.2	Quantification of MSC Engraftment in murine livers following via portal vein infusion.....	82
2.16	Measurement of serum amyloid protein (SAP): an inhibitor of fibrocyte differentiation .....	83
2.16.1	Quantification of Serum Amyloid Protein (SAP) in liver samples by Sandwich ELISA.....	83
2.17	Statistical Analyses .....	90
CHAPTER 3: EFFECTS OF MSC DETACHMENT METHODS ON VIABILITY, TRI-LINEAGE DIFFERENTIATION, IMMUNOMODULATION AND CHEMOKINE RECEPTOR EXPRESSION.....		91
3.1	Introduction.....	92
3.2	Results.....	95

3.2.1	MSC express high levels of intracellular CCR but negligible levels of cell surface CCR when in suspension. ....	95
3.2.2	Non-enzymatic detachment preserves functionally active cell surface CCR expression on MSC.....	107
3.2.3	MSC viability, re-plating ability and proliferation in culture are altered according to detachment methodology.....	110
3.2.4	Non-enzymatic detachment with CDB results in increased autophagy as a response to increased cellular stress. ....	115
3.2.5	Impact of detachment method on the differentiation and immunomodulatory capabilities of MSC .....	123
3.3	Discussion.....	129
CHAPTER 4: EFFECTS OF CYTOKINES ON MIGRATION AND IMMUNOMODULATION BY MSC .....		138
4.1	Introduction.....	139
4.2	Results.....	148
4.2.1	MSC express a consistent profile of intracellular and cell surface CCR expression. ....	148
4.2.2	TGFβ1, IL4 and IL10 stimulation significantly increases surface CCR expression by MSC.....	155
4.2.3	TGFβ1 and IL4 stimulation increases MSC migration to CXCR3 ligand IP10/ CXCL10 and CCR4 ligand TARC/ CCL17. ....	164
4.2.4	TGFβ1 stimulated MSC show increased binding to hepatic sinusoidal endothelium in cirrhotic livers and in culture.....	171
4.2.5	Upregulation of cell surface CXCR3 modulates increased engraftment of TGFβ1 stimulated MSC in mice with carbon tetrachloride induced liver injury. ....	175
4.2.6	TGFβ1 stimulation of MSC increases binding and engraftment of enzyme detached MSC to injured mouse livers.....	183
4.2.7	TGFβ1 stimulation of MSC does not significantly alter tri-lineage differentiation of MSC and does not increase intracellular stress or the production of pro-fibrotic factors.....	188
4.2.8	TGFβ1 stimulation of MSC increases cell surface CD44 expression and secretion of CCL2 and IL-6.....	192
4.2.9	TGFβ1 stimulated MSC exhibit increased exhibit increased suppression of CD4 T cell proliferation mediated by increased PGE2.....	198
4.2.10	Treatment of MSC with serum from cirrhotic ALD patients reduces cell surface CCR expression and increases levels of β1 integrin. ....	200

4.2.11	Treatment of MSC with normal or end stage cirrhotic ALD patient serum can alter tri-lineage differentiation of the MSC without inducing intracellular stress.....	205
4.3	Discussion.....	209
CHAPTER 5: FIBROCYTE ISOLATION AND PHENOTYPING.....		223
5.1	Introduction.....	224
5.1.1	HSC derived fibrocytes .....	224
5.1.2	Fibrocytes in diseased organs .....	226
5.1.3	The contribution of fibrocytes to liver disease .....	229
5.1.4	Are fibrocytes likely to contaminate cultures of MSC? .....	231
5.1.5	Current methodologies used to isolate and culture fibrocytes.....	232
5.2	Results.....	235
5.2.1	Murine liver injury results in increased levels of Serum Amyloid Protein (SAP) levels in liver and serum.....	235
5.2.2	PBMC isolated from peripheral blood separated on Lympholyte-H gradient and grown on tissue culture plastic do not express a fibrocyte phenotype. ....	239
5.2.3	PBMC isolated from peripheral blood separated on Ficoll-Paque gradient and grown on fibronectin coated Cell Bind tissue culture plastic vary between donors and on occasion small numbers of cells with a fibrocyte phenotype can be detected. ....	242
5.2.4	PBMC isolated directly from blood or pre-prepared buffy coat using Ficoll-Paque or Lympholyte-H show no significant differences in cell number upon isolation.....	246
5.2.5	The effect of culture substrate and cell seeding density on morphological appearance.....	248
5.2.6	Significantly higher numbers of fibrocyte-like spindle shaped cells are observed when PBMC are cultured on tissue culture plastic.....	252
5.2.7	Improvement in yield of fibrocytes using collagen-coated plastic and pre-selection of cells .....	257
5.2.8	Spindle shaped-cells isolated from peripheral blood do not consistently express fibrocyte markers.....	262
5.2.9	Expression of $\alpha$ SMA and collagen-1 by fibroblast populations.....	264
5.2.10	CD45 <sup>+</sup> cells isolated from HSEC isolation waste from ALD livers have a spindle shaped fibrocyte-like phenotype compared to normal livers.....	273
5.3	Discussion.....	275
5.3.1	SAP in fibrocyte differentiation .....	276
5.3.2	Isolation of fibrocytes from whole blood .....	279

5.3.3	Fibrocytes in circulation and effects of cell culture conditions.....	283
5.3.4	Fibrocytes presence in explanted cirrhotic livers .....	287
5.3.5	Conclusion .....	290
CHAPTER 6: FINAL REMARKS.....		294
6.1	Cell dissociation buffer (CDB) mediated preservation of surface CCR expression after MSC detachment.....	295
6.2	Increased engraftment in injured liver via TGFβ1 up-regulated MSC surface CXCR3 expression.....	299
6.3	Unsuccessful isolation and identification of fibrocytes with current protocols, markers and antibodies .....	306
6.4	Future perspectives .....	310
6.4.1	Immediate experiments.....	310
6.4.2	Longterm experiments.....	311
LIST OF REFERENCES .....		313

## LIST OF FIGURES

Figure 1.1: Changes in the hepatic architecture in disease.....	4
Figure 1.2: Drivers of hepatic inflammation and fibrosis. ....	8
Figure 1.3: Proposed mechanisms of MSC engraftment into the liver. ....	33
Figure 1.4: CCR signalling.....	39
Figure 1.5: Schematic diagram of typical Integrin structure.....	43
Figure 2.1: Standard Curve for Alizarin red Staining.....	71
Figure 2.2: Standard curve for TGFβ1 Sandwich ELISA.....	73
Figure 2.3: Schematic diagram of the Boyden migration chambers.....	77
Figure 2.4: Standard Curve for mouse SAP Sandwich ELISA.....	84
Figure 2.5: Standard Curve from human SAP Sandwich ELISA.....	85
Figure 3.1: Surface and intracellular CCR expression by MSC.....	97
Figure 3.2: Effect of passage and cytokine stimulation upon MSC surface CCR expression. ....	98
Figure 3.3: Pre-labelling and fixation of cells, and treatment in absence of serum do not alter surface chemokine expression.....	<b>Error! Bookmark not defined.</b>
Figure 3.4: The effect of serum on MSC surface receptor expression after cytokine stimulation.....	103
Figure 3.5: Expression of surface CCR on viable cells after CDB detachment.....	105
Figure 3.6: Expression and function of CCR expression of MSC after non enzymatic detachment.....	108
Figure 3.7: Measurement of MSC viability and growth of re-plated cells.....	112
Figure 3.8: Morphology of re-plated MSC on tissue culture plastic. <b>Error! Bookmark not defined.</b>	
Figure 3.9: Measurement of Autophagy in detached MSC.....	117
Figure 3.10: Impact of serum supplementation on viability and proliferation of MSC detached with CDB.....	118
Figure 3.11: Impact of centrifugation speed on viability and proliferation of MSC detached with CDB.....	120
Figure 3.12: Impact of detachment method on the differentiation capabilities of MSC.....	125
Figure 3.13: Confirmation of efficiency of CD3 <sup>+</sup> CD4 <sup>+</sup> CD25 <sup>-</sup> T cells sorting from peripheral blood. ....	127
Figure 3.14: Impact of detachment method on the immunomodulatory capabilities of MSC. ....	128
Figure 4.1: MSC CCR expression.....	150
Figure 4.2: PBMC CCR expression. ....	152
Figure 4.3: QPCR analysis of MSC CCR expression. ....	153
Figure 4.4: Immunohistochemical analysis of MSC CCR expression. ....	154
Figure 4.5: Expression of MSC CCR after cytokine stimulation.....	157
Figure 4.6: Confirmation of Flow cytometry results for chemokine expression on multiple donors. ....	159

Figure 4.7: Effects of short term stimulation with TGFβ1 on receptor expression.....	161
Figure 4.8: Confirmation of effects of cytokines on CCR expression by QPCR.....	162
Figure 4.9: MSC dose response to chemokine ligand. ....	165
Figure 4.10: MSC migration to chemokine ligands. ....	168
Figure 4.11: Impact of TGFβ1, IL4 and IL10 stimulation on MSC migration to chemokine ligands.....	170
Figure 4.12: Impact of cytokine stimulation on adhesion of MSC. ....	172
Figure 4.13: Carbon tetrachloride induced liver injury in Rag2 <sup>-/-</sup> IL-2r <sup>γ</sup> <sup>-/-</sup> mouse models. ....	177
Figure 4.14: Carbon tetrachloride induced liver injury in C57BL/6 mouse models. ....	178
Figure 4.15: Impact of TGFβ1 stimulation on MSC adhesion and engraftment.....	180
Figure 4.16: Impact of TGFβ1 stimulation on MSC after enzymatic detachment.....	185
Figure 4.17: Effect of TGFβ1 stimulation on production of pro-fibrotic factors, tri-lineage differentiation and intracellular stress in MSC.....	189
Figure 4.18: TGFβ1 stimulated MSC surface integrin and adhesion molecule expression. ...	194
Figure 4.19: Cytokines and angiogenic factors in TGFβ1 stimulated MSC supernatant.....	196
Figure 4.20: Adhesion molecules on HSEC after culture with cytokine stimulated MSC supernatant.....	197
Figure 4.21: TGFβ1 stimulated MSC mediated suppression of CD4 T cell proliferation. ....	199
Figure 4.22: Impact of ALD serum on MSC surface receptor expression.....	202
Figure 4.23: Effect of ALD serum on MSC adhesion.....	204
Figure 4.24: Effect of ALD serum on cellular stress.....	206
Figure 4.25: Impact of ALD serum on tri-lineage differentiation.....	207
Figure 5.1: Sources of fibrocytes, fibroblasts and myofibroblasts in inflammation and fibrosis. ....	228
Figure 5.2: SAP levels in serum and liver during liver injury.....	236
Figure 5.3:PBMC isolated from peripheral blood on Lympholyte-H. ....	240
Figure 5.4: PBMC isolated from peripheral blood on Ficoll-Paque. ....	243
Figure 5.5: Number of PBMC isolated from blood or pre-prepared buffy coat using Ficoll-Paque or Lympholyte-H. ....	247
Figure 5.6: PBMC isolated from blood or pre-prepared buffy coat using Ficoll-Paque or Lympholyte-H cultured on fibronectin coated Cell Bind tissue culture plastic. ....	249
Figure 5.7: PBMC isolated from buffy coat using Ficoll-Paque cultured on fibronectin, Cell Bind tissue culture plastic, or tissue culture plastic.....	250
Figure 5.8: PBMC isolated from buffy coat using Ficoll-Paque cultured on tissue culture plastic at low and high cell densities. ....	251
Figure 5.9: Number of spindle shaped cells arising from PBMC isolated from blood or buffy coat using Ficoll-Paque or Lympholyte-H cultured on fibronectin, Cell Bind tissue culture plastic, or tissue culture plastic.....	254
Figure 5.10: PBMC cultured on normal, fibronectin coated and collagen coated tissue culture plastic.....	258
Figure 5.11: Adherent PBMC cultured on normal, fibronectin coated and collagen coated tissue culture plastic. ....	259

Figure 5.12: CD14 <sup>+</sup> and CD14 <sup>-</sup> PBMC cultured on normal, fibronectin coated and collagen coated tissue culture plastic. ....	260
Figure 5.13: Non adherent PBMC cultured on normal, fibronectin coated and collagen coated tissue culture plastic. ....	261
Figure 5.14: Expression of fibrocyte markers on PBMC isolated from buffy coat and cultured on tissue culture plastic. ....	263
Figure 5.15: Expression of procollagen-1 on PBMC isolated from buffy coat obtained from peripheral blood. ....	265
Figure 5.16: Collagen-1 and $\alpha$ SMA expression on CD90 <sup>+</sup> synovial fibroblasts. ....	267
Figure 5.17: Collagen-1 and $\alpha$ SMA expression on CD90 <sup>+</sup> synovial fibroblasts and PBC liver derived myofibroblasts. ....	269
Figure 5.18: CD45 and collagen-1 co-expression in human liver injury. ....	270
Figure 5.19: CD45 <sup>+</sup> selected cells from HSEC and BEC depleted, digested liver slices. ....	274



## LIST OF TABLES

Table 1.1: Proposed markers for prospective MSC isolation.....	14
Table 1.2: Chemokine receptors.....	37
Table 1.3: Integrins subfamily.....	41
Table 2.1: Cells used for this study and details of culture media used for propagation.....	50
Table 2.2: Antibodies for IHC.....	57
Table 2.3: CCR and Integrin antibodies for used for flow cytometry.....	61
Table 2.4: Cytokines used for MSC stimulation.....	63
Table 2.5: 18S rRNA Thermal Profile and Primers.....	64
Table 2.6: 18S rRNA PCR Reagents.....	65
Table 2.7: 18S rRNA PCR Electrophoresis Buffer.....	65
Table 2.8: QPCR Primers.....	67
Table 2.9: QPCR Thermal Profile.....	67
Table 2.10: QPCR reagents.....	68
Table 2.11: QPCR primers for $\alpha$ SMA and coll1 $\alpha$ 1.....	69
Table 2.12: Components of QPCR reagents for $\alpha$ SMA and coll1 $\alpha$ 1.....	69
Table 2.13: Antibodies used for cell based ELISA.....	74
Table 2.14: Chemokine ligands used in Boyden chamber migration assays.....	78
Table 2.15: Buffers for SDS PAGE.....	87
Table 2.16: Gel components for SDS PAGE.....	88
Table 2.17: Reagents for Western Blot.....	88

## ABBREVIATIONS

$\alpha$ SMA	$\alpha$ smooth muscle actin
(d)dH <sub>2</sub> O	(Double) distilled water
7AAD	7-Aminoactinomycin D
AIH	Autoimmune hepatitis
ALD	Alcoholic liver disease
APC	Antigen presenting cell
APC	Allophycocyanin
APS	Ammonium persulfate
BEC	Biliary epithelial cells
bp	Base pairs
BSA	Bovine serum albumin
C57BL/6	C57 black 6
CCl	Calcium chloride
CCl <sub>4</sub>	Carbon tetrachloride
CCR	Chemokine receptor
CD	Cluster differentiation
CDB	Cell dissociation buffer
cDNA	Complimentary DNA
CFSE	Carboxyfluorescein succinimidyl ester
CFU-F	Colony forming unit fibroblasts
Col-1	Type 1 collagen
Col1 $\alpha$ 1	Type 1 collagen
ct	Cycle threshold
CXCL	C-X-C motif chemokine
DAB	3,3'-Diaminobenzidine
DAG	Diacyl-glycerol
DAPI	4', 6-diamidino-2-phenylindol
DC	Dendritic cell
DCF	Dichlorofluorescein
DMEM	Dulbecco's modified eagle's medium
DMSO	Dimethyl Sulfoxide
DNA	Deoxyribonucleic acid
dNTP	Deoxyribonucleotide triphosphate
ECL	Electrochemiluminescence
ECM	Extracellular matrix
EDTA	Ethylenediaminetetra-acetic acid
EGF	Epideral growth factor
EGFR	Epidermal growth factor receptor
ELISA	Enzyme linked immunosorbent assay

FACS	Fluorescently activated cell sorting
FCS	Foetal calf serum
FGF4	Fibroblast growth factor 4
FHF	Fulminant hepatic failure
FITC	Fluoresceinisoithiocyanate/ fluoresceinisoithiocyanate
FS	Forward scatter
FW	Formula weight
GAPDH	Glyceraldehyde 3-phosphate dehydrogenase
GDP	Guanosine diphosphate
GFP	Green fluorescent protein
GRK	G protein coupled receptor kinases
GTP	Guanosine triphosphate
GVDH	Graft versus host disease
H <sub>2</sub> O <sub>2</sub>	Hydrogen peroxide
HBSS	Hanks balanced salt solution
HCC	Hepatocellular carcinoma
HCl	Hydrochloric acid
HGF	Hepatocyte growth factor
HIV	Human Immunodeficiency virus
HLA-G5	Human leukocyte antigen G5
HO-1	Heme oxygenase 1
Hr(s)	Hour(s)
HRP	Horse radish peroxidase
HSC	Hematopoietic stem cells
HSEC	Hepatic sinusoidal endothelial cells
ICAM	Intercellular adhesion molecule
IDO	Indoleamine 2,3-Dioxygenase
IF	Immunofluorescence
IFN	Interferon
IGF-1	Insulin like growth factor
IgG	Immunoglobulin
IHC	Immunohistochemistry
IL	Interleukin
IMC	Isotype matched control
IMS	Industrial methylated spirit
IP	Intraperitoneal
IP10	Interferon gamma-induced protein 10
IP3	Phosphatidylinositol 1, 4, 5-triphosphate
IROS	Intracellular reactive oxygen species
ITAC	Interferon Inducible T-Cell Alpha Chemoattractant
kDa	Kilodaltons
LPS	Lipopolysaccharide

MCP	Monocyte chemoattractant protein
MDC	Monodansylcadaverine
MDC	Macrophage-derived chemokine
MEC	Mucosae-associated epithelial chemokine
MF	Myofibroblast
MFI	Median fluorescence intensity
MgCl <sub>2</sub>	Magnesium chloride
MIG	Monkine induced by gamma interferon
Min(s)	Minute(s)
MIP	Macrophage inflammatory protein
MMP	Matrix metalloproteinase
mRNA	Messenger RNA
MSC	Human bone marrow derived mesenchymal stem cells
MSCGM	Mesenchymal stem cell growth media
MTT	3-(4, 5-dimethylthiazol-2-yl)-2, 5-diphenyl-2H-tetrazolium bromide
NASH	Non alcoholic steatotic hepatitis
NEAA	Non essential amino acids
NK	Natural killer cells
NO	Nitric oxide
nt	Nucleotides
OSM	Oncostatin M
PB	Pacific blue
PBC	Primary Biliary Cirrhosis
PBMC	Peripheral blood mononuclear cells
PBS	Phosphate buffered saline
PCR	Polymerase chain reaction
PDGF	Platelet derived growth factor
PE	Phycoerythrin
PGE2	Prostaglandin E2
PIP2	Phosphatidylinositol 4, 5-bisphosphate
PKC	Protein kinase C
PLC <sup>2</sup>	Phospholipase C $\beta$ 2
PMA	Phosphomolybdic acid
PO	Pacific orange
polyI:C	Polyinosinic – polycytidylic acid sodium
Procol-1	Type 1 Collagen
PSC	Primary Sclerosing Cholangitis
PSG	Penicillin, Streptomycin, Glutamine
QPCR	Quantitative PCR
RNA	Ribonucleic acid
RPMI	Roswell park memorial institue
rRNA	Ribosomal RNA

SAP	Serum amyloid protein
SDF	Stromal cell derived factor
SDS-PAGE	Sodium dodecyl sulfate polyacrylamide gel electrophoresis
SEM	Standard error of mean
SS	Side scatter
TARC	T cell-directed CC chemokine
TEMED	N,N,N',N'-tetramethylethylenediamine
TGF	Transforming growth factor
TLR	Toll-like receptor
TNF	Tumour Necrosis Factor
Treg	T regulatory cells
VCAM	Vascular cellular adhesion molecule
VEGF	Vascular endothelial growth factor
WT	Wild type

# **CHAPTER 1: INTRODUCTION**

## **1.1 The Liver**

### **1.1.1 Liver function**

The liver is the largest gland and solid organ in the body and its size appropriately reflects its complexity and functional importance for survival. The primary role of the liver is to process material from systemic and portal vein-derived blood and hence the liver has a dual blood supply from the hepatic artery and the hepatic portal vein. To process the blood the liver performs over 500 metabolic functions. Examples of such functions include metabolism of carbohydrates, fats and proteins to glucose, fatty acids/glycerol and amino acids respectively. The liver is able to convert glucose to glycogen and vice versa allowing rapid utilization of glucose when needed. The liver produces bile which aids fat digestion and absorption, and helps excretion of substances such as waste products from metabolism, hormones, drugs and bilirubin. The liver is involved in synthesis of plasma proteins and blood clotting factors. The phagocytes in the liver also produce acute phase proteins and immune factors in response to microbes in the liver (Wallace *et al.*, 2008). On a cellular level these metabolic reactions are carried out by many powerful enzymes which are contained within specialised liver cells called hepatocytes (Friedman, 1993). The capillary system of the liver, also known as the sinusoids, plays a pivotal role in liver function (Wallace *et al.*, 2008). Sinusoids are lined with endothelial cells and phagocytic Kupffer cells, and the fenestrated endothelial layer ensures blood constituents can penetrate into the Space of Disse where hepatocytes take up nutrients and oxygen as they come into direct contact with the blood components (Figure 1.1).

### **1.1.2 Liver Disease**

According to the British Liver Trust, liver disease is the only major cause of death that has risen year-on-year since the seventies compared to diabetes, cancer, stroke, heart diseases, respiratory diseases, and road accidents, which have remained stable or even decreased. Liver disease ranks as the fifth commonest cause of death in England and Wales and kills more people than diabetes and road deaths combined. 16087 people in the UK have died from liver disease in 2008, a 4.5% increase since 2007 and a 12% increase since 2005 and 100% increase since 1991. Since 2005 the total number of deaths is 46244 and deaths are predicted to double in 20 years if the current trend continues ([www.britishlivertrust.org.uk](http://www.britishlivertrust.org.uk), 2008).

There are a number of causes of liver disease including alcohol excess, hepatitis virus infection, obesity, non-alcoholic fatty liver disease and autoimmune diseases. Liver disease can manifest as an acute disease or in a chronic form depending on the cause. Although the causes can vary, the disease progression is much the same following sustained injury. Liver injury disrupts the normal function of the liver cells, usually by causing mass death of normal cells either resulting in, or as a cause of concurrent inflammation. When the inflammatory response to liver injury or the injurious cause is sustained without resolution, this leads to a buildup of scar tissue without the counterbalanced stimulus for the breakdown of this scar tissue, by matrix metalloproteases (MMP). This continued process may eventually lead to fibrosis and decreased liver function. Eventually sustained fibrosis can lead to cirrhosis, altering the cellular composition and liver architecture causing liver function to seriously deteriorate (Figure 1.1). Cirrhosis is usually followed by complete loss of liver function known as liver failure.



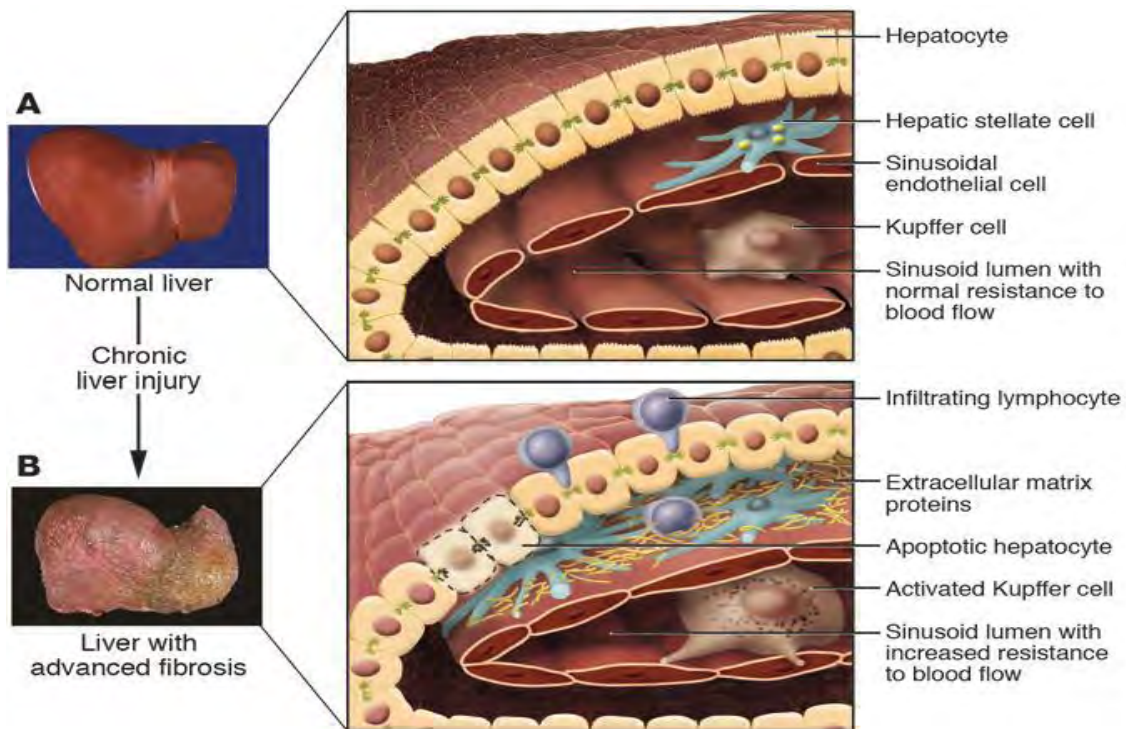


**Figure 1.1: Changes in the hepatic architecture in disease**

Appearance of normal liver (A) and liver in advanced liver fibrosis (B): Inflammatory lymphocytes infiltrate the hepatic parenchyma after injury. Hepatocytes can undergo apoptosis after being damaged, and Kupffer cells activate, releasing fibrogenic mediators. Stellate cells become active and proliferate, secreting large amounts of extracellular matrix proteins. Figure reproduced from (Bataller and Brenner, 2005).

Resolution of liver inflammation and fibrosis leading to a return to normal histology has been observed in humans and in mouse models of inflammation and fibrosis when the sustained injury has been stopped (Tsukada *et al.*, 2006). It has also been shown that levels of fibrosis can be reached after which resolution cannot occur. At this stage in humans, treatment focuses on preventing further progression to cirrhosis and liver failure. Symptoms of cirrhosis include ascites (fluid retention in the abdominal cavity), increased risk of infection, hepatic

encephalopathy and a poor quality of life (Wallace *et al.*, 2008). The forms of therapy that currently exist have significant drawbacks. Anti inflammatory medication like corticosteroids stop the release of proliferative fibrogenic cytokines but these rarely offer complete suppression. The other alternative is liver transplantation, but this too has significant drawbacks, the main being a lack of donors and immune rejection.

The British Liver Trust suggests that at the end of March 2009 there were 338 people on the remaining on the waiting list for a liver transplant, despite 644 liver transplants from deceased donors during the preceding 12 months. This illustrates how there a continuous need for liver donors, but there was a distinct shortage in donor organs from 2007 to 2008 where only 58% of the 1121 patients waiting received transplants while 25% were still waiting at the end of the year. Between 2002 and 2007, the three commonest reasons for a liver transplant included alcoholic cirrhosis, hepatitis C related cirrhosis and primary biliary cirrhosis ([www.britishlivertrust.org.uk](http://www.britishlivertrust.org.uk), 2008). Considering these statistics, there is clearly a need for the development of new, non invasive therapies that work on a cellular level to reduce or reverse inflammation and fibrosis. To do this, the mechanisms causing liver fibrosis at a cellular level need to be thoroughly understood and factors which increase, reverse or have the potential to reduce fibrosis need to be identified manipulated and used as effective therapies.

On a cellular level, when liver injury causes sustained inflammation, resident hepatic stellate cells in the Space of Disse become activated and take on a myofibroblast-like phenotype and rapidly proliferate (Figure 1.1). When activated, these cells are responsible for depositing components of extracellular matrix including fibril forming collagens 1 and 3, matrix

glycoconjugates including fibronectin, hyaluronic acid, and proteoglycans which make up the connective tissue that causes scarring and fibrosis. This matrix fills the subendothelial space (which normally contains minimal basement membrane constituents) causing impaired hepatocyte function and loss of cell pores, which further activates hepatic stellate cells, creating a vicious cycle. The collagen and proteoglycans that are produced by these fibroblasts contribute to formation of significant connective scar tissue which may be up to 6 times more abundant in cirrhotic liver than in normal liver (Tsukada *et al.*, 2006).

### **1.1.3 Liver Inflammation**

Inflammation in liver is characterised by recruitment and retention of circulating immune cells during an immune response and can clinically be defined as acute or chronic, when inflammation continues for over 6 months. Liver injury or infection causes resident macrophages or Kupffer cells to initiate an immune response and mediate inflammation which usually precedes stellate cell activation and the development of fibrosis (Figure 1.2). During liver injury, there is a mass of apoptotic cells which are phagocytosed by Kupffer cells, and in response release cytokines such as TNF $\alpha$ , IL1, IL6 and IL8, which drive recruitment of leukocytes. Recruited leukocytes can then exert further damaging effect on the liver tissue promoting fibrosis (Liaskou *et al.*, 2012).

The role of Kupffer cells in linking inflammation with fibrosis is shown in studies in mice with carbon tetrachloride induced liver injury (Titos *et al.*, 2003), where a reduction of Kupffer cells, subsequently reduced fibrosis. Kupffer cells also produce IL8 which is specific for the recruitment of neutrophils from circulation (Liaskou *et al.*, 2012). IL10 is an anti-

inflammatory cytokine which serves to reduce neutrophil recruitment in the liver (Nelson *et al.*, 2000). In IL10 knockout mice neutrophil recruitment was increased resulting in increased fibrosis, furthermore increased IL10 was shown to have anti-fibrotic effects (Louis *et al.*, 1998). An obvious way to reduce inflammation would therefore be to selectively deplete macrophages to avoid fibrosis. However subsequent studies have found that the presence of Kupffer cells is essential during resolution of fibrosis and these cells play an active role in this mechanism through the use of MMP which degrade deposited collagen (Duffield *et al.*, 2005, Stramer *et al.*, 2007). This highlights the important fact that fibrosis is an essential repair mechanism which leads to the resolution of injury providing that the initial insult can be stopped. Kupffer cells are an essential part of the recovery mechanism (Figure 1.2).

The problem occurs when the cause of injury cannot be stopped. In this instance Kupffer cells still function to promote inflammation and release factors such as TGF $\beta$ 1, a major cytokine involved in fibrosis (Kershenovich Stalnikowitz and Weissbrod, 2003). TGF $\beta$ 1 is responsible for preventing Kupffer cells from degrading deposited collagen via an up-regulation of TIMP which inhibits MMP function (Kershenovich Stalnikowitz and Weissbrod, 2003). Such cytokines can cause hepatic stellate cells to differentiate to myofibroblasts which further express TGF $\beta$ 1 forming a perpetual loop in activating stellate cells and promoting fibrosis (Kershenovich Stalnikowitz and Weissbrod, 2003). Myofibroblasts also have antigen presenting capabilities suggesting they can further promote inflammation and are also able to induce T cell proliferation (Kershenovich Stalnikowitz and Weissbrod, 2003). Myofibroblasts further perpetuate inflammation by enhancing recruitment of lymphocytes and promoting cellular damage in the liver (Fernandez-Cruz *et al.*, 1978, Holt *et al.*, 2009). This presents a challenge where the inflammation in the liver environment needs to be controlled and

suppressed while the fibrotic process is encouraged to resolve the tissue damage. Bone marrow derived mesenchymal stem cell therapy provides an option with the means to achieve this end.

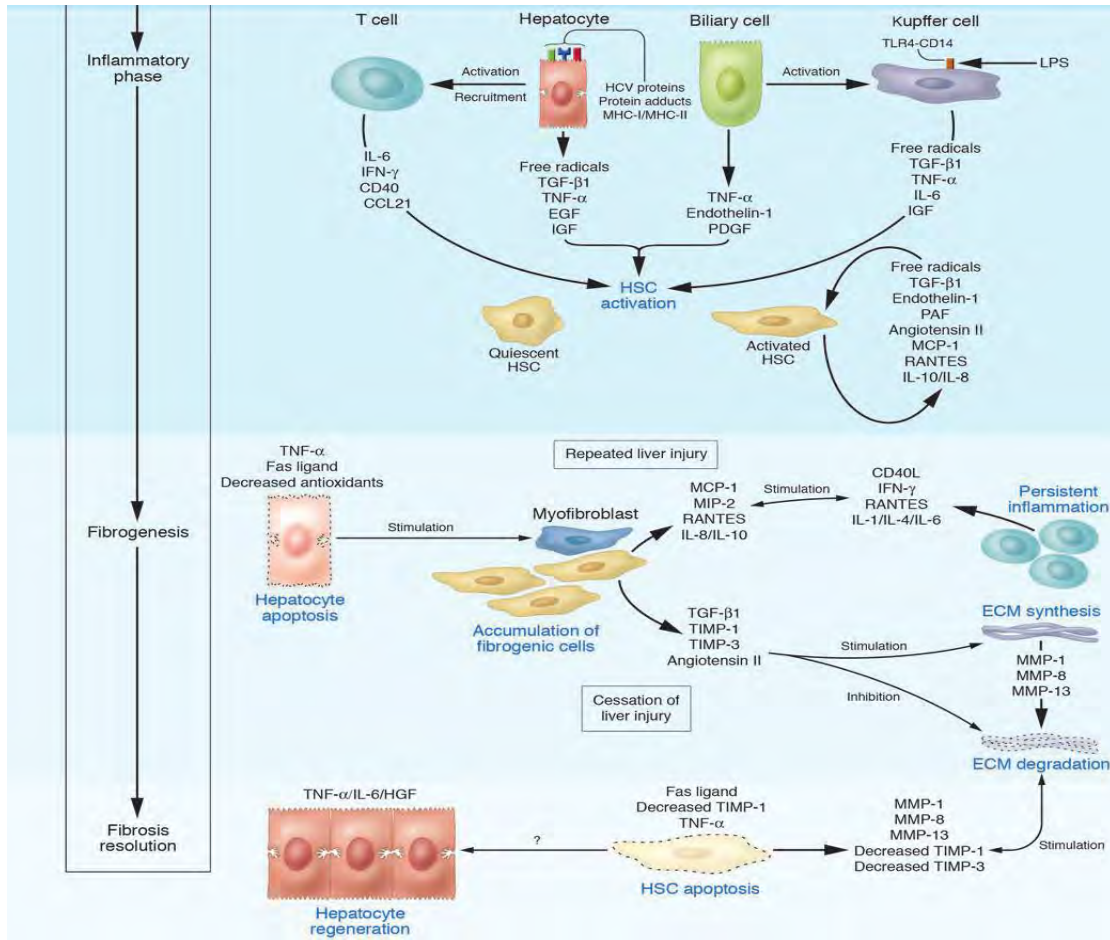


**Figure 1.2: Drivers of hepatic inflammation and fibrosis.**

Damaged hepatocytes and biliary cells release soluble inflammatory factors that activate Kupffer cells and recruit activated T cells. Hepatic stellate cells are activated by these conditions into fibrogenic myofibroblasts and secrete cytokines that perpetuate their activated state. If the cause of injury is not stopped, this leads to an accumulation of activated stellate cells and portal myofibroblasts, synthesizing large amounts of ECM proteins, leading to tissue fibrosis. ECM degradation is inhibited by the actions of TIMP. Apoptosis of damaged hepatocytes stimulates the fibrosis via

stellate cells. If the cause of the liver injury is removed, fibrosis can resolve through stellate cell apoptosis and hepatocyte regeneration. TIMP expression reduces leading to increased MMP activity, which causes collagen degradation. Reproduced from (Bataller and Brenner, 2005).

## **1.2 Human Bone Marrow derived Mesenchymal Stem Cells (MSC)**

### **1.2.1 MSC Markers**

This thesis will investigate the process of exogenously applied MSC engraftment into the liver, and their potential therapeutic effects. Conflicting reports exist regarding the molecules involved in MSC recruitment to organs and the effects they can impart. A potential reason for this could be the heterogeneity reported in MSC populations. It is therefore important to review current methods of identifying MSC. The first observation of a stromal precursor was made from bone marrow from rabbits or rodents, which when seeded at low densities in medium containing serum gave rise to discrete colonies of plastic adherent, non phagocytic fibroblast-like cells. Each colony was generated from a single cell and these cells were termed colony forming units-fibroblasts (CFU-F) (Friedenstein *et al.*, 1974). Subsequent research into these cells identified differentiation towards cartilage tendon and muscle and fat (Pittenger *et al.*, 1999). Human bone marrow mesenchymal stem cells (MSC) are similarly defined as spindle shaped, cell culture plastic adherent and are positive for a profile of mesenchymal receptors including SH2, SH3, CD29, CD44, CD71, CD90, CD106, CD120a, CD124, CD105, CD73 (Dominici *et al.*, 2006). They can be distinguished from hematopoietic stem cells by their lack of hematopoietic receptors including CD11b, CD14, CD34, CD45, CD79a, CD19, HLA-DR (Dominici *et al.*, 2006). For cells to be termed MSC, they must have the ability to replicate as undifferentiated cells and display at least tri-lineage plasticity to adipocytes, chondrocytes and osteoblasts (Dominici *et al.*, 2006).

Current isolation methods involve culturing whole human bone marrow on tissue culture plastic for a number of passages to deplete all non adherent cells or more recently culturing

bone marrow in a bioreactor (Boxall and Jones, 2012, Mareschi *et al.*, 2009). The phenotype of adherent cells is then confirmed for MSC markers and tri-lineage potential. Of note, an accepted and universally used prospective MSC isolation method does not currently exist. Although a single specific marker for prospective mesenchymal stem cell isolation from bone marrow has not yet been identified, there have been attempts to isolate MSC with a number of markers (Table 1.1). CD73, CD90 and CD105 are commonly used as markers of MSC however these markers do not vary with MSC age, potency or differentiation potential, suggesting these markers only serve a purpose in characterising these cells and these are not a specific combination of markers for MSC but may encompass various other populations (Boxall and Jones, 2012).

Stro1 is a well known marker of MSC identifying a purer population of cells with tri-lineage potential and stem-like qualities. However, Stro1 is not specific for MSC and is expressed by other cell populations in the bone marrow (Simmons and Torok-Storb, 1991). On MSC, Stro1 is a marker that is lost with time on MSC in culture. The function of Stro-1<sup>+</sup> is not known but it has been implicated in MSC migration and attachment to extracellular matrix, similar to CD106 expression (Bensidhoum *et al.*, 2004). Subsequently, CD106 has been coupled with Stro-1<sup>+</sup> as a marker to isolate a purer MSC population (Gronthos *et al.*, 2003). Like Stro1, CD106 expression also reduces with time in culture but also after tri-lineage differentiation, suggesting it may be a true marker of potency and tri-lineage potential in expanded MSC cultures (Jung *et al.*, 2011a, Liu *et al.*, 2008). PODXL has also been highlighted as a marker of highly proliferative MSC and, so could indicate increased potency and stem cell potential but this marker is also down regulated in culture over time (Boxall and Jones, 2012). It is possible that proliferation potential and age of the cell is closely linked with differentiation



potency and CD106, PODXL and Stro1 could be markers of this (Boxall and Jones, 2012). However there are reports of certain markers identifying populations which are primed to differentiate to a specific cell type, acting as a mesenchymal progenitor rather than a true stem cell, such as CD106<sup>+</sup> cells, which have shown a propensity to differentiate towards adipogenic more than osteogenic cells (Boxall and Jones, 2012). A recently described MSC marker is CD271 which when coupled with CD73 expression has yielded consistently potent MSC populations (Cuthbert *et al.*, 2012, Veyrat-Masson *et al.*, 2007). However, like Stro1, CD271 is also found on hematopoietic populations in bone marrow (Cuthbert *et al.*, 2012, Simmons and Torok-Storb, 1991). During isolation hematopoietic cells can be gated out isolating only the non hematopoietic fraction and in situ CD271 can be couple with CD146, a pericyte marker identified on cells with non-hematopoietic MSC-like properties to yield pure MSC populations (Boxall and Jones, 2012). Furthermore, W8B2-MSCA 1, a marker for uncultured bone marrow MSC and an enzyme known to promote bone mineralisation, has been seen consistently expressed on CD271 positive cells and could serve to further purify the MSC population (Boxall and Jones, 2012).

In common with a lack of definitive phenotypic marker, a universally used prospective MSC isolation method from bone marrow does not exist. As culture expansion to large cell numbers is an unavoidable necessity in MSC therapy, potent MSC populations need to be selected prospectively and cultured to larger numbers. Furthermore as most markers which have been implicated in this role are rapidly lost in culture, it is essential that we can prospectively isolate MSC using these markers. A further argument for prospective isolation is because contaminating cell types could serve to compete against MSC for oxygen and space making conditions less favourable for MSC growth particularly as MSC are now being

produced in bioreactors rather than undergoing multiple passages in culture to decrease contaminating cell numbers. Such protocols could increase MSC variability and produce inconsistencies between multiple MSC isolations. To avoid such inconsistencies in this project we utilised MSC that were acquired commercially from the same source. This eliminates variability to some extent and allows us to focus on the therapeutic benefits of MSC, which can in future studies be enhanced through purification of the current MSC populations we use.

**Table 1.1: Proposed markers for prospective MSC isolation**

Markers	Function	Expression	Specificity	Reference
STRO1	Unknown (potentially MSC migration)	Diminished with age.	Labels hematopoietic cells	Simmons and Torok-Storb, 1991 (Simmons and Torok-Storb, 1991)
CD146	Unknown (potentially endothelial junction protein)	Diminished with age. <i>In-vivo</i> distribution when coupled with CD271.	Labels pericytes	Covas <i>et al.</i> , 2008 (Covas <i>et al.</i> , 2008)
CD106	MSC migration	Diminished with age.	Labels hematopoietic cells	Gronthos <i>et al.</i> , 2003 (Gronthos <i>et al.</i> , 2003)
PODXL	Sialomucin	Diminished with age.	Labels hematopoietic cells	Lee <i>et al.</i> , 2009 (R. H. Lee <i>et al.</i> , 2009)
CD271	Receptor for neurotrophins	Diminished with age.	Labels hematopoietic cells	Quirici <i>et al.</i> , 2002 (Quirici <i>et al.</i> , 2002)
W8B2	Promote bone mineralisation	Strong prospective marker when coupled with CD271.	Labels CD271 bone marrow cells	Buhring <i>et al.</i> , 2009 (Buhring <i>et al.</i> , 2009)

### 1.1.1 Function in Niche

Mouse bone marrow derived mesenchymal stem cell colonies seeded under the renal capsule of animal models gave rise to bone and bone marrow with hematopoietic cells of host origin, suggesting that certain cellular components from this population generated the correct microenvironment for hematopoietic stem cell (HSC) homing and growth (Friedenstein *et al.*, 1970). Stem cells in the bone marrow exist in specialised niches within a highly regulatory microenvironment (Spradling *et al.*, 2001). Mesenchymal stem cells provide this environment for HSC and maintain them in the bone marrow (Dexter *et al.*, 1977). The most primitive HSC are located in the endosteal region, co localised with osteoblasts, suggesting these cells play a central role in maintaining stem potential in HSC (Moore, 2004). Progenitor cells derived from primitive HSC are found localised in the central vascular region of the marrow space,

the cells of which include MSC derived cells (Kopp *et al.*, 2005). This suggests that MSC are potentially the source of all cell populations responsible for supporting HSC development.

It is clear that the MSC provide regulation of the HSC niche, however it is less apparent how the MSC niche is regulated. MSC can control their own niche using autocrine signals but HSC can also provide signals to control the MSC niche. This is best shown in conditions of culture expanded MSC where cell cluster size and organisation can regulate the niche (Delorme *et al.*, 2006, Simmons and Torok-Storb, 1991). The niche is an immunoprivileged environment and acts as a shelter which sequesters stem cells from differentiation stimuli, apoptosis and other stimuli which could challenge stem cells acting as a lifelong source for differentiated cells (Moore and Lemischka, 2006). It is not unsurprising that MSC have been reported to have powerful immunosuppressive and immunomodulatory properties considering they are responsible for this role. Furthermore MSC in the niche are responsible for safeguarding against excessive stem cell proliferation which could lead to cancer. This effect of suppression and protection against challenging stimuli can be observed in some of the therapeutic applications of MSC.

### **1.3 Therapeutic uses of MSC in disease**

#### **1.3.1 MSC as a vector to deliver cellular treatment**

Perhaps due to their original function in the stem cell niche MSC have to be poor antigen presenters so that they do not initiate any immune response in the niche. For this reason MSC have no MHC II molecules (Puglisi *et al.*, 2011). As a result for therapeutic purposes, MSC are well tolerated and due to a lack of co stimulatory molecules CD80, CD86, CD40, CD40L,

MSC do not suffer from host versus graft response after transplant (Ryan *et al.*, 2005). This not only makes them ideal tools for carrying out whatever intrinsic therapeutic properties they have as a cell, but also makes them ideal candidates for cellular delivery of treatments for various diseases. MSC can be engineered for use as vectors to deliver therapies in cases where there are genetic deficiencies as in the case of  $\alpha$ -1-anti-trypsin deficiency (Li *et al.*, 2011). MSC have also been reported to home to hepatocellular carcinoma (HCC) (Garcia *et al.*, 2011) so, coupled with their use as vectors, they can be manipulated to carry cancer killing signals or agents, like TRAIL (Loebinger *et al.*, 2009) or suicide genes (Niess *et al.*, 2011), to tumours after infusion. This type of therapy is central to the focus of this thesis, which is to try and understand the mechanism of engraftment to the liver so that this mechanism can be manipulated and enhanced to deliver treatment for diseases or to attack tumours.

### **1.3.2 MSC administration to pre-clinical models of liver disease**

This thesis will investigate exogenous delivery of MSC to injured liver, so it is important to consider methods that have previously been used and the effects of MSC infusion. The common method for MSC infusion in most models of liver injury is intravenous administration. However a common problem observed in mice with intravenous injection of MSC, potentially due to their large size, is lodging of these cells in the pulmonary vasculature (Karp and Leng Teo, 2009). This problem may be overcome using vasodilatory mechanisms, but currently experiments suggest only a small reduction in cell lodging (Gao *et al.*, 2001). Interestingly Ezquer *et al* who also used intravenous infusion observed no MSC in lungs, but found MSC only in the liver, bone marrow, heart and kidney (Ezquer *et al.*, 2011). This could have been due to long term nature of their engraftment experiments where MSC may have

ultimately been cleared from the lungs. Infusions through the portal vein as more commonly being tested to circumvent problems encountered by using intravenous injections and are showing promising results (Li and Li, 2012). Most notably infusions of MSC into pigs with Fulminant Hepatic Failure (FHF) were rescued using this method of infusion of MSC (Li and Li, 2012).

Transplanted MSC have been shown to home to sites of injury to ensure continued delivery of molecules or signals which assist in resolving injury (Yagi *et al.*, 2009). To develop MSC transplantation as a viable clinical therapy for liver disease, the administration of these cells need to be carried out using the least invasive methods as possible. Infusion methods can be intrahepatic, intraportal-vein, intrasplenic or intravenous injection and have all shown efficacy in resolving liver diseases (Cao *et al.*, 2012, Kuo *et al.*, 2008, Zhao *et al.*, 2012). Studies have also investigated infusion via the jugular vein and showed minimal engraftment compared to portal vein infusions in a D-galactosamine induced liver injury model (Parekkadan *et al.*, 2007b). Intrahepatic infusions are invasive procedures and have been shown to have weaker effects than intravenous injections in liver therapy (Zhao *et al.*, 2012).

### 1.3.3 Therapeutic effect of MSC through transdifferentiation into hepatocytes

The focus of this thesis is to further understand and enhance MSC migration to the injured liver when administered as a therapy. It is therefore important to review the therapeutic effects of MSC that have been documented in the liver and other organs or diseases. As we are interested in the therapeutic effects of MSC, I will review some of the therapeutic properties of MSC and also some potential safety considerations that may exist with MSC therapy. Initial reports focus on MSC transdifferentiation into hepatocytes to restore liver function. *In-vitro* differentiation of MSC to hepatocytes in response to liver specific factors has been proven (Chivu *et al.*, 2009), specifically Dong *et al* have shown fibroblast growth factor 4 (FGF-4), hepatocyte growth factor (HGF) and oncostatin M (OSM) are potent inducers of hepatocyte differentiation of mouse bone marrow derived mesenchymal stem cells (Dong *et al.*, 2010). Subsequent *in-vivo* experiments have confirmed differentiation of MSC into hepatocytes via expression of markers like human serum albumin, cytokeratin 18,  $\alpha$ -1-anti-trypsin and  $\alpha$ -fetoprotein after engraftment into immunocompromised mice (Kuo *et al.*, 2008, Tao *et al.*, 2009). Tao *et al* suggest that hepatocyte differentiation may be mediated by cell contact between resident hepatocytes and the transplanted MSC in the injured liver (Tao *et al.*, 2009). Later work by Mohamadnejad *et al* implicated adenosine as responsible for MSC retention and differentiation into hepatocytes in the liver (Mohamadnejad *et al.*, 2010). Infusion of MSC into pigs with fulminant hepatic failure (FHF) induced by D-galactosamine injury showed cells differentiated to hepatocytes in hepatic lobules and increased survival rates for over 6 months compared with only 96 hours in pigs without infusion (Li and Li, 2012). However there is limited evidence to suggest that such a mechanism can significantly reduce or resolve liver injury, particularly as the number of differentiated MSC is so small.

Pre-differentiation of MSC to hepatocyte-like cells before infusion into CCL<sub>4</sub> injured mice has sought to resolve this but with little success (Kuo *et al.*, 2008).

Zhao *et al* pre-differentiated MSC to hepatocyte-like cells and rescued CCL<sub>4</sub> induced liver injury in Sprague Dawley rats implicating an IL10 mediated reduction of fibrotic factors and cytokines (Zhao *et al.*, 2012). Hepatocyte-like cells differentiated from MSC on nanofibers before transplantation were also reported to reduce liver fibrosis due to increased differentiation (Piryaei *et al.*, 2011). However this study seems inconclusive as control MSC derived hepatocyte-like cells which were not grown on nanofibers also showed differentiation into hepatocyte-like cells and there was no clear link in fibrosis resolution and hepatocyte differentiation. Engraftment of MSC derived hepatocyte like cells has been shown to be long lasting but the beneficial effects of this procedure are limited. Alternatively MSC have exhibited long term engraftment for 15-20 weeks in pigs with FHF and have shown significant beneficial effects in these animals (Li and Li, 2012).

#### **1.3.4 Paracrine anti-fibrotic effects of MSC in liver disease**

Experiments with human placenta derived MSC infusions into Chinese miniature pigs with D-galactosamine induced liver injury resulted in significantly resolved injury through a paracrine effect (Cao *et al.*, 2012). It is rather more likely that the reparative anti-fibrotic effect is due to MSC and their release of paracrine factors rather than reconstitution of hepatocytes. Although Tao *et al* showed presence of MSC in injured liver, they did not report any significant reduction in injury (Tao *et al.*, 2009). Kuo *et al* reported similar results but went further in their findings to suggest that MSC were able to restore liver function and



ameliorate injury. They went on to show that this beneficial effect was not dependent on MSC differentiation to hepatocytes, although differentiation was observed in some rare cases. Alongside MSC, hepatocytes derived from MSC in *in-vitro* conditions were also infused but showed significantly less effect compared with MSC (Kuo *et al.*, 2008).

The resolution of injury and repair of the injured liver was likely to be a result of the MSC capacity to resist and reduce the typically high levels of oxidative stress, and the release of other paracrine factors which encouraged the repopulation of endogenous hepatocytes (Kuo *et al.*, 2008). Certainly MSC seem to have an intrinsic ability to reduce oxidative stress. Kanazawa *et al* observed reduced hepatocyte apoptosis during ischemic injury in rats after infusion of MSC, with an associated reduction of collagen deposition, reduced  $\alpha$ SMA expression and TGF $\beta$ 1 production, and increased stellate cell apoptosis, compared to injured controls (Kanazawa *et al.*, 2011). Increased MMP9 expression, involved in ECM degradation and reduction of fibrosis, was also observed in MSC infused rats (Higashiyama *et al.*, 2007).

The role of MSC derived paracrine factors in anti-fibrotic effects of MSC have also been highlighted in work by Pan *et al* who showed that MSC are able to suppress stellate cell activation by inhibiting the activation of the Dlk-1 protein in CCl<sub>4</sub> injured mice (Pan *et al.*, 2011). A powerful paracrine effect via bioactive factors of MSC was perhaps a more likely explanation to how MSC executed their beneficial effects. This was proven in great detail in reports where MSC conditioned media was administered as a bolus or systemically infused into rat models of FHF (Parekkadan *et al.*, 2007b). The effects of experiments using conditioned media did not last as long as those where MSC were transplanted and could deliver local and sustained tropic signalling molecules to the liver environment (Banas *et al.*,

2008, Yagi *et al.*, 2009), thus illustrating the importance of persistent signals derived from local MSC. Mechanisms by which MSC can act upon the liver microenvironment have not been fully defined. However MSC have been shown to directly interact with stellate cells in order to reduce fibrosis (Wang *et al.*, 2009a). Parekkadan *et al* have shown that increased IL6 from activated stellate cells induces MSC to produce IL10 and increased HGF, which reduce stellate cell proliferation and collagen production (Parekkadan *et al.*, 2007a). HGF is able to selectively induce apoptosis of activated stellate cells but not normal stellate cells (Parekkadan *et al.*, 2007a). Further, Wang *et al* showed that MSC can produce TGF $\beta$ 3 which behaves in a similar way to HGF and can inhibit collagen 1 and 3 production by activated stellate cells by inhibiting ERK1/2 phosphorylation; however the introduction of PDGF into the environment can override this inhibition. PDGF is abundant in the liver environment so in order for this effect to be observed, PDGF would have to be simultaneously blocked or reduced (Wang *et al.*, 2009a).

MSC transplantation into carbon tetrachloride injured mice resulted in recovery from FHF again suggesting paracrine mode of action. Although there were rare events where MSC differentiated into albumin secreting hepatocyte like cells, liver regeneration seemed to be mediated by a reduction of oxidative stress in the liver and by an increase in the proliferation and viability of endogenous hepatocytes (Kuo *et al.*, 2008) induced by the MSC. Furthermore Mohamadnejad *et al* showed that infusions of MSC into peripheral veins in cirrhotic patients was able to significantly restore liver function and reduce MELD scores in half the patients that were treated after 6 months (Mohamadnejad *et al.*, 2007).

### 1.3.5 Immunomodulatory effects of MSC

As part of this thesis we will investigate immunomodulatory effects of MSC and also how these may be affected by techniques used enhance engraftment of MSC in the liver. The immunomodulatory effects can manifest in a number of ways. Anti-inflammatory effects can be carried out through direct cell to cell contact or through paracrine mechanisms. Infiltration of inflammatory cells is an essential step leading to liver injury and is an important part in causing chronic damage. MSC have a range of effects on immune cells from both the innate and adaptive immune systems. MSC may dampen or reduce persistent immune responses that can promote fibrosis. MSC are able to suppress the proliferation of cells involved in innate immunity including monocytes, dendritic cells (DC), macrophages, natural killer cells (NK) (Sotiropoulou *et al.*, 2006) and neutrophils (Puglisi *et al.*, 2011). Jiang *et al* have reported that MSC are able to prevent monocytes from differentiating into DC and can cause mature DC to lose stimulatory molecules and cytokines resulting in impaired T cell stimulation (Chiesa *et al.*, 2011, Jiang *et al.*, 2005). Early stage DC maturation can be prevented by MSC via IL4, GM-CSF and PGE2 (Spaggiari *et al.*, 2009). PGE2 has also been implicated in the MSC induced suppression of  $\gamma\delta$  T cells and invariant NK cell proliferation and activation in autoimmune disease without affecting the cell antigen presenting capabilities (Prigione *et al.*, 2009).

Eosinophil infiltration can also be inhibited by MSC during an innate immune response in ragweed induced mouse asthma (Nemeth *et al.*, 2010). The mechanism of action appears to involve IL4 and IL13 induction of STAT6 which increases TGF $\beta$ 1 release and therefore eosinophil inhibition by MSC (Nemeth *et al.*, 2010). MSC can also have direct effects on

adaptive immunity by suppressing NK and T cell responses, blocking B cell differentiation and interfering with function of antigen presenting cells. However it is unclear whether this occurs via soluble mediators or through cell to cell contact (Puglisi *et al.*, 2011).

### **1.3.6 Effects of cytokines on immunomodulatory properties of MSC**

A key element in this thesis will be to try and identify ways in which cytokines can increase the engraftment and therapeutic properties of MSC. There is currently a lot of evidence to suggest cytokines can enhance the immunomodulatory properties of MSC. IFN $\gamma$  and TNF $\alpha$  pre-stimulation of MSC has increased immunosuppressive capabilities in numerous reports (English *et al.*, 2007, Krampera *et al.*, 2005). In particular, IFN $\gamma$  stimulated MSC have been implicated as being integral to the prevention of graft versus host disease (Polchert *et al.*, 2008). IFN $\gamma$  has been identified as the cytokine released by T cells which is responsible for the increase in MSC surface B7-H1 which is implicated in T cell suppression through cell to cell contact (Sheng *et al.*, 2008). Reports suggest MSC can induce contact-dependent suppression on a number of immune cells, but significant non contact dependent suppression of immune cell proliferation can only occur after IFN $\gamma$  stimulation of MSC, with the exception of B cells. Perhaps due to the lack of IFN $\gamma$  expression by B cells, cytokine stimulation of MSC is necessary to observe any suppression of B cell proliferation either through contact or non contact mechanisms (Krampera *et al.*, 2006). Spaggiari *et al* report that MSC are able to reduce B cell function either by direct contact or through paracrine factors, while reducing CD8 T cell proliferation and increasing CD4 T helper cell and regulatory cell numbers (Spaggiari *et al.*, 2009). MSC can exert the immunosuppressive effects in a number of ways, through TGF $\beta$ 1 (Soleymaninejadian *et al.*, 2012), IL10 (Yang *et al.*, 2009), PGE2

(Soleymaninejadian *et al.*, 2012), IDO (Soleymaninejadian *et al.*, 2012), NO (Ren *et al.*, 2008), HGF (Soleymaninejadian *et al.*, 2012), HO-1 (Mougiakakos *et al.*, 2011), HLA-G5 (Selmani *et al.*, 2008) and galectins (Sioud, 2011). Of note, it is now accepted that the NO mediated MSC immunosuppressive effects are restricted to mice and not present in humans (Ren *et al.*, 2008).

### **1.3.7 MSC Immunotherapy in liver specific models**

Reports of MSC immunotherapeutic effects in models of liver injury are limited. In rat models of allogeneic liver transplant, MSC infusions are associated with significantly reduced graft rejection (Wang *et al.*, 2009b). Most immunoregulatory effects of MSC as in this case seem to work via recruitment and induction of CD4<sup>+</sup>CD25<sup>+</sup>FoxP3<sup>+</sup> T regulatory cells (Tregs) (Di Ianni *et al.*, 2008, Ghannam *et al.*, 2010, Maccario *et al.*, 2005, Prevosto *et al.*, 2007, Ye *et al.*, 2008), which are able to assist in suppressing inflammation (Kavanagh and Mahon, 2011), similar effects were seen in a cardiac allograft model (Zhou *et al.*, 2006). In a polyinosinic – polycytidylic acid sodium (polyI:C) induced model of liver injury similar to PBC in humans, MSC were able to reduce monocyte infiltration around bile ducts and a simultaneous increase in Treg induction was also reported in the circulation and lymph nodes (Wang *et al.*, 2011). In a high fat-induced NASH model, obese mice given infusions of mesenchymal stem cells from other obese mouse bone marrow showed signs of steatosis only without significant hepatitis (Ezquer *et al.*, 2011). Anti-inflammatory effects have also been reported in an acute pancreatitis model where there was significantly reduced inflammatory cell infiltration after MSC infusion (Jung *et al.*, 2011b). Hong *et al* showed that infusion of IFN $\gamma$  boosts MSC immune suppression in an *in-vivo* orthotopic liver transplant model

suggesting that cytokine treatment of MSC can enhance their therapeutic effects (Hong *et al.*, 2009).

### **1.3.8 The effects of MSC in Cancer**

The intrinsic ability of MSC to home to tumours highlights a potentially grey area in MSC therapy, the possibility that MSC might support tumour growth (Puglisi *et al.*, 2011). MSC may transform into tumours themselves or via their potent immunosuppressive abilities, suppress anti-tumour responses, possibly by increasing T regulatory cell numbers (Patel *et al.*, 2010). MSC effects in cancer are variable and there are contradictory reports in the existing literature. MSC associated transplants with colon cancer cells resulted in larger tumours developing in nude mice due to the increased angiogenesis and reduced tumour apoptosis caused by MSC. MSC can also promote the migration and metastases of tumour cells through soluble molecules (Shinagawa *et al.*, 2010). Studies have suggested that MSC can contribute to B cell lymphomas but research also shows that MSC can reduce terminal differentiation and proliferation of B cells after engraftment into the spleen (Asari *et al.*, 2009, Che *et al.*, 2012). In contrast to reported tumour promoting effects, MSC have also been described as protective against tumour development. Aziz *et al* have shown MSC were able to suppress tumours in a rat HCC model through down regulation of Wnt signalling of target genes related to anti-apoptosis, mitogenesis, cell proliferation, and cell cycle regulation (Abdel aziz *et al.*, 2011). Other reports also suggest MSC can prevent cancer or reduce it. Recent studies involving autologous MSC transplantation in liver failure patients caused by hepatitis B were assessed for long term and short term contributions to tumour development but none were

observed (Peng *et al.*, 2011). Secchiero *et al* have also suggested that MSC play an insignificant role and have a modest effect on survival of lymphomas (Secchiero *et al.*, 2010)

### **1.3.9 MSC contribution to fibrosis**

This thesis will investigate MSC recruitment to a very hostile and damaged environment during liver disease. This means MSC will encounter high levels of factors which may have an uncontrolled or unforeseen effect on MSC. Therefore an important question to address in this study is whether exogenously administered MSC can contribute to accelerated fibrosis in a liver environment. Forbes *et al* have previously identified that recruitment of other cells from the bone marrow occurs during liver fibrosis which take on a myofibroblast phenotype and contribute to scarring by depositing excessive levels of extracellular matrix in the injured liver (Forbes *et al.*, 2004). Here, cases of gender mismatch transplants in humans with liver cirrhosis showed that there were extrahepatic cells and more specifically, cells from the bone marrow contributing to the scarring population of myofibroblasts. Morphological studies and in-situ hybridisation techniques identified cells that were originally extrahepatic but had possibly differentiated to myofibroblasts. Further gender mismatch studies of cirrhotic livers suggested that perhaps these cells were from the bone marrow, they infiltrated the liver during fibrosis and had subsequently differentiated to a myofibroblast phenotype (di Bonzo *et al.*, 2008). The presence of bone marrow derived myofibroblast-like cells was clearly identified in this study, but data was lacking in respect to how, if at all, these cells contributed to fibrosis.

Subsequently the contribution of these bone marrow derived cells to fibrosis was investigated using gender mismatched studies in mouse models of chronic liver disease by Russo *et al*

(Russo *et al.*, 2006). Female mouse livers were injured in separate experiments by carbon tetrachloride and thioacetamide, which cause mass hepatocyte death, and these mice were then transplanted with bone marrow from healthy male mice. The study suggested that the level of liver fibrosis indicated by  $\alpha$ SMA, collagen deposition and transcriptional regulation was dependent on recruitment of bone marrow derived cells. Increased cell recruitment caused a corresponding increase in myofibroblasts in the liver and contributed to the deposition of scar tissue including collagen. To further show that bone marrow cell-dependent liver fibrosis played a significant part in scarring of liver tissue, transgenic male *Col1 $\alpha$ 1<sup>rr</sup>* bone marrow which expressed collagenase-resistant collagen was transplanted into female mice (Russo *et al.*, 2006). Upon injury these mice showed significantly more fibrotic tissue in their livers than in their control counterparts with wild type bone marrow transplants. The highly up-regulated fibrosis in the livers of mice with transgenic bone marrow suggests that the bone marrow derived cells make a significant contribution to the scar tissue in fibrotic livers. In the same livers the colocalisation of Y chromosome single cells and  $\alpha$ SMA corroborates this conclusion.

Thus, the bone marrow has been identified as significant contributor to fibrosis in a fibrotic organ. However the bone marrow is a mixture of both HSC and MSC. To develop an efficient cellular therapy or target it is important to determine what role each of these types of bone marrow cells is responsible for within a fibrotic organ. To this end, Russo *et al* transplanted female mice with male bone marrow mesenchymal stromal cells and female HSC and other females with female bone marrow stromal cells and male HSC and then induced liver injury in these mice with carbon tetrachloride. Through tracking with in-situ hybridisation of the Y chromosome Russo identified that female mice with male stromal cells had significantly more



Y chromosome-positive myofibroblasts in their fibrotic livers compared to their counterparts, suggesting bone marrow stromal cells are the preferentially recruited cells during liver fibrosis (Russo *et al.*, 2006). More recently, Sphingosine-1-Phosphate has been identified as a multi-functional mediator which may be involved in migration of MSC to liver, and TGF $\beta$ 1 has been identified as a mediator of MSC differentiation to myofibroblasts (Li *et al.*, 2009). On the contrary, Higayashima showed that such cells rarely took on a myofibroblast phenotype and contributed very little to collagen deposition in the liver in models of bile duct ligation (Higashiyama *et al.*, 2009).

Research into cells in the bone marrow suggests that hematopoietic stem cells could also contribute to the stromal cell compartment in culture (Bucala *et al.*, 1994, Ogawa *et al.*, 2006). A commonly overlooked contaminating cell which resembles MSC both in terms of marker expression and tri-lineage potential, but unlike MSC, promotes fibrosis and inflammation, is the fibrocyte. The isolation of MSC is still an unrefined method and as HSC derived cells can also be adherent, such cells could dampen down therapeutic effects (Ogawa *et al.*, 2006). Little is known of such cells and phenotyping these cells will allow us to identify these cells and prospectively exclude them from cultures. The last chapter in this thesis will consider mechanisms for isolation and culture of these cells.

### **1.3.10 Bone marrow derived stromal cells contributing to hepatic fibrosis: HSC derived fibrocytes**

This thesis will investigate the introduction of MSC to an inflammatory and potentially fibrotic environment in the liver. It is therefore essential that we administer a population of

cells which will not in any way contribute to the inflammation or fibrosis and will have a maximum beneficial effect on the liver. Although MSC have a robust profile of markers for their identification from humans and mice, mouse MSC have been shown to express CD34, and in some reports isolated populations of human MSC express CD34 but gradually lose expression in culture (Delorme *et al.*, 2006). The evidence discussed above suggests that cells responsible for laying down scar tissue during liver injury appear to be resident of bone marrow derived hepatic myofibroblasts which were shown to be derived from cells enriched for mesenchymal stromal cells (Russo *et al.*, 2006). However, in this study there were also some myofibroblast like cells that originated from cells enriched for HSC.

Both sets of evidence may reflect a contribution to the myofibroblast population from monocyte-derived cells of HSC origin known as fibrocytes. Fibrocytes can be found in tissue and in the circulation, they are derived from a hematopoietic lineage and express a combination of hematopoietic markers and mesenchymal markers at different stages of their maturation (Peng and Herzog, 2012). They are elongated, spindle shaped, cell culture plastic adherent cells found in healing wounds and fibrotic lesions (Peng and Herzog, 2012). Fibrocytes represent a relatively recently discovered cell, and although literature on fibrocytes grew rapidly when they were first identified, research on fibrocytes has equally rapidly diminished. Thus further research is needed to characterise these cells and to develop a standardised method of isolation. However it seems clear there is a definite presence of these cells in fibrotic tissue (Kisseleva *et al.*, 2006) and it is therefore important to identify how these cells may be involved in fibrosis.

We have investigated these cells in the current study and our reasons for phenotyping fibrocytes further is so that a marker can be determined which allows differentiation between fibrocytes and mesenchymal stem cells. Both cell types are plastic adherent, they have a similar morphological phenotype, surface antigen profile and tri-lineage differentiation potential (Peng and Herzog, 2012). The only reported difference between the two cell types is that fibrocytes contribute to inflammation and fibrosis whereas MSC have anti-inflammatory and anti-fibrotic properties. There are even similarities in the migratory properties of the two cell types. Fibrocytes pose a problem in that without prospective identification isolation and depletion of these cells from MSC isolation of bone marrow, these cells may be competing with MSC for oxygen and space and not allowing conditions for MSC isolation to be as optimal as perhaps they could be.

#### **1.3.11 The mechanism of MSC engraftment**

There has been much experimental work investigating direct transplantation of MSC into injured liver. However as a valid therapy it is likely that most cells will be delivered to target organs using a less invasive method of delivery via the circulation. Thus it is necessary to investigate the mechanism of MSC recruitment to the injured liver from circulation. There are two potential hypotheses for this mechanism (Figure 1.3). The first is an active mechanism similar to the leukocyte recruitment cascade and the second, a passive mechanism where the MSC due to their large size get wedged in the small sinusoids within the liver (Karp and Leng Teo, 2009). Due to their vast variations in size it is likely that MSC recruitment is a combination of these two hypotheses, where the MSC are recruited either actively or by getting stuck and then they transmigrate into the liver where they are recruited to specific

areas within the liver. At present MSC recruitment to the tissue is loosely based on the model of leukocyte migration from peripheral blood circulation to tissue (Ponte *et al.*, 2007). Initial contact between the cells and tissue is mediated by adhesion molecules like Selectins and  $\beta$ 1 integrins causing a rolling motion of weakly adherent leukocytes which may be regulated by chemokines (Chen *et al.*, 2010). Chemokines (chemotactic cytokines) are a large superfamily of small (8-10kda) glycoproteins involved in many biological processes including leukocyte trafficking and MSC trafficking. Chemokines on endothelial cells trigger integrin activation and cause arrest of the leukocytes which is followed by transendothelial migration of the leukocyte into the tissue (Ley *et al.*, 2007). Evidence suggests this transendothelial migration is mediated by molecules including PECAM-1, CD99, junction adhesion molecules and ICAM-1 (Ley *et al.*, 2007). Once inside the tissue the cells migrate along localised chemokine gradients, and finally adhere to target cells or extracellular matrix (Ley *et al.*, 2007).

It seems that leukocytes use molecules such as L-Selectin and  $\alpha$ 4 integrins amongst others to become captured upon endothelial layers before transmigration into tissue (Ley *et al.*, 2007). Interestingly MSC do not use L-Selectin, suggesting that although the mechanism for migration of the two different cells may be similar, different adhesion molecules and chemokines are involved. It is likely that MSC recruitment into tissue will involve processes of arrest in tissue vasculature followed by transmigration across the endothelium. Based on these processes, there are potentially two important mechanisms for MSC recruitment. Firstly the cell may become lodged in narrow tissue vasculature, alter the blood flow through the capillary and as a result of a chemokine gradient in the inflammatory part of the tissue or the firm attachment of adhesion molecules, the cell may transmigrate. The second potential pathway is more akin to the leukocyte mechanism where the MSC may tether and roll at a

part of a tissue where a chemokine gradient exists due to injury in that area. The cell without changing the blood flow would then quickly flatten and spread onto the endothelium and probably transmigrate. It is still unclear what may occur during the lodged MSC transmigration but the second method could involve P-Selectin, VLA-4 and VCAM-1 during rolling, ICAM-1, VLA-4 and VCAM-1 during firm adhesion and VLA-4, VCAM-1, MMP and TIMP during transmigration (Karp and Leng Teo, 2009). Ruster *et al* have shown with knockout mice that P-Selectin is involved in mediating the rolling of human MSC along endothelium via a novel carbohydrate ligand expressed by the MSC (Ruster *et al.*, 2006). Various other adhesion molecules are expressed by MSC including VCAM-1, ICAM-1, ICAM-3, ALCAM and endoglin/ CD105, as well as many integrin molecules including  $\alpha$  1, 2, 3, 4, 5, v;  $\beta$ 1, 3 and 4 (Karp and Leng Teo, 2009). In particular  $\alpha$ 4 $\beta$ 1 integrin has been shown to be involved in firm adhesion of MSC to endothelial cells under shear flow conditions via VCAM-1 (Karp and Leng Teo, 2009). We have previously described the role of  $\beta$ 1 integrin and CD44 in MSC engraftment in injured liver but the role of CCR within this mechanism has not been elucidated (Aldridge *et al.*, 2012).

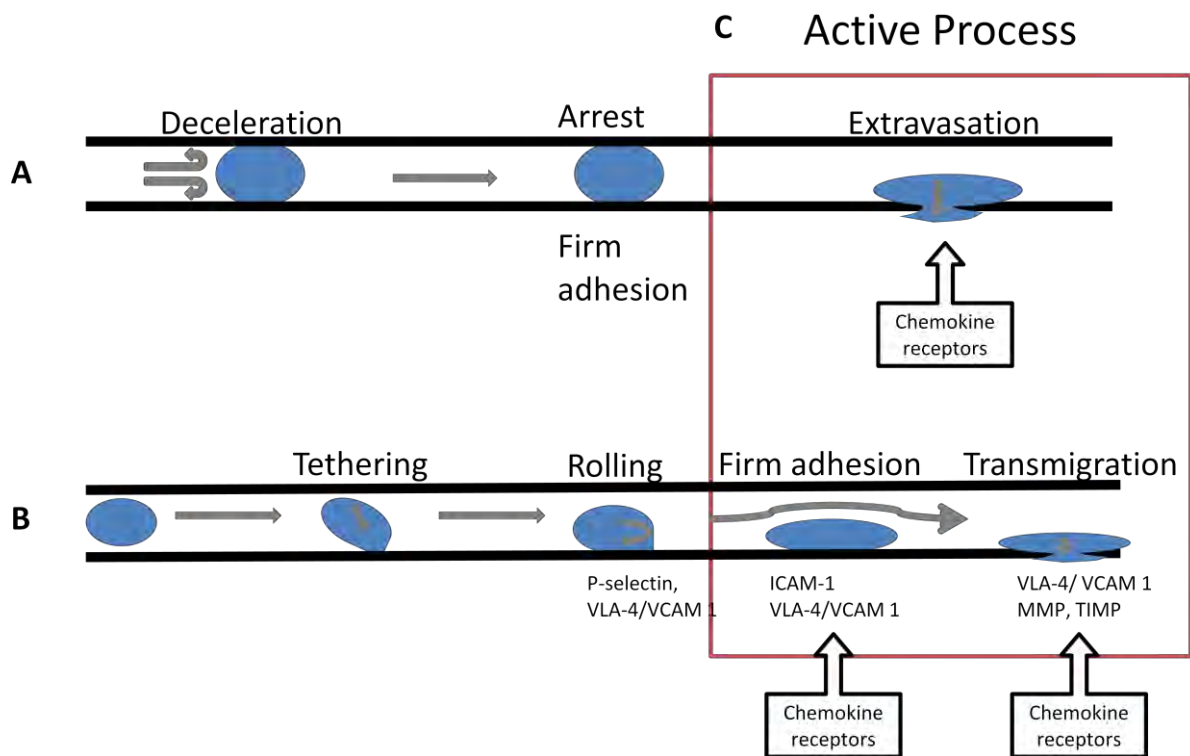


**Figure 1.3: Proposed mechanisms of MSC engraftment into the liver.**

There are two potential hypotheses for the mechanism of engraftment. A passive mechanism where the MSC due to their large size get wedged in the small sinusoids within the liver (A) or an active mechanism similar to the leukocyte recruitment cascade (B). In the active process rolling occurs due to the actions of P Selectin, followed by firm adhesion through ICAM-1 and finally by MMPs and TIMPs. VLA-4 and VCAM-1 seem to interact throughout this process. Due to their vast variations in size, it is likely that initial stages of MSC recruitment are a combination of these two hypotheses, where the MSC are recruited either, actively or by getting stuck. However later stages of recruitment involving transendothelial recruitment must occur through a shared active mechanism (C). CCR may play a role in multiple stages of this recruitment which have not yet been elucidated.

To try and understand the role of CCR in the MSC recruitment mechanism to the liver, we can look to the well characterised recruitment of the hematopoietic stem cell. A larger body of research into HSC adhesion and recruitment has suggested the CXCR4-SDF1 $\alpha$  /CXCL12

(which is up-regulated in tissue injury and inflammation) CCR-ligand interaction is responsible for HSC migration to injured tissue (Fox *et al.*, 2007). As CXCR4 is also a well established migratory chemokine in leukocytes, it was hypothesised that MSC may also use the CXCR4-SDF1 $\alpha$  /CXCL12 axis to migrate and engraft to injured tissue (Wynn *et al.*, 2004). This was investigated by Ip *et al* using blocking assays with murine MSC in mice with heart injury. However their hypothesis investigated whether CXCR4 was responsible for cell engraftment into tissue and unsurprisingly they found the adhesion molecule  $\beta$ 1 integrin and not CXCR4 was responsible for engraftment. The findings of Ip *et al* suggest  $\beta$ 1 integrin may be important for the adhesion mechanism but do not exclude CXCR4 from playing some part in the entire mechanism of homing, perhaps as part of the rolling mechanism prior to adhesion, or as a localisation signal once the cell has entered the tissue (Ip *et al.*, 2007). Interestingly, in culture, MSC show little or no expression of CXCR4 and some groups suggest that only a subset of cells demonstrate extracellular expression of CXCR4 (Fox *et al.*, 2007, Wynn *et al.*, 2004). However this may be due to a downregulation of adhesion receptors and CCR when MSC are cultured *in-vitro*. Receptor profiles are further distorted on these cells when cells are trypsinised and detached from their culture surfaces. Cell detachment mediums, like TrypLE may be responsible for cleaving some receptors off the cells and resting the cells in suspension before using them has been shown to cause the cells to regain some of their original receptor expression (Chamberlain *et al.*, 2007, Chamberlain *et al.*, 2008).

It seems that due to this changeable extracellular phenotype, reported MSC CCR profiles tend to vary between different groups and even between isolations when the procedure is kept the same. Due to the complexity of the MSC there seems to be an ever increasing amount of data

emerging about their migration mechanisms. This suggests that small changes in an environment and particularly the systemic and local inflammatory state of the environment can alter the chemokine profiles of MSC and may influence cell mobilisation and their subsequent homing to injured tissues.



### **1.3.11.1 Chemokine Receptors (CCR)**

This thesis will investigate the role of CCR in engraftment of MSC and so it is important to review the way in which these CCR function. As we are interested in MSC recruitment I will review the major CCR likely to be of importance. CCR (Table 2.2) are membrane bound, 7 transmembrane domain receptors coupled to G-proteins. Generally CCR measure approximately 350 amino acids in length and are very similar to each other in their primary sequences. They have a short extracellular acidic N terminus and may be sulphated on tyrosine residues and contain N linked glycosylation sites. Receptors have an intracellular C terminus containing serine and threonine residues that act as phosphorylation sites for receptor regulation. On their 7  $\alpha$  helical transmembrane domains, they have 3 extracellular and 3 intracellular connecting loops composed of hydrophilic amino acids and these domains are positioned perpendicularly to the plasma membrane. A disulphide bond links highly conserved cysteines in extracellular groups 1 and 2. G proteins are coupled through the C terminus segment and possibly through the third intracellular loop (Murdoch and Finn, 2000). There are a number of CCR, but two of the families of CCR we will focus on in this study are listed in Table 1.2.

**Table 1.2: Chemokine receptors (CCR)**

Group	Receptor	Ligand
CC	CCR1	MIP1 $\alpha$ /CCL3, Rantes/CCL5 MCP3/CCL7, MCP2/CCL8, MCP4/CCL13, HCC1/MIP1 $\delta$ /CCL15, HCC4/CCL16, MPIF/CCL23
	CCR2	MCP1/CCL2, MCP3/CCL7, MCP2/CCL8, MCP4/CCL13
	CCR3	Rantes/CCL5, MCP3/CCL7, MCP2/CCL8, Eotaxin/CCL11, MCP4/CCL13, HCC1/MIP1 $\delta$ /CCL15, Eotaxin2/CCL24, Eotaxin3/CCL26
	CCR4	Rantes/CCL5, TARC/CCL17, MDC/CCL22
	CCR5	MIP1 $\alpha$ /CCL3, MIP1 $\beta$ /CCL4, Rantes/CCL5, MCP2/CCL8
	CCR6	MIP3 $\alpha$ /CCL20
	CCR7	6Ckine/CCL21
	CCR8	I309/CCL1, TARC/CCL17
	CCR9	Teck/CCL25
	CCR10	CTACK/CCL27, CCL28
CXCR	CXCR1	IL8/CXCL8
	CXCR2	GRO $\alpha$ /CXCL1, GRO $\alpha$ / $\beta$ /CXCL2 GRO $\gamma$ /CXCL3, ENA78/CXCL5, GCP2/CXCL6, NAP2/CXCL7, IL8/CXCL8
	CXCR3	MIG/CXCL9, IP10/CXCL10, ITAC/CXCL11, PF4/CXCL4
	CXCR4	SDF1 $\alpha$ /CXCL12
	CXCR5	BCA1/CXCL13
	CXCR6	CXCL16
	CXCR7	SDF1 $\alpha$ /CXCL12

Intracellular signalling via CCR (Figure 1.4) with the exception of CXCR7 depends on coupling to heterotrimeric G proteins. CXCR7 is a scavenger receptor so signals differently to other receptors in its group. During ligand binding CCR bind G proteins and activate them. G

proteins are activated when their subunit which is usually bound to guanosine diphosphate (GDP) is exchanged for guanosine triphosphate (GTP), which causes the G protein to dissociate into  $\alpha$  and  $\beta$  subunits.  $G\beta$  subunits are able to activate the membrane associated enzyme phospholipase C $\beta$ 2 (PLC<sup>2</sup>) which in turn cleaves phosphatidylinositol 4, 5-bisphosphate (PIP<sub>2</sub>) to form the intracellular second messengers phosphatidylinositol 1, 4, 5-triphosphate (IP<sub>3</sub>) and diacyl-glycerol (DAG). IP<sub>3</sub> mobilises calcium from intracellular stores but DAG acts in conjunction with calcium to activate various isoforms of protein kinase C (PKC). PKC and other calcium sensitive protein kinase activation catalyse protein phosphorylation, thus activating a series of co-ordinated signalling events leading to cellular responses. G coupling can lead to activation of several downstream effectors including the Rock and Rho, phospholipase A<sub>2</sub>, phosphatidylinositol-3-kinase, tyrosine kinases and the MAP kinase pathway (Murdoch and Finn, 2000). After stimulation, CCR become partially or totally desensitized to repeat stimulation with same or other agonists. This process involves serine and threonine residue phosphorylation in the C tail of the receptor by G protein coupled receptor kinases and receptor sequestration by internalisation. This may be a critical process for the receptor to sense chemokine gradients (Murdoch and Finn, 2000).

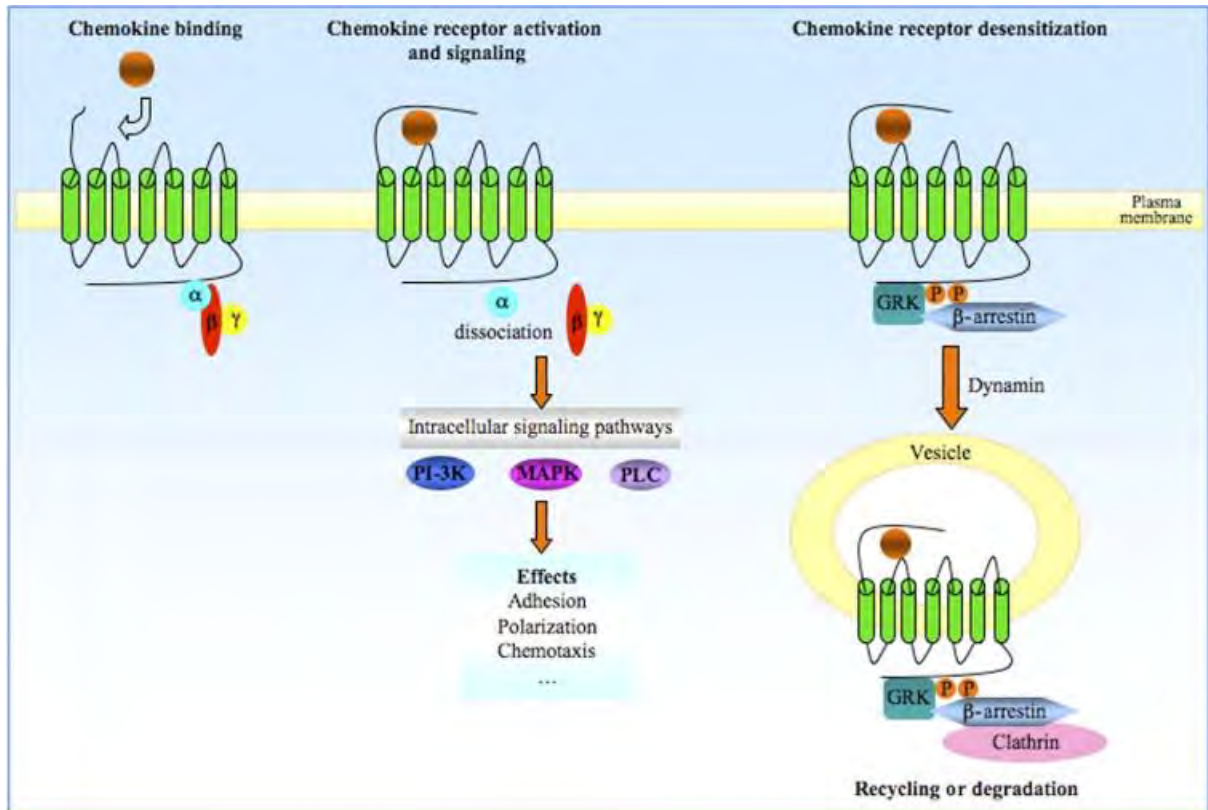


**Figure 1.4: CCR signalling.**

CCR recognise and bind ligand, to initiate signalling with G protein activation, characterised by dissociation of  $\alpha$  and  $\beta\gamma$  unit heterotrimers. Down-stream effectors include MAPK, PI-3K and PLC. Desensitisation starts with C terminal CCR tail phosphorylation, increasing the affinity of  $\beta$  arrestin proteins for the receptor and prevents further interaction between CCR and G proteins. Clathrin mediated internalisation of the ligated CCR into vesicles is promoted by G protein coupled receptor kinases (GRK) -  $\beta$  arrestin complex and requires GTPase activity of dynamin. The internalised receptor is then degraded or recycled. Illustration reproduced from (Savarin-Vuillat and Ransohoff, 2007).

CXCR7 acts as a decoy receptor responsible for clearing chemokines from an inflammatory environment preventing or resolving inflammation. It therefore controls the availability of chemokines for leukocyte trafficking via CXCR4 and thus regulates innate or adaptive immune responses acting as a guidance cue. Unlike other CC or CXC family receptors, CXCR7 is classified as a 7TMD-receptor and not as a GPCR because G protein coupling

cannot be demonstrated after ligand activation (Thelen and Thelen, 2008). Recent research demonstrates that the SDF-1 $\alpha$ /CXCL12-CXCR7 signalling pathway regulates genes distinct from the SDF-1 $\alpha$ /CXCL12-CXCR4 pathway, involved in cell cycle control, amino acid metabolism and ligase activity (Yoshida *et al.*, 2009).

### **1.3.11.2 Integrins**

For the purposes of this study which is mainly based on CCR function in MSC engraftment it is important to also consider the role of integrins, which have been shown to play a major role in MSC engraftment to the injured liver (Aldridge *et al.*, 2012). I, therefore describe the various groups of integrins and methods by which integrins are known to function. Integrins are one of the major families of cell adhesion and matrix binding receptors. There are 24  $\alpha/\beta$  heterodimers which anchor cells to ECM, plasma proteins or counter-receptors on other cells (Humphries *et al.*, 2006). In vertebrates integrins can be separated into four categories listed in Table 1.3.

**Table 1.3: Integrins subfamily**

Group	Integrins	Bind
RGD binding integrins	$\alpha 5\beta 1$ , $\alpha 8\beta 1$ , $\alpha 11\beta 3$ , $\alpha V\beta 1$ , $\alpha V\beta 5$ , $\alpha V\beta 6$ , $\alpha V\beta 8$	ECM glycoproteins, fibronectin, vitronectin, fibrinogen
Non- $\alpha$ A-domain-containing laminin-binding integrins	$\alpha 3\beta 1$ , $\alpha 6\beta 4$ , $\alpha 6\beta 1$ , $\alpha 7\beta 1$	Laminins
LDV-binding integrins SVVYGLR*	$\alpha 4\beta 1$ , $\alpha 4\beta 7$ , $\alpha 9\beta 1$ , $\alpha E\beta 7$	Fibronectin, VCAM-1, MAdCAM-1, Osteopontin*
A-domain $\beta 1$ integrins (subgroup)	$\alpha 1\beta 1$ , $\alpha 2\beta 1$ , $\alpha 10\beta 1$ , $\alpha 11\beta 1$ ( $\alpha D\beta 2$ , $\alpha E\beta 7$ , $\alpha L\beta 2$ , $\alpha M\beta 2$ , $\alpha X\beta 2$ )	Laminin, collagen (Leukocytes, collagen)

The first integrin group recognises the arginine-glycine-aspartic acid motif which binds at an interface between  $\alpha$  and  $\beta$  subunits. The arginine residue binds to a cleft in a  $\beta$  propeller module in the  $\alpha$  subunit and the D residue coordinates a cation bound in the von Willibrand factor A-domain in the  $\beta$  subunit.  $\beta 3$  integrins bind to a large number of ECM and soluble vascular ligands. Ligands are shared by these integrins but the rank order of ligand affinity varies reflecting the precision fit of RGD conformation within the specific  $\alpha$ - $\beta$  active site pocket (Humphries *et al.*, 2006, Ivaska and Heino, 2011). The second group is widespread in the animal kingdom.  $\beta 4$  integrin is structurally unique among all integrins due to a large intracellular domain with several phosphorylation sites serving as a docking site for many signalling proteins. The LDV connecting ligand in fibronectin lies in its Type III connecting segment (Humphries *et al.*, 2006, Ivaska and Heino, 2011). The third group includes the  $\beta 2$  integrin family subgroup, which has a different mode of ligand binding. The major interaction takes place through an inserted A-domain in  $\alpha$  subunit.  $\beta 1/\beta 7$  ligands employ an aspartate residue for cation coordination whereas  $\beta 2$  integrins use glutamate (Humphries *et al.*, 2006, Ivaska and Heino, 2011). The fourth group of integrins, have proteins which are structurally different from all other subunits. They contain an extra  $\alpha$  inserted domain similar to von

Willebrand factor A and these are found only in chordates. A crystal structure of a complex between the  $\alpha 2$  A-domain and a triple-helical collagenous peptide has revealed the structural basis of the interaction, a critical glutamate within a collagenous GFOGER motif providing the key cation-coordinating residue (Humphries *et al.*, 2006, Ivaska and Heino, 2011).

The ECM regulates cell proliferation, survival, differentiation and metabolism and integrins are the main mediators of ECM generated cellular signals. As integrins do not possess any enzyme activity, signalling is dependent on binding of short cytoplasmic integrin domains to intracellular proteins.  $\beta$  integrins interact with lots of cytoskeletal and signalling proteins whereas  $\alpha$  subunits play an important role in heterodimer specific signalling. Transmission of signals through the plasma membrane occurs through ligand induced conformational changes in  $\beta$  subunits. Receptors activate after separation of  $\alpha$  and  $\beta$  subunits (Humphries *et al.*, 2006, Ivaska and Heino, 2011). Integrins also mediate mechanical stress related signals. Mechanical forces stretch integrin associated intracellular proteins to unveil novel cryptic binding sites and in this manner create new protein-protein interactions. High resolution microscopy allows visualisation of integrin generated adhesion sites (Figure 1.5) (Ivaska and Heino, 2011).

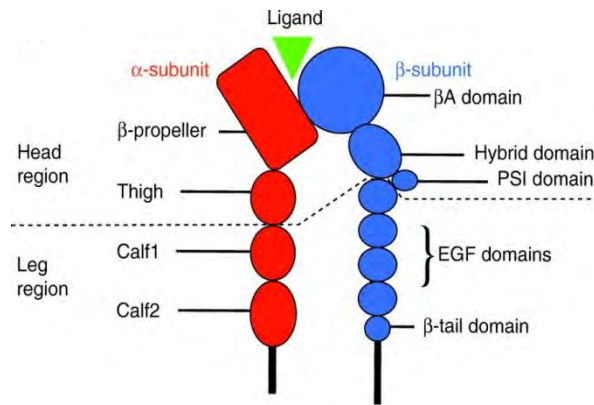


**Figure 1.5: Schematic diagram of typical Integrin structure**

(A) Schematic diagram of integrin structure. The overall structure is of a head region [propeller and thigh domains of  $\alpha$  subunit and the  $\beta$ A (also known as  $\beta$ 1), hybrid and PSI domains of the  $\beta$  subunit] supported on calf1 and calf2 domains in the  $\alpha$  subunit, EGF repeats and  $\beta$  tail domain in the  $\beta$  subunit. The binding of ligands takes place at an interface between the propeller domain and the  $\beta$ A domain. Image reproduced from (Askari *et al.*, 2009).

## 1.4 Hypotheses and Aims

To date, major limitations in MSC therapy which lead to low efficacy are the inefficient engraftment of MSC after infusion or the crude isolation methods of MSC due to an apparent lack of a marker for prospective isolation. As part of this project I attempt to address both these aspects of limited engraftment and impure MSC populations obtained during isolation.

During liver disease there is a major influx of inflammatory immune cells from circulation. This is largely mediated by increased cytokine levels in the liver which are able to induce recruitment of circulating cells through interaction with corresponding surface ligands such as chemokine receptors. Thus I hypothesise that *ex vivo* stimulation of MSC with these cytokines



may increase recruitment of MSC to diseased liver environments through chemokine receptor upregulation.

Due to the lack of specific MSC marker allowing for the prospective isolation of MSC it is necessary to be able to refine or purify the MSC populations that are isolated in order to get maximum and reproducible efficacy. Previously, combinations of markers have been used to try and isolate MSC but with limited success. Fibrocytes are a bone marrow derived population of cells which could remain undetected in MSC isolations and reduce the therapeutic potential of the MSC. There is no known marker which is retained by fibrocytes in culture that can allow it to be identified from MSC isolations. Fibrocytes can be isolated from the blood as adherent CD45<sup>+</sup> cells which express collagen-1 in long term culture and eventually lose their CD45 expression. However in the literature, phenotypic data regarding fibrocytes is limited and contradictory. Thus I hypothesise that if fibrocytes can be isolated from blood and kept in long term culture, they may express markers which could allow them to be distinguished and depleted from MSC isolations to yield refined and purer populations of therapeutic MSC.

This project focuses on three main areas of MSC biology. The mechanism for MSC recruitment to injured liver is likely to closely resemble the leukocyte recruitment cascade where CCR play an integral role. However studies investigating CCR expression on MSC report an inconsistent repertoire of receptors. A reason for this may be the method by which MSC are detached from tissue culture plastic. Our first goal focuses on the effects of MSC detachment methods on viability, tri-lineage differentiation potential, and immunomodulatory capabilities of the MSC and CCR expression.

Studies have shown that cytokine stimulation of MSC can alter their CCR expression and as a result, their migratory and adhesive potential. However treatment of MSC with cytokines has also been reported to differentiate MSC to a progenitor phenotype and alter their anti-inflammatory properties. Therefore our second goal investigates the effect of prevalent cytokines in liver injury on MSC CCR expression and subsequent engraftment in animal models of liver injury.

The ultimate goal for research into MSC therapy is for it to be used as a viable clinical intervention. However based on recent research some reports have raised concerns about the safety of using MSC clinically. One of the concerns is that MSC could contribute to fibrosis and this could be the result of contaminating cells called fibrocytes. In the final chapter we have attempted to isolate and phenotype fibrocytes using existing and modified techniques with a view to identify and deplete cells which are responsible for pro-fibrotic effects, from future studies where we may attempt to isolate MSC from human bone marrow.

The specific aims of this project were to:

- (i) Assess the effects of MSC detachment methods on viability, tri-lineage differentiation potential, immunomodulation and CCR expression.
- (ii) Test the effects of prevalent cytokines in liver injury on MSC CCR expression and subsequent engraftment in animal models of liver injury and immunomodulatory properties.

- (iii) Isolate and phenotype fibrocytes using existing and modified techniques with a view to identify and deplete cells responsible for pro-fibrotic effects, from future studies where we may attempt to isolate MSC from human bone marrow.

## **CHAPTER 2: MATERIALS AND METHODS**

## **2.1 Human Tissue**

Human liver tissue was obtained from explanted diseased livers including Alcoholic liver disease (ALD), Autoimmune hepatitis (AIH), Primary Biliary Cirrhosis (PBC), Primary Sclerosing Cholangitis (PSC), Non-alcoholic steatohepatitis (NASH) patients, after transplantation. Normal tissue was also taken, which was surplus to transplantation requirements, or from tumour margins collected during resection surgery from patients at the Queen Elizabeth Hospital, Birmingham, UK. Peripheral blood was obtained from patients undergoing routine venesection for haemochromatosis at Queen Elizabeth Hospital, Birmingham, UK. Serum was also collected from normal patients and patients admitted to the Queen Elizabeth Hospital Liver Unit with Alcohol-induced liver injury. All human tissue and blood samples were collected with local research ethics committee approval and written, informed patient consent.

## **2.2 Isolation of human hepatic sinusoidal endothelial cells (HSEC), biliary epithelial cells (BEC) and hepatic myofibroblasts (MF) and peripheral blood mononuclear cells (PBMC).**

Cells were isolated from explanted diseased human livers using standard protocols (Crosby *et al.*, 2009). Liver tissue was finely chopped and digested with collagenase type 1A (0.4mg/ml, Sigma), filtered through a fine mesh into a beaker, washed several times with PBS and separated on a 77% and 33% Percoll (GE Healthcare) gradient to remove parenchymal cells. The band of cells at the interface was removed, and washed several times with PBS. Anti-HEA 125 antibody (5µg/ml Progen Biotec) bound to magnetic goat anti-mouse Dynabeads

(Invitrogen) was used to positively select BEC. The remaining unselected cells were exposed to anti CD31 antibody (10 $\mu$ g/ml, Invitrogen) bound to magnetic goat anti-mouse Dynabeads (Invitrogen) to collect HSEC. HSEC and BEC were cultured in appropriate media (Table 2.1) on rat tail collagen (Sigma) coated flasks.

Myofibroblasts (MF) were also isolated from human livers for adhesion assays and as positive control cells for alpha smooth muscle actin ( $\alpha$ SMA) and collagen-1 expression. Following positive selection of BEC and HSEC from tissue digests, CD45<sup>+</sup> cells in the remainder were selected using anti CD45 antibody (R and D Systems, 10 $\mu$ g/ml) and Dynabeads (Invitrogen) as before. Selected cells were plated in fibroblast media or on occasion RPMI-1640 containing 10% FCS, 1% PSG, 1% NEAA and 1% Sodium Pyruvate (all Invitrogen). Fibrocytes were isolated from whole blood or buffy coats layered onto a density separation gradient (Lympholyte, Cedarlane Laboratories or Ficoll-Paque, GE healthcare) and centrifuged for 30 minutes at 900xg. The mononuclear cell layer was removed, washed with buffer (PBS or HBSS, both Sigma) and the pellet was re-suspended in medium (DMEM containing 20% Heat Inactivated FBS, and 1% PSG (all Invitrogen)). Cells were then plated into 'Cell-Bind' (Corning, Appleton Woods Ltd), or conventional 24 well plates or culture flasks, with or without a fibronectin (10 $\mu$ g/ml in PBS, Sigma) coating.

To ensure removal of contaminating T cells, B cells and monocytes from fibrocyte cultures, isolated PBMC were cultured for 5 days without washing and then media was changed regularly for a further 14 days. Cells were then removed from plates using Accutase (Innovative Cell Technologies) and negatively selected by removal of CD2<sup>+</sup>, CD19<sup>+</sup> and

CD14<sup>+</sup> contaminating cells using CD2 (4x10<sup>8</sup>beads/ml), CD19 (4x10<sup>8</sup>beads/ml) and CD14 (4x10<sup>8</sup>beads/ml) conjugated Dynabeads (all Invitrogen).

On occasion the effects of different cell detachment and isolation methods on fibrocyte cultures were assessed. Again total PBMC were isolated from blood and suspended in a known volume of media. Cells isolated using Lympholyte or Ficoll-Paque were counted to compare cell yields using a haematocytometer as described below (section 3.3).

**Table 2.1: Cells used for this study and details of culture media used for propagation**

Cells				
Name	Species: Tissue	Split ration	Growth media and Source	Cell origin
MSC	Human: Bone marrow	1:3	MSC Growth Medium (MSCGM™) (Lonza)	Primary mesenchymal stem cells (MSC) isolated from human bone marrow, purchased from Lonza.
HSEC	Human: Liver	1:2	Human Endothelial Basal Growth Medium (Invitrogen), 1% Glutamine, Penicillin, Streptomycin (PSG, Invitrogen), 10% Heat Inactivated Human Serum, 10ng/ml Hepatocyte Growth Factor (HGF), 10ng/ml Vascular Endothelial Growth Factor (VEGF, PeproTech).	Human sinusoidal endothelial cells (HSEC), isolated as primary cultures from human liver tissue.
BEC	Human: Liver	1:2	DMEM (Invitrogen), 10% Heat-Inactivated Human Serum, 2mM Glutamine, 10ng/ml HGF (PeproTech), 10ng/ml EGF (PeproTech), 2mg/ml Hydrocortisone,	Biliary epithelial cells (BEC), isolated as primary cultures from human liver tissue

			10ng/ml Cholera toxin (Sigma Aldrich), 2nM Tri-iodo-thyronine (Sigma Aldrich) 0.124U/ml Insulin 100IU/ml Penicillin and 100mg/ml Streptomycin (Invitrogen).	
MF	Human: Liver	1:2	Dulbeccos modified Eagle Medium (DMEM, Invitrogen), 10% Heat Inactivated Foetal Calf Serum (FCS, Invitrogen), 1% PSG	Liver myofibroblasts (MF), isolated as primary cultures from human liver tissue
Fibroblasts	Human: Synovial fluid	1:2	RPMI-1640 (Invitrogen), 20% FCS, 1% PSG, 1% Non Essential Amino Acids (NEAA; Invitrogen), 1% Pyruvate (NEAA; Invitrogen)	Primary synovial fibroblasts were a gift from Professor Chris Buckley and Dr Andy Filer, of The Rheumatology group, Immunity and infection. University of Birmingham.
Lymphocytes	Human: Peripheral blood	-----	RPMI-1640, 10% FCS, 1% PSG	Lymphocytes, isolated as primary cultures from human peripheral blood
PBMC	Human: Peripheral blood	-----	RPMI-1640, 10% FCS, 1% PSG	Peripheral blood mononuclear cells (PBMC), isolated as primary cultures from human peripheral blood

### 2.3 Cell culture and viability measurement

All primary cells used in this study are detailed in Table 2.1 with details of the media in which they were propagated. Cells were maintained in sterile tissue culture flasks or well plates as required, and grown at 37°C in 5% CO<sub>2</sub>. All tissue culture was carried out in a class II microflow safety cabinet using aseptic technique and cell growth was monitored using an inverted phase contrast microscope.



To passage cells, media was removed and cells were washed with PBS (Phosphate Buffered Saline, Oxoid UK). In general, adherent cells were passaged using TrypLE (Invitrogen), followed by incubation at 37°C with gentle agitation. The enzymatic activity of the TrypLE was neutralised using spent media and cells were collected by centrifugation at 550xg for 5 minutes. For cultures of non-adherent cells in suspension which did not require detachment, cells were centrifuged at 550xg for 5 minutes. Cell pellets were then re-suspended in new media and seeded into new culture flasks.

In contrast, several detachment methods were used for cultures of multiple human MSC donors. MSC were purchased from a commercial source called Lonza, designated P1 upon arrival from and were grown through multiple passages and used at P4. All experiments were repeated with multiple MSC isolates/ donors. MSC were detached from culture flasks using enzymatic and non-enzymatic methods. For enzymatic detachment MSC were incubated at 37°C with either TrypLE (Invitrogen) or Accutase (ebiosciences) for 5 minutes and gently agitated until cells detached, at which point enzyme activity was neutralised with MSCGM™. Non-enzymatic methods included incubation of cells with Cell Dissociation Buffer (CDB, Sigma) or EDTA (Sigma) at 37°C in a CO<sub>2</sub> incubator for 5 minutes with gentle agitation until they detached. MSC were also detached by gentle scraping with cell scrapers (BD Biosciences).

For long-term storage, cells were cryopreserved in liquid nitrogen. Briefly cells were detached, pelleted and re-suspended in freezing media (FCS 5% dimethylsulfoxide (DMSO; Sigma)). 1ml aliquots of cells were placed in cryovials at -80°C in a Mr Frosty™ freezing

container (Wessington Cryogenics) to permit gradual cooling to minimise cell damage. After 24 hours, cryovials were transferred to liquid nitrogen for long term storage.

The viability of cells was measured using several methodologies. Firstly, following detachment, cells were diluted 1:5 in Trypan blue (Sigma) and 5µl was added to a haematocytometer. Viable (unstained) cells were counted and total cell number was calculated by multiplying viable cell counts by the dilution factor (5) and by  $10^4$  to yield total cell count (cells/ml). Alternatively viability of MSC was also determined cytometrically. For details of labelling protocols see section 2.6 below. Here, after detachment MSC were incubated with an APC labelled live dead cell marker (Invitrogen, 1ul per  $1 \times 10^6$  cells/ml, according to manufacturers instructions) and analysed using a Dako Cyan ADP flow cytometer and Summit version 4.3 software. Live and dead MSC were identified by two characteristic peaks on an APC histogram. The APC low peak was characteristic of a viable cell population and the APC high peak of non viable cells.

Ability of detached MSC to reattach to plastic was also used to assess their functional viability. Here MSC were washed with PBS alone or PBS supplemented with PBS 1% FCS and centrifuged for 5 minutes at a speed of 900xg or 500xg, before re-suspension in MSCGM<sup>TM</sup> and re-plating on tissue culture plastic. Representative phase contrast microscopic images of MSC were captured at 1, 3 and 5 days after re-plating. In addition MTT (3-(4, 5-dimethylthiazol-2-yl)-2, 5-diphenyl-2H-tetrazolium bromide, Sigma) was used to assess function of re-plated cells. MSC were incubated with 0.4mg/ml of MTT for 1 hour at 37°C before washing with PBS. Incorporated formazan salts were solubilised with 600µl DMSO for 5 minutes with agitation. Supernatants were added to 96 well plates in triplicate and

absorbance values were determined at 570nm. Background absorbance signals from DMSO alone were subtracted from test values.

## **2.4 Attachment of cells onto microscope slides using Cytospin**

Suspensions of lymphocytes, myofibroblasts or synovial fibroblasts were washed in PBS and re-suspended in PBS 0.1% BSA to a concentration  $1 \times 10^6$  cells/ml. The total cell number was adjusted to yield  $1.5 \times 10^5$  cells per slide in 150  $\mu$ l volume and then aliquots were cytopun (Shandon Cytospin) for 5 minutes at 2300xg onto poly-l-lysine (10%, Sigma) coated slides. Slides were then air dried, fixed with acetone for 5 minutes, wrapped in foil and stored at -20°C until used in staining experiments

## **2.5 Immunohistochemistry**

Immunohistochemical analysis was used to quantify receptor expression within human liver sections and cytopins or wells of cultured cells. Tissue section slides and cytopin cell slides were acetone fixed for 5 minutes, air dried, wrapped in foil and stored at -20°C until needed at which time they were thawed for 30 minutes at room temperature. Cells grown in well plates were fixed with methanol for 5 minutes, washed with PBS and then stored in PBS at 4°C before staining was carried out in wells. A reservoir was created around tissue sections using a wax pen (The Binding Site) and subsequent staining was carried out in a humidified chamber.

Sections were incubated with H<sub>2</sub>O<sub>2</sub> (Sigma 0.3% in methanol (VWR)) for 30 minutes at room temperature on a rocking platform to block non specific endogenous peroxidase activity. Following a wash with PBS 0.1% Tween 20, Casein (Vector) 10% in goat serum (Sigma) was used to block the specimen for 30 minutes at room temperature on a rocking platform. If a biotinylated primary antibody was to be used with streptavidin secondary antibodies, an Avidin/Biotin blocking kit (Vectorlabs) was used to reduce any background staining. The specimen was incubated in Avidin D solution for 15 minutes at room temperature and with Biotin solution for a further 15 minutes, and rinsed briefly before the primary antibody was added.

Pre-determined optimal concentrations of primary antibody (Table 2.2) were diluted in PBS and incubated on sections at room temperature on a rocker for 1 hour. Sections were washed three times with PBS 0.1% Tween 20 and then HRP-conjugated secondary antibody was diluted to the working concentration (Table 2.2) in PBS and added to the specimens for 1 hour. Sections were washed as before and incubated with DAB substrate (DAB reagent and substrate, ABD serotec) for 2 to 5 minutes and then washed with tap water. Similar protocols were used for cytopins of cultured cells. Finally, sections or cells were counterstained with Mayer's Haematoxylin (VWR) for 15-30 seconds and washed under running tap water to "blue". Sections were dehydrated through graded alcohol (IMS gradient 50%, 70%, and 100% for 3 minutes) and incubated twice for 2 minutes in Clearene (Leica Microsystems) before mounting with a coverslip (Leica Microsystems Surgipath, Premier Coverglass) using DPX mountant (Leica Biosystems). Cells stained in wells were similarly treated with alcohol gradient but then washed and covered with PBS and viewed using an inverted microscope.

MSC grown to confluence on glass coverslips in 24 well plates and fixed with methanol were stained using similar protocols to those described above. However following applications of primary (Table 2.2) and secondary antibodies (Table 2.2), cells were treated with Nova red substrate (Vectorlabs) for 2 to 5 minutes, washed with tap water, counterstained with Mayer's Haematoxylin for 30 seconds and "blued" under running tap water. MSC were dehydrated and stored in PBS before bright field microscopic images were captured at x40 magnification.

PBMC were isolated and seeded in 24 well plates and fixed with methanol. Endogenous peroxidase in PBMC was blocked with H<sub>2</sub>O<sub>2</sub> (0.3% methanol), and casein 10% goat serum. PBMC were incubated with pre-determined optimal concentrations of unconjugated primary antibodies for collagen 1, CD45, CXCR4, and  $\alpha$ SMA for 1 hour alongside controls listed in Table 3.2. PBMC were washed with and incubated with Vectastain ABC kit (Vector Labs). PBMC were washed and incubated with DAB (Sigmafast Diaminobenzidine tablets, Sigma) substrate for 2 to 5 minutes, washed with tap water, counterstained with Mayer's Haematoxylin for 30 seconds and "blued" under running tap water. PBMC were dehydrated and stored in PBS before bright field microscopic images were captured at x10, x20 and x40 magnification. Fibroblasts cytopun on glass slides were used as positive controls for collagen 1,  $\alpha$ SMA and lymphocytes for CXCR4 and CD45.

Paraffin embedded mouse livers were sectioned using a microtome and stained using a standard Van Geison protocol. Briefly, after dewaxing and sections were stained with Celestin Blue (Leica Biosystems) for 5 minutes, rinsed in dH<sub>2</sub>O and stained in Mayer's haematoxylin for 5 minutes. Sections were washed well in running tap water for 5 minutes and flooded with

Van Gieson stain for 5 minutes. Finally sections were then dehydrated rapidly in alcohols, cleared and mounted in DPX.

Hematoxylin and Eosin (Leica Biosystems) staining was carried out on PBMC in 24 well plates to identify cell morphology. Sections were raised in dH<sub>2</sub>O stained in Haematoxylin for 4 minutes, in 0.3% acid alcohol for 30 seconds, tap water for 5 minutes and eosin for 2 minutes with intermittent 5 minute tap water rinses between each step.

**Table 2.2: Antibodies for IHC**

CCR antibodies					
1°Antibody	Type	Working Conc.	Source		
Anti-human CCR4	Goat IgG	50ug/ml	Pierce antibodies, ThermoScientific		
Anti-human CCR5	Rabbit IgG	20ug/ml	Abcam		
Anti-human CCR9	Rabbit IgG	10ug/ml	Pierce antibodies, ThermoScientific		
Anti-human CXCR3	Rabbit IgG	20ug/ml	Abcam		
Anti-human CXCR4	Rabbit IgG	20ug/ml	Abcam		
Anti-human CXCR7	Mouse IgG2A	25ug/ml	R and D Systems		
Controls					
Rabbit IgG	-----	20ug/ml	R and D Systems		
Rabbit IgG (CCR9)	-----	10ug/ml	R and D Systems		
Rabbit IgG2A (CXCR7)	-----	25ug/ml	Dako		
Goat IgG		50ug/ml	R and D Systems		
Secondary antibodies					
Goat anti Rabbit HRP	-----	1 in 1000	Abcam		
Rabbit anti Goat HRP	-----	1 in 1000	Abcam		
Rabbit anti mouse HRP	-----	1 in 1000	Abcam		
Fibrocyte phenotyping antibodies					
Antibodies	Type	IHC Conc.	IF Conc.	Flow Cytometry	Source
Anti-human CD45	Mouse IgG1	5ug/ml	-----	5ug/ml	R and D

Anti-human Collagen 1	Mouse IgG1	5ug/ml	5ug/ml	5ug/ml	Sigma
Anti-human Collagen 1	Rabbit biotinylated	-----	20ug/ml	20ug/ml	Rockland
Anti-human $\alpha$ SMA	Mouse IgG2A	10ug/ml	-----	-----	Dako
Anti-human CD45	Mouse IgG2A	-----	10ug/ml	-----	Abcam
Anti-human CXCR4	Mouse IgG2B	2.5ug/ml	2.5ug/ml	2.5ug/ml	R and D Systems
Anti-human Procol 1	Rat IgG1	-----	-----	1:50	Abcam
Controls					
Mouse IgG1	-----	5ug/ml	5ug/ml	5ug/ml	Dako
Rabbit IgG biotinylated	-----	-----	20ug/ml	20ug/ml	Rockland
Mouse IgG2A	-----	10ug/ml	10ug/ml	10ug/ml	Dako
Mouse IgG2B	-----	2.5ug/ml	-----	-----	R and D Systems
Rat IgG1	-----	-----	-----	1:10	Abcam
Secondary					
Goat anti mouse FITC	Mouse IgG1	-----	1:50	1:50	Southern Biotech
Goat anti mouse Texas red	Mouse IgG2A	-----	1:50	1:50	Southern Biotech
Goat anti mouse (streptavidin) FITC	Streptavidin	-----	1:50	1:50	Southern Biotech
Goat anti rat FITC	Rat IgG1	-----	1:50	1:50	Abcam
Goat anti mouse Alexaflour 488	Mouse IgG1	-----	-----	1:500	Invitrogen
Goat anti mouse Alexaflour 546	Mouse IgG2A	-----	-----	1:500	Invitrogen

## 2.6 Flow Cytometric analysis of cells

Cell surface or intracellular chemokine and integrin expression, cell viability and autophagy were all assessed using cytometric techniques. Specifically, MSC were detached from tissue culture plastic by incubating with CDB or TrypLE (other adherent cell types) at 37°C for 3 to 5 minutes. MSC were washed with PBS and centrifugation for 5 minutes at 900xg with the brake at 3 and re-suspended in FACS Buffer at a concentration of  $1 \times 10^6$  cells/ml. PBMC were

grown in culture for 2 weeks and scraped from tissue culture plastic. PBMC were washed and incubated with procollagen-1 (Abcam) for 30 minutes at 4°C. Isolated PBMC were washed and incubated for 30 minutes with a rabbit anti rat FITC conjugated secondary antibody (Abcam). Fibroblasts were tested for procollagen1, collagen1 and  $\alpha$ SMA as a positive control, and lymphocytes were tested for CXCR4 and CD45 listed in Table 2.3. Cells in suspension were washed and re-suspended in FACS buffer (PBS 1% FCS), counted and diluted to  $1 \times 10^6$  cells/ml and if necessary labelled with a live/dead marker (Invitrogen) after incubation for 30 minutes at 4°C. Labelled cells were washed twice with FACS buffer and re-suspended at  $1 \times 10^5$  cells per tube. The APC labelled fixable live/dead cell marker was added to the cell suspension to identify viable MSC upon detachment. Where necessary cells were permeabilised for intracellular staining using BD Cytotfix Fixation/ Permeabilisation kit (BD Biosciences) according to manufacturers instructions, washed and cells were labelled with antibodies in BD Wash Buffer. Once re-suspended in FACS buffer (for cell surface staining) or BD Wash buffer (for intracellular staining), cells were labelled with pre-determined optimal concentration of antibody (Table 2.3) and incubated for 30 minutes at 4°C in the dark. For MSC surface staining, cells were washed twice with FACS buffer. PE-conjugated anti-human CCR antibodies (CCR1-10, CXCR1-7, all from R and D Systems) or anti-human integrin antibodies listed in Table 2.3 were incubated with MSC at pre-determined optimal concentrations (typically 1:10) alongside individual controls. PE-conjugated anti-human CCR antibodies (CCR1-10, CXCR1-7, all from R and D Systems) or anti-human integrin antibodies listed in Table 2.3 were incubated with MSC at pre-determined optimal concentrations (typically 1:10) alongside individual controls. Cells were washed and then re-suspended in 500 $\mu$ l FACS buffer. Labelled cells were analysed using Dako Cyan ADP flow cytometer and Summit version 4.3 software (Dako).



MSC were stimulated with cytokines detailed in Table 2.4 for 10 minutes and 24 hours in MSC Growth Medium (MSCGM™) and normal or ALD cirrhotic patient serum (1:10) in an incubator with 5% CO<sub>2</sub> at 37°C. All serum and cytokines were diluted in complete MSC Growth Medium (MSCGM™). MSC were detached using various methods (section 2.3) from flasks, washed with FACS buffer and incubated with live dead cell marker as above. CCR expression on treated MSC was then determined as described above.

## **2.7 Quantification of autophagy and cell stress**

After detachment, MSC were incubated with an APC-labelled viability marker for 30 minutes. Autophagy of MSC was measured by incubating cells with 1µM Pacific orange-labelled Monodansylcadaverine (MDC, Sigma) for 30 minutes. Intracellular reactive oxygen species (IROS), apoptosis, necrosis and autophagy was also measured using a 4 colour reporter assay system. IROS accumulation was determined by incubation with 30µM of fluorescent probe 2', 7'-dichlorofluorescein (DCF; Merck) for 30 minutes. DCF binds to hydrogen peroxide and fluoresces in the fluorescein isothiocyanate (FITC) channel. Simultaneously, levels of autophagy were determined by incubating cells with 1µM Monodansylcadaverine (MDC; Sigma), which fluoresces in the Pacific orange channel, for 30 minutes. Cells were also incubated for 15 minutes with 0.25µg/ml annexin V (Invitrogen), a marker of apoptosis, which is detected in the Pacific blue channel, and with 1µg/ml 7AAD (ebiosciences), a marker of cellular necrosis, fluorescent in the Pe-Cy5 channel. Data were expressed as mean fluorescence intensity (MFI) of the cells.

**Table 2.3: CCR and Integrin antibodies used for flow cytometry**

Antibody name	Dilution of manufacturers stock	Type	Species	Source
Anti-human CCR1 PE	1/10	IgG2B	Mouse	R and D systems
Anti-human CCR2 PE	1/10	IgG2B	Mouse	R and D systems
Anti-human CCR3 PE	1/10	IgG2A	Rat	R and D systems
Anti-human CCR4 PE	1/10	IgG2B	Mouse	R and D systems
Anti-human CCR5 PE	1/10	IgG1	Mouse	R and D systems
Anti-human CCR6 PE	1/10	IgG2B	Mouse	R and D systems
Anti-human CCR7 PE	1/10	IgG2A	Mouse	R and D systems
Anti-human CCR8 PE	1/10	IgG2B	Rat	R and D systems
Anti-human CCR9 PE	1/10	IgG2A	Mouse	R and D systems
Anti-human CCR10 PE	1/10	IgG2A	Rat	R and D systems
Anti-human CXCR1 PE	1/10	IgG2A	Mouse	R and D systems
Anti-human CXCR2PE	1/10	IgG2A	Mouse	R and D systems
Anti-human CXCR3 PE	1/10	IgG1	Mouse	R and D systems
Anti-human CXCR4 PE	1/10	IgG2A	Mouse	R and D systems
Anti-human CXCR5 PE	1/10	IgG2B	Mouse	R and D systems
Anti-human CXCR6 PE	1/10	IgG2B	Mouse	R and D systems
Anti-human CXCR7 PE	1/10	IgG2A	Mouse	R and D systems
Anti-human $\alpha$ 1 integrin PE	1/10	IgG1	Mouse	ABD Serotec
Anti-human $\alpha$ 2 integrin PE	1/10	IgG2A	Mouse	R and D systems
Anti-human $\alpha$ 3 integrin PE	1/10	IgG1	Mouse	R and D systems
Anti-human $\alpha$ 4 integrin PE	1/10	IgG1	Mouse	R and D systems
Anti-human $\alpha$ 5 integrin PE	1/10	IgG1	Mouse	R and D systems

Anti-human $\alpha 6$ integrin PE	1/10	IgG1	Mouse	ABD Serotec
Anti-human $\alpha 8$ integrin PE	1/10	IgG2B	Mouse	R and D systems
Anti-human $\alpha V$ integrin PE	1/10	IgG1	Mouse	Abcam
Anti-human $\alpha V\beta 3$ integrin PE	1/10	IgG1	Mouse	R and D systems
Anti-human $\alpha V\beta 3$ integrin PE	1/10	IgG1	Mouse	R and D systems
Anti- human $\beta 1$ integrin PE	1/10	IgG1	Mouse	R and D systems
Anti- human $\beta 2$ integrin PE	1/10	IgG1	Mouse	R and D systems
Anti-human $\beta 3$ integrin PE	1/10	IgG2A	Mouse	R and D systems
Anti-human CD44 PE	1/10	IgG2B	Mouse	BD Pharmigen
Anti-human $\beta 7$ integrin PE	1/10	IgG2A	Rat	R and D systems
Anti human $\beta 4$ integrin Unconjugated	1/10	IgG2b	Mouse	R and D systems
Controls				
Mouse IgG1 PE	1/10	-----	-----	R and D systems
Mouse IgG2A PE	1/10	-----	-----	R and D systems
Mouse IgG2B PE	1/10	-----	-----	R and D systems
Rat IgG2A PE	1/10	-----	-----	R and D systems
Rat IgG2B PE	1/10	-----	-----	R and D systems
Mouse IgG2B Unconjugated	1/10	-----	-----	R and D systems
Secondary				
Anti-mouse IgG PE	1/10	IgG	Goat	R and D systems

**Table 2.4: Cytokines used for MSC stimulation**

Treatment	Final Concentration	Source
TNF $\alpha$	10ng/ml	PeptoTech
IFN $\gamma$	25ng/ml	PeptoTech
TNF $\alpha$ + IFN $\gamma$	10ng/ml + 20ng/ml	PeptoTech
TGF $\beta$ 1	5ng/ml	PeptoTech
LPS	200ng/ml	Sigma
IL1 $\beta$	10ng/ml	PeptoTech
IL4	10ng/ml	PeptoTech
IL6	10ng/ml	PeptoTech
IL8	10ng/ml	PeptoTech
IL10	50ng/ml	PeptoTech

## **2.8 Polymerase Chain Reaction (PCR)**

### **2.8.1 RNA extraction and cDNA preparation from cytokine stimulated MSC**

MSC were stimulated with cytokines detailed in Table 2.4 or media alone, for 24 hours in MSC Growth Medium (MSCGM<sup>TM</sup>) at 37°C in 25cm<sup>2</sup> flasks. Media was aspirated, cells were washed with PBS and RNA was extracted using the RNeasy mini kit (Qiagen) according to the manufacturers instructions. RNA purity was tested using a Nanodrop spectrophotometer (Implen GeneFlow) and samples were stored at -80°C. Purity was assessed using the 260/ 280 absorbance ratio to give an indication of protein contamination, and samples with a value less than 1.8 were not used.

CDNA was prepared from RNA using the Biorad iScript<sup>TM</sup> cDNA Synthesis Kit (Biorad) according to the manufacturers instructions. Briefly, 4 $\mu$ l of 5x iScript reaction mix and 1 $\mu$ l iScript reverse transcriptase was added to a mixture to nuclease-free water and RNA

(0.25µg/µl) resulting in a reaction volume of 20µl in PCR tubes (Thermoscientific). The complete reaction mixture was incubated in a PCR machine (Geneflow TC512) for 5 minutes at 25°C, 30 minutes at 42°C and 5 minutes at 85°C. The cDNA was then stored at -20°C. Control samples were prepared using water substituted for Reverse Transcriptase.

### 2.8.1.1 Use of 18S rRNA PCR to test for RNA contamination of cDNA samples

**Table 2.5: 18S rRNA Thermal Profile and Primers**

	Forward Primer	Reverse Primer
18S rRNA primers	Gtaacccggtgaacccatt	ccatccaatcggtagtagcg
Number of Cycles: 30	Temperature (°C)	Time (seconds)
	95	225
Denaturing	95	45
Annealing	55	45
Extension	72	45

Reverse transcription was carried out using 18S rRNA primers (Table 2.5) to assess integrity of cDNA and to identify any potential contamination in negative controls. The Hyperladder IV DNA ladder (Bioline) was used as amplicon length marker. 1µl of cDNA or RT negative sample was added to 1µl of ready mixed primers (Sigma), 3µl nuclease free water and 5µl of Mastermix (Bioline) in a PCR tube. 7µl of oil was layered over the samples to avoid any evaporation of sample. The thermal profile of the 18S rRNA primers and the reagents that were used in the 18S rRNA PCR are shown in Table 2.5 and 2.6 respectively.

**Table 2.6: 18S rRNA PCR Reagents**

Reagents	Final Concentration	Source
Mastermix (Biomix)	x1	Bioline
MgCl <sub>2</sub>	1mM	Bioline
dNTPs	0.8mM (total)	Promega, Southampton
Ready Mixed Primers	10µM	Sigma
cDNA	250µg/µl	MSC

The PCR product for 18S rRNA was visualised on a 2% agarose gel stained with ethidium bromide (10mg/ml, Sigma) using standard protocols. Samples were loaded alongside a lane of Hyperladder IV to indicate the size of the bands and run in electrophoresis buffer (Table 2.7). The gel was removed and photographed on Genegenius Bioimaging System Imaging machine.

**Table 2.7: 18S rRNA PCR Electrophoresis Buffer**

TBE x10 Electrophoresis Buffer			
Reagents	Molecular Weight (FW)	Final Concentration	Source
Trisma Base	121.14	0.89M	Sigma
Boric Acid	61.83	0.89M	Sigma
Na <sub>2</sub> EDTA.2H <sub>2</sub> O	442.5	0.5M	Sigma-Aldrich
ddH <sub>2</sub> O	1000ml		

### 2.8.2 Use of quantitative PCR (QPCR) to assess expression of CCR by MSC

QPCR experiments were carried out using commercially available QPCR kits (Roche) on the Roche Lightcycler 480 instrument. Cytokine stimulated MSC cDNA was tested for the CCR CCR4, CCR5, CCR9, CXCR3, CXCR4 and CXCR7 using primers designed by the Roche

primer design library listed in Table 2.8 and reagents in Table 2.10. 1µl of the forward primer and 1µl of the reverse primer, 0.4µl of the probe, 5.6µl RNase free H<sub>2</sub>O and 10µl of probes master (Roche QPCR Kit) was added to 2µl cDNA to give a total reaction volume of 20µl in a well of a Roche LC 480 multi-well, 96 well plate alongside a positive control sample (from PBMC), β Actin as a housekeeping gene and an endogenous control. Each β Actin reaction mixture contained 2µl cDNA, 0.4µl primer mixture, 0.4µl probe, 7.2µl nuclease free water and 10µl probes master. Similarly, unstimulated MSC and TGFβ1 stimulated MSC cDNA was analysed for alpha smooth muscle actin (αSMA) and collagen 1 (col1α1) (Table 2.11), at the thermal profile shown in Table 2.9 using reagents in Table 2.12 by QPCR. Human β-actin was used as internal control to which the threshold cycle (Ct) values of the target gene were normalised. Multi-well plates were covered with Lightcycler 480 sealing film (Roche) before they were inserted into the Lightcycler 480 QPCR machine. Differential expression levels were calculated according to the  $2^{-\Delta\Delta Ct}$  method and the results were analysed using Lightcycler 480 SW 1.5 software.

**Table 2.8: QPCR Primers**

Gene name	Gene ID	Forward Primer	Reverse Primer	Roche Probe No	Amplicon length (nt)
CCR4	NM_005508.4	ttgtgctctgccaatactgtg	taagatgagctgggggtgctc	25	64
CCR5	ENST00000479006.1  ENSG00000160791.9	cccttgaaaagacatcaagca	Tgcacaatcatatgagacagaaca	63	72
CCR5	ENST00000426816.1  ENSG00000160791.9	cttgggtggtggctgtgt	gaccagccccaagatgacta	14	129
CCR9	ENST00000422395.1  ENSG00000173585.10	caccatgacaccacagact	agcgagggaaggtgatctg	25	63
CCR9	ENST00000357632.2  ENSG00000173585.10	cagctctttccccagacact	catggtgggtcagtcagatg	56	101
CCR9	ENST00000395963.2  ENSG00000173585.10	tttccccagacactgagagc	tcagccatgtaggaataggg	36	87
CCR9	ENST00000357632.2  ENSG00000173585.11	caccacagacttcacaagc	tcacagtagaagtcagtgaaagttgaa	21	111
CXCR3	ENST00000373691.4  ENSG00000186810.6	ccagccatggtccttgag	tccagggccgtacttct	58	136
CXCR3	ENST00000373693.3  ENSG00000186810.6	gccatggtccttgaggtg	ctccatagtcataaggaagagctga	79	94
CXCR4	ENST00000466288.1  ENSG00000121966.4	ttaagcgcctggtgactgtt	gccatttctcctggttag	47	67
CXCR7	ENST00000272928.3  ENSG00000144476.5	tcacagtgttgcaaaagtct	gcagatccatcgttctgagg	36	138
$\alpha$ SMA	NM_001141945.1	ctgtccagccatcctcat	tcatgatgctgtttaggtggt	58	70
Col1 $\alpha$ 1	NM_000088.3	aggtcccctggaagaa	aatcctcagcacctga	79	96
Control					
ACTB (Roche)		ACTB 05046165001 Primer		ACTB 05046165001 Probe	

**Table 2.9: QPCR Thermal Profile**

QPCR Thermal Profile			
Number of Cycles: 50	Temperature (°C)	Time (seconds)	Ramp rate (°C/s)
	95	10	4.4
Denaturing	95	10	4.4
Annealing	60	30	2.2
Extension	72	1	4.4
Cooling	40	30	2.2



**Table 2.10: QPCR reagents**

CCR	
Reagents	Final Volume
Primers	0.5µM
Probe	0.4µl
Roche Mastermix	x1
cDNA	0.5µg/ml
RNase free water	5.6µl
Beta Actin	
Reagents	Final Volume
Primer Mix	0.4µl
Probe	0.4µl
Roche Mastermix	x1
cDNA	0.5µg/ml
RNase free water	7.2µl

### 2.8.3 Measurement of collagen-1 (coll1a1) and alpha smooth muscle actin (αSMA) mRNA levels in injured mouse livers by QPCR.

Levels of αSMA and coll1a1 mRNA were measured in carbon tetrachloride injured and uninjured C57 Black 6 mouse livers (section 2.14.2) using a Taqman Gene Expression Assay. RNA was extracted from frozen carbon tetrachloride injured and uninjured C57BL/6 mouse livers using the Qiagen RNeasy mini kit as described above. RNA purity was tested using a Nanodrop spectrophotometer, and cDNA was prepared from RNA using the Biorad iScript™ cDNA Synthesis Kit (Biorad) as before. For analysis of relative expression of coll1a1 and αSMA Taqman gene expression assays were run on an ABI Prism 7900 sequence detector (at University of Birmingham, UK). Coll1a1 and αSMA Ct values were normalised to murine GAPDH Ct levels which were used as an internal control. Differential expression levels were calculated according to the  $2^{-\Delta\Delta Ct}$  method as above.

**Table 2.11: QPCR primers for  $\alpha$ SMA and  $coll1\alpha1$** 

	Primer/ Probe Assay ID	Source
$\alpha$ SMA	Mm00801666_g1	Applied Biosystems, Invitrogen
Coll1 $\alpha$ 1	Mm00725412_s1	
GAPDH	Mm99999915_g1	
Expendables		
Taqman® Universal PCR Master Mix		
Taqman® 2x Master Mix		
MicroAmp® Optical 96-well reaction plate-0.1ml		
MicroAmp® Optical adhesive film		

**Table 2.12: Components of QPCR reagents for  $\alpha$ SMA and  $coll1\alpha1$** 

Reagents	Final Concentration [single reaction (20 $\mu$ l)] ( $\mu$ l)
20 $\times$ TaqMan® Gene Expression Assay	1
2 $\times$ TaqMan® Gene Expression Master Mix	10
cDNA	4
RNase free water	5

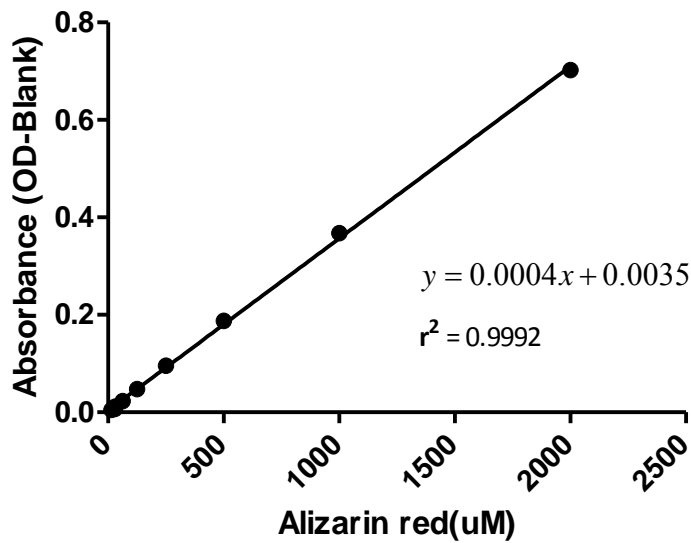
## 2.9 Measurement of MSC tri-lineage differentiation capacity

The effects of cell dissociation protocol and cytokine (TGF $\beta$ 1) stimulation on the adipogenic, osteogenic and chondrogenic differentiation capacity of MSC was assessed at P4 using commercially available differentiation kits. MSC were seeded at equal densities in 24 well plates and cultured in osteogenic and adipogenic differentiation media according to manufacturer's instructions (Lonza) alongside controls, which were cultured in maintenance medium for approximately 3 weeks.

Adipogenic differentiation was indicated by the morphological appearance of lipid droplets when stained with oil red O according to standard protocols. Stock oil red O solution (0.5% in isopropanol) was diluted to 60% in dH<sub>2</sub>O prior to experimentation. Cells were fixed with formalin and then incubated with 60% isopropanol for 5 minutes. Cells were then incubated with oil red O working reagent for 15 minutes, followed by isopropanol for 5 minutes and then washed twice with dH<sub>2</sub>O. Bright field microscopic images were captured at x20 magnification and percentage area staining red was calculated using Image J Software (<http://rsbweb.nih.gov/ij/>).

Osteogenic differentiation was measured using an osteogenesis assay kit (Millipore) according to the manufacturers protocol. Briefly, cells were washed with HBSS, fixed with formalin for 5 minutes and washed with dH<sub>2</sub>O. Cells were incubated with 1ml/well of Alizarin red stain solution at room temperature for 20 minutes and washed with dH<sub>2</sub>O. 400µl 10% acetic acid was added to each well and incubated for 30 minutes with shaking. The contents were scraped from the wells and vortexed vigorously for 30 seconds. Samples were heated at 85°C for 10 minutes, put on ice for 5 minutes and centrifuged for 15 minutes at 550xg. Samples were neutralised with Ammonium Hydroxide and read at an optical density 405nm against high and low standards from the kit, in order to permit assessment of concentration of Alizarin red present (Figure 2.1).

**Figure 2.1: Standard Curve for Alizarin red Staining**

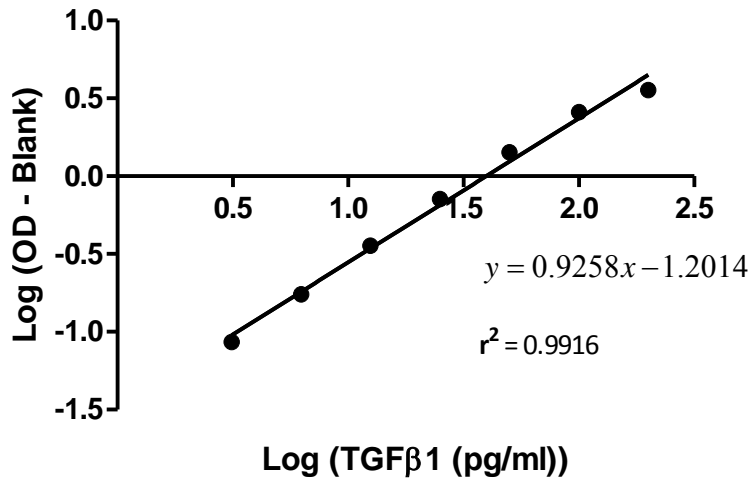


To assess chondrogenic differentiation capacity of MSC, cell pellets were formed in polypropylene falcon tubes and cultured in chondrogenic differentiation media (supplemented with TGF $\beta$ 3 at a final concentration of 10ng/ml) according to manufacturers instructions (Lonza) alongside controls, which were cultured in maintenance medium. Cell pellets were stored at 37°C in a cell culture incubator, and caps were loosened to allow gas exchange. 500 $\mu$ l medium was replenished every 2 to 3 days for 2/ 3 weeks. Cell pellets were snap frozen in liquid nitrogen and stored at -80°C until sections were cut using a cryostat. Slides were stored at -20°C until sections were analysed for chondrogenic differentiation as indicated by the presence of collagen II (Millipore) detected by immunohistochemistry.

## **2.10 Quantification of TGF $\beta$ 1 in MSC Supernatants by ELISA**

Unstimulated and TGF $\beta$ 1 stimulated MSC supernatant was collected from P4 MSC in culture. Supernatants were tested using ELISA for active TGF $\beta$ 1 using an ELISA kit (R and D Systems), according to the manufacturers instructions. Briefly, 96 well plates (Nunc Maxisorp) were coated with TGF $\beta$ 1 capture antibody from the TGF $\beta$ 1 DuoSet ELISA kit (R and D Systems). Plates were loaded with kit standards, serum from 3 normal volunteers and from 3 with patients ALD cirrhosis and supernatant from 3 unstimulated MSC isolates and 3 TGF $\beta$ 1 stimulated MSC isolates. Plates were incubated, washed with PBS 1% Tween 20 and then incubated with a biotinylated TGF $\beta$ 1 detection antibody conjugated to HRP. Wells were washed and finally streptavidin-HRP was added to wells. Upon addition of substrate, a blue colour developed, at which point a stop solution was added. Plates were read on a microplate reader set to 450nm with the wavelength correction set to 540nm. Triplicate readings were averaged and the average zero standard optical density was subtracted. The mean absorbance for each standard curve was plotted against the concentrations on the x axis and a line of best fit was drawn (Figure 2.2). Samples had been diluted, so the concentration read from the standard curve was multiplied by the dilution factor to determine actual concentrations.

**Figure 2.2: Standard curve for TGFβ1 Sandwich ELISA**



### **2.11 Adhesion molecule expression of HSEC after stimulation by MSC conditioned media**

This experiment assessed the effect of cytokine stimulated MSC conditioned media on HSEC adhesion molecules expression. HSEC were cultured on collagen coated 96 well ELISA plates and pre-stimulated with TNF $\alpha$  (20ng/ml, PeproTech), IFN $\gamma$  (100ng/ml, PeproTech) or control media for 24 hours, and then for a further 24 hours in cytokine stimulated MSC supernatant as shown in Table 4. After 24 hours, cells were methanol fixed in 96 well plates, washed with PBS and blocked with PBS 1% Bovine Serum Albumin (BSA, Sigma) for 1 hour. ICAM1, VCAM1, CD31, P-Selectin, E-Selectin expression on HSEC was then analysed using primary antibodies listed in Table 2.13. Cell based ELISA was the method used to do this. Briefly, wells were washed with PBS 0.1% Tween 20 and then incubated with a goat anti mouse HRP

conjugated secondary antibody (Dako) at 1:1000 dilution for 1 hour. OPD substrate (Dako) was used to quantify antibody binding. The ELISA substrate was used according to manufacturers instructions and absorbance values of triplicate wells were determined at 490nm.

**Table 2.13: Antibodies used for cell based ELISA.**

Primary antibody	Working concentration	Source
VCAM1	5 µg/ml	R and D Systems
ICAM1	5 µg/ml	R and D Systems
E Selectin	5 µg/ml	R and D Systems
P Selectin	5 µg/ml	Abcam
CD31	5 µg/ml	DAKO
Control		
Mouse IgG1	5 µg/ml	R and D Systems

### 2.11.1 Quantification of cytokine and pro-angiogenic mediators in MSC supernatants

TGFβ1 stimulated MSC supernatants were tested for changes in secreted angiogenic factors and cytokines using the Cytokine/ Angiogenesis kit (R and D systems), according to the manufacturers instructions. Briefly array membranes with already bound capture antibodies were blocked to prevent non specific binding. Samples were added to the membranes with a detection antibody and incubated overnight at 4°C. Membranes were washed, incubated with streptavidin-HRP for 1 hour and washed again. Membranes were then exposed to Supersignal chemiluminescent reagent (Thermoscientific) as described by the manufacturer, covered with plastic wrap and exposed to for 1 minute to enhanced chemiluminescence detection film (Amersham Biosciences) and developed using a Kodak X-Omat 1000 processor. Data were

analysed using Image J software. A template was created to analyse pixel density for each spot of the array. The average signal (pixel density) of the pair of duplicate spots representing each angiogenesis or cytokine related protein was determined and the average background signal from blank control spots was subtracted.

## **2.12 Use of an immunosuppression assay to assess ability of MSC to inhibit T effector cell proliferation**

CD3<sup>+</sup>CD4<sup>+</sup>CD25<sup>-</sup> T effector cells were isolated from human peripheral blood. Briefly, blood was layered onto a Lympholyte®-H (Axis Shield) density separation gradient and centrifuged at 900xg for 20 minutes. The cell layer was collected from the density gradient interface, washed with PBS and incubated in MACS buffer (1L PBS, 4ml EDTA, 5ml FCS)) with a cocktail of selection antibodies (CD3 PB, (4µg/ml, BD Pharmigen), CD4 PE (4µg/ml, BD Pharmigen), CD25 APC (4µg/ml, Invitrogen). CD3<sup>+</sup>CD4<sup>+</sup>CD25<sup>-</sup> Cells were then sorted using the Mo flow XDP cell sorter (Beckman Coulter). Control or TGFβ1-stimulated MSC, treated with or without Indomethacin (Sigma Aldrich), a PGE2 blocker, were cultured with the CD3<sup>+</sup>CD4<sup>+</sup>CD25<sup>-</sup> T effector cells and T regulatory suppression inspector beads (Miltenyi). Cells were cultured for 5 days in RPMI 1640 (Invitrogen) with 10% human serum (Invitrogen) and 5% Glutamine-Streptomycin-Penicillin (PSG) (Invitrogen) at 37<sup>0</sup>C in round bottom 96 well plates (BD Falcon). Finally CD3<sup>+</sup>CD4<sup>+</sup>CD25<sup>-</sup> T effector cells were aspirated, washed and re-suspended in 200µl PBS. 20µl Accucheck counting beads (Invitrogen) were added to the tubes and samples run on the Dako Cyan ADP flow cytometer. CD3<sup>+</sup>CD4<sup>+</sup>CD25<sup>-</sup> T effector cells labelled with CellTrace™ Violet Cell Proliferation Kit (Invitrogen) were gated and total number of cells/µl was obtained.



### **2.13 Use of a modified Boyden chamber migration assay to assess MSC migration towards chemokines**

MSC chemotaxis was determined in a modified 48-well Boyden chamber (Figure 2.3). Pre-determined concentrations (in the range 0-500ng/ml) of chemokines listed in Table 2.14 in serum-free media were placed in the lower wells. A polycarbonate membrane with 8µm pores (Neuroprobe) was used, and MSC (control or pre-stimulated with TGFβ1, IL4, IL10 (Table 2.14)) detached with either TrypLE or CDB were re-suspended in serum free media and placed the upper wells. After incubation at 37°C for 24 hours, filters were removed, air-dried and stained using Diffquick (Medion Diagnostics). Migrated MSC on the lower face of the membrane were counted in 5 fields of view (x40 magnification) per well using a brightfield microscope.

**Figure 2.3: Schematic diagram of the Boyden migration chambers**

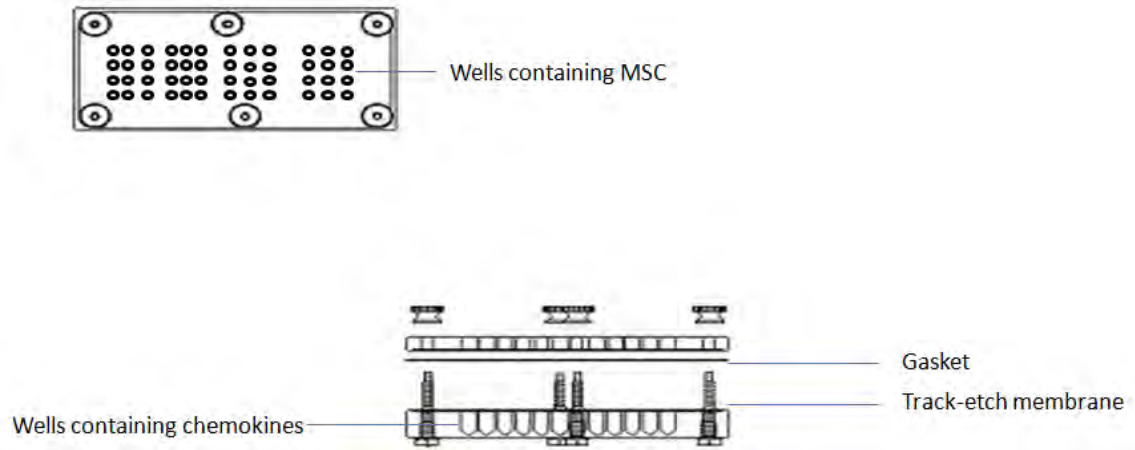


**Table 2.14: Chemokine ligands used in Boyden chamber migration assays**

Chemokine	Source	Corresponding receptor	Concentration range	Optimal concentration
Human TARC/ CCL17	PeproTech	CCR4	10-500ng/ml	100ng/ml
Human MDC/ CCL22	PeproTech	CCR4	10-500ng/ml	500ng/ml
Human MIP-1 $\beta$ / CCL4	PeproTech	CCR5	10-500ng/ml	500ng/ml
Human MCP-1/ CCL2	PeproTech	CCR4	10-500ng/ml	-----
Human IP-10/ CXCL10	PeproTech	CXCR3	10-500ng/ml	50ng/ml
Human ITAC/ CXCL11	PeproTech	CXCR3	10-500ng/ml	500ng/ml
Human PF-4/ CXCL4	PeproTech	CXCR3	10-500ng/ml	-----
Human MIG/ CXCL9	PeproTech	CXCR3	10-500ng/ml	-----
Human TECK/ CCL25	PeproTech	CCR9	10-500ng/ml	100ng/ml
Human RANTES/ CCL5	PeproTech	CCR5	10-500ng/ml	10ng/ml
Human SDF1 $\alpha$ / CXCL12	PeproTech	CXCR4, CXCR7	10-500ng/ml	50ng/ml
Human MIP-1 $\alpha$ / CCL3	PeproTech	CCR5	10-500ng/ml	-----
Human MCP-2/ CCL8	PeproTech	CCR5	10-500ng/ml	100ng/ml

## **2.14 Use of murine liver injury models to assess the hepatic trafficking of infused MSC**

### **2.14.1 The CCl<sub>4</sub> injury model**

Carbon tetrachloride (Sigma Aldrich) diluted 1/4 in mineral oil (Sigma) was administered by intraperitoneal (IP) injections of 100ul each into 9 week old (weight: approx 20g) C57BL/6 wild type mice, twice weekly for 6 to 8 weeks. Immune-compromised Rag2<sup>-/-</sup>IL-2r<sup>γ</sup><sup>-/-</sup> mice were also injured with carbon tetrachloride IP injections at a 1/40 dilution in mineral oil, twice weekly, for 9 or 12 weeks. After the course of administration, mice were used for portal vein infusion experiments and culled. Livers were snap frozen in liquid nitrogen and stored at -80°C to be sectioned by a cryostat. Alternatively livers were fixed in formalin to be cut as wax sections and embedded in paraffin.

### **2.14.2 Measuring injury in carbon tetrachloride injured mice**

#### **2.14.2.1 Picrosirius red staining for quantification of fibrosis**

Paraffin sections from injured and uninjured C57BL/6 and Rag2<sup>-/-</sup>IL-2r<sup>γ</sup><sup>-/-</sup> mouse livers were dewaxed using Clearene, and passed through a graded ethanol series. These and frozen sections from 6 week C57BL/6 injured/ uninjured mice or normal/ diseased human liver section were washed with dH<sub>2</sub>O and incubated with 0.5 % phosphomolybdic acid (PMA, Sigma) for 5 minutes. 100ml of 0.1% Sirius red stain (Direct red 80 in saturated picric acid; Sigma) was added to the sections for 2-3 hours and sections were dipped in 0.01M HCl

(Sigma) in dH<sub>2</sub>O. Finally sections were counterstained with Mayer's Haematoxylin, dehydrated and mounted in DPX. Bright field microscopic images were captured at x20 and x40 magnification and analysed by Image J analysis for area fraction that had stained red to measure and score fibrosis.

#### **2.14.2.2 Serum albumin levels**

Albumin levels were measured in uninjured and carbon tetrachloride injured mouse serum using the Quantichrom™ BCG Albumin Assay Kit (Bioassay Systems) according to the manufacturers instructions. Briefly, standards were diluted in dH<sub>2</sub>O, samples were diluted two fold and 5µl of each was added to the wells of a 96 well plate. 200µl of working reagent was added to each well, the plate was tapped lightly to mix, incubated at room temperature for 5 minutes and the optical density was read at 620nm. Triplicate readings were averaged and the average zero standard optical density was subtracted. The log of mean absorbance for each standard curve was plotted against the log of concentrations on the x axis and a line of best fit was drawn. The concentration read from the standard curve was multiplied by the dilution factor to determine actual concentrations.

#### **2.14.2.3 Serum bilirubin quantification**

Bilirubin levels were measured in uninjured and carbon tetrachloride injured mouse serum using the Quantichrom™ Bilirubin Assay Kit (Bioassay Systems) according to the manufacturers instructions. Briefly, standards and samples were diluted in working reagent and incubated for 10 minutes at room temperature and the optical density was read at 540nm.

Triplicate readings were averaged and the average zero standard optical density was subtracted. The log of mean absorbance for each standard curve was plotted against the log of concentrations on the x axis and a line of best fit was drawn. The concentration read from the standard curve was multiplied by the dilution factor to determine actual concentrations.

## **2.15 Quantification of MSC adhesion and recruitment into injured tissue**

### **2.15.1 Use of modified Stamper Woodruff assays to assess adhesion of MSC to injured human liver sections**

10µm cryosections cut from explanted human livers (Normal, ALD, AIH, PSC, PBC and NASH) were fixed in acetone for 5 minutes, air-dried and wrapped in foil. Sections were stored at -80°C until required for adhesion assays. Cultured MSC were detached, washed and re-suspended with PBS 0.1% BSA in a conical bottomed 15 ml polypropylene tubes. The cells were incubated with 1µM CFSE per ml for 10 minutes at 37°C. CFSE was washed with 2ml FCS and cells were centrifuged for 5 minutes at 900xg to stop binding of excess CFSE and to help remove unbound CFSE from the cell suspension. This wash was repeated twice with cold PBS to remove unincorporated CFSE. Finally MSC were re-suspended in cold PBS and stored on ice in the dark for 5 minutes to allow leaching of any residual CFSE. MSC were washed again and re-suspended in PBS 0.1% BSA (Sigma) at the desired concentration.

Tissue sections were thawed at room temperature for 30 minutes, and transferred to a humidified chamber. Alternatively for liver cell monolayers (including HSEC, BEC and MF) grown in 24 or 6 well plates, media was aspirated and wells were washed with PBS. 10<sup>5</sup>

CFSE-labelled or unlabelled MSC were added to sections or wells in PBS and incubated for 60 minutes at room temperature. Slides or wells were washed PBS and fixed for 5 minutes in acetone or methanol respectively. Adherent MSC were quantified by microscopic counting of CFSE labelled or haematoxylin counterstained MSC. Microscopic images of cell monolayer adherent CFSE labelled MSC were taken at x40 magnification using an inverted fluorescence microscope. Fluorescence on these images was measured by Image J analysis and measured as the area fraction of the pictures which were fluorescent. Alternatively counterstained or CFSE labelled adhered MSC on tissue sections were counted in 30 fields of view at x40 magnification using a brightfield microscope. Where MSC were labelled with CFSE, all procedures were carried out in the dark.

### **2.15.2 Quantification of MSC Engraftment in murine livers following via portal vein infusion**

Cytokine stimulated MSC labelled with CFSE, were re-suspended in PBS 0.1% BSA at appropriate concentration, typically  $5 \times 10^6$  to  $10 \times 10^6$  cells/ml. Where indicated, MSC were pre-incubated with blocking antibodies raised against CCR for 15 minutes at  $37^\circ\text{C}$ , washed and re-suspended in PBS 0.1% BSA. MSC were infused into the portal vein of uninjured or injured (carbon tetrachloride for 8 weeks) mice. Post injection, bleeding was encouraged to clot using sterile cotton wool buds and Spongostan (Ethicon, acquired through National Veterinary Services). Bleeding was stopped and mice were kept under anaesthetic for 15 minutes to allow engraftment of infused cells. Mice were culled, and livers were immediately snap frozen in liquid nitrogen and stored at  $-80^\circ\text{C}$ . Finally livers were cryosectioned into serial sections and CFSE-labelled cells were counted under a fluorescent microscope at varying

depths within the liver samples. Cells were counted in 10 fields of view on 4 sections over 4 depths from each mouse liver.

## **2.16 Measurement of serum amyloid protein (SAP): an inhibitor of fibrocyte differentiation**

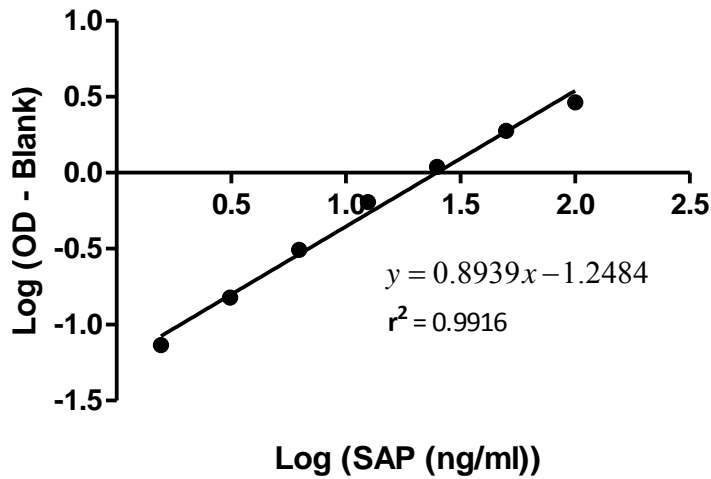
### **2.16.1 Quantification of Serum Amyloid Protein (SAP) in liver samples by Sandwich ELISA**

Serum Amyloid Protein (SAP) or Pentraxin 2 has been implicated in the differentiation of fibrocytes. Serum Amyloid Protein (SAP) or Pentraxin 2 levels in injured and non injured C57 BL/6 mouse liver lysates and serum were tested using a sandwich ELISA kit (R and D Systems). All reagents, samples and working standards were prepared as directed in the manufacturers instructions and the manufacturers protocol was followed. Briefly, 50 $\mu$ l of calibrator diluent was added to each well followed by 50 $\mu$ l of control, standard, or sample and incubated for 3 hours at room temperature on a horizontal orbital microplate shaker. The wells were washed 5 times with 400 $\mu$ l wash buffer. 100 $\mu$ l of mouse Pentraxin 2 conjugate was then added to each well and incubated for 1 hour at room temperature. 100 $\mu$ l of substrate solution was added to each well and incubated for 30 minutes at room temperature in the dark. Finally 100 $\mu$ l of stop solution was added and the optical density of each well was determined within 30 minutes at 450nm with the wavelength correction set to 540nm. Triplicate readings were averaged and the average zero standard optical density was subtracted. The log of mean absorbance for each standard curve was plotted against the log of concentrations on the x axis



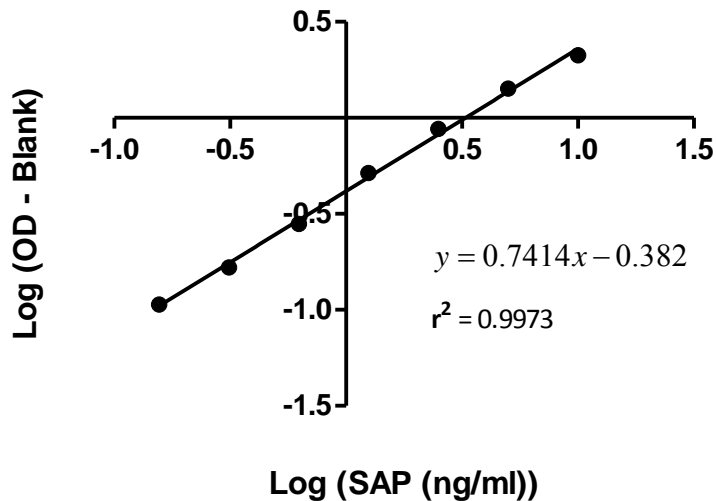
and a line of best fit was drawn (Figure 2.4). The concentration read from the standard curve was multiplied by the dilution factor to determine actual concentrations.

**Figure 2.4: Standard Curve for mouse SAP Sandwich ELISA**



Serum Amyloid Protein (SAP) or Pentraxin 2 levels in diseased and normal patient liver lysates and serum were tested using a sandwich ELISA kit (Abnova) according to the manufacturers protocol, similar to the mouse Pentraxin ELISA kit (R and D systems). The log of mean absorbance for each standard curve was plotted against the log of concentrations on the x axis and a line of best fit was drawn (Figure 2.5).

**Figure 2.5: Standard Curve from human SAP Sandwich ELISA**



#### **2.16.1.1 Quantification of SAP using Western blotting**

Protein lysates were made from human livers including ALD, AIH, PBC, NASH, and normal livers. Livers were also collected from 6 and 8 week carbon tetrachloride injured and uninjured mice. All tissues were frozen and buffers were pre-cooled or stored on ice. Frozen tissue was defrosted on ice and 70-90mg of tissue was homogenised in a Miltenyi Gentle MACS M-Tube with ice cold lysis buffer [(20µl CellLytic MT Buffer; Sigma, 1x Protease Inhibitor cocktail; Sigma, 5U/ml DNase; Roche) per mg of tissue] and digested using programme Protein-01 on the Gentle MACS (Miltenyi). The tube was centrifuged at 3000xg or 3 minutes and lysate collected in a 1.5ml eppendorf tube. Samples were continuously agitated for 1 hour at 4°C and then centrifuged at 16000xg for 30 minutes at 4°C. The resulting supernatant was aspirated and stored at -80°C. For use, protein concentration was

determined using a Bio-Rad DC Protein Assay performed according to manufacturers instructions and samples were diluted to 5ug/ml in PBS 0.1% Tween 20. Normal/ uninjured and diseased/ injured liver lysates were then tested for levels of serum amyloid protein (SAP) using western blot analysis, the reagents for which are listed in Table 2.15 and the buffer dilutions in Table 2.16.

Serum was also tested for levels of serum amyloid protein (SAP) using western blot analysis. Here, normal human serum was collected from healthy volunteers and compared with serum from patients with end stage ALD cirrhosis. Serum was also collected from 6 and 8 week carbon tetrachloride injured and uninjured mice. Here blood was collected by cardiac puncture, allowed to clot and then spun down at  $\geq 8000xg$  for 15 minutes to separate serum. Serum was then stored at  $-80^{\circ}C$  in working aliquots. Samples were diluted 1:20000 in PBS 0.1% Tween 20 before use.

**Table 2.15: Buffers for SDS PAGE**

Buffer	Constituents	Storage
10x running/electrophoresis buffer	30.3g Trizma Base, 144g Glycine, 10g SDS, 1000ml dH <sub>2</sub> O	Room Temperature
Transfer buffer	28.8g Glycine, 6.0g Trizma Base, 400ml Methanol, 1g SDS, 1600ml dH <sub>2</sub> O	4°C
Resolving gel buffer	1.5M Trizma Base pH 8.8	Room Temperature
Stacking gel buffer	0.5M Trizma Base pH 6.8	Room Temperature
5x SDS-PAGE sample buffer	200mM Trizma Base pH 6.8, 20% Glycerol, 10% SDS, 0.05% bromophenol blue, 10mM β-ME	Room Temperature
Blocking buffer	TBS + 0.02% Tween 20, 10% non fat milk (25ml per membrane)	Room Temperature
Stripping buffer	20.0ml 10% SDS, 12.5ml 0.5M Trizma Base-HCL pH 6.8, 67.5ml dH <sub>2</sub> O, 0.8ml β-ME	Room Temperature
10% SDS	10g SDS, 100ml dH <sub>2</sub> O	Room Temperature
TBS-0.1%Tween 20	2000ml TBS pH7.6, 2ml Tween 20	Room Temperature

**2.16.1.2 SDS Polyacrylamide Gel Electrophoresis (SDS-PAGE)**

Serum or tissue lysates were loaded in the wells of a 4% polyacrylamide stacking gel (Table 2.15) which was layered above a 15% resolving gel (Table 2.15) using the BioRad Mini Trans Blot Cell System. Samples were diluted in 1x SDS-PAGE sample buffer with β-mercaptoethanol and boiled at 100°C for 10 minutes on a heat block. Heated protein samples were centrifuged and set aside to cool before loading 20ul into wells created in the gel using a plastic comb. Pre-stained rainbow molecular weight markers (Amersham, GE Healthcare) were used as size markers. Electrophoresis was performed at 200V for 1 hour until the dye reached the bottom of the gel.

**Table 2.16: Gel components for SDS PAGE**

	4% Stacking Gel	15% Resolving Gel
dH <sub>2</sub> O	6.1ml	2.4ml
30% Acrylamide mix (Biorad)	1.3ml	5ml
Stacking Gel Buffer	2.5ml	-----
Resolving Gel Buffer	-----	2.5ml
10% SDS	0.1ml	0.1
10% ammonium persulfate (APS) (Sigma Aldrich)*	40µl	40µl
N,N,N',N'-tetramethylethylenediamine (TEMED) (Sigma Aldrich)*	20µl	20µl

Components of SDS-PAGE gels. \*APS and TEMED were added immediately prior to pouring of gels, as the oxygen free radicals released from the reaction between APS and the tertiary amine TEMED are responsible for the polymerisation of bis-acrylamide.

**Table 2.17: Reagents for Western Blot**

Reagents	Molecular Weight (FW)	Source	
Trizma Base	121.14	Sigma	
NaCl	58.44	Sigma	
Glycine	75.07	Sigma	
Sodium Dodecyl Sulfate (SDS)	288.38	Sigma	
Methanol	-----	Fischer Scientific	
Glycerol	-----	Fischer Scientific	
Bromophenol blue	-----	Sigma	
Betamercaptoethanol	78.13	Sigma	
Tween 20	-----	Sigma	
Trizma HCl		Sigma	
Non fat milk	-----	Marvel	
Antibodies			
Primary	Type	Working dilution/ concentration	Source
Mouse Serum Amyloid Protein (T-15)	Goat Polyclonal	1 in 100	Santa-Cruz
Human Serum Amyloid	Mouse IgG1	1 in 1000	Abcam

Protein (6E6)			
Secondary			
Rabbit anti goat HRP	Goat polyclonal	1 in 5000	Abcam
Goat anti mouse HRP	Mouse IgG1	1 in 1000	Dako
Control			
Mouse GAPDH	Rabbit Polyclonal	0.2µg/ml	Sigma
Human GAPDH	Mouse IgG1	0.5µg/ml	Sigma

### 2.16.1.3 Western Blot Transfer

Resolved proteins on the gel were transferred onto a nitrocellulose membrane (Hydrobond ECL Amersham Biosciences) at 100V for 1 hour using standard protocols. Efficient transfer was confirmed by staining the membrane with Ponceau red solution (0.1% Ponceau S in 5% acetic acid, Sigma) for 5 minutes followed by rinsing with water to visualise successful protein transfer. Non-specific protein binding sites on transferred membranes were then blocked for 1 hour using milk. The membrane was then stained with primary SAP antibodies, in non-fat dry milk overnight. After several washes in PBS-Tween 20, blots were stained with a HRP conjugated secondary. Membranes were exposed to Supersignal chemiluminescent reagent as described by the manufacturer, covered with plastic wrap and exposed to enhanced chemiluminescence detection film (Amersham Biosciences) for 5 minutes and developed using a Kodak X-Omat 1000 processor .

After SAP levels were quantified, bound antibodies were stripped from membranes by incubation in stripping buffer (Table 2.15) for 45 minutes at 50°C and several washes in dH<sub>2</sub>O. The membranes were then blocked with 10% non-fat milk and re-probed with an endogenous control and incubated overnight. HRP conjugated secondary was added to the membrane followed by exposure to chemiluminescent reagent and film as described

previously. Protein density was measured by quantifying signal from the human SAP: 25-28kDa, mouse SAP: 26kDa and human GAPDH: 37kDa mouse GAPDH: 38kDa bands using Image J analysis. Pixel density of SAP protein bands was measured relative to control GAPDH bands (Table 2.17).

## **2.17 Statistical Analyses**

Student's t-test was used to analyse data when comparing numerical variables between two groups. In situations where more than two groups were compared against each other, data was analysed using a one way ANOVA with Bonferroni post test. All statistical analysis was performed using the GraphPad Prism software version 4. Data were considered statistically significant when  $p < 0.05$ . Levels of significance were expressed as follows: \*,  $p < 0.05$ ; \*\*,  $p < 0.01$ ; \*\*\*,  $p < 0.001$ ; \*\*\*\*,  $p < 0.0001$ .

**CHAPTER 3: EFFECTS OF MSC DETACHMENT  
METHODS ON VIABILITY, TRI-LINEAGE  
DIFFERENTIATION, IMMUNOMODULATION AND  
CHEMOKINE RECEPTOR EXPRESSION**



### 3.1 Introduction

Human bone marrow derived mesenchymal stromal cells (MSC) are multipotent stem cells capable of self-renewal and tri-lineage differentiation into adipocytes, chondrocytes and osteoblasts (Jiang *et al.*, 2002, Pittenger *et al.*, 1999). MSC have also been shown to transdifferentiate into other cell types including hepatocytes (Lee *et al.*, 2004, Pittenger *et al.*, 1999), neuronal cells (Brazelton *et al.*, 2000, Pittenger *et al.*, 1999), endothelial cells (Oswald *et al.*, 2004), cardiac cells (Pittenger *et al.*, 1999) and connective tissue (Pittenger *et al.*, 1999). In addition, MSC have been shown to have potent immunomodulatory properties (Uccelli *et al.*, 2008), with anti-inflammatory actions having been demonstrated in a range of murine models of disease including diabetes (Ding *et al.*, 2009), graft versus host disease (GVHD) (Ren *et al.*, 2008) and sepsis (Nemeth *et al.*, 2009). Moreover, allogeneic MSC have been used in clinical trials of GVHD with evidence of efficacy (Le Blanc *et al.*, 2008), with larger trials ongoing in patients with ischaemic heart disease, inflammatory bowel disease and diabetes ([www.osiris.com](http://www.osiris.com)). The diverse functions of MSC and proven efficacy in clinical trials, combined with their transdifferentiation abilities suggests they are well equipped to assist regeneration and recovery of injured organs. In support of this MSC have been shown to reduce tissue damage and to exhibit anti cancer properties (Secchiero *et al.*, 2010) by a multitude of pathways (Jung *et al.*, 2011b, Lin *et al.*, 2011) indicating their possible therapeutic utility.

However, other significant aspects of MSC function, such as an understanding of the mechanisms regulating their adhesion and incorporation into tissue, remain less well delineated. Although direct transplantation of MSC into injured organs has been shown to contribute to recovery (Amado *et al.*, 2005), gaining such direct access is not always practical,

and it is more likely that therapeutic cells will be delivered by systemic infusion. Indeed, up-regulation of adhesion molecules in injured organs increases homing of cells such as leukocytes to the site of injury, in a manner critically dependent on the expression of specific adhesion molecules and cell surface CCR (Aldridge *et al.*, 2012, Ley *et al.*, 2007, Thankamony and Sackstein, 2011). We (Aldridge *et al.*, 2012), and others have demonstrated that similar mechanisms operate for MSC recruitment (Chamberlain *et al.*, 2011, Ji *et al.*, 2004, Karp and Leng Teo, 2009, Sarkar *et al.*, 2010, Wu and Zhao, 2012) although the importance of CCR for MSC for tissue homing remains uncertain (Ciuculescu *et al.*, 2011, Ponte *et al.*, 2007, Ringe *et al.*, 2007, Sordi *et al.*, 2005). This is particularly relevant as MSC are cultured on tissue plastic and are commonly detached with enzymatic methods which may cleave surface CCR prior to *in vivo* delivery (Lubis *et al.*, 2011). Certainly surface receptor expression and function on leukocytes alters according to the way they are handled *ex vivo* and this can have an effect on their subsequent adherence to endothelium (Faint *et al.*, 2011). However, there has been no comprehensive study of the impact of different methods of MSC detachment on the functionality, viability and homing ability of the cells (Frith *et al.*, 2010, Girdlestone *et al.*, 2009, Heng *et al.*, 2009, Liu *et al.*, 2011a).

Based on current data I hypothesise that MSC have a reproducible and robust chemokine receptor profile but as these receptors are susceptible to proteolytic degradation, enzymatic dissociation methods may reduce surface CCR expression leaving them undetectable. Although non enzymatic detachment methods may preserve receptor expression, there is a significant lack of data reporting the effects of the less commonly used non enzymatic detachment methods on MSC properties such as tri-lineage potential and immunotherapy. I predict that non enzymatic methods may, as reported, reduce viability and alter MSC

properties through increased levels of stress and damage to the cells. A comparison of non enzymatic detachment methods may yield a method which is least detrimental to MSC upon dissociation.

Therefore, in this chapter, we specifically considered how culture and detachment of MSC may alter their cell surface CCR expression and whether cell processing could influence the targeting of intravenously administered cells to injured organs. We also documented how preparation techniques may alter receptor expression and also affect viability, multipotency, immunomodulatory and migratory properties. These investigations will have important implications for the design of methodologies for applications.

The aims of this chapter were:

- (i) To identify the most appropriate method to detach viable MSC from tissue culture plastic while maintaining functional cell surface CCR expression.
- (ii) To assess the effects of the detachment method on MSC tri lineage differentiation.
- (iii) To measure the effects of detachment on the immunosuppressive properties of MSC.

## **3.2 Results**

### **3.2.1 MSC express high levels of intracellular CCR but negligible levels of cell surface CCR when in suspension.**

Intracellular and cell surface CCR expression was measured on enzymatically detached MSC from tissue culture plastic using flow cytometry. High proportions of MSC expressed intracellular CCR4, CXCR3 and CCR5 (Figure 3.1A) but cell surface expression of all CCR we investigated (CCR1-10, CXCR1-7) was negligible and often absent (Figure 3.1B). To investigate whether CCR expression changed in response to cell passage, intracellular and cell surface CCR expression was measured at P2, P4 and P6. Intracellular CCR4, CCR5 and CXCR3 were detectable at all passages (Figure 3.2A) but cell surface CCR was negligible (Figure 3.2B). Furthermore, stimulation of MSC with inflammatory cytokines, TNF $\alpha$  and IFN $\gamma$ , had no effect on receptor expression and cell surface CCR levels remained absent or negligible (Figure 3.2C). Cytokine efficacy was confirmed by treatment of positive control cells. TNF $\alpha$  stimulation of HSEC increased cell surface VCAM-1 expression (Figure 3.2E) and IFN $\gamma$  stimulation increased CD40 in a hepatoma cell line (PLC/PRF/5 Alexander, Figure 3.2D). To assess whether cell detachment altered CCR receptor expression adherent MSC were stimulated with cytokines and pre-labelled with CCR antibodies in culture and fixed with PFA. If MSC were then detached using TrypLE they still did not express any surface CCR (Figure 3.3A and B). Of note, although serum was identified as a potential mediator of CCR internalisation in previous data (Figure 3.1A and 3.1B), expression upon cells under serum-free culture conditions was similar to MSC tested in serum culture conditions (Figure 3.3A and B). Similarly when MSC were stimulated with TNF $\alpha$  and IFN $\gamma$  in culture with and

without serum little expression was evident (Figure 3.4A and B). A small shift was noted in the absence of serum but back gating the positive population onto the MSC dot plot histogram suggested localisation on a dead cell population, or due to debris and not upon the viable MSC population (Figure 3.4C). Importantly use of non enzymatic means (CDB) to detach cells resulted in much higher surface CCR levels (Figure 3.5A), although use of a viability marker to exclude non viable cells reduced the signal somewhat (Figure 3.5B). Nevertheless a population of viable cells expressing cell surface CCR was evident (Figure 3.5C).

### Figure 3.1: Surface and intracellular CCR expression by MSC

Representative flow cytometry plots of A: Permeabilised MSC (gate R1) and B: Non-permeabilised MSC (gate R1). Representative flow cytometry histograms for, A: intracellular and, B: cell surface CCR4, CCR5, CXCR3 (green) compared to Isotype-matched negative control (red). Representative of n=3 donors, cells were detached using TrypLE.

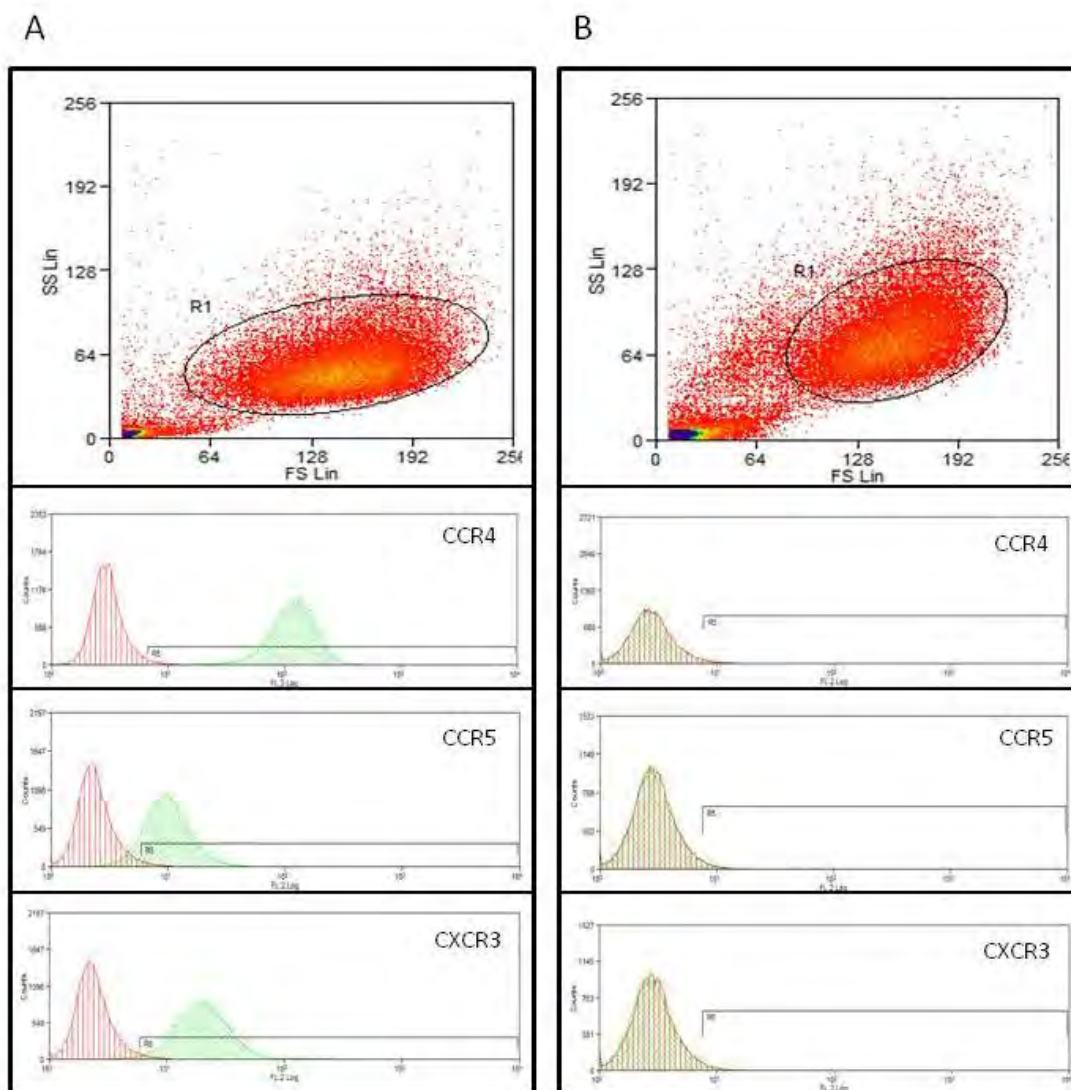
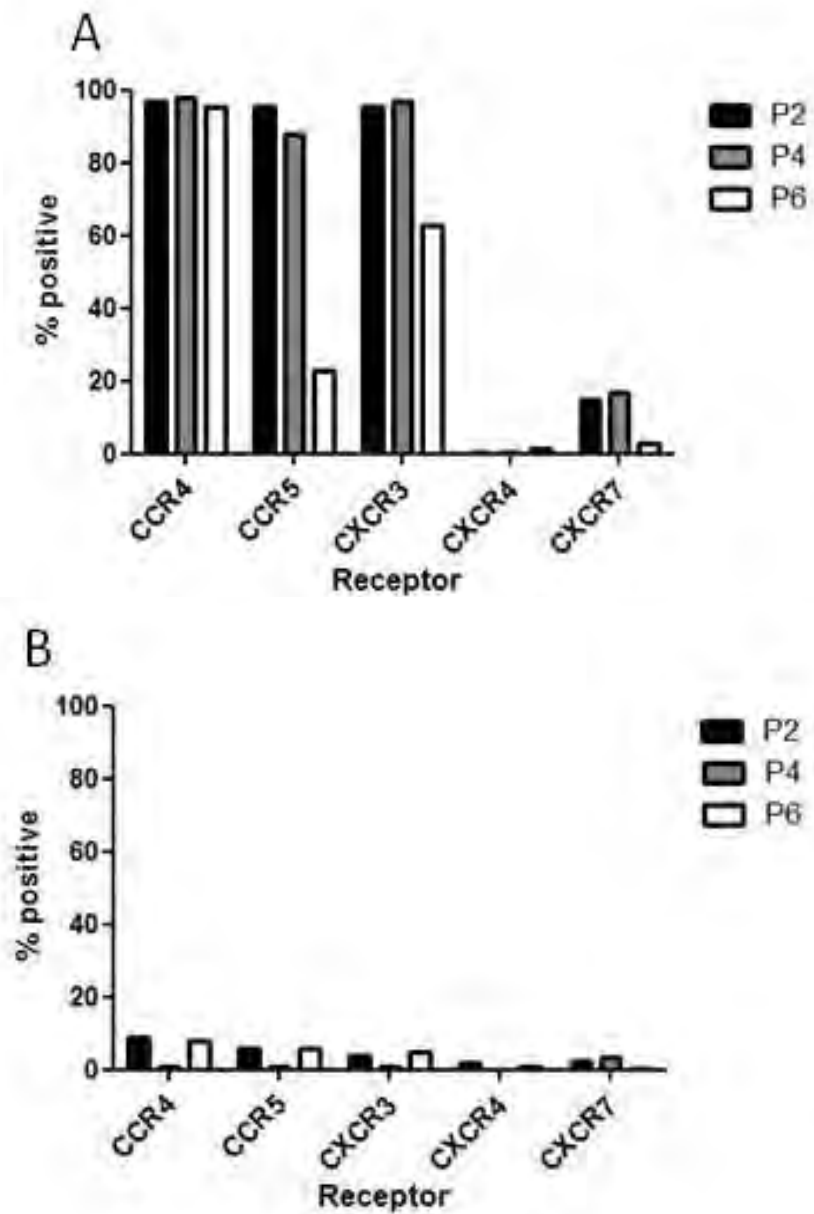
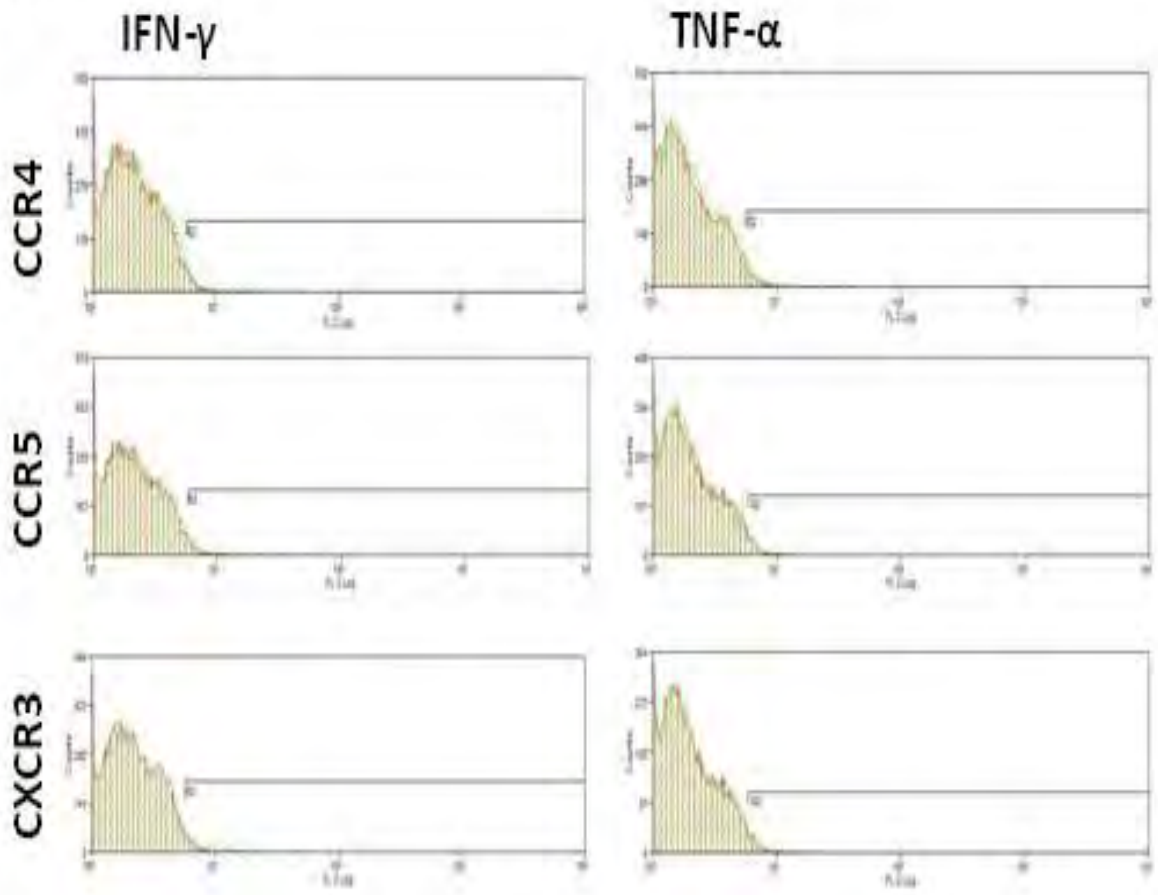


**Figure 3.2: Effect of passage and cytokine stimulation upon MSC surface CCR expression.**

Flow cytometry analysis for CCR4, CCR5 and CXCR3, expressed as, A: percentage of MSC positive for intracellular CCR expression at passage 2, 4 and 6; and B: percentage of MSC positive for surface CCR expression at passage 2, 4 and 6. Bars represent n=1 donor. C: Representative flow cytometry histograms of CCR4, CCR5, CXCR3 (green) expression compared to immunoglobulin matched negative control (red) after TNF $\alpha$  (10ng/ml) and IFN $\gamma$  (25ng/ml) stimulation. D: Representative flow cytometry histogram of VCAM-1 expression on unstimulated (red) and stimulated HSEC (green) compared to an isotype-matched negative control (blue). E: Representative flow cytometry histogram of CD40 expression on unstimulated and TNF $\alpha$  stimulated hepatoma cell line (PLC/PRF/5 Alexander: green) compared to an isotype-matched negative control (red). Representative of n=3 donors.



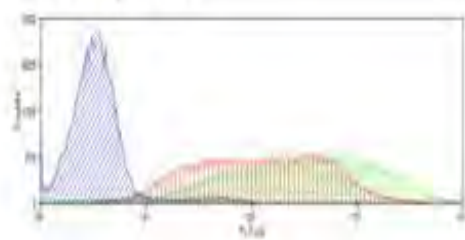
C





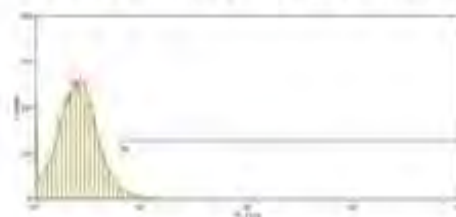
D

IFN- $\gamma$  Test



E

TNF- $\alpha$  Test: Unstimulated



TNF- $\alpha$  Test: Stimulated

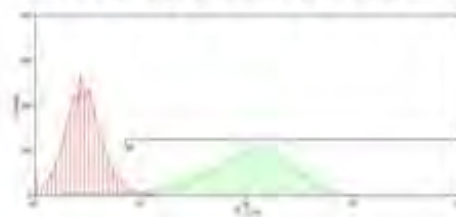
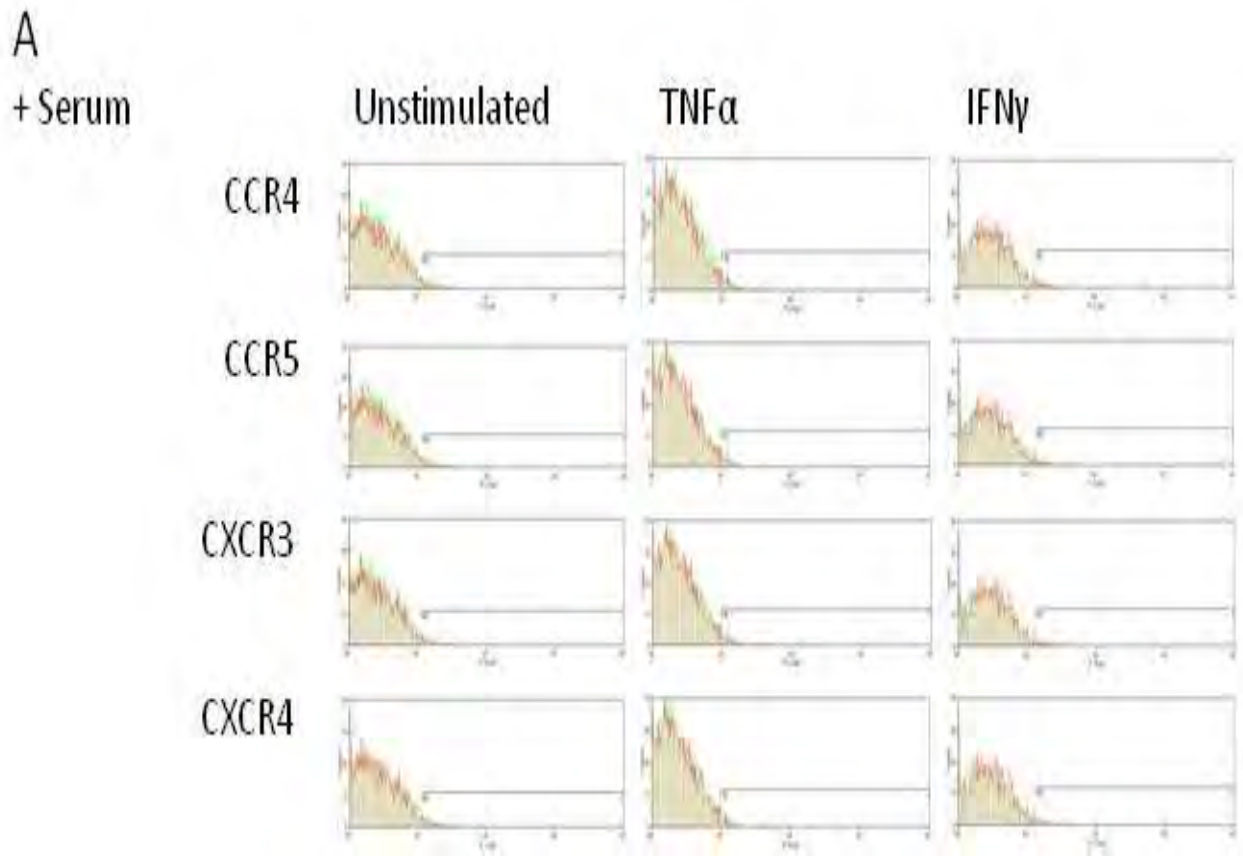


**Figure 3.3: Pre-labelling and fixation of cells, and treatment in absence of serum do not alter surface chemokine expression.**

Representative flow cytometry histograms of pre-detachment, antibody labelled and PFA fixed MSC surface CCR4, CCR5, CXCR3, CXCR4 expression (green) on unstimulated, TNF $\alpha$  and IFN $\gamma$  stimulated MSC compared to isotype matched negative control (red) in the A: presence and B: absence of serum. Representative of n=3 donors.



**B**  
- Serum

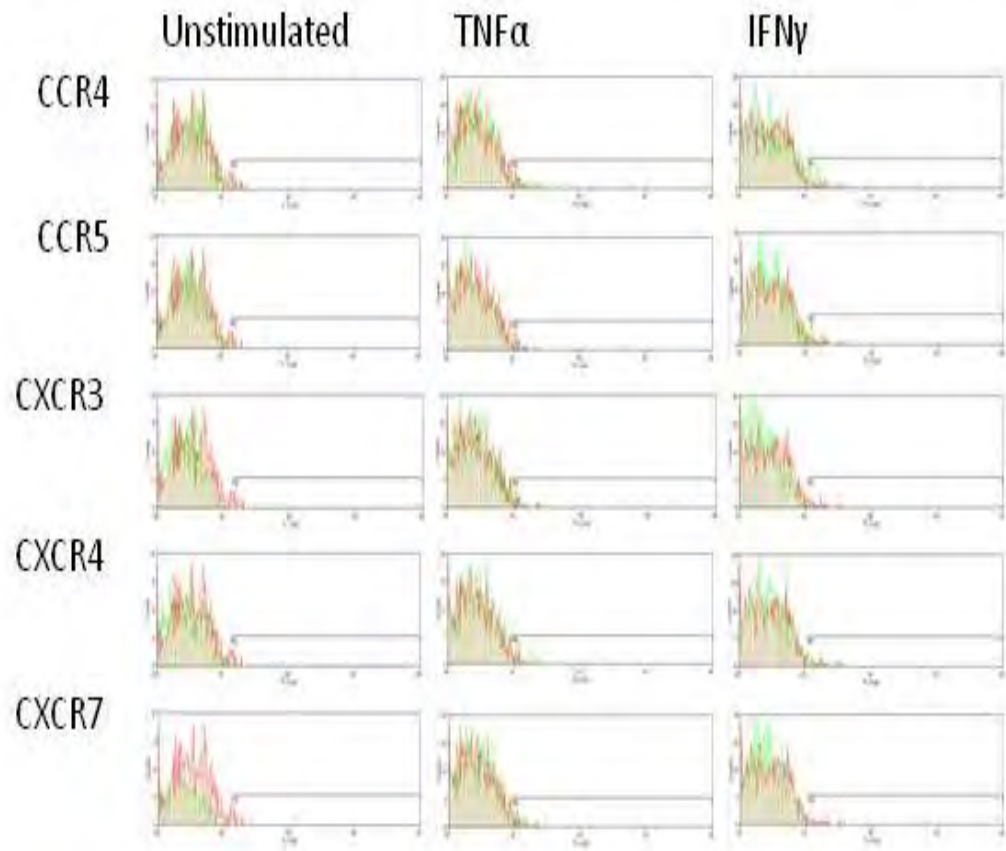
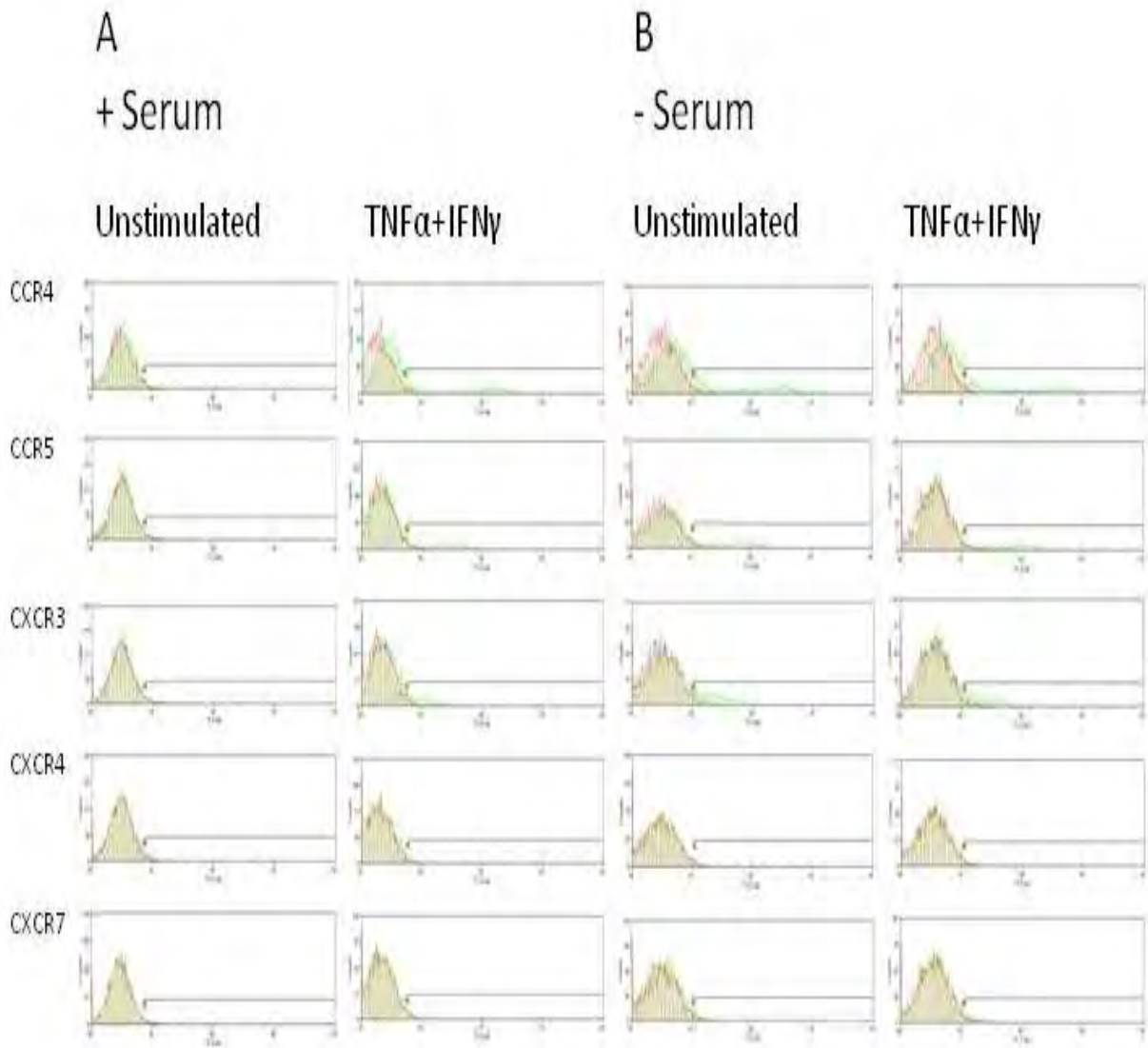


**Figure 3.4: The effect of serum on MSC surface receptor expression after cytokine stimulation.**

Representative flow cytometry histograms of MSC surface CCR4, CCR5, CXCR3, CXCR4 (green) on unstimulated, TNF $\alpha$  and IFN $\gamma$  stimulated MSC compared to isotype matched negative control (red) in the A: presence and B: absence of serum. C: Representative flow cytometry plot of MSC (gate R8) of surface CCR positive (blue) and negative (red) MSC population with representative flow cytometry histograms of CCR4, CCR5 and CXCR3 positive cells (blue). Representative of n=3 donors.



C

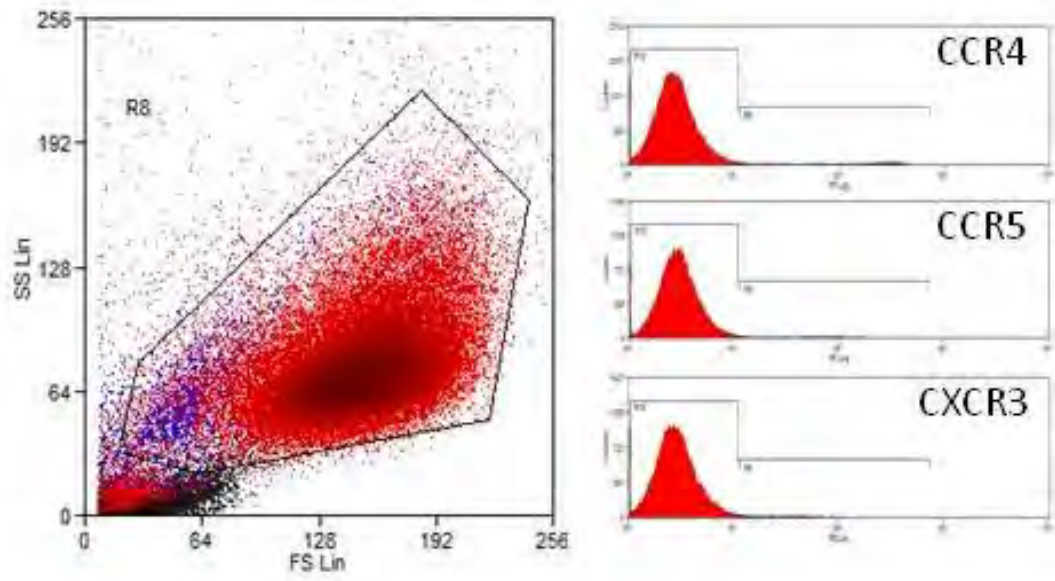
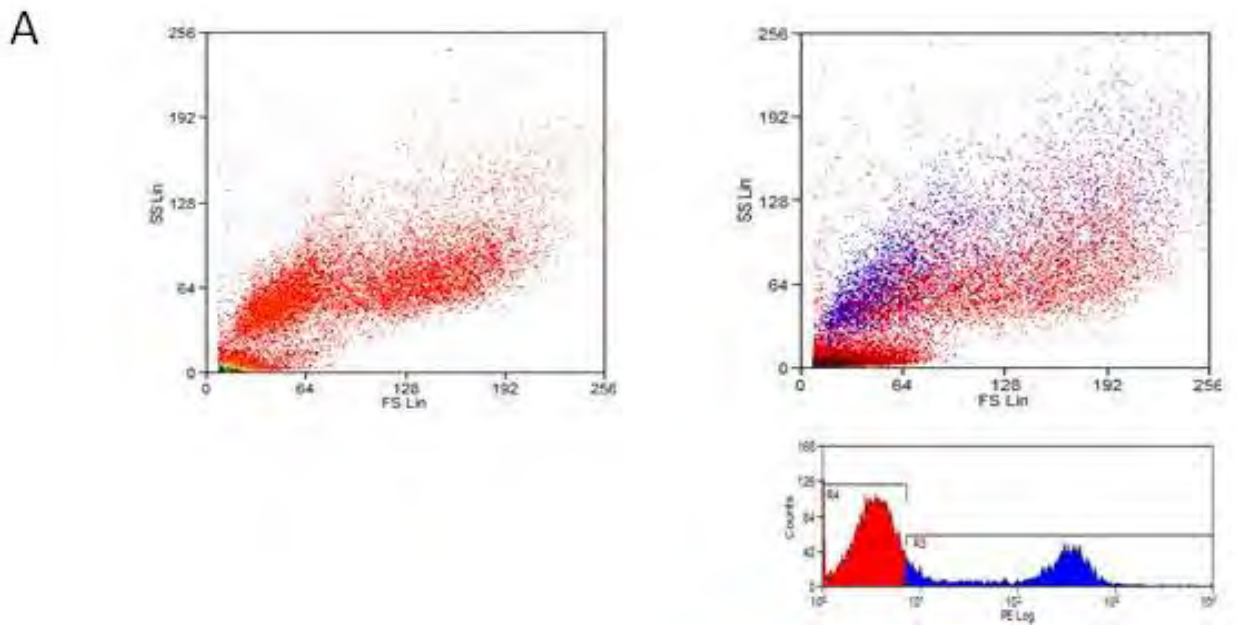
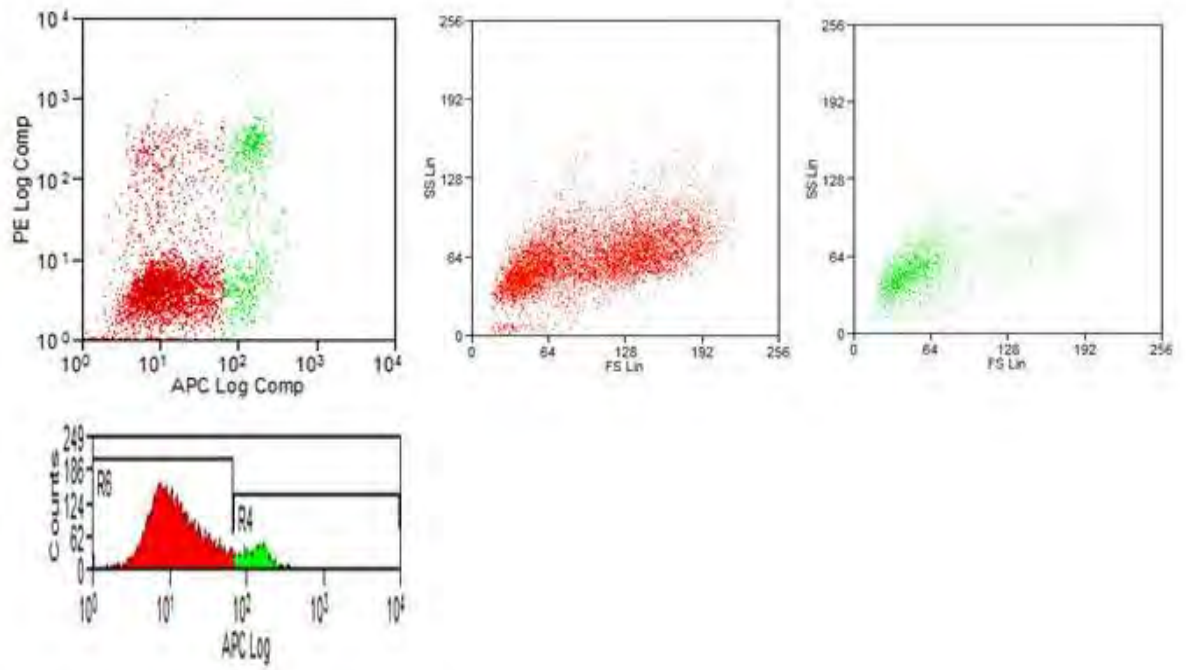


**Figure 3.5: Expression of surface CCR on viable cells after CDB detachment.**

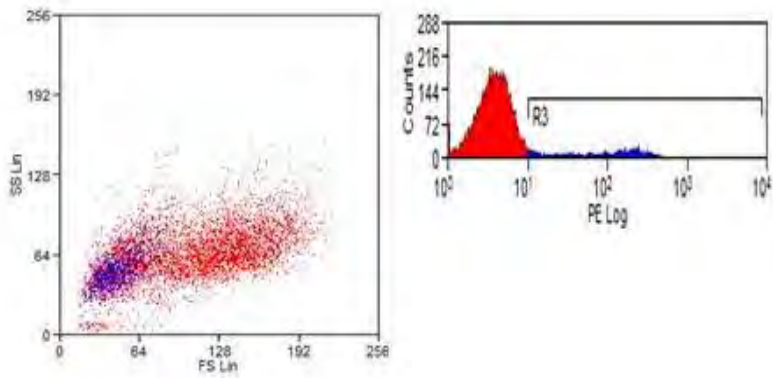
A: Representative flow cytometry plots of MSC detached with CDB (red) and CCR4 expressing MSC (blue). B: Representative flow plots of MSC detached with CDB (red) and labelled with a fixable viability marker to identify non viable MSC (green). C: Representative flow cytometry plots of viable MSC after CDB detachment expressing cell surface CCR4 (blue). Representative of n=3 donors.



B



C



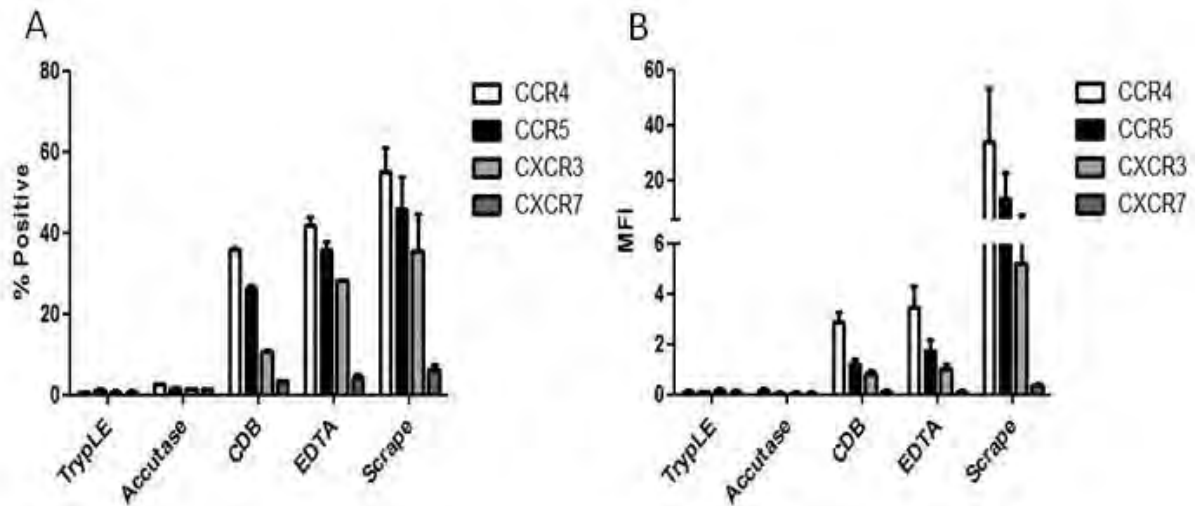
### **3.2.2 Non-enzymatic detachment preserves functionally active cell surface CCR expression on MSC**

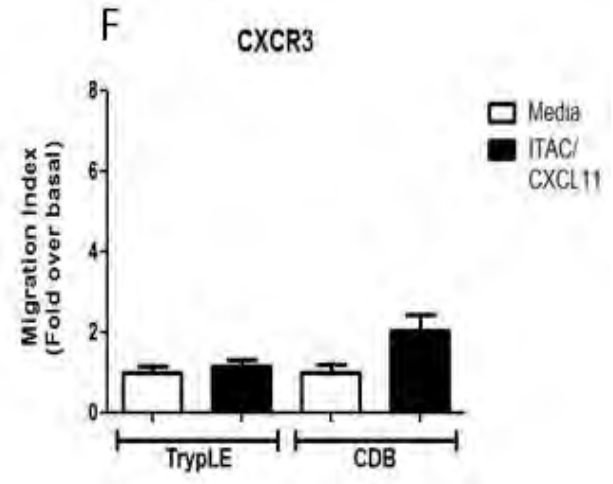
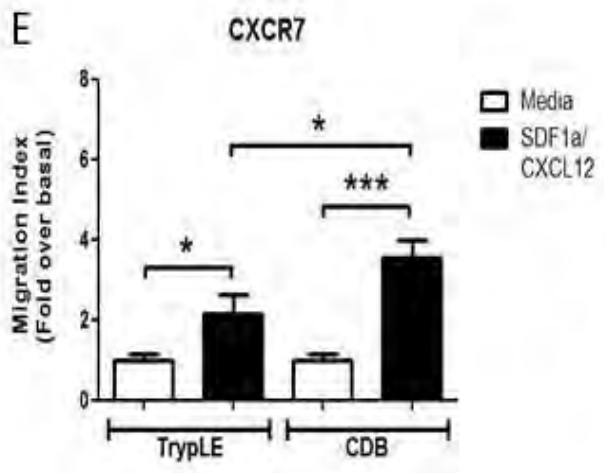
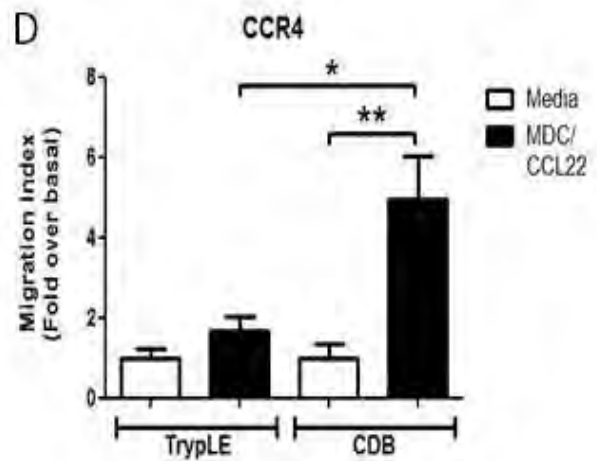
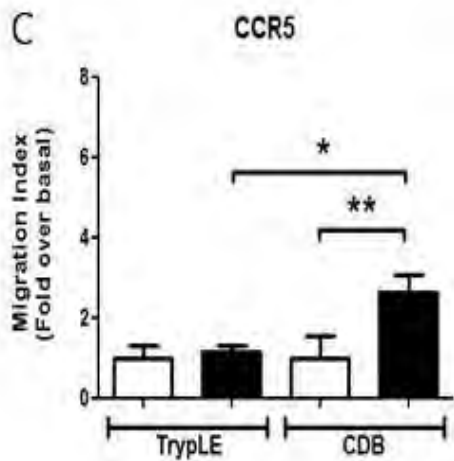
Enzymatically detached MSC had very low CCR expression on their cell surface, with less than 2.5% of cells positive for the CCR tested (Figure 3.6A) and those present had very low median channel fluorescence values (Figure 3.6B). In contrast, cells detached non-enzymatically had significantly higher CCR expression and MFI, with the highest levels seen in cells detached by scraping. After detachment by scraping MSC were; 55.25±5.878% positive for CCR4, 46±7.782% for CCR5, 35.28±9.387% for CXCR3 and 6.25±1.187% positive for CXCR7 (Figure 3.6A and B). 35.8±0.494% MSC detached with CDB were positive for CCR4, 26.24±0.658% for CCR5, 10.65±0.518% for CXCR3 and 3.31±0.198% for CXCR7 (Figure 3.6A and B). Of the non-enzymatic detachment methods CDB offered the best compromise of retention of CCR expression and cell viability. Hence this method was compared with TrypLE (as the most effective enzymatic detachment method) to assess the functional status of CCR on MSC. There was significantly improved migration of cells detached using CDB towards CCL22 (4.944±1.098 vs. 1.667±0.3630) ( $p<0.05$ ), CXCL12 (3.528±0.4739 vs. 2.133±0.5051) ( $p<0.05$ ) and CCL4 (2.643±0.4320 vs. 1.161±0.1385) ( $p<0.05$ ), as compared with TrypLE. A trend for improved migration of cells detached using CDB was observed, with approximately twice as many cells transmigrating towards CXCL11, however this response was not statistically significant (Figure 3.6C-F).



**Figure 3.6: Expression and function of CCR expression of MSC after non enzymatic detachment.**

Flow cytometry analysis for CCR4, CCR5, CXCR3 and CXCR7 expressed as, A: percentage of MSC positive for surface CCR expression, B: median fluorescence intensity (MFI) of MSC. Bars represent mean  $\pm$  SEM of n=3 donor samples. Migration of MSC to C: RANTES/ CCL22 (CCR5 ligand) (500ng/ml), D: MDC/ CCL5 (CCR4 ligand) (500ng/ml), E: SDF1a/ CXCL12 (CXCR7 ligand) (50ng/ml) and F: ITAC/ CXCL11 (CXCR3 ligand) (500ng/ml) normalised to control/ basal (serum free media only) was assessed by Boyden Chamber assays. Optimal concentrations for migration were found by dose response curves. Data is expressed as fold over basal migration. Bars represent mean  $\pm$  SEM of n=3 donor samples, \*, p<0.05; \*\*, p<0.01; \*\*\*, p<0.001.





### **3.2.3 MSC viability, re-plating ability and proliferation in culture are altered according to detachment methodology.**

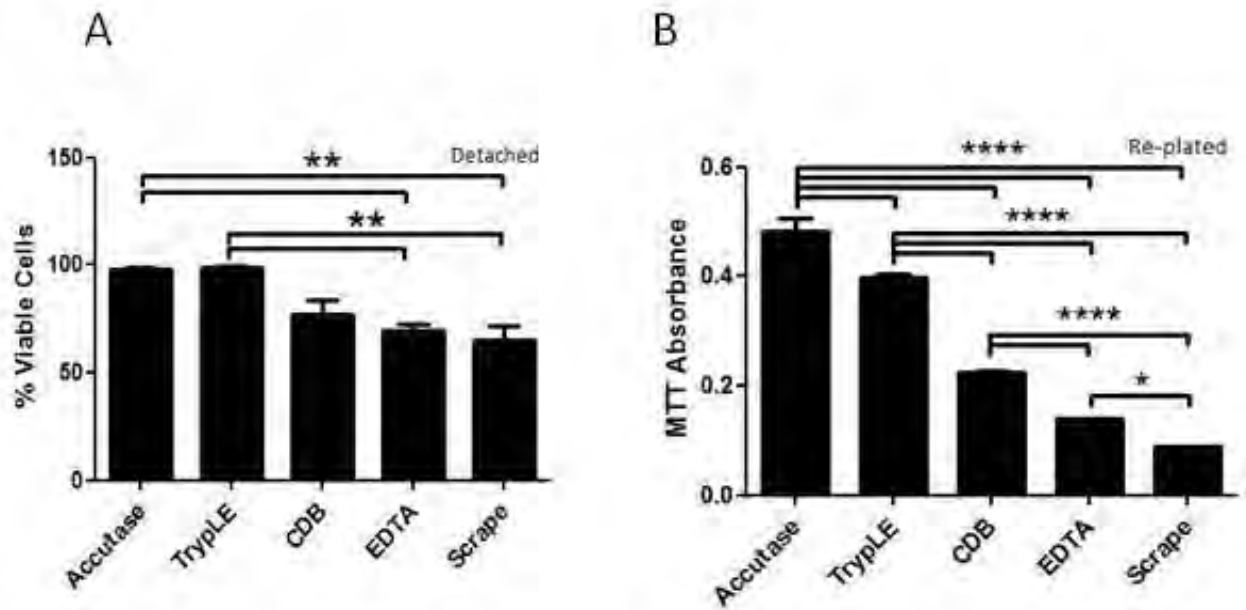
Cultured Human MSC were detached from cell culture plastic using a range of enzymatic and non-enzymatic methods. Viability was best retained following detachment with enzymatic methods TrypLE ( $98.38 \pm 0.89\%$ ) and Accutase ( $98.35 \pm 0.37\%$ ) as depicted in Figure 3.7A. Of the non-enzymatic detachment methods EDTA ( $69.32 \pm 3.2\%$ ) and cell scraping ( $64.78 \pm 6.67\%$ ) demonstrated the greatest reduction in viability immediately after detachment ( $p < 0.001$ ). Similarly CDB caused a reduction in MSC viability ( $77.29 \pm 6.51\%$ ). In view of the findings of altered viability following detachment we sought to determine whether this would have an impact on the ability of MSC to re-plate and proliferate. Following detachment MSC were re-plated and functionally viable numbers remaining bound after 24 hours were quantified by measuring their ability to reduce MTT. Enzymatic detachment resulted in higher levels of MTT signal suggesting greater numbers of bound MSC (MTT absorbance values; TrypLE,  $0.397 \pm 0.008$  and Accutase,  $0.483 \pm 0.0218$  after 24 hours in culture (Figure 3.7B), compared to non-enzymatic detachment (CDB  $0.225 \pm 0.003$ , EDTA  $0.140 \pm 0.001$ , and by scraping  $0.089 \pm 0.001$ ).

Altered viability following detachment and re-plating was accompanied by changes in morphological appearance. MSC re-plated after detachment with enzymatic methods retained spindle-shaped fibroblast-like morphology, typical of MSC (Figure 3.8A(i) and (ii)), whereas, MSC detached by EDTA and scraping exhibited quite different morphology with most cells taking on a retracted, circular shape, similar to dying cells with large gaps between cells (Figure 3.8A(iii) and (iv)). Notably, MSC detached with CDB mostly retained typical MSC-

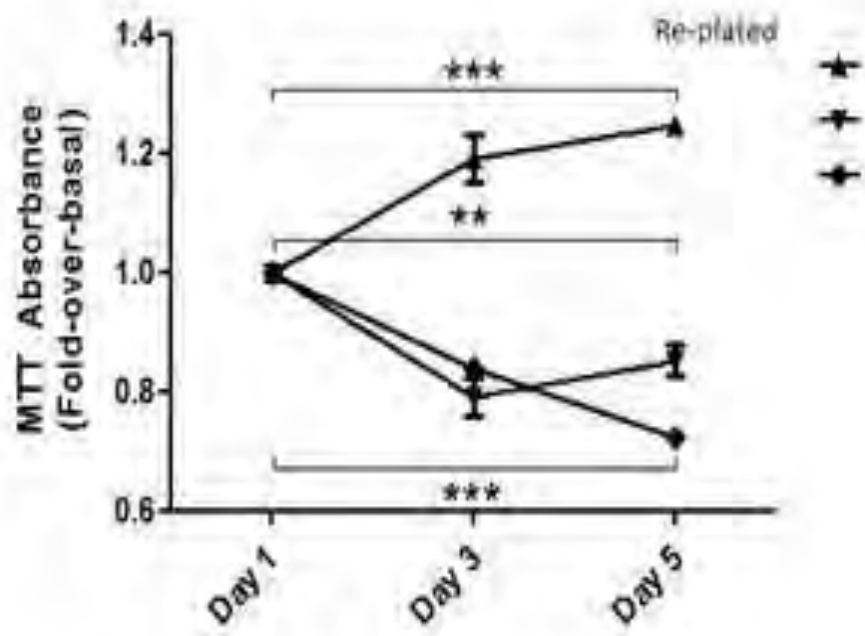
like morphology (Figure 8B(ii)) and proliferated to confluence after re-plating ( $p < 0.001$ ) (Figure 3.7C). In contrast, MSC detached using other non enzymatic methods (EDTA/scraping) showed no proliferation after 5 days in culture, coupled with a decline in viable cells (EDTA ( $p < 0.01$ )/ scraping ( $p < 0.001$ ), possibly as a result of cell death and detachment in culture (Figure 7B and C). However enzymatically recovered cells showed higher viability upon re-plating thus quickly reaching confluence and causing cell numbers to plateau (Figure 3.7D).

**Figure 3.7: Measurement of MSC viability and growth of re-plated cells.**

A: MSC viability after detachment from tissue culture plastic measured using flow cytometry staining for live/ dead cell marker. Bars represent mean  $\pm$  SEM of n=3 different donor samples; \*\*, p<0.01. B: Cell viability by MTT analysis of re-plated cells after 24 hours, expressed as an MTT absorbance value. Bars represent mean  $\pm$  SEM of n=3 samples, \*, p<0.05; \*\*\*\*, p<0.0001. C: Cell proliferation indicated by fold change in cell viability after 3 and 5 days measured by MTT assay from basal MTT readings at 24 hours culture of re-plated cells after non enzymatic detachment and after, D: enzymatic detachment methods. Data represent mean  $\pm$  SEM of n=3 samples, \*\*, p<0.01; \*\*\*, p<0.001.



C



D

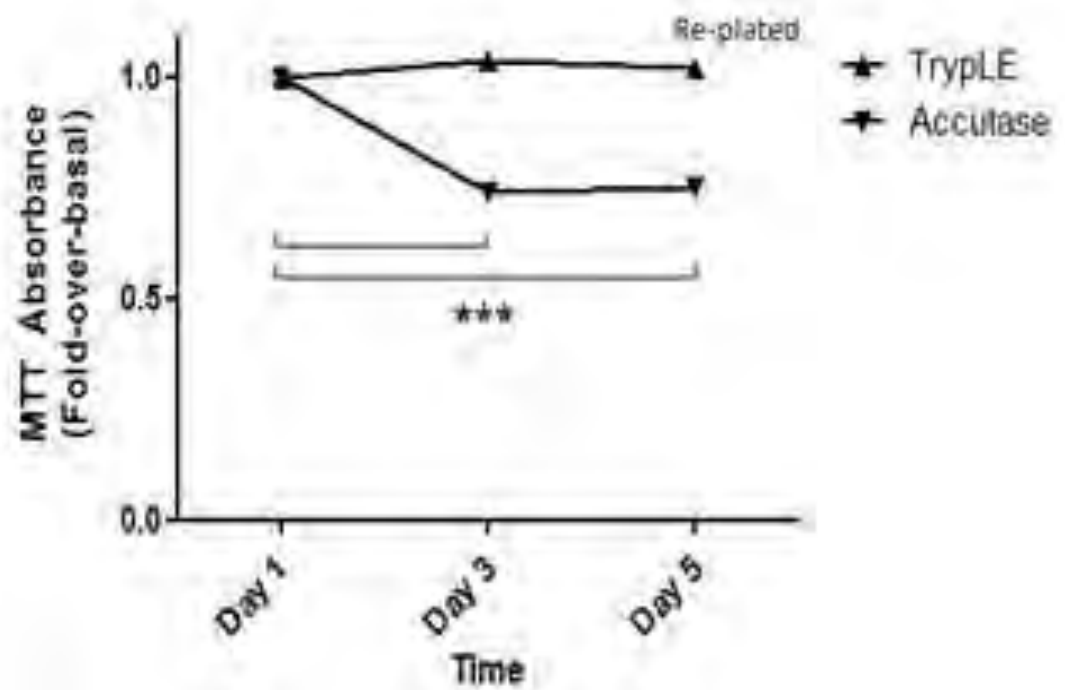
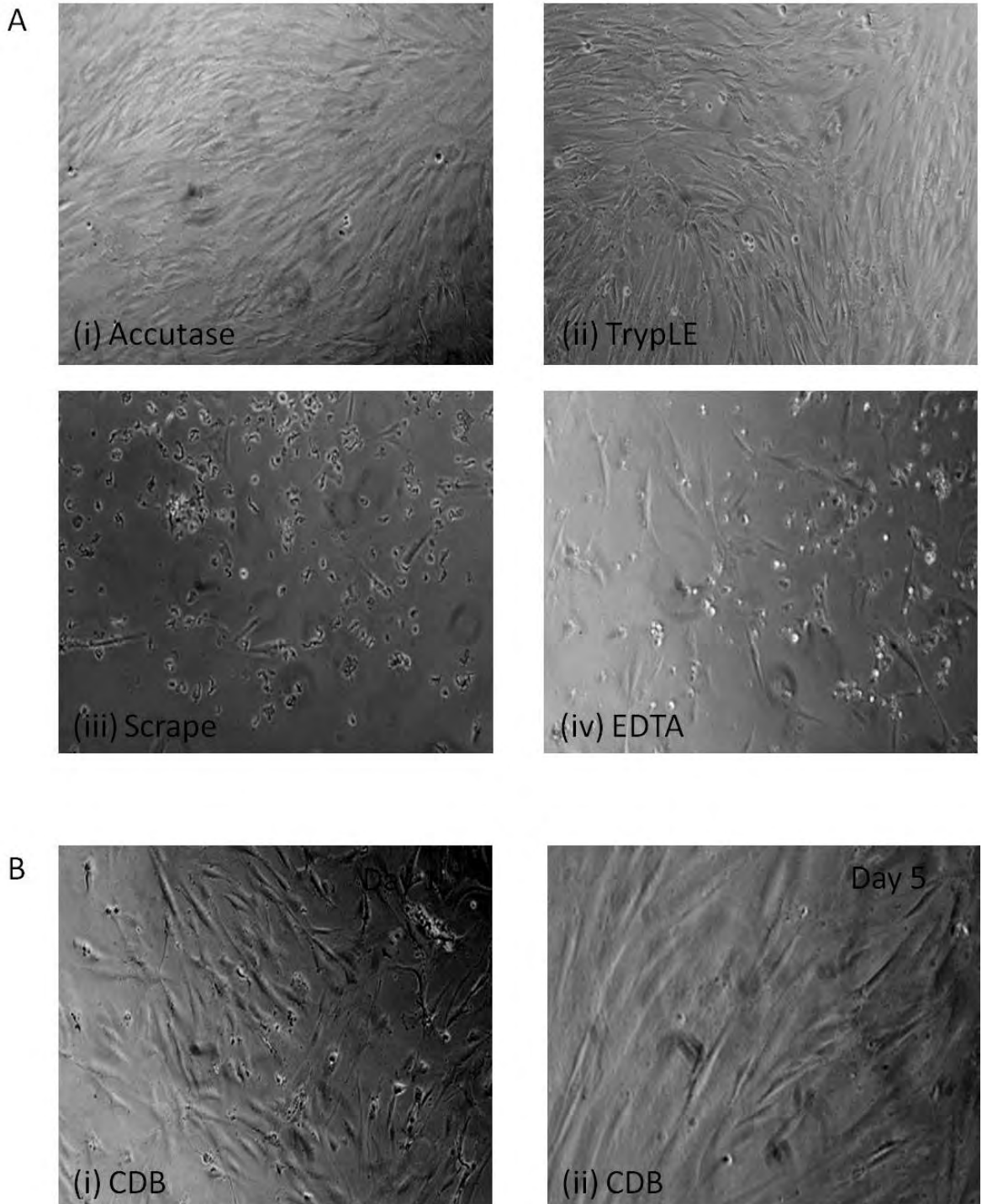


**Figure 3.8: Morphology of re-plated MSC on tissue culture plastic.**

A: Representative images of re-plated MSC 24 hours after detachment with (i) Accutase, (ii) TrypLE, (iii) EDTA and (iv) Scraping; n=3 samples. B: Representative images of re-plated MSC detached by CDB after (i) 24 hours, (ii) 120 hours; n=3 samples. Original magnification x10, images captured using phase contrast microscopy.



### **3.2.4 Non-enzymatic detachment with CDB results in increased autophagy as a response to increased cellular stress.**

To determine why of the non-enzymatic methods used to detach MSC, only CDB was associated with subsequent viable expansion, the presence of cellular survival strategies such as autophagy were examined. We observed that,  $13.77 \pm 0.81\%$ , ( $p < 0.0001$  compared to cells only, unlabelled control) of MSC detached with CDB underwent autophagy (Figure 3.9A) compared with much lower levels for all other detachment methods (EDTA,  $3.00 \pm 0.71\%$ , and cell scraping,  $2.39 \pm 0.74\%$ ). To better understand the impact of detachment method on cellular stress, intracellular reactive oxygen species, and levels of apoptosis & necrosis were also measured. Based on our earlier data, this analysis was focussed on the most effective detachment methods (TrypLE and CDB). MSC detached with CDB exhibited higher levels of autophagy (MFI:  $18.06 \pm 1.39$  vs.  $11.59 \pm 0.97$  ( $p < 0.05$ ), Figure 3.9B) and intracellular reactive oxygen species (MFI:  $200.7 \pm 1.09$  vs.  $180 \pm 19.24$ , Figure 3.9B) compared with TrypLE detached MSC. In addition, CDB detached MSC displayed a corresponding increase in apoptosis (MFI:  $10.39 \pm 1.16$  vs.  $8.35 \pm 1.6$ , Figure 3.9B) and necrosis (MFI:  $11.74 \pm 1.1$  vs.  $10.04 \pm 1.34$ , Figure 3.9B) compared with values seen following TrypLE detachment.

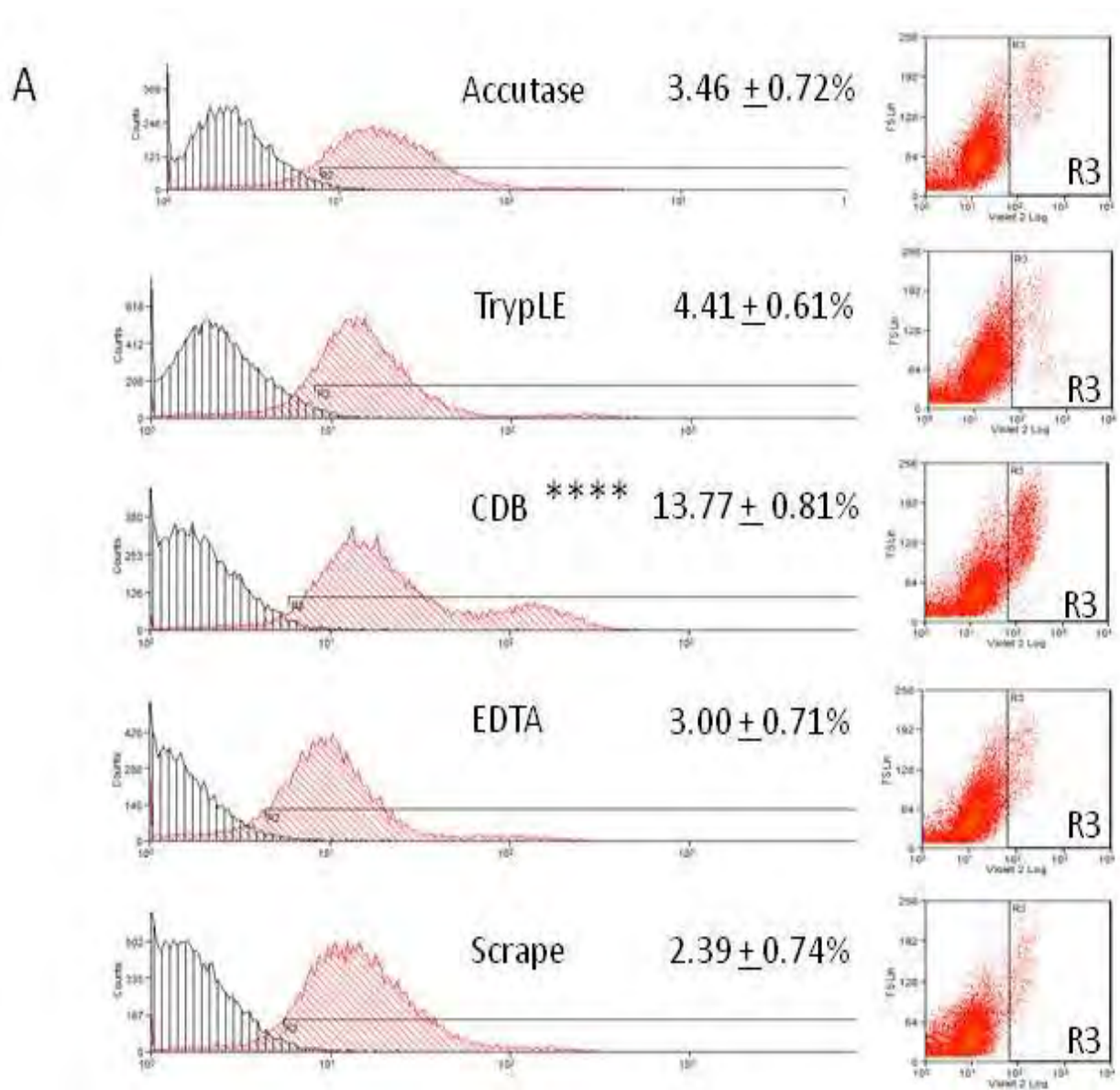
Addition of serum during CDB detachment and subsequent washing steps resulted in a marked increase in viable MSC numbers re-plating at day 1 (MTT absorbance values; serum<sup>+</sup> v serum<sup>-</sup>,  $0.753 \pm 0.003$  vs.  $0.210 \pm 0.001$ ). By day 5 cells proliferated significantly more when serum was used compared to cells re-plated after washing without serum (MTT absorbance values; serum<sup>+</sup> v serum<sup>-</sup>,  $1.275 \pm 0.013$  ( $p < 0.0001$ ) vs.  $0.243 \pm 0.002$  ( $p < 0.01$ )) (Figure 3.10A and B). Re-plated MSC washed with PBS alone remained in clumps and seeded sparsely



(Figure 3.10C); whereas inclusion of 1% fetal calf serum resulted in fewer, smaller clumps and the cells converged into a complete monolayer by day 5. This effect was also observed following use of slower centrifugation speeds (1500 vs. 2000 rpm) during washing (Figure 3.11A and B).

**Figure 3.9: Measurement of Autophagy in detached MSC.**

A: Representative cytometry histograms for unlabelled MSC (black) and MSC stained with autophagy marker, monodansylcadaverine-Pacific Orange (MDC-PO) (red). Representative flow cytometric plots, including unlabelled cells. Dots in gate R3 represent percentage of cells undergoing autophagy with representative cytometry histograms. Data represents mean  $\pm$  SEM of n=3 different donors, \*\*\*, p<0.0001. B: Levels of stress on TrypLE (enzymatic) and Cell Dissociation Buffer (non enzymatic) detached cells. Representative cytometry histogram for CDB detached MSC (red) and TrypLE detached MSC (black), stained with A: Autophagy marker, monodansylcadaverine (MDC), B: IROS marker, 2', 7'-dichlorofluorescein (DCF), C: Apoptosis marker, annexin V, D: Necrosis marker, 7AAD; with corresponding Median Fluorescent Intensity (MFI) values. Data represents mean  $\pm$  SEM of n=3 different donors, \*, p<0.05.



B

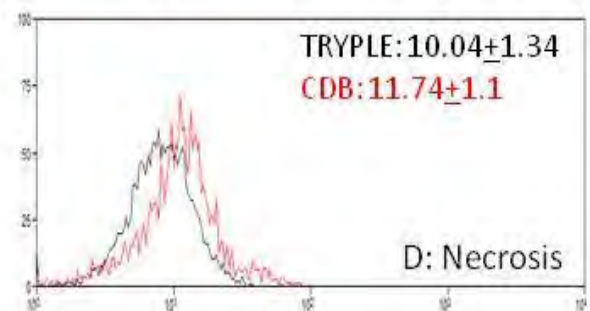
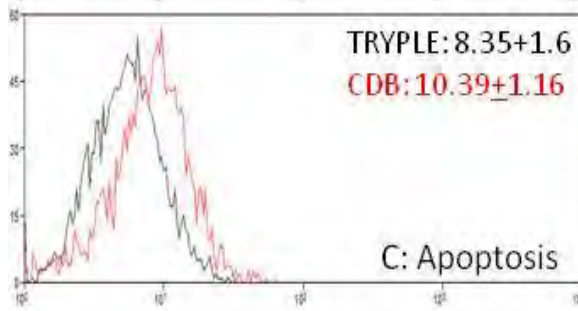
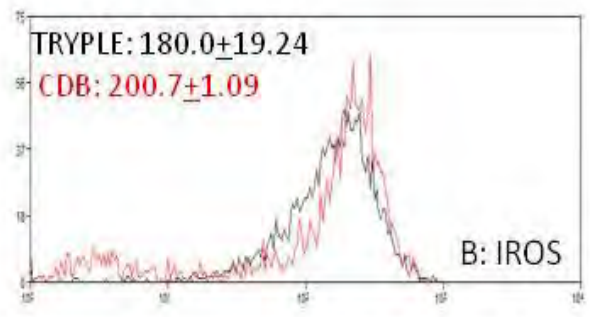
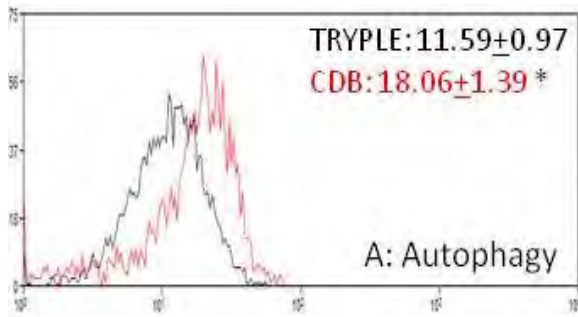
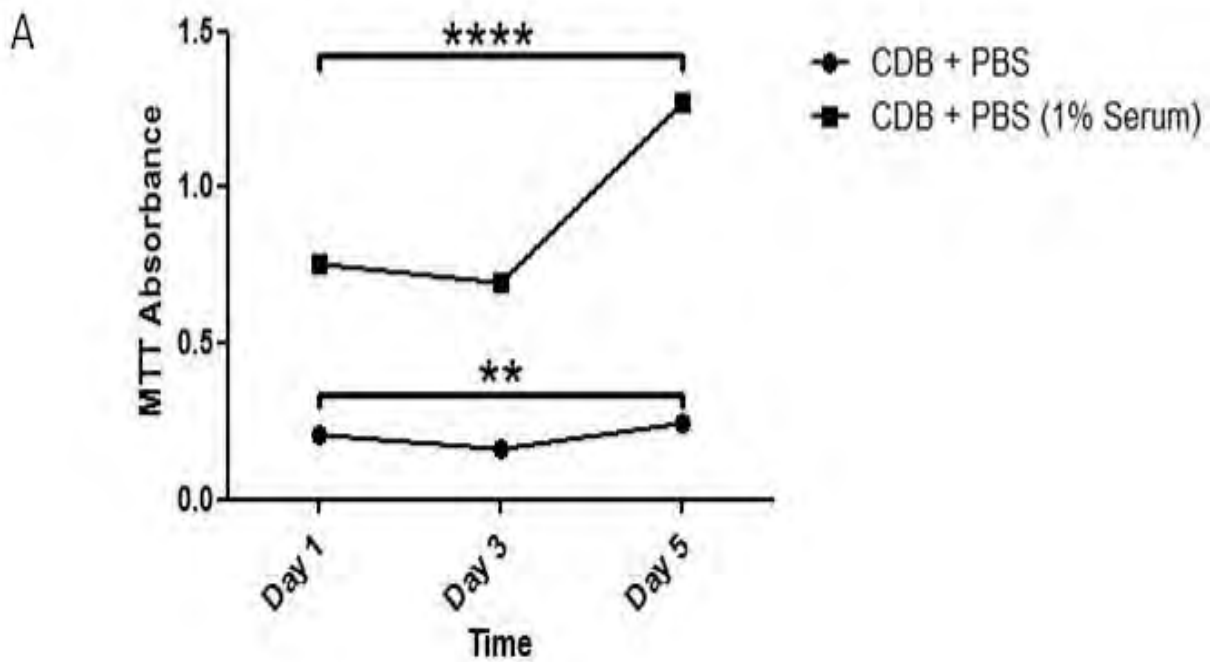


**Figure 3.10: Impact of serum supplementation on viability and proliferation of MSC detached with CDB.**

A: Cell proliferation and survival of re-plated cells indicated by absorbance of MTT after 1, 3 and 5 days measured by MTT assay after detachment with CDB and wash with PBS with or without 1% serum. Data represent mean  $\pm$  SEM of n=3 samples. \*\*, p<0.01; \*\*\*, p<0.001. B: Representative images of re-plated MSC detached with CDB and washed with PBS with or without 1% serum, taken after 1, 3 and 5 days; n=3 samples. Original magnification x10, images captured using phase contrast microscopy.

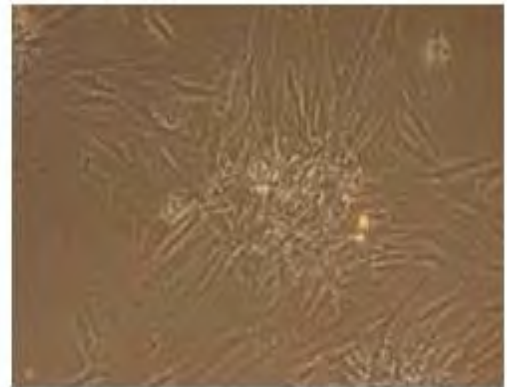


B

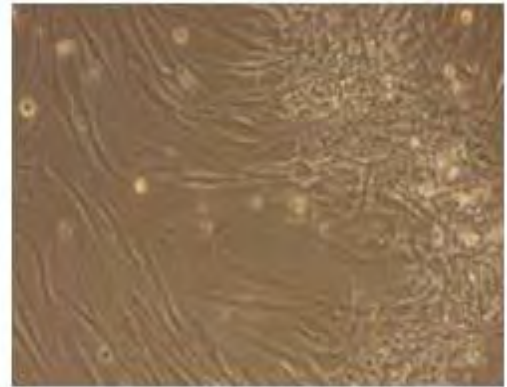
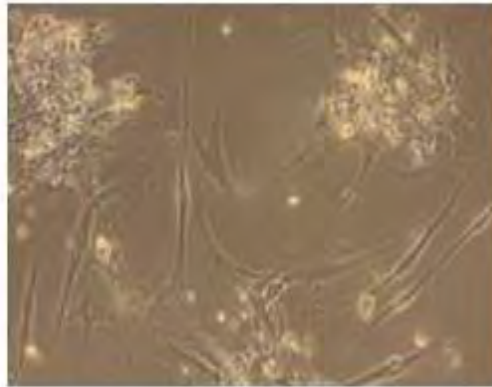
No Serum

1% Serum

Day 1



Day 3

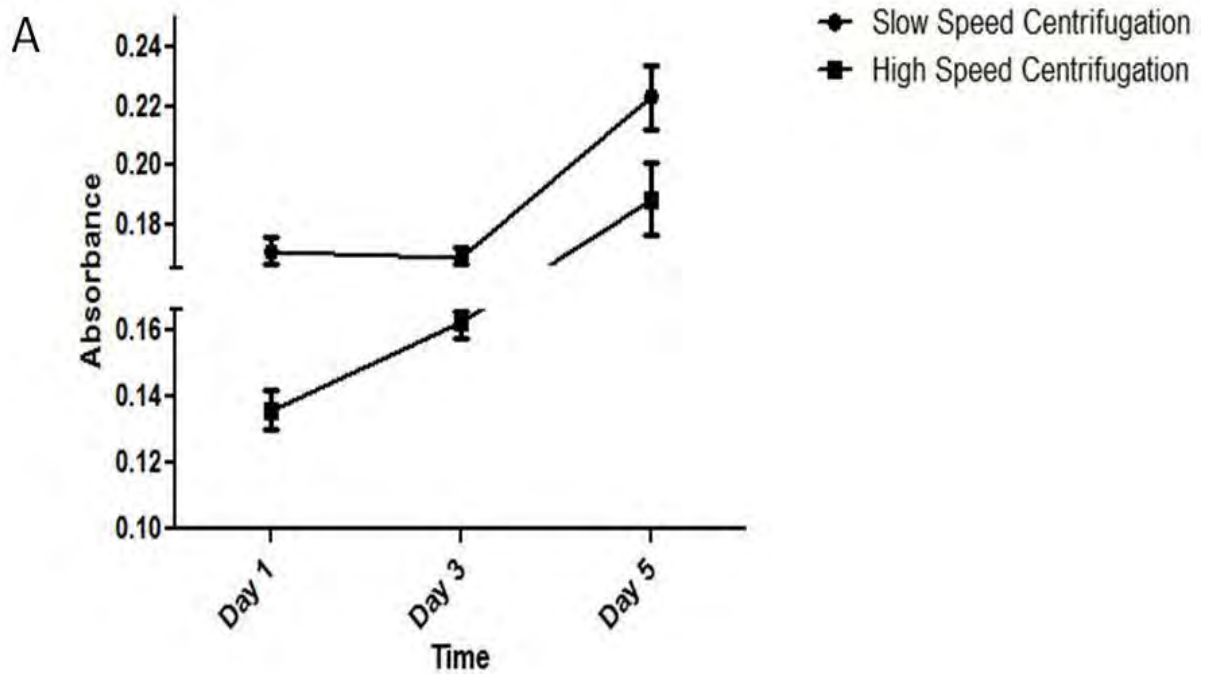


Day 5



**Figure 3.11: Impact of centrifugation speed on viability and proliferation of MSC detached with CDB.**

A: Cell proliferation and survival of re-plated cells indicated by absorbance of MTT after 1, 3 and 5 days measured by MTT assay after detachment with CDB, washed with PBS with 1% serum at high (2000RPM) and low speed (1500RPM) centrifuge. Data represent mean  $\pm$  SEM of n=3 samples. B: Representative images of re-plated MSC detached with CDB, washed with PBS 1% serum and centrifuged at high and low speeds, taken after 1, 3 and 5 days; n=3 samples. Each point represents mean  $\pm$  SEM of n=3 different donors, \*, p<0.05; \*\*, p<0.01; \*\*\*, p<0.001. Original magnification x10, images captured using phase contrast microscopy.

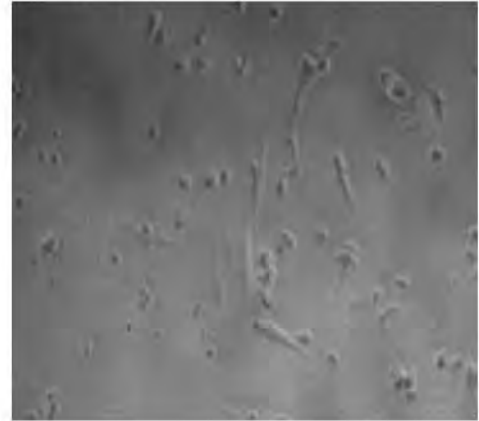
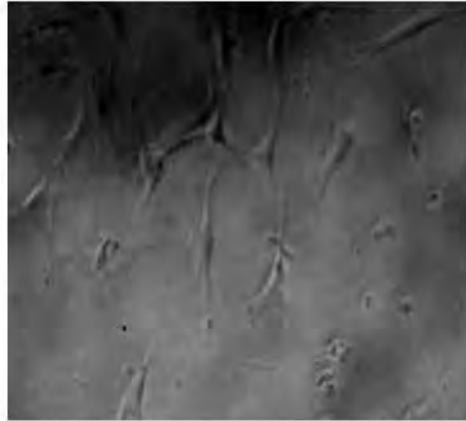


B

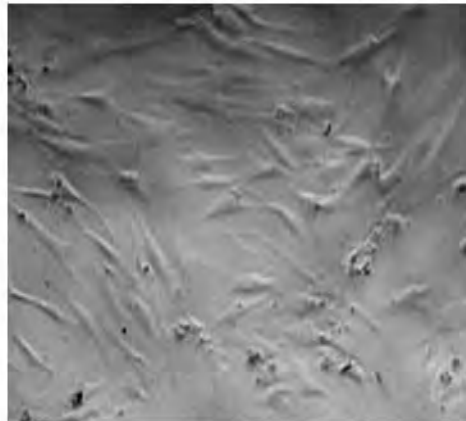
Low Speed

High Speed

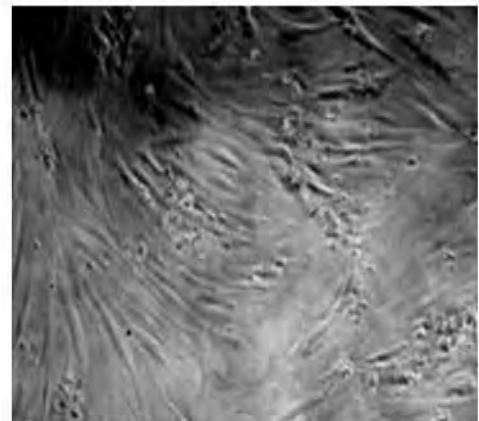
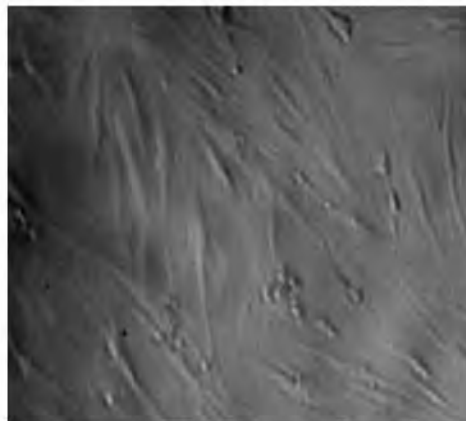
Day 1



Day 3



Day 5



### **3.2.5 Impact of detachment method on the differentiation and immunomodulatory capabilities of MSC**

Adipogenic differentiation was markedly reduced following detachment with non-enzymatic methods in particular EDTA and cell scraping (Figure 3.12A), although a degree of differentiation did occur following CDB detachment ( $p < 0.001$ ). In contrast, detachment by cell scraping resulted in a much higher calcium concentrations ( $188.3 \pm 50.92$ ,  $p < 0.05$ ), indicative of greater differentiation into osteoblasts ( $p < 0.05$ ) (Figure 3.12B). Chondrogenic differentiation seemed to be maintained in cells detached by both enzymatic (TrypLE) and non enzymatic (CDB) methods (Figure 3.12C).

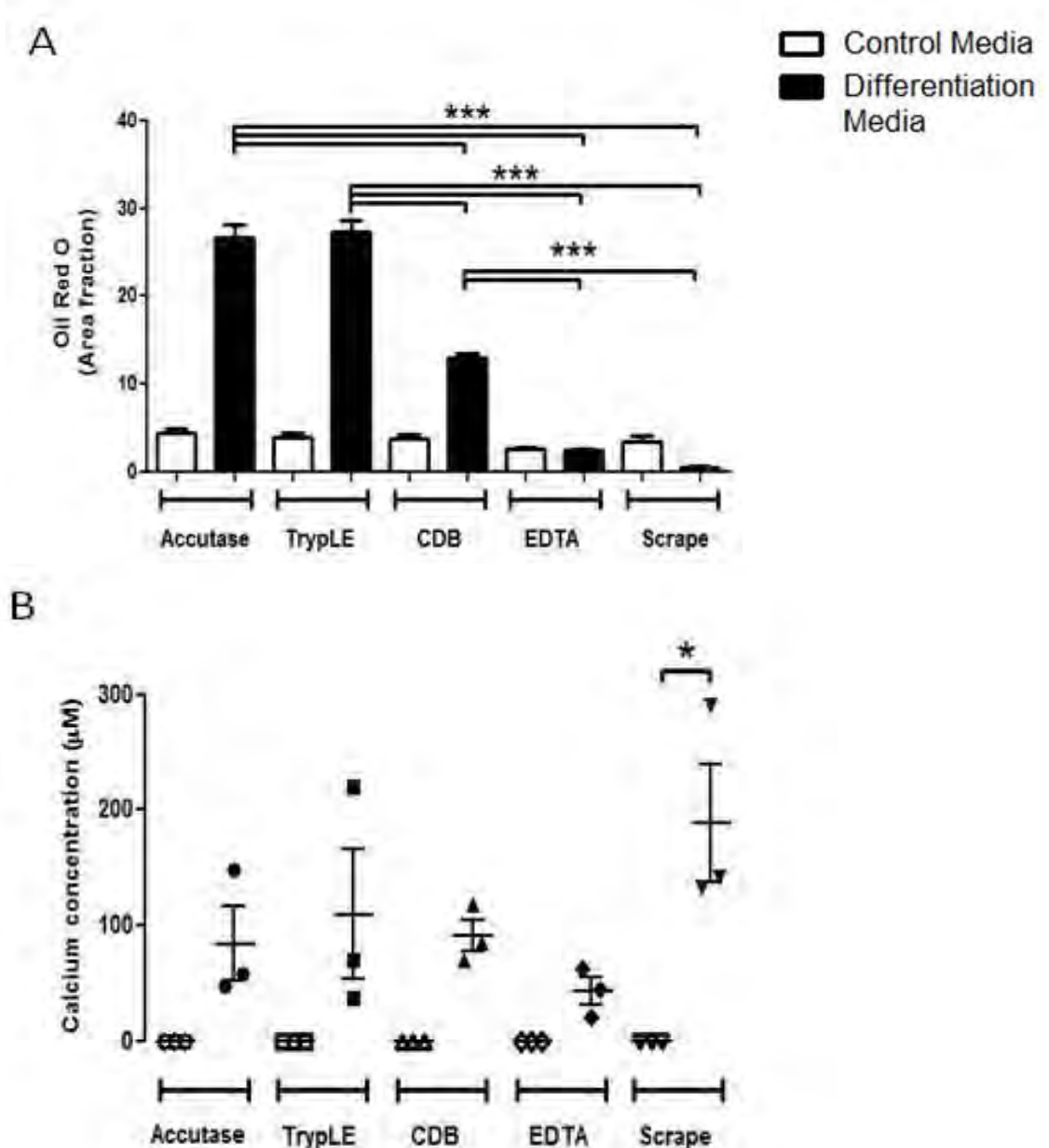
Proliferation of activated  $CD3^+CD4^+CD25^-$  T effector cells (Figure 3.13) has been shown to be suppressed by co-culture with MSC. Indeed, MSC detached with both TrypLE and CDB are able to significantly suppress activated  $CD3^+CD4^+CD25^-$  T effector cell proliferation when co-cultured at a ratio of 1:5 (Figure 3.14A and B). T effector cells cultured without MSC proliferated to  $3271 \pm 146.1$  cells/ $\mu$ l and  $3221 \pm 101.2$  cells/ $\mu$ l but were significantly suppressed at a ratio of 1:5 in the TrypLE ( $1540 \pm 338.3$  cells/ $\mu$ l,  $p < 0.001$ ) and CDB ( $2188 \pm 47.07$  cells/ $\mu$ l,  $p < 0.05$ ) assays, respectively. However it appears that TrypLE detached cells are more potent immunosuppressors as they were able to significantly suppress proliferation to lower numbers than CDB dissociated cells. TrypLE detached MSC were able to significantly suppress T effector cell numbers,  $2281 \pm 189.3$  cells/ $\mu$ l at a ratio of 1:10 ( $p < 0.05$ ) compared with CDB detached cells ( $2636 \pm 187.9$  cells/ $\mu$ l) which did not significantly suppress T effector cell proliferation at this ratio. This is particularly evident at a 1:20, MSC:



T cell ratio where there was significant suppression by the TrypLE detached MSC population ( $27.37 \pm 4.85\%$ ,  $p < 0.05$ ) whereas T effector cells cultured with CDB detached MSC seemed to proliferate with little suppression ( $1.2 \pm 1.2\%$ ) (Figure 3.14C).

**Figure 3.12: Impact of detachment method on the differentiation capabilities of MSC.**

A: Image J analysis of oil red O staining of MSC differentiated into adipocytes. MSC were re-plated after various ways of detachment from tissue culture plastic and differentiated into adipocytes. Bars represent oil red O stained mean area fraction  $\pm$  SEM of n=3 samples; \*\*\*, p<0.001. B: Alizarin red staining of MSC differentiated into osteoblasts. MSC were re-plated after various ways of detachment from tissue culture plastic and differentiated into osteoblasts. Bars represent mean calcium concentration ( $\mu$ M)  $\pm$  SEM of n=3 samples; \*, p<0.05. C: Representative images of DAB staining of collagen II as a marker of MSC differentiated into chondrocytes at x20 magnification. MSC were cultured as pellets after detachment from tissue culture plastic using CDB and TrypLE and differentiated into chondrocytes.



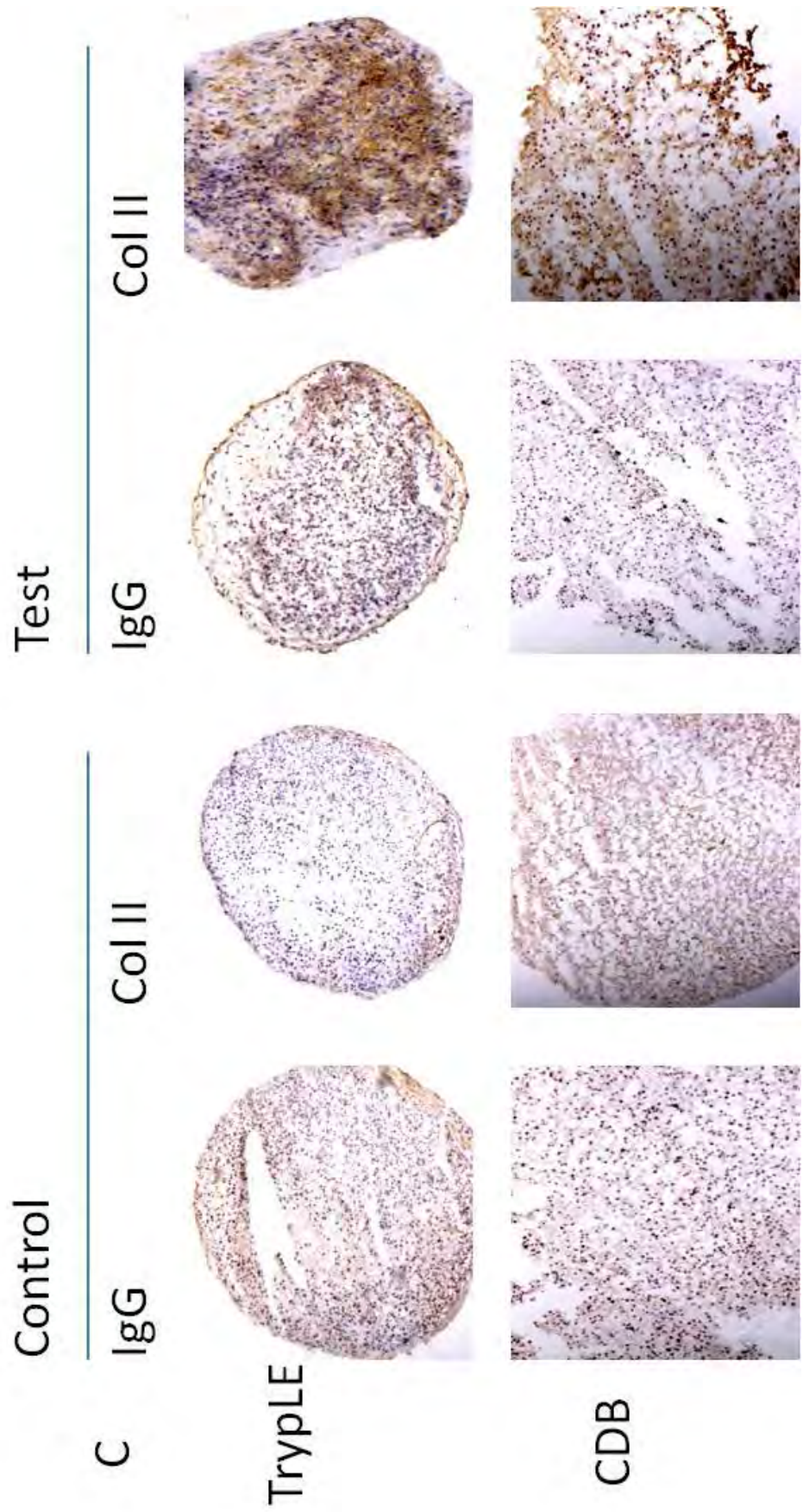


**Figure 3.13: Confirmation of efficiency of CD3<sup>+</sup>CD4<sup>+</sup>CD25<sup>-</sup> T cells sorting from peripheral blood.**

A: Peripheral blood T cells were gated on forward scatter (FS) side scatter (SS) histogram plots. B: CD3<sup>+</sup> cells were gated from the peripheral blood T cell population. C: Effector T cells were identified by gating on CD4<sup>+</sup>CD25<sup>-</sup> cells from the CD3<sup>+</sup> T cell population. D: Sorted CD3<sup>+</sup>CD4<sup>+</sup>CD25<sup>-</sup> T effector cells were 98% pure.

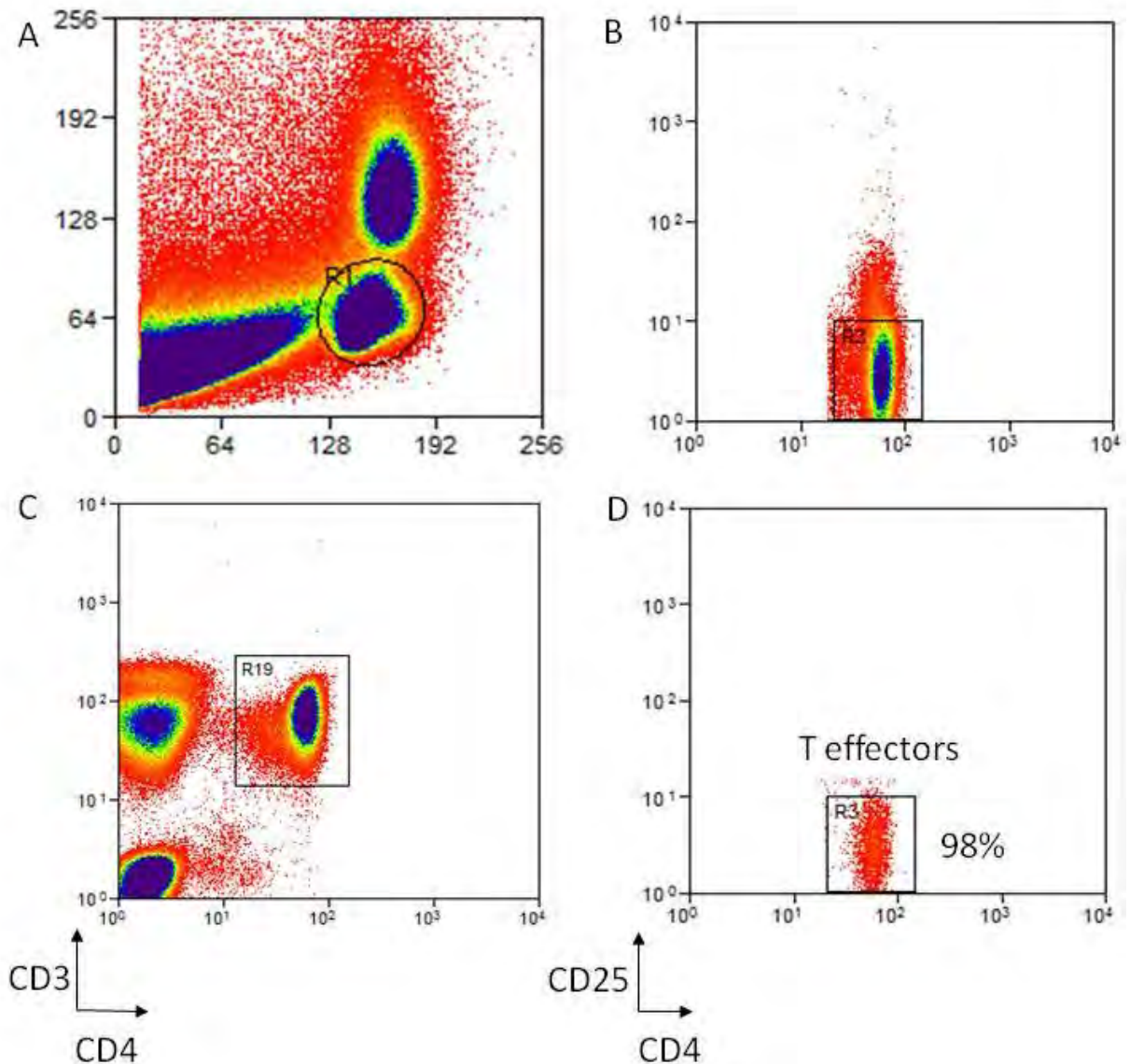
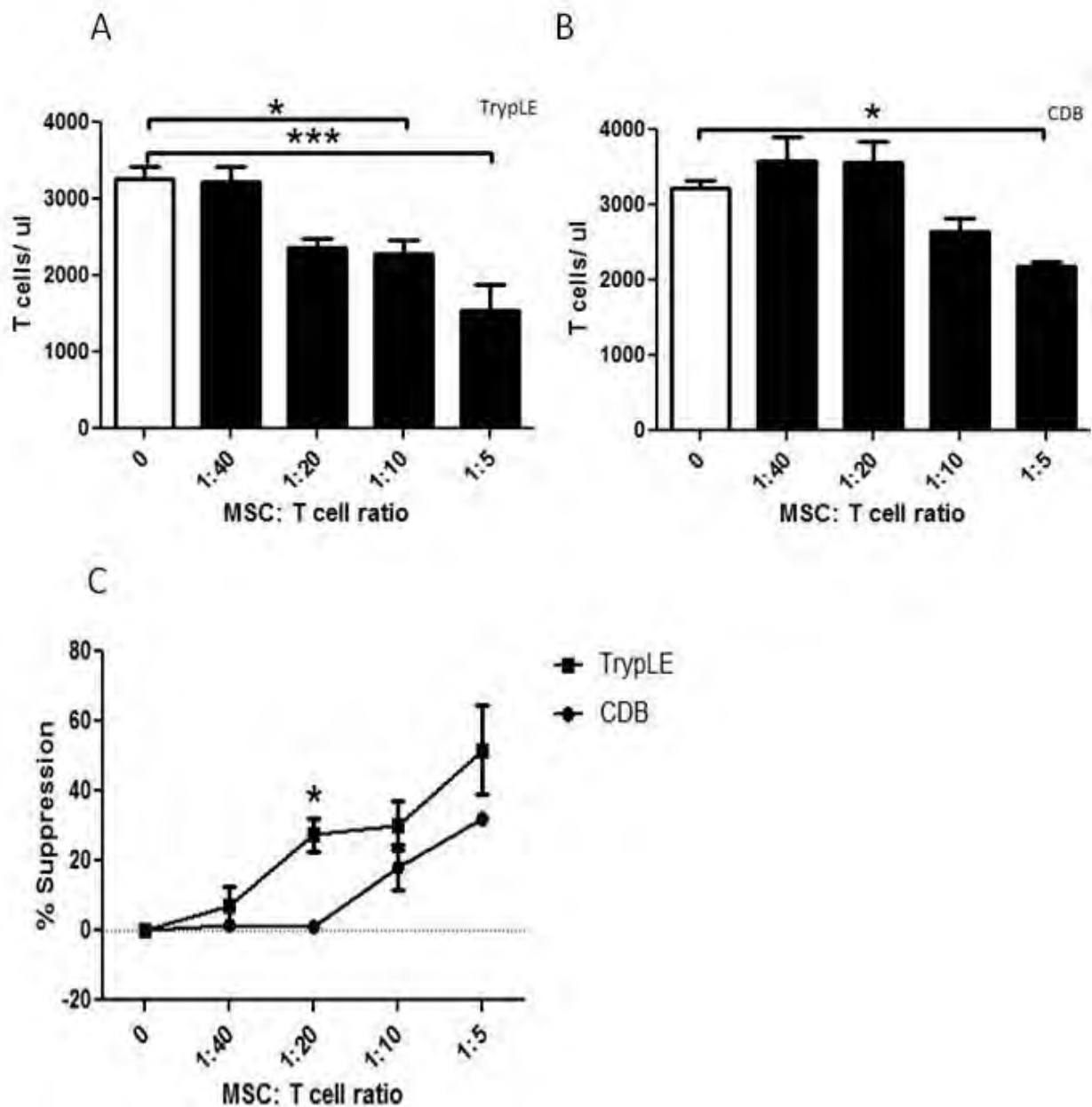


**Figure 3.14: Impact of detachment method on the immunomodulatory capabilities of MSC.**

Flow cytometry analysis of activated  $CD3^+CD4^+CD25^-$  T effector cell proliferation labelled with CellTrace™ Violet and analysed with PE labelled Accucheck counting beads. MSC were co-cultured with activated  $CD3^+CD4^+CD25^-$  T effector cell at ratios of 1:5, 1:10, 1:20, 1:40, 1:80, respectively and compared to  $CD3^+CD4^+CD25^-$  T effector cell proliferation without MSC after, A: TrypLE detachment and B: CDB detachment. C: Comparisons at each ratio were made of percentage  $CD3^+CD4^+CD25^-$  T effector cell suppression. Bars represent mean  $\pm$  SEM of n=3 different donors, \*, p<0.05; \*\*\*, p<0.001.



### 3.3 Discussion

MSC have been shown to possess powerful therapeutic qualities including immunomodulatory (Lin *et al.*, 2011), anti-fibrotic (Zhao *et al.*, 2012) and anti-cancer (Secchiero *et al.*, 2010) properties as well as potential for use as vectors for gene therapy (Ley *et al.*, 2007, Loebinger *et al.*, 2009, Niess *et al.*, 2011). This repertoire of clinical uses has led to an increasingly large number of clinical trials (Houlihan and Newsome, 2008) that assess MSC as a cell therapy in a variety of diseases. The typically low yield of cells obtained after isolation means that MSC have to be expanded in artificial culture conditions, prior to their clinical use (Lubis *et al.*, 2011). Consequently there is a high degree of non-physiological manipulation involved in the pre-clinical preparation of MSC. Unfortunately until recently there has been no standardised way to do this and a variety of modified methods have been employed to isolate, grow and detach MSC for therapeutic use (Wagner *et al.*, 2006). Although MSC are commercially available and thus culture conditions are now more standardized, one potential preclinical variable that remains to be investigated is the method of detachment of MSC from tissue culture plastic (Heng *et al.*, 2009). Thus it is vital to investigate how pre-clinical manipulation and treatment of these cells could affect their downstream functions including recruitment, engraftment and their anti-inflammatory effect at the site of injury.

In the present chapter we have investigated whether different methods of detachment, including enzymatic and non enzymatic methods, can affect MSC differentiation, immunomodulation and migration via cell surface CCR expression. Previous work has shown that enzymatic detachment, specifically using Trypsin can reduce MSC CCR expression

whereas EDTA preserves cell surface expression (Chamberlain *et al.*, 2008). Studies using embryonic stem cell populations also suggest that detachment strategies such as scraping which maintain small groups of cells rather than complete single-cell disaggregation may be more successful in terms of maintaining viability (Buzzard *et al.*, 2004, Mitalipova *et al.*, 2005). I have shown in this chapter that enzymatic, detachment of cells from tissue culture plastic preserves cell viability and their adipogenic and osteogenic differentiation but causes proteolytic cleavage of cell surface CCR. In contrast, non-enzymatic detachment methods did not increase intracellular stress on MSC during detachment, but reduced cell viability and adipogenic and osteogenic differentiation capabilities. CDB and EDTA both work to dissociate cells by chelating calcium but as there is an apparent difference between the effects of both methods (Heng *et al.*, 2009) this cannot solely explain the loss in cell viability. Since the loss of viability seems to occur at the point of dissociation from plastic (Heng *et al.*, 2009) the physical trauma associated with scraping cells may explain the highest degree of cell death following this treatment. This is in agreement with data from adherent cell cultures (Batista *et al.*, 2010) which shows damage to plasma membrane domains following cell scraping.

Despite reduced viability following non-enzymatic detachment, cells maintained functional cell surface CCR expression, resulting in increased migration towards corresponding chemokine ligands, compared to TrypLE detached MSC. This suggests that although viability is compromised upon cellular detachment, surviving cells may retain functional capabilities if allowed to recover. Thus we investigated how the cells behave once allowed to reattach in culture. Here, the morphology, viability and growth dynamics of the differentially detached MSC was monitored and recorded after 1, 3 and 5 days. Viability of equal densities of

adherent cells in culture after 24 hours seemed to reflect the initial pattern of viability upon detachment. However, in all cases, we observed fewer cells attaching to plastic than would be indicated by the numbers of viable cells present. This may reflect the relative insensitivity of Trypan blue for identifying cells undergoing early stages of cell death or apoptosis. Over 5 days in culture compared to other non-enzymatic methods, CDB-detached MSC appeared to exhibit the greatest recovery of growth in culture despite initially lower viability post detachment, and their morphology was similar to enzymatic detached cells. EDTA-detached and scraped cells showed little or no recovery over 5 days and exhibited a denatured and damaged appearance in culture. In contrast, possibly due to higher survival of plated cells and rapid development of confluence, resulting in contact inhibition, TrypLE and Accutase detached MSC maintained or started to reduce in cell number, respectively, over time.

Centrifugal washing of cells post-detachment is a highly stressful but vital stage of the cell preparation protocol. We have shown that post-detachment washing at reduced speed using a buffer supplemented with foetal calf serum preserves viability. Low centrifugation speeds during washing stages may increase yield of viable cells by minimising the proportion of dead cells accumulating in the cell pellets. Similarly the inclusion of serum may increase subsequent reattachment by either reducing cell clumping or providing substrates for attachment (Horiuti *et al.*, 1982) thus preventing anoikis (Yu *et al.*, 2012). In support of this, detachment of rat MSC from temperature responsive platforms suggests the presence of ECM proteins around or within the cell membranes can preserve viability (Yang *et al.*, 2012).

We hypothesised that CDB may result in a high percentage of cells entering a cell survival mechanism known as autophagy, which has been demonstrated in highly stressed cells



(Bhogal *et al.*, 2012). During autophagy cells begin a process of self degradation through a lysosomal degradation pathway (Bhogal *et al.*, 2012, Levine and Yuan, 2005) with preservation of cytoskeletal elements until later stages (Bhogal *et al.*, 2012, Levine and Yuan, 2005). Autophagy was first identified as a pre-apoptotic or a pre-necrotic mechanism, which would ultimately lead to the death of the cell (Schweichel and Merker, 1973). However recent studies have shown that prevention of autophagy does not necessarily prevent cell death (Levine and Yuan, 2005) and suggest that autophagy is a cell survival mechanism which may precede cell death, or which cells can recover from (Levine and Yuan, 2005). The role of autophagy in cell survival is best characterised in nutrient deficiency but has been shown to occur in cells under hypoxic stress (Bhogal *et al.*, 2012). During this process, autolysosomes generate free fatty acids and amino acids through degradation of membrane lipids and proteins to fuel mitochondrial ATP energy production and protein synthesis to promote cell survival (Bhogal *et al.*, 2012, Levine and Yuan, 2005). Alternatively, autophagy may activate in cells committed to die by apoptosis or necrosis so the cell contents are targeted for degradation by its own lysosomes (Levine and Yuan, 2005). This provides a mechanism to clear dead cells in the absence of phagocytes (Levine and Yuan, 2005) but in cultured cells this may protect surrounding cells from cytotoxic contents of dead or dying cells, thus preventing the formation of a necrotic environment. Recent evidence has shown that autophagy in hepatocytes can be mediated by increased intracellular reactive oxygen species (IROS) due to hypoxic stress (Bhogal *et al.*, 2012). CDB treated cells did not demonstrate increased IROS levels compared with cells detached using TrypLE. We therefore suggest that CDB seems to preserve long-term viability of MSC compared to the other non enzymatic detachments by promoting autophagy. This may operate as a recoverable pre death state, or as a self clearance mechanism which protects the viability of surrounding cells.

We observed that non-enzymatic detachment methods resulted in reduced adipogenic differentiation. Cell scraping is a standard technique which could be employed to passage cells before differentiation; our findings suggest that such methods could be detrimental to adipogenic differentiation of MSC perhaps as a result of cellular damage during detachment. Alternatively methods such as scraping or EDTA cell detachment results in clumps of cells rather than single cells. This could mean receptors otherwise used for adipogenic differentiation are not exposed to differentiation factors. In contrast, osteogenic differentiation was maintained in cells detached by all methods and there was significantly increased differentiation when cells were scraped. Evidence suggests that increased cellular stress levels induced by shearing cells can push MSC towards an osteogenic phenotype (Yourek *et al.*, 2010) and thus scraping cells may activate similar processes. This mechanism may be designed to drive osteogenesis upon bone fracturing (Carter *et al.*, 1988), and thus shearing MSC in culture to drive osteogenic progenitor phenotype may have implications in cell therapy for orthopaedics. A recently described alternative method of cell detachment that has not been explored in this chapter is the use of temperature responsive platforms. Here cells are cultured on poly-N-isopropylacrylamide (PNIPAAm) copolymer films and detached by rapidly reduction in temperature (Yang *et al.*, 2012). Rat MSC grown on the copolymer films showed significantly higher degrees of differentiation to adipocytes compared with trypsinised controls but no significant difference in osteogenic differentiation (Yang *et al.*, 2012). Such studies also suggest significantly higher levels of viability than enzymatic detachment. We have noted reduced adipogenic differentiation and that MSC immunomodulatory capacity was diminished following cell scraping and such differences with other detachment studies highlight the need to standardise methodology for specific

downstream applications. Also we showed that a lower concentration of TrypLE detached MSC are able to inhibit T effector cell proliferation compared with CDB detached MSC, suggesting CDB detached MSC lose some of their immunosuppressive ability.

The loss of immunosuppression is likely to be due to the detachment method. CDB detached MSC have a significantly altered morphology, reduced viability and they appear damaged after 24 hours of reattachment to plastic compared with TrypLE detached MSC. This could serve to explain why we see a significant decrease in CDB detached MSC immunomodulatory capabilities which are tested after 24 hours of reattachment to plastic. There could be a number of reasons for this based on our findings. Firstly we see recovery of CDB detached cells after 5 days, up to this point MSC may be undergoing autophagy as we have shown, thus reducing the production of immunomodulatory cytokines involved in immunosuppression. Secondly, the reduced viability of CDB detached cells suggests that some cells seeded onto plastic after detachment will be dead or dying, thus reducing production of immunosuppressive cytokines. Finally, MSC are an adherent cell type and are not physiologically designed to migrate in suspension or through the circulation. Exogenous administration of MSC would mean infusing MSC in suspension. To identify receptors that MSC may use to migrate through the circulation, MSC need to be analysed for the receptors they express whilst non-adherent and in suspension. To identify the receptors on detached MSC, CDB is a more appropriate method as TrypLE would cleave off receptors. Alternatively to carry out immunosuppressive functions it may be essential for the cell to be adhered. TrypLE detached MSC appear to be regain their normal morphology after 24 hours when reattached to plastic. TrypLE is perhaps the best method of detachment to enable MSC to retain immunosuppressive potential, although receptor expression when in suspension is minimal.

An important obstacle in MSC therapy is the application of MSC to the site of injury and the method of administration of MSC in the patient. Direct transplantation of MSC to injured organs has been shown to contribute to recovery of the organ (Amado *et al.*, 2005) however this type of invasive procedure is not always feasible. Therefore a non-invasive method of MSC delivery to areas of injury needs investigation, possibly through intravenous administration and organ targeting via specific adhesion. According to the well established paradigm of leukocyte recruitment to organs, adhesion molecules and cell surface CCR play an integral role in cell recruitment (Ley *et al.*, 2007). However, there are inconsistent reports on CCR expression on MSC (Ciuculescu *et al.*, 2011, Ponte *et al.*, 2007, Ringe *et al.*, 2007, Sordi *et al.*, 2005). In this study we have investigated affects of detachment methods on cell surface CCR expression and function. We chose a panel of CCR, namely, CCR4, CCR5, CXCR3 and CXCR7 that were retained on the MSC surface when detached by non enzymatic methods and demonstrated significantly increased migration towards chemokine ligands, suggesting a functional preservation of cell surface CCR expression. We have shown there was significant migration towards the respective CCR4 and CCR5 ligands, MDC/ CCL22 (Imai *et al.*, 1998) and MIP1B/ CCL4 (Raport *et al.*, 1996) when MSC were detached with CDB and no difference compared to control when MSC were detached with TrypLE. Migration towards the CXCR3 ligand, ITAC/ CXCL11 (Loetscher *et al.*, 2001) showed a similar trend but this was not significant. Our data supports previous work by Chamberlain *et al* (Chamberlain *et al.*, 2008) which suggests CCR expression on MSC surface and their function is preserved with non-enzymatic detachment methods but significantly reduced after detachment with enzymatic methods possibly through proteolytic cleavage.

Our studies also suggest that migration towards the CXCR4/ CXCR7 ligand SDF1a/ CXCL12 (Dambly-Chaudiere *et al.*, 2007) is maintained after detachment. However, there appears to be increased migration of CDB detached MSC to SDF1a/ CXCL12. This is of interest as the receptor CXCR4 is expressed at negligible levels on MSC and so alternate receptors must be responsible. One possible alternative is CXCR7, an unusual CCR implicated mainly in scavenging and not in cell migration (Naumann *et al.*, 2010). Although few reports do provide evidence for CXCR7 mediated migration, others suggest that CXCR7 forms heterodimers with CXCR4 to enhance migration of cells (Decaillot *et al.*, 2011). Our lack of CXCR4 expression on MSC suggests CXCR7 may function independently in this case. CXCR7 is a cytoplasmic receptor not usually found on the cell surface, with the majority of its function dictated by the intracellular tail of the receptor (Ray *et al.*, 2012). Thus enzymatic detachment of MSC would have little effect on its function, and cells may retain sustained migration towards SDF1a/ CXCL12 via CXCR7 independently or through association with other CCR. The reduced migration of TrypLE detached MSC to SDF1a/ CXCL12 supports the hypothesis that other enzymatically-sensitive surface receptors may dimerise with CXCR7 in order for the cell to migrate towards SDF1a/ CXCL12. Alternately cytoplasmic CXCR7 may also be able to mobilise to the cell surface during our migration experiments (Dambly-Chaudiere *et al.*, 2007, Naumann *et al.*, 2010).

Clinical studies have shown that although very large numbers of MSC are infused into patients during non invasive applications only a very low number of cells engraft in the sites of injury (Lin *et al.*, 2011). Furthermore, the immunosuppressive efficacy of these cells has been shown to directly correlate with the number of cells engrafted (Lin *et al.*, 2011). Therefore an increased number of cells engrafting would lead to greater therapeutic efficacy

(Lin *et al.*, 2011). Importantly such trials have all used enzymatic detachment methods. Since our results show reduced migration after enzymatic detachment we infer that the low level of engraftment in these trials may be due to the loss of important receptors during detachment. As MSC migration to sites of injury, binding and retention in organs is highly dependent on their cell surface CCR expression (Sordi *et al.*, 2005, Wynn *et al.*, 2004) cleavage of these receptors could affect their immediate functional capabilities when detached. Migration is not the only function of CCR which also play a role in firm adhesion and cell retention, both of which can be abrogated by loss of cell surface CCR (Chamberlain *et al.*, 2008). The loss of CCR could also have implications on other TrypLE/ enzyme sensitive receptors on MSC cell surfaces. This report highlights the need for the development of a method of detachment that can preserve viability and cell surface receptor profile of MSC.

In conclusion, our data suggest that the optimal choice of MSC detachment method depends on the ultimate downstream application of the MSC. For example, if efficient organ delivery is likely to require cell surface CCR which are susceptible to proteolytic degradation, TrypLE is not a reliable method. However TrypLE preserves viability and the multi-lineage differentiation potential to a higher degree than CDB. Thus if cells can be delivered directly to the target organ, enzymatic dissociation may be possible. Therefore handling and manipulation, of MSC prior to experimental or clinical use has direct implications on the downstream outcome. As a result we have to very carefully consider how detachment of cells may have downstream effects on cell function otherwise we need to enhance our efforts to maintain the natural phenotype of MSC after detachment and before their use as a powerful and potent cell therapy.

## **CHAPTER 4: EFFECTS OF CYTOKINES ON MIGRATION AND IMMUNOMODULATION BY MSC**

## 4.1 Introduction

The therapeutic properties of MSC are well established and research suggests MSC can have significant beneficial effects in liver disease (Kuo *et al.*, 2008, Lin *et al.*, 2011, Puglisi *et al.*, 2011). Previous studies suggest that infused MSC are able to migrate to and enter the site of injury and thereby ensure a continued local delivery of mediators order to enact their therapeutic properties (Karp and Leng Teo, 2009, Lin *et al.*, 2011). It has been shown that a significant reparative or beneficial impact can be carried out by very few MSC and the benefit is directly dependent on the number of cells that engraft into the site of injury (Lin *et al.*, 2011). Thus, for use as a therapeutic intervention in liver disease, MSC need to be infused into the patient and then to enter the liver. However the quantity of transplanted MSC needs to be far greater than the amount of MSC that are expected to carry out an effect as it is unlikely that all transferred cells will end up at the required location (Lin *et al.*, 2011). In animal studies, the quantity of transplanted MSC used is usually approximately  $10^6 - 10^7$  cells (Lin *et al.*, 2011). Transfer of larger numbers does not seem to increase the therapeutic effects, which were seen to plateau (Lin *et al.*, 2011). However such numbers are still very large and require a significant degree of cell culture and expansion prior to infusion (Karp and Leng Teo, 2009) which may mean that the purity of the cells is difficult to maintain. It is therefore important to develop a method to improve MSC transplantation and subsequent engraftment in order to improve therapeutic efficacy rather than simply transferring increasing numbers of cells. Recent research into MSC recruitment to organs such as the liver is helping better understand this process, so that we can try and enhance MSC engraftment.



Exogenously administered MSC, like most cells in circulation attempting to enter tissue, will potentially arrest in the vasculature of the tissue followed by transmigration across the endothelium (Karp and Leng Teo, 2009, Oo and Adams, 2010). It has been hypothesised that MSC may be recruited to an organ either through an active process which mimics the existing paradigm of leukocyte recruitment or through a physical lodging into small vessels and then an active process of extravasation into the organ (Karp and Leng Teo, 2009, Oo and Adams, 2010). MSC have been shown to actively roll in post capillary venules in mice using intravital microscopy via a P-Selectin mediated process (Ruster *et al.*, 2006). This has led to the development of SLex containing protein which couples to the surface of MSC and promoted shear resistant low affinity interactions or rolling on vascular endothelium via P-Selectin (Sarkar *et al.*, 2008). Subsequent firm adhesion on TNF $\alpha$  activated umbilical vein endothelium occurs due to MSC interacting through the  $\beta$ 1 ligands, VCAM-1 and VLA-4 (Ruster *et al.*, 2006, Segers *et al.*, 2006), and blocking  $\beta$ 1 integrin on MSC reduces their engraftment in ischemic myocardium (Ip *et al.*, 2007). Firm adhesion may follow an initial rolling interaction which is the case for leukocytes. Alternatively, large MSC may lodge in the narrow vessels of the post-capillary vasculature (Chavakis *et al.*, 2008). To mimic this process, researchers have used flow based assay methodology, where they paused the flow to allow MSC to adhere to endothelium prior to resumption of flow. Such studies confirm that  $\beta$ 1 integrin and CD44 are involved in the firm adhesion of MSC to sinusoidal endothelium (Aldridge *et al.*, 2012). Such studies also suggest that MSC rolling on sinusoidal endothelium is mediated by  $\beta$ 1 integrin and further, engraftment in carbon tetrachloride injured mouse liver is mediated by  $\beta$ 1 integrin and CD44. This is important as hepatic sinusoidal endothelium does not express P-Selectin (Aldridge *et al.*, 2012) and thus requires alternate routes for capturing recruited cells.

CCR play a large part in leukocyte recruitment, during firm adhesion and transendothelial migration stages (Oo and Adams, 2010). Research into the role of CCR in MSC adhesion and migration are inconclusive as some suggest that although MSC express CCR, there is no contribution of CCR to MSC recruitment (Thankamony and Sackstein, 2011). Alternate studies measuring mouse MSC retention to murine aortic endothelium under shear (Chamberlain *et al.*, 2011) suggest a functional role for CCR in the firm adhesion, crawling and transmigration of MSC. Hence, ITAC/ CXCL9 on TNF $\alpha$  activated endothelium could significantly increase the number of MSC that remained firmly adhered under shear stress of which a high proportion actively crawled on endothelium in a ITAC/ CXCL9 dependent manner. Mouse MSC were also shown to migrate towards CXCL16, ITAC/ CXCL9, MIP3 $\alpha$ / CCL20 and TECK/ CCL25, using corresponding CCR, CXCR6, CXCR3, CCR6 and CCR9. These investigators have previously reported the expression of these CCR and CXCR2 on mouse MSC cell membrane, with other CCR (except CCR3) present on negligible proportions of MSC (Chamberlain *et al.*, 2008). Furthermore they showed that human MSC expressed similar functional receptors on large proportions of cells but also expressed CCR1, CCR2, CCR3, CCR5, CCR7, CCR10, CXCR1, CXCR4, and CXCR5. Negligible proportions of human MSC were found to express CCR4 and CCR8 (Chamberlain *et al.*, 2008).

However, there are many inconsistencies in functional CCR profiles of MSC in reports from various groups. Isolated human MSC have been reported to express functional CCR1, CCR7, CXCR4, CXCR6 and CX3CR1 and could migrate towards corresponding ligands CCL3 (MIP1 $\alpha$ ), CCL19 (MIP3 $\beta$ )/ CCL21 (6Ckine), CXCL12 (SDF1 $\alpha$ ), CXCL16 and CX3CL1 (Fractalkine) respectively (Sordi *et al.*, 2005). Other groups have detected the expression of

CCR1, CCR2, CCR4, CCR6, CCR7, CCR8, CCR9, CCR10, CXCR1, CXCR2, CXCR3, CXCR4, CXCR5, CXCR6, CX3CR1 and XCR at the mRNA level (Honczarenko *et al.*, 2006, Ringe *et al.*, 2007). Protein expression of CCR8, CCR9 and CXCR1-6 has also been detected on MSC, of which CXCR1 and CXCR2 were proven to have a functional migratory response towards CXCL8/ IL8 (Ringe *et al.*, 2007). Growth factors, including PDGF AB, IGF-1, EGF and HGF were better chemotactic agents than chemokines, nonetheless, MSC expressed high levels of CCR3, CXCR4 and CXCR5, and intermediate levels of CCR2, CCR4 and CCR5 and showed migration to SDF1 $\alpha$ / CXCL12, Rantes/ CCL5 and MDC/ CCL22, suggesting a functional role for CCR4, CXCR4, CCR3 and CCR5 (Ponte *et al.*, 2007). There have been particular inconsistencies in reports suggesting presence of CXCR4 on MSC. Many reports suggest MSC do not express CXCR4 (Karp and Leng Teo, 2009) but others suggest CXCR4 is central to MSC migration (Son *et al.*, 2006). Studies have also identified organ specific chemokines and receptors on MSC which could be responsible for MSC recruitment. For example, the importance of CCR2 has been highlighted in homing of MSC to injured myocardium (Belema-Bedada *et al.*, 2008), and MSC have been proven to migrate towards pancreatic islets, mediated by the CXCR4/ CXCL12 (SDF1 $\alpha$ ) and CX3CR1/ CX3CL1 (Fractalkine) pathway (Sordi *et al.*, 2005). Similarly, transplanted rat MSC have been reported to migrate to recombinant human SDF-1 $\alpha$ / CXCL12 in an *in vivo* chemotaxis assay and could use the CXCR4/ CXCL12 (SDF1 $\alpha$ ) and CX3CR1/ CX3CL1 (Fractalkine) axis during left hypoglossal nerve injury to the brain (Ji *et al.*, 2004).

Various chemokines have been shown to be expressed on different cell types at specific sites in the liver during injury including CCL3 (MIP1 $\alpha$ ), CCL4 (MIP1 $\beta$ ) and CCL5 (Rantes) (Berres *et al.*, 2010, Kirovski *et al.*, 2010) in portal vessels; CXCL9 (ITAC) (Wasmuth *et al.*,

2009), CXCL10 (IP-10), CXCL11 (MIG) and CXCL16 in liver sinusoids; CCL28 (MEC), CXCL16, CX3CL1 (Fractalkine), CXCL12 (SDF1 $\alpha$ ) in biliary epithelium; and CCL19 (MIP3 $\beta$ ), CCL21 (6Ckine) in portal associated lymphoid tissue (Oo and Adams, 2010). CCL17 (TARC) and CCL22 (MDC) are highly expressed on immune cells and upregulated CCL25 expression has been reported on hepatic endothelium (Oo and Adams, 2010). CCL2 is upregulated on stellate cells during NASH on ballooning hepatocytes and on Kupffer cells (Lalor *et al.*, 2007). In steatotic diseased livers, CCL21 (6Ckine) is also often observed in lymphatics and in stromal cells (Lalor *et al.*, 2007). CXCL4 has been is upregulated in experimental liver fibrosis as a result of infiltrating platelets (Zaldivar *et al.*, 2010). CXCL1 (GRO1), CXCL5 (LIX), CXCL8 (IL8) are also observed in inflamed portal tracts usually due to infiltrating leukocytes and injured endothelium (Lalor *et al.*, 2007). Thus we were interested to determine whether receptors for such chemokines were robustly expressed on human MSC populations to determine whether they may play a role in hepatic localisation of infused cells.

Whilst documentation of basal chemokine receptor expression by MSC is of value, it is likely that pre-infusion expansion strategies may alter expression and furthermore that culture conditions could be manipulated to maximise expression of desired hepatic homing cues. Before use, MSC have to be expanded to large numbers in culture where cells may encounter high levels of confluence and multiple passages, in these cases MSC can lose their migratory ability and expression of certain CCR involved in migration, respectively (Karp and Leng Teo, 2009). MSC treated with a cocktail of cytokines can increase surface CXCR4 expression with corresponding increased migration towards CXCL12/ SDF1 $\alpha$  (Shi *et al.*, 2007). Stimulation of MSC with TNF $\alpha$  also increases surface expression of CCR3 and increased

migration to CXCL12/ SDF1 $\alpha$ , CCL5/ Rantes and CCL22/ MDC (Ponte *et al.*, 2007). Cytokines like TNF $\alpha$  have been reported to increase expression of CCR5 and CCR10 on MSC and thus the migration of MSC toward Rantes/ CCL5 and MEC/ CCL28 (Hemeda *et al.*, 2010). As well as modifying pre-infusion treatment of MSC it is likely that cells will be exposed to soluble mediators upon infusion into a diseased environment. There are vast increases in cytokine levels during liver injury (Lalor *et al.*, 2007), and these may act upon local and systemic MSC to increase their homing and migratory capabilities. Cytokines such as TNF $\alpha$  can induce the invasion by human MSC into extracellular matrix (Bocker *et al.*, 2008) and can enhance MSC engraftment into infarcted myocardium (Kim *et al.*, 2009). In some cases successful engraftment can be limited by cell survival (Burst *et al.*, 2010), however manipulation with LPS stimulation of mouse MSC has been shown to enhance survival after engraftment (Yao *et al.*, 2009). There has been much research into engineering or priming MSC to increase migration and engraftment including IL1 $\beta$  stimulation of MSC which has been reported to increase MSC migration (Carrero *et al.*, 2012). Thus we wanted to investigate whether cytokines from a selected panel induced during liver injury could enhance migration and engraftment when transplanted via increases in CCR expression, specifically, TNF $\alpha$  (Lalor *et al.*, 2007), IFN $\gamma$  (Lalor *et al.*, 2007), TGF $\beta$ 1 (Achyut and Yang, 2011, Lalor *et al.*, 2007, Marek *et al.*, 2005, Weng *et al.*, 2009), LPS (Su, 2002) , IL1 $\beta$  (Gieling *et al.*, 2009), IL4 (Lalor *et al.*, 2007), IL6 (Danese and Gao, 2010, Lalor *et al.*, 2007), IL8 (Lalor *et al.*, 2007, Maltby *et al.*, 1996) and IL10 (Lalor *et al.*, 2007, Thompson *et al.*, 1998, Zhang *et al.*, 2011). MSC have been reported to have receptors for most of these cytokines including TNFI and IIR, IFN $\gamma$ R, TGF $\beta$ RI and RII, (Docheva, 2008) TLR4 (Tomchuck *et al.*, 2008), IL-1R, IL-4R, IL-6R (Rattigan *et al.*, 2010), IL8R (CXCR1) (Docheva, 2008) and IL10R (Silva *et al.*, 2003).

Chemicals such as dexamethasone have been reported to significantly increase the migratory potential and motility of human MSC (Yun *et al.*, 2011) as have growth factors such as HGF (Forte *et al.*, 2006). Hypoxic culture conditions can also be employed to upregulate the migration of MSC by upregulating MMP (Karp and Leng Teo, 2009) and also possibly through increases in intracellular reactive oxygen species (IROS) as increases in IROS have been implicated in inducing cell migration and motility (Novo *et al.*, 2011). Interestingly hydrogen peroxide, an inducer of IROS, has been shown to upregulate surface CCR5 on monocytes (Lehoux *et al.*, 2003) and may also be how migratory properties of MSC may increase.

Retrovirus vectors encoding CXCR4 have been introduced into MSC and subsequently enhanced migration (Karp and Leng Teo, 2009). Similarly an adenoviral vector in MSC has been used to upregulate the  $\alpha 4$  subunit which dimerise with the  $\beta 1$  integrin to form the VLA-4 integrin and thus increased MSC migration into the bone marrow (Karp and Leng Teo, 2009). Cell surface glycans on MSC have been chemically engineered into an E-Selectin binding motif in order to encourage engraftment to endothelium that expresses high levels of E-Selectin (Sackstein *et al.*, 2008).

We wanted to specifically explore the effects of cytokines on MSC engraftment in the injured liver via increased CCR expression and function. However a consideration of using such cytokine stimulation is that other therapeutic MSC properties such as immunomodulation that has been described in the liver after MSC transplantation (Popp *et al.*, 2009) may also be modulated.  $\text{TNF}\alpha$ ,  $\text{IFN}\gamma$ ,  $\text{IL}1\alpha$  and  $\text{IL}1\beta$  have been shown to augment the immunosuppressive

capabilities, particularly with regard to T cell suppression, but not all cytokines may act in this way (Krampera *et al.*, 2006, Prasanna *et al.*, 2010, Ren *et al.*, 2008). Therefore it must be taken into consideration that cytokines which may enhance engraftment could alter the immunomodulatory properties of MSC, and so such properties will also be assessed in this chapter. A final consideration is the effect of the cytokine on multipotency of the MSC. As the MSC retain stem cell properties they are liable to be pushed towards a particular lineage during cytokine stimulation. IL1 $\beta$  and TNF $\alpha$  stimulation have been proven to inhibit osteogenic differentiation of MSC and thus influencing certain properties of the cell that may diminish the therapeutic potential (Lacey *et al.*, 2009). TGF $\beta$ 1 may induce chondrogenic differentiation of MSC or may push the MSC towards a cardiomyogenic or myofibroblast-like phenotype (Li *et al.*, 2009, Mohanty *et al.*, 2011). In this case, a myofibroblast could contribute to the fibrosis in the liver. Therefore within this chapter we phenotyped the MSC after cytokine stimulation to ensure the cells retained characteristic MSC tri-lineage potential.

The current literature has led to my hypothesis that cytokine stimulation, particularly by inflammatory or pro-fibrotic cytokines can increase chemokine receptor expression and function and thus the potential of MSC to engraft in the liver. A comprehensive panel of cytokines has not yet been tested with most studies focussing primarily on common inflammatory cytokines TNF $\alpha$  and IFN $\gamma$ . Pro-fibrotic cytokines such as TGF $\beta$ 1 and LPS which are responsible for activation of liver resident stromal cells could have similar effects on MSC thus increasing their migratory potential. With this, I predict that cytokine stimulation could also have beneficial effects on other aspects of the MSC phenotype, but limited stimulation protocols (maximum 24 hours) could minimise any detrimental effects on the cell phenotype including loss of tri-lineage differentiation potential.

The aims of this chapter were:

- (i) To measure the intracellular and cell surface CCR profile (CCR1-10, CXCR1-7) of MSC.
- (ii) To use a panel of cytokines typically upregulated during liver disease to identify those that could functionally increase surface CCR expression on MSC.
- (iii) To measure effects of selected cytokines on MSC adhesion to diseased human livers and isolated cell monolayers.
- (iv) To measure effects of selected cytokine stimulation on adhesion of MSC to mouse livers *in vitro* and engraftment into *in vivo* models of liver injury and to elucidate any CCR mediated mechanisms.
- (v) To measure effects of selected cytokine stimulation on tri-lineage differentiation potential, and on immunomodulatory potential of MSC.



## 4.2 Results

### 4.2.1 MSC express a consistent profile of intracellular and cell surface CCR expression.

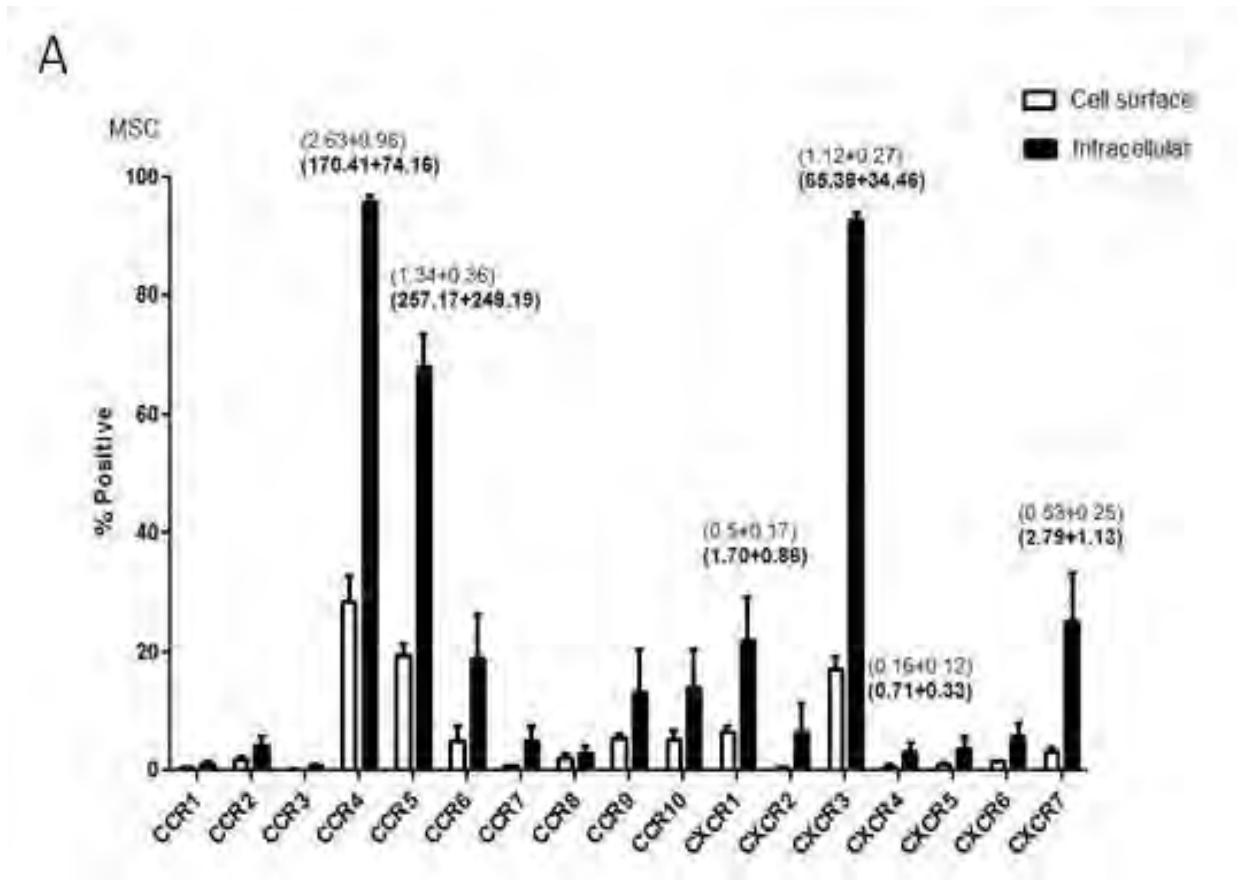
Flow cytometry was used to measure intracellular and MSC surface CCR expression (CCR1-10 and CXCR1-7) by MSC detached from tissue culture plastic. A large percentage of MSC contain large intracellular stores of CCR4 (95.84±0.88%), CCR5 (67.96±5.54%), and CXCR3 (92.69±1.26%) with correspondingly high MFI (Figure 4.1A and B). A smaller percentage of MSC have low levels of CCR6 (18.92±7.56%), CCR9 (13.2±7.16%), CCR10 (13.99±6.39%), CXCR1 (22.1±7.12%), and CXCR7 (25.02±8.22%). Very small percentages of MSC expressed CCR2 (4.11±1.66%), CCR7 (5.07±2.55%), CCR8 (2.9±1.28%), CXCR2 (6.51±4.81%), CXCR4 (3.14±1.57%), CXCR5 (3.73±1.93%) and CXCR6 (5.78±2.24%) at low levels. Intracellular CCR1 and CCR3 were expressed at negligible levels in a minimal percentage of MSC (Figure 4.1A). In all cases we observed that MSC cell surface CCR expression was low compared with intracellular stores of CCR. We found CCR4 (28.51±4.28%), CCR5 (19.34±2.01%), and CXCR3 (17.2±1.87%) to be exhibited on the cell surface by the greatest proportion of MSC. CCR6 (4.84±2.60%), CCR9 (5.38±0.81%), CCR10 (5.32±1.37%), CXCR1 (6.62±0.84%) and CXCR7 (3.11±0.76%) were also expressed but at lower levels on MSC cell surface. The lowest MSC surface expression was of CCR2 (1.9±0.58%), CCR8 (2.05±0.72%), CXCR5 (1.13±0.33%) and CXCR6 (1.57±0.13%) with CCR1, CCR3, CCR7, CXCR2 and CXCR4 absent or negligible on MSC cell surface (Figure 1A). PBMC isolated from peripheral blood were used as positive control cells and we measured positive expression of all CCR on PBMC. Although there was positive expression

of CCR3 and CCR8, these were expressed in a very low percentage of PBMC (Figure 4.2A and B).

A specific set of MSC surface CCR: CCR4, CCR5, CCR9, CXCR3, CXCR4 and CXCR7, were selected for confirmatory analysis by QPCR to measure mRNA levels of receptor expression (Figure 4.3). Expression closely followed that seen cytometrically with CCR4 ( $21.58 \pm 1.36$ ) and CCR5 ( $20.35 \pm 0.43$ ) mRNA expressed at high levels. CXCR3 ( $6.86 \pm 3.43$ ) and CCR9 ( $6.85 \pm 3.425$ ) were expressed at lower but more variable levels. We saw consistent levels of CXCR7 ( $7.75 \pm 0.45$ ) mRNA expression among multiple donors at a similar level to CCR9 and CXCR3 (Figure 4.3). CXCR4 expression was near absent as a protein (Figure 4.1B) and was also not detectable relative to  $\beta$ -actin levels (Figure 4.3). Immunohistochemical techniques were used to image and detect CCR protein expression for CCR4, CCR5, CCR9, CXCR3, CXCR4 and CXCR7. In support of findings using flow cytometry and QPCR, MSC expressed high levels of CCR4, CCR5 and CXCR3, lower levels of CCR9 and CXCR7 and no detectable CXCR4 (Figure 4.4)

**Figure 4.1: MSC CCR expression.**

A: Flow cytometry analysis of CCR1-10, CXCR1-7 CCR expression shown as percentage of CDB detached MSC positive for surface (open bars) and intracellular (closed bars) CCR with median fluorescence intensity (MFI) shown for CCR of interest, specifically CCR4, CCR5, CCR9, CXCR3, CXCR4 and CXCR7. Bars and MFI represent mean  $\pm$  SEM of n=3 different donor samples. B: Representative cytometry histograms for cell surface and intracellular CCR4, CCR5, CCR9, CXCR3, CXCR4 and CXCR7 expression of MSC (green) compared with immunoglobulin matched control (IMC) (red) of n=3 samples.



B

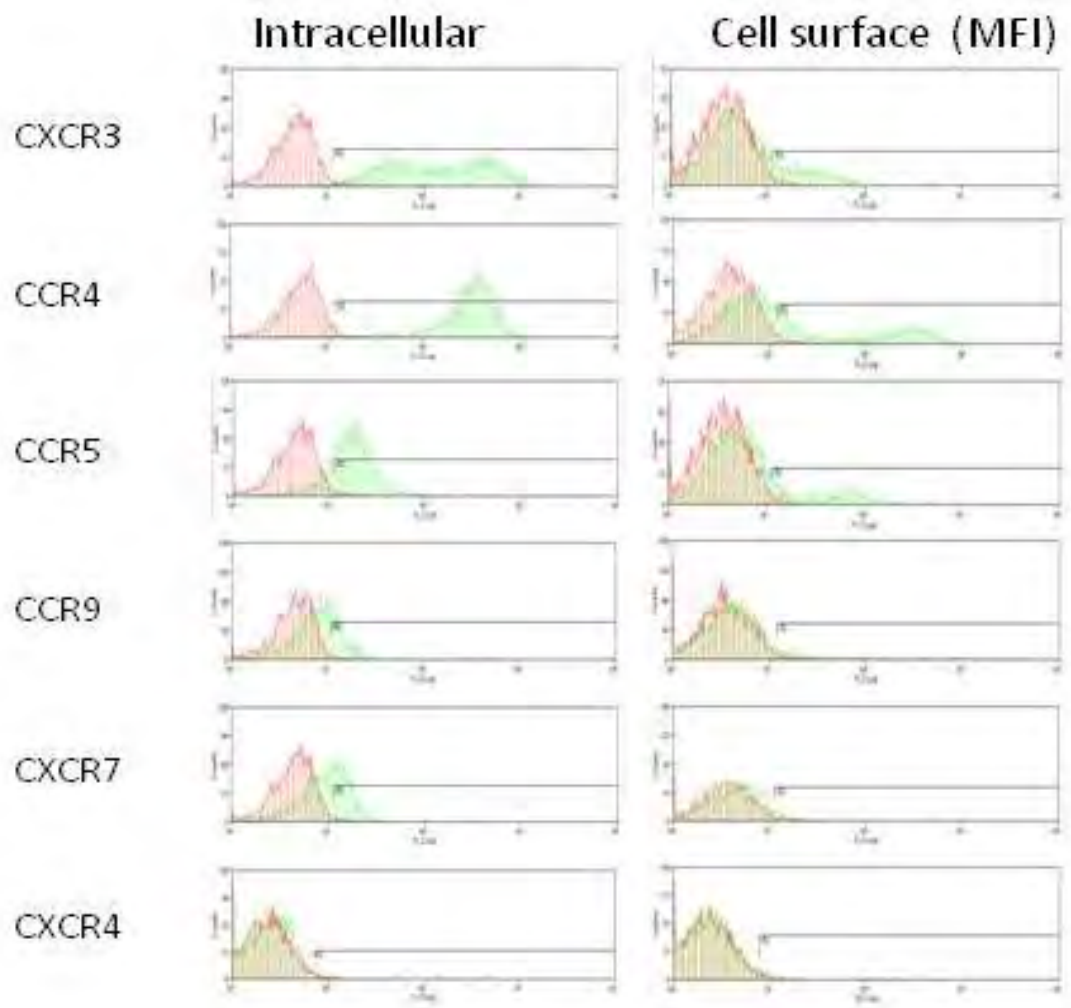


**Figure 4.2: PBMC CCR expression.**

Flow cytometric analysis of cell surface CCR1-10, CXCR1-7 CCR on PBMC as, A: percentage positive and B: MFI. Bars and MFI represent n=1 donor sample.

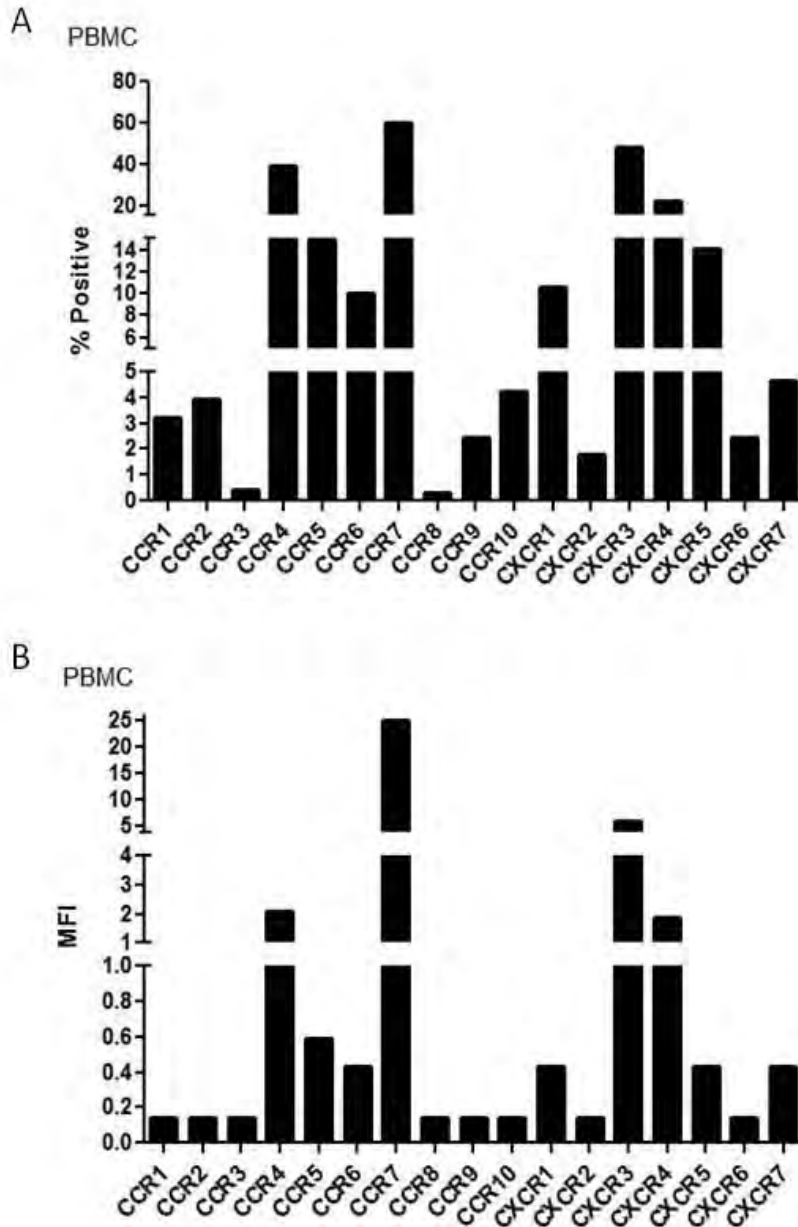


**Figure 4.3: QPCR analysis of MSC CCR expression.**

Quantitative analysis of total CCR4, CCR5, CCR9, CXCR3, CXCR4 and CXCR7 gene levels in MSC, measured by Real Time Polymerase Chain Reaction (QPCR) analysis and expressed as relative to endogenous MSC  $\beta$ -actin levels. The results were calculated by the comparative threshold cycle (Ct) method, with the Ct for  $\beta$ -actin used to normalise the results. Expression of each gene was calculated with the endogenous level of  $\beta$ -actin in MSC defined as 1. Bars represent mean  $\pm$  SEM of n=3 different donor samples, performed in triplicate.

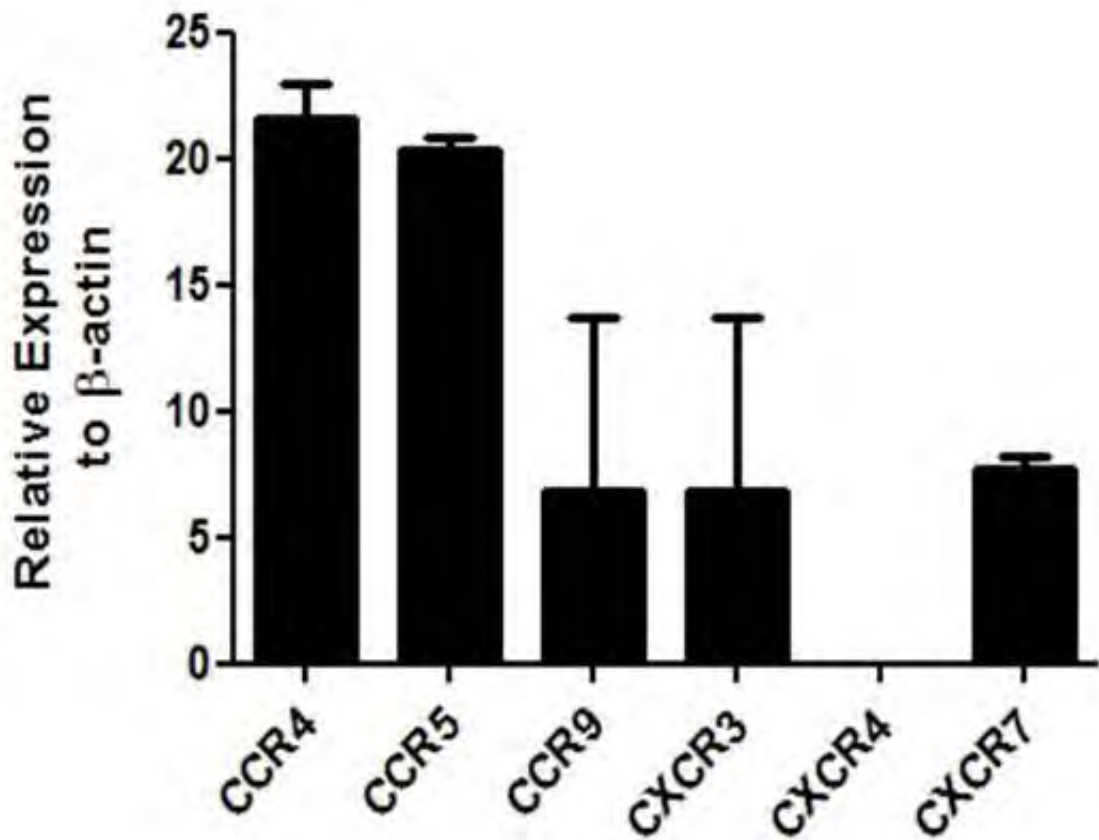
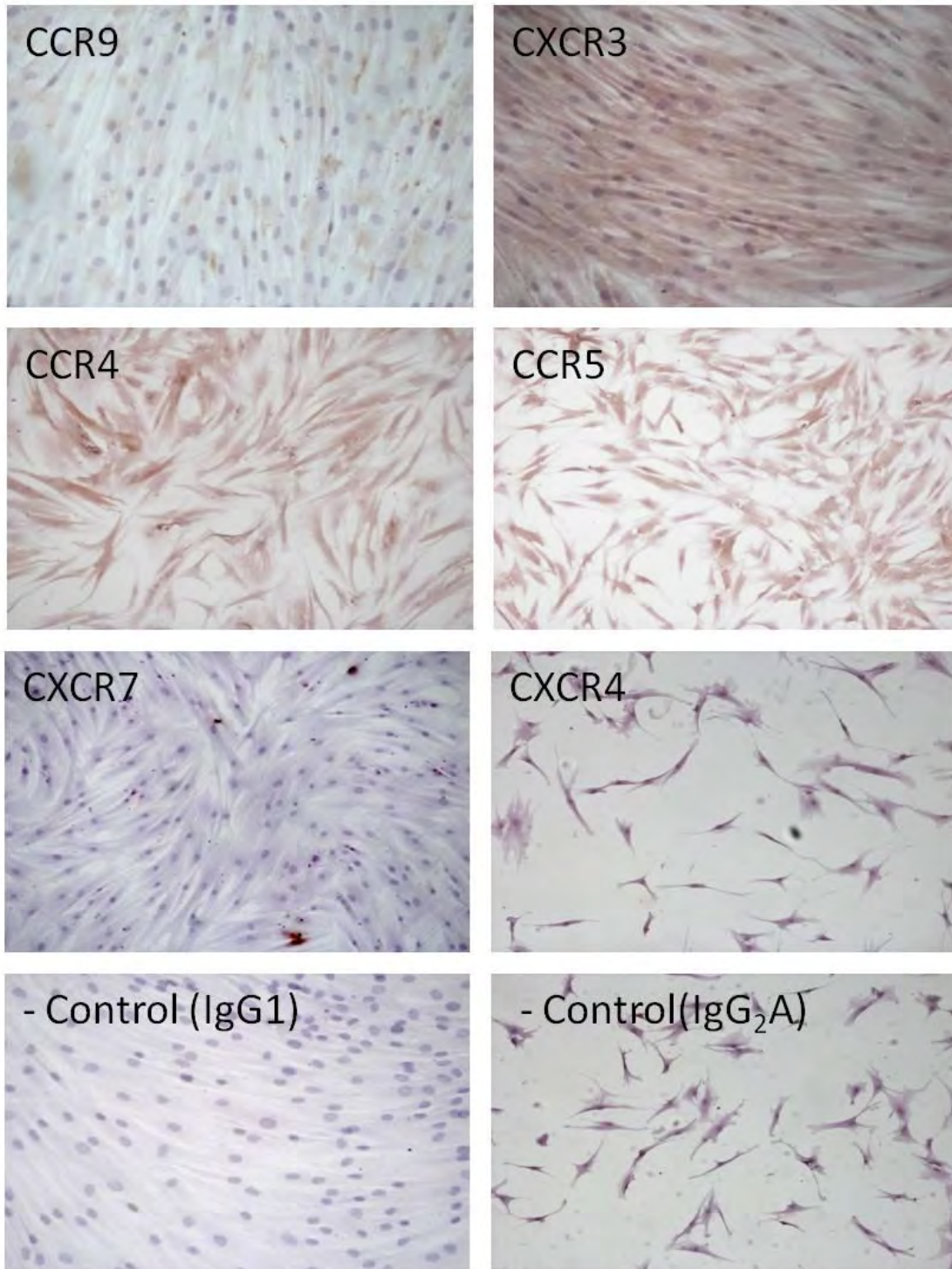


**Figure 4.4: Immunohistochemical analysis of MSC CCR expression.**

Representative images of immunohistochemical staining with Nova red (red/ brown) of CCR4 (IgG1), CCR5 (IgG1), CCR9 (IgG1), CXCR3 (IgG1), CXCR7 (IgG1), CXCR4 (IgG2a), compared to concentration matched controls. MSC are grown on glass cover-slips and counterstained with Mayer's Haematoxylin (n=3 donors at x20 magnification).



#### **4.2.2 TGFβ1, IL4 and IL10 stimulation significantly increases surface CCR expression by MSC**

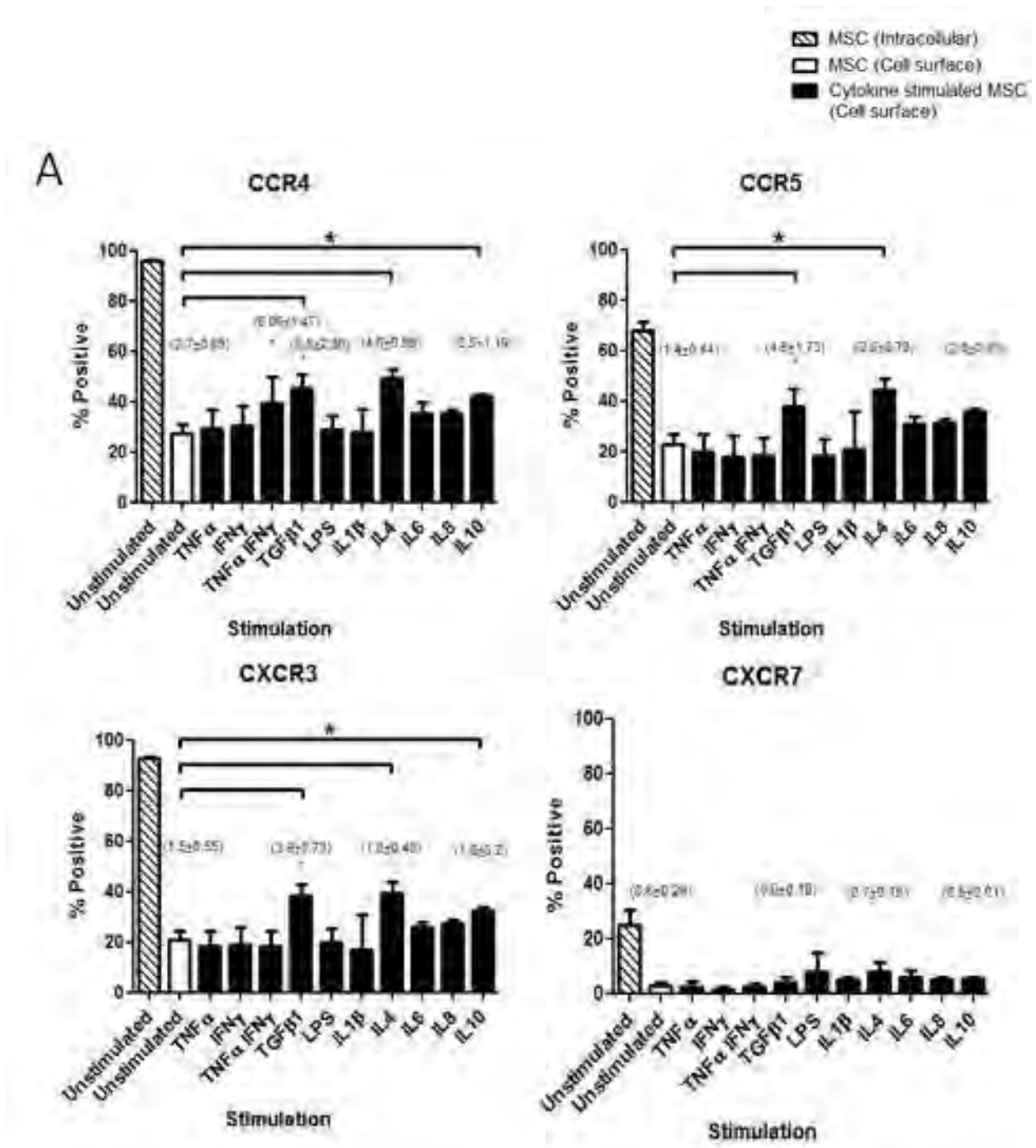
Flow cytometry was used to measure the percentage of MSC expressing cell surface CCR4, CCR5, CCR9, CXCR3, CXCR4 and CXCR7 before and after cytokine stimulation for 24 hours. TGFβ1 (unstimulated: 23.36±7.2, stimulated: 45.56±5.41; p<0.05), IL4 (unstimulated: 30.91±3.32, stimulated: 49.15±3.78; p<0.05) and IL10 (unstimulated: 30.19±3.32, stimulated: 41.62±1.29; p<0.05) stimulation of MSC significantly increased the percentage of MSC with CCR4 surface expression. Similarly, TGFβ1 (unstimulated: 18.49±6.94, stimulated: 38.34±4.73; p<0.05), IL4 (unstimulated: 23.57±1.68, stimulated: 39.26±4.44; p<0.05) and IL10 (unstimulated: 23.57±1.68, stimulated: 32.54±1.39; p<0.05) significantly increased the percentage of MSC with surface CXCR3 surface expression. However, only TGFβ1 and IL4 stimulation significantly increased the percentage of MSC with CCR5 surface expression (Figure 4.5A and B). TGFβ1 stimulation significantly increased MSC CCR4 (3.21±0.52 fold; p<0.05), CCR5 (3.28±0.78 fold; p<0.05) and CXCR3 (3.27±0.92 fold; p<0.05) expression compared to unstimulated MSC. TNFα/IFNγ stimulation also significantly increased CCR4 (2.26±0.31 fold; p<0.05) surface expression on MSC. As we further increased the number of donors (Figure 4.6A), we found that TGFβ1 stimulation significantly increased the percentage of cells which expressed CCR9 (unstimulated: 4.1±0.88%, stimulated: 10.54±2.28%; p<0.05) and that IL10 caused a significant increase in CCR5 (unstimulated: 25.26±3.06, stimulated: 33.24±2.65; p<0.05), CCR9 (unstimulated: 4.11±0.88, stimulated: 8.5±3.21; p<0.01), CXCR4 (unstimulated: 0.69±0.30, stimulated: 1±0.38; p<0.05) and CXCR7 (unstimulated: 4.07±1.34, stimulated: 5.24±0.53; p<0.0001). IL4 stimulation also significantly increased expression of CXCR4 (unstimulated: 0.69±0.30, stimulated: 0.86±0.23; p<0.05) on the cell surface

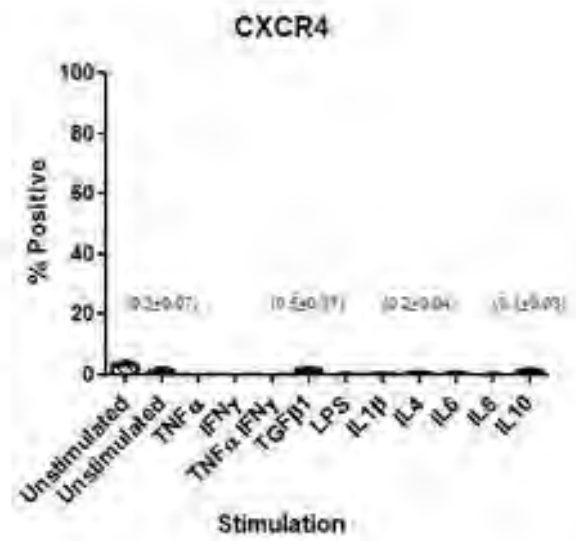
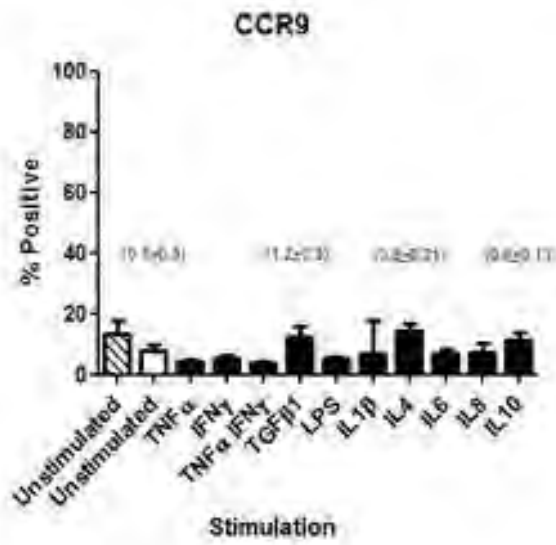




although only a very small percentage of MSC were positive (Figure 4.6B). We additionally tested whether we could see a significant increase in the percentage of MSC expressing CCR4, CCR5 or CXCR3 and a corresponding increase of surface CCR expression in the MSC after 10 minutes stimulation with TGF $\beta$ 1. There was not a significant increase in CCR4, CCR5 or CXCR3 expression in MSC or as a percentage of expression after 10 minutes TGF $\beta$ 1 stimulation (Figure 4.7). To measure changes in the selected CCR mRNA before and after cytokine stimulation in MSC we used quantitative PCR (QPCR). Here in contrast to protein expression changes, we found there was no significant change in CCR mRNA levels after cytokine stimulation of MSC (Figure 4.8). However in the case of CCR4, statistical analysis using Analysis of Variance (ANOVA) tests and subsequent post-hoc tests showed no significant difference in expression after IL8 stimulation, but an individual T test showed a significant increase in CCR4 expression. 18S rRNA PCR was used to confirm that no RNA contamination of cDNA samples occurred (not shown).

**Figure 4.5: Expression of MSC CCR after cytokine stimulation.**

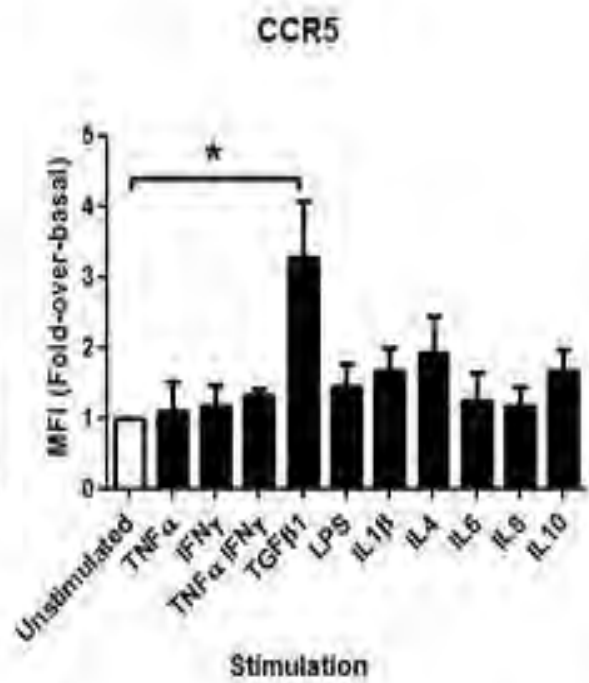
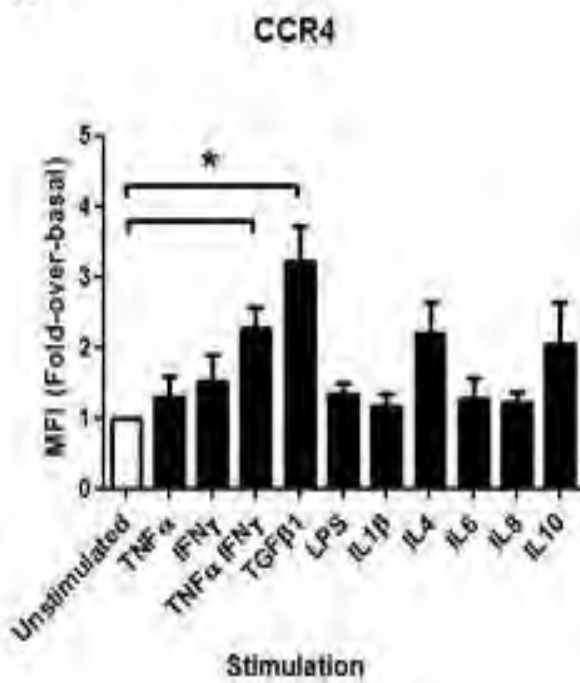
Flow cytometry analysis for surface CCR4, CCR5, CCR9, CXCR3, CXCR4 and CXCR7 after 24 hour cytokine stimulation [TNF $\alpha$  (10ng/ml), IFN $\gamma$  (25ng/ml), TGF $\beta$ 1 (5ng/ml), LPS (200ng/ml), IL1 $\beta$  (10ng/ml), IL4 (10ng/ml), IL6 (10ng/ml), IL8 (10ng/ml), IL10 (50ng/ml)] compared with basal CCR levels expressed as A: percentage positive MSC, and B: MFI. Bars represent mean  $\pm$  SEM of n=3 donor samples.

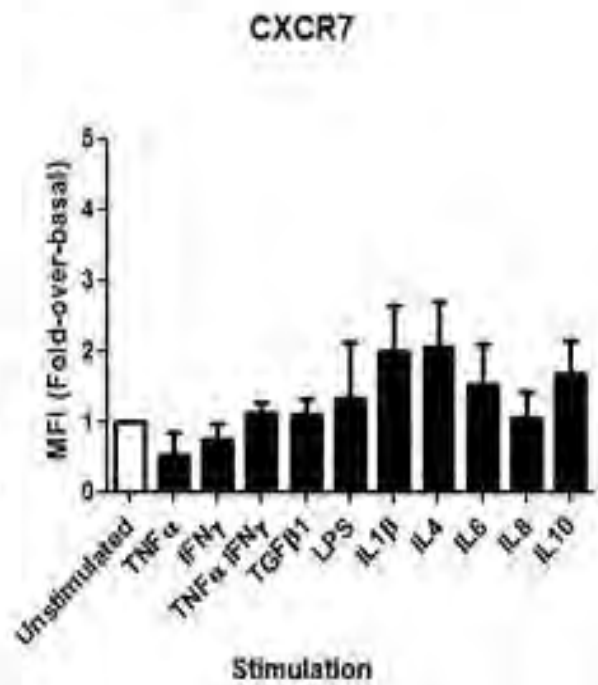
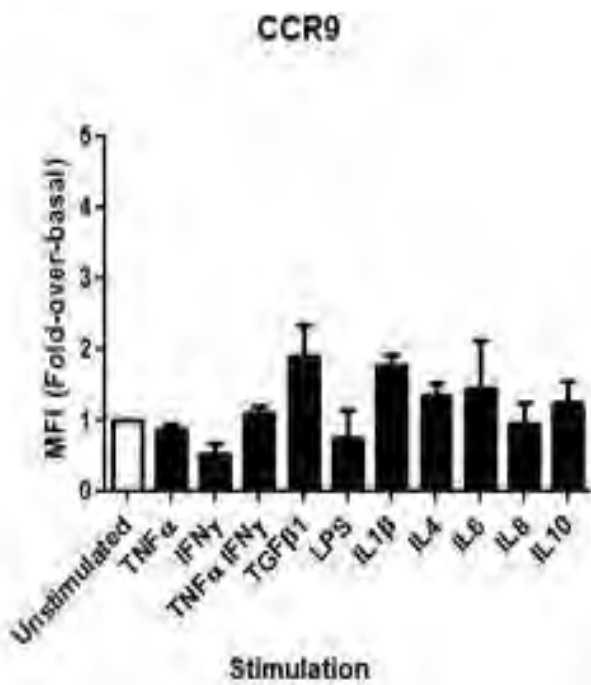
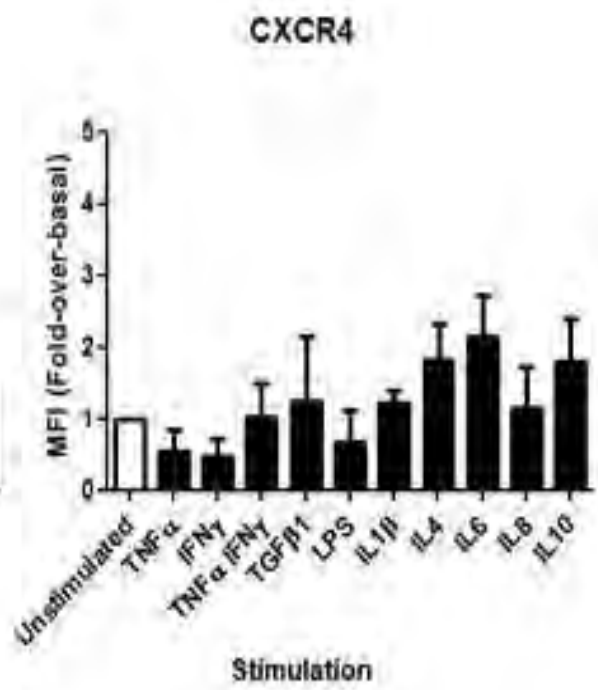
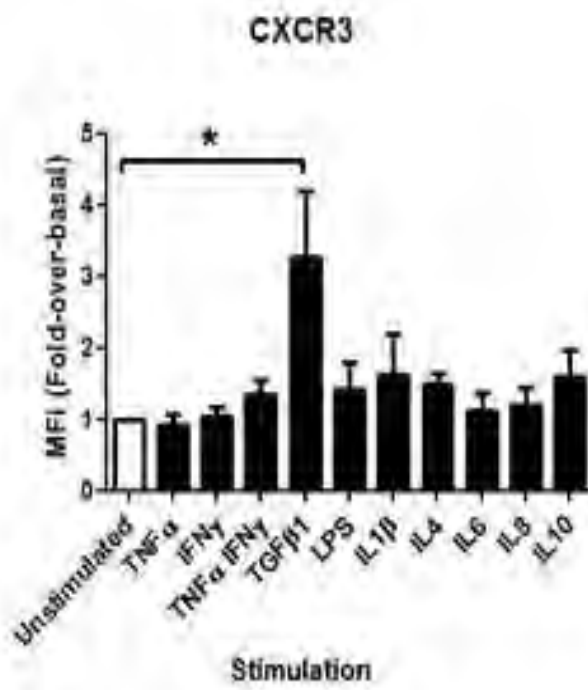




 MSC (Cell surface)  
 Cytokine stimulated MSC (Cell surface)

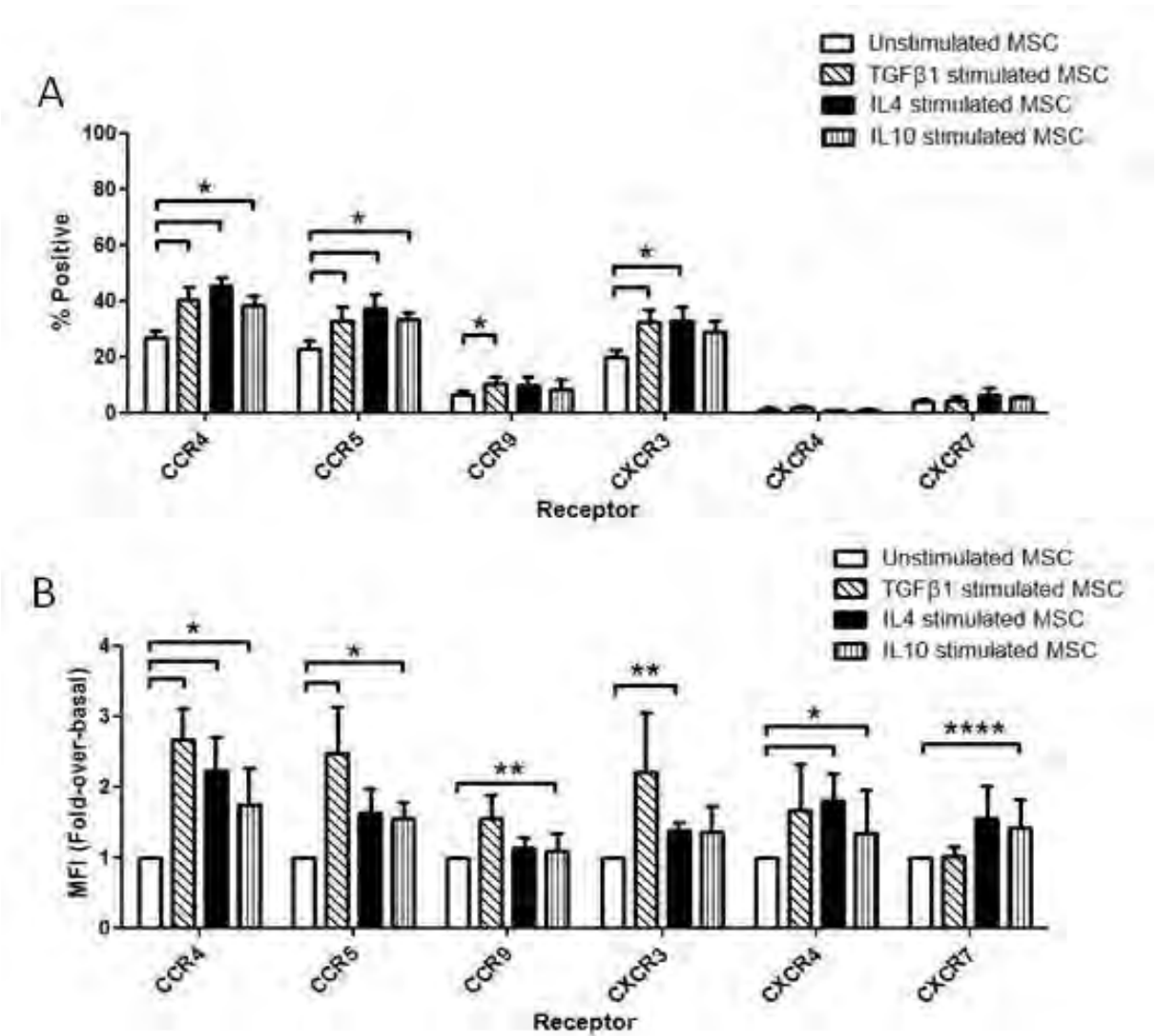
**B**





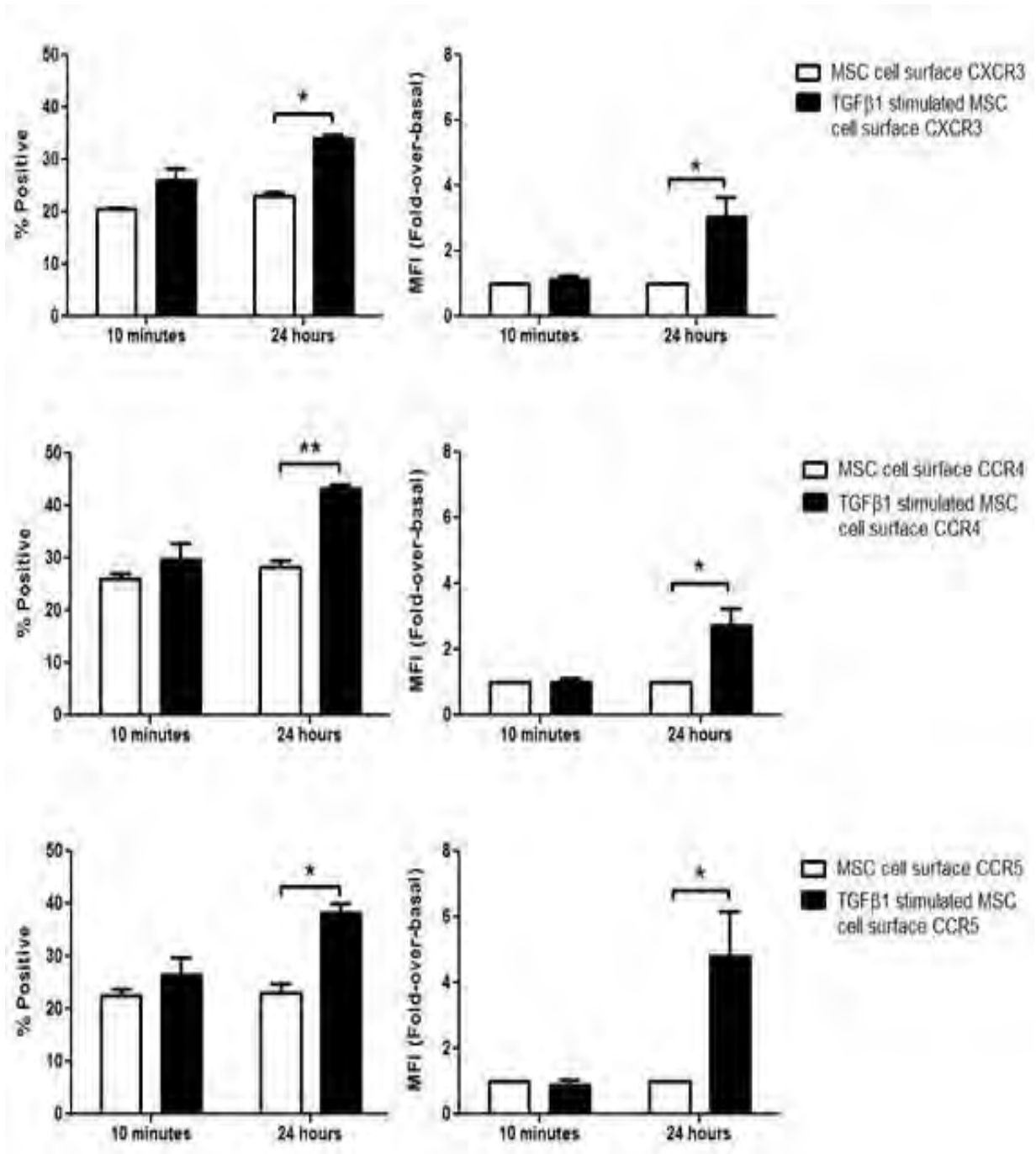
**Figure 4.6: Confirmation of Flow cytometry results for chemokine expression on multiple donors.**

Analysis for surface CCR4, CCR5, CCR9, CXCR3, CXCR4 and CXCR7 after TGFβ1, IL4, IL10 stimulation compared with basal CCR levels expressed as A: percentage positive MSC, and B: MFI. Bars represent mean ± SEM of n=5 donor samples, \*, p<0.05, \*\*, p<0.01, \*\*\*\*, p<0.0001.



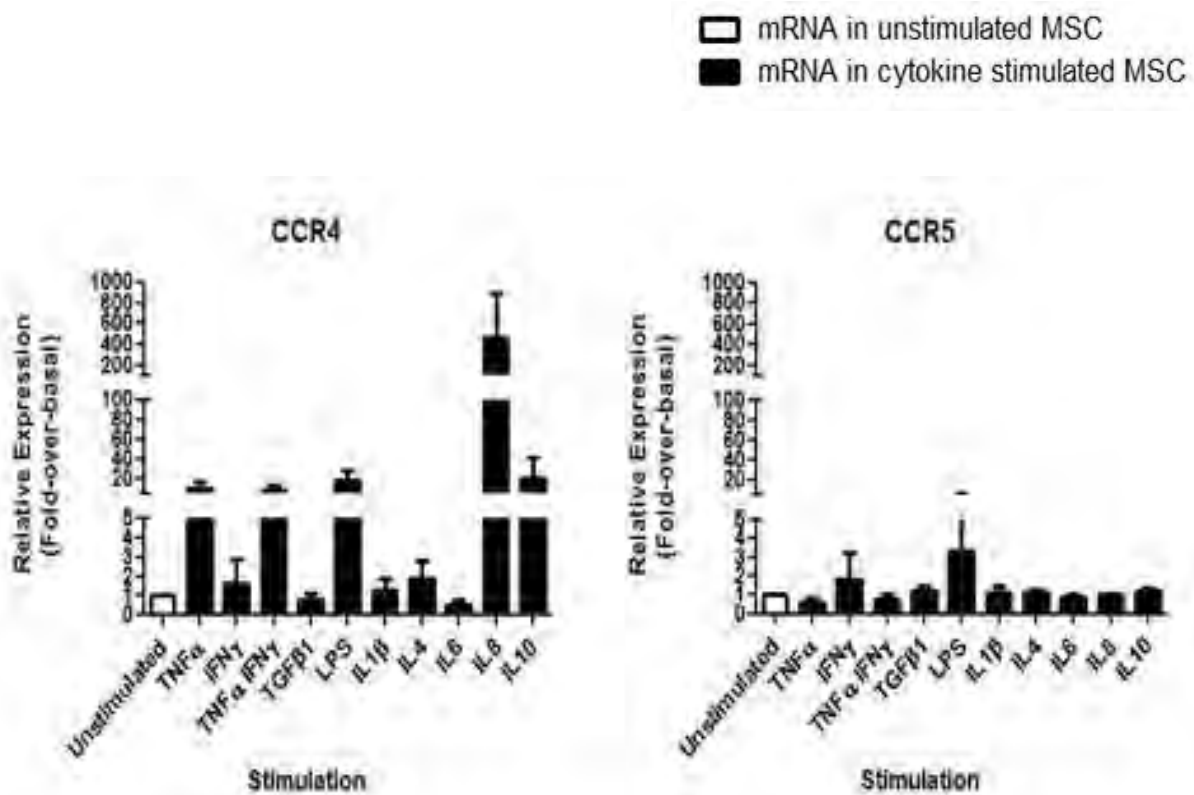
**Figure 4.7: Effects of short term stimulation with TGFβ1 on receptor expression.**

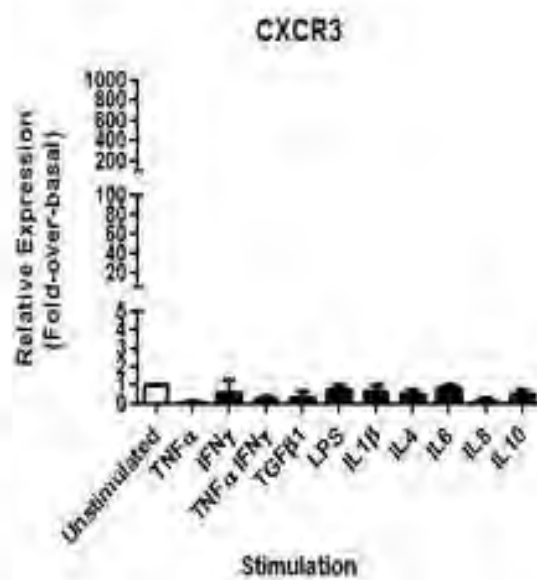
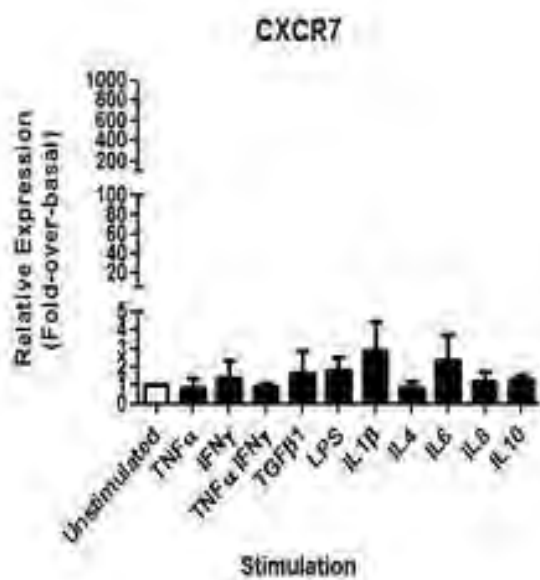
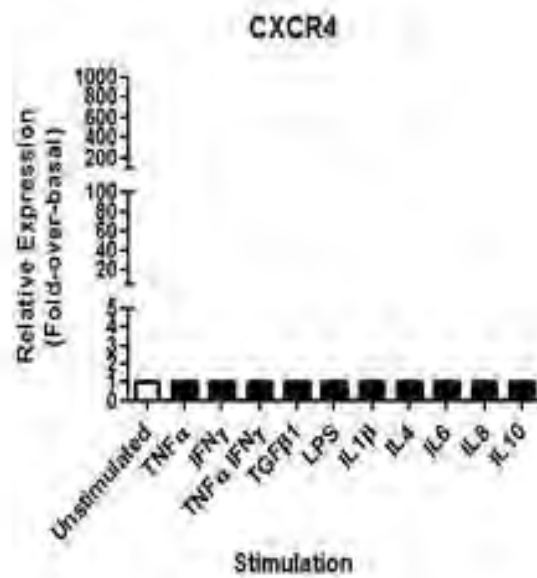
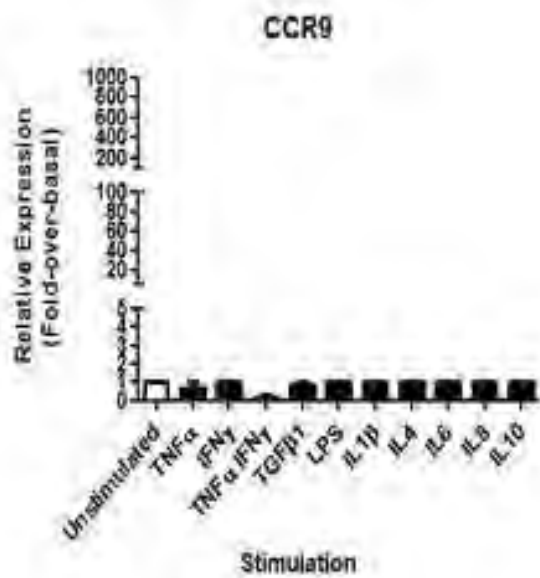
Flow cytometry analysis for surface CCR4, CCR5, and CXCR3 after TGFβ1 stimulation compared with basal CCR levels for 10 minutes and 24 hours. Bars represent mean ± SEM of n=5 donor samples. MFI of CCR levels in stimulated MSC (closed bars) are expressed as fold change over basal MFI levels of CCR in unstimulated MSC (open bars).



**Figure 4.8: Confirmation of effects of cytokines on CCR expression by QPCR.**

Quantitative analysis of total CCR4, CCR5, CCR9, CXCR3, CXCR4 and CXCR7 gene levels in cytokine stimulated MSC, measured by Real Time Polymerase Chain Reaction (QPCR) analysis. Stimulated MSC gene levels relative to endogenous  $\beta$ -actin levels (closed bars) in stimulated MSC were expressed as fold change over basal levels of CCR in un-stimulated MSC (open bars). The results were calculated by the comparative threshold cycle (Ct) method, with the Ct for  $\beta$ -actin in cytokine treated and untreated MSC used to normalise the results. Expression of each gene was calculated with the difference in basal CCR levels and endogenous level of  $\beta$ -actin in untreated MSC defined as 1 (open bars). Bars represent mean  $\pm$  SEM of n=3 different donor samples, performed in triplicate.







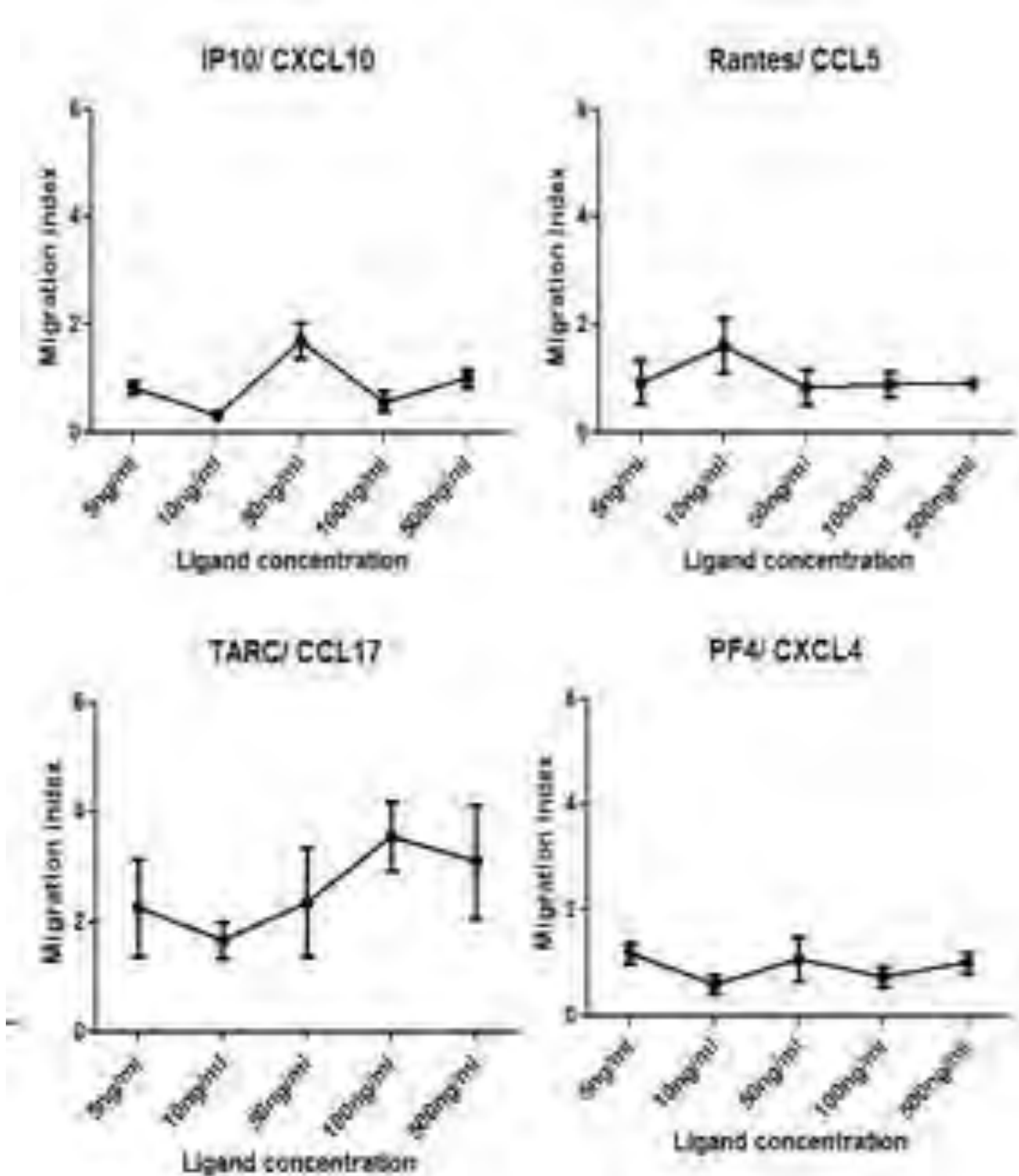
### **4.2.3 TGFβ1 and IL4 stimulation increases MSC migration to CXCR3 ligand IP10/ CXCL10 and CCR4 ligand TARC/ CCL17.**

Using Boyden chamber assays the migration of MSC towards chemokine ligands for selected CCR was measured across a range of concentrations. Optimal concentrations of ligands where maximal MSC migration was observed were identified for further investigation (Figure 4.9). There was significant migration of MSC to SDF1α/ CXCL12 (control:  $0.4 \pm 0.12$ , ligand:  $1.77 \pm 0.34$ ;  $p < 0.01$ ), ITAC/ CXCL11 (control:  $1.6 \pm 0.24$ , ligand:  $3.23 \pm 0.93$ ;  $p < 0.05$ ), MCP2/ CCL8 (control:  $0.85 \pm 0.22$ , ligand:  $2.83 \pm 0.91$ ;  $p < 0.05$ ), Teck/ CCL25 (control:  $1.65 \pm 0.43$ , ligand:  $4.57 \pm 0.91$ ;  $p < 0.05$ ). We were also interested in further investigation of specific ligands where although not significant, there was some suggestion of a small degree of MSC migration, namely, MDC/ CCL22 (control:  $0.45 \pm 0.15$ , ligand:  $2.22 \pm 0.70$ ), MIP1β/ CCL4 (control:  $1.4 \pm 0.66$ , ligand:  $3.7 \pm 1.07$ ), TARC/ CCL17 (control:  $2.7 \pm 0.27$ , ligand:  $3.57 \pm 0.63$ ), Rantes/ CCL5 (control:  $0.45 \pm 0.13$ , ligand:  $1.6 \pm 0.51$ ) and IP10/ CXCL10 (control:  $0.95 \pm 0.26$ , ligand:  $1.7 \pm 0.33$ ) (Figure 4.10).

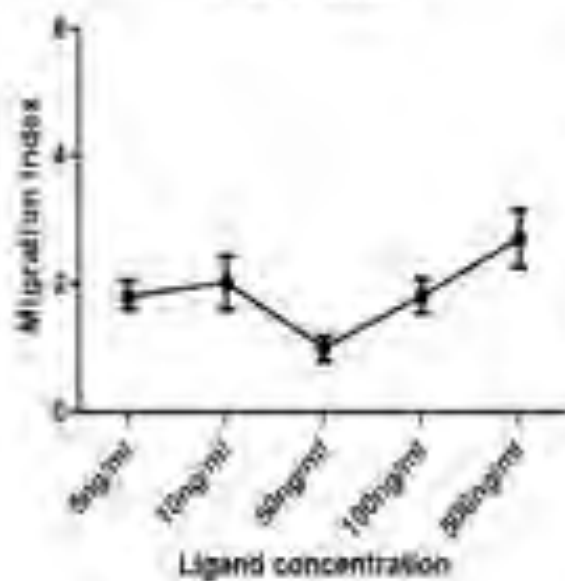
When migration of MSC towards chemokine was normalised to controls, the different stimulations were compared by how much they influence migration of MSC towards each ligand. There did not seem to be any significant difference in migration of MSC after cytokine stimulation to most ligands. There was significantly increased MSC migration towards TARC/ CCL17 ( $2.6 \pm 0.18$  fold;  $p < 0.05$ ) after IL4 stimulation of MSC. TGFβ1 stimulation significantly increased MSC migration towards IP10/ CXCL10 ( $2.3 \pm 0.49$  fold;  $p < 0.05$ ) (Figure 4.11).

**Figure 4.9: MSC dose response to chemokine ligand.**

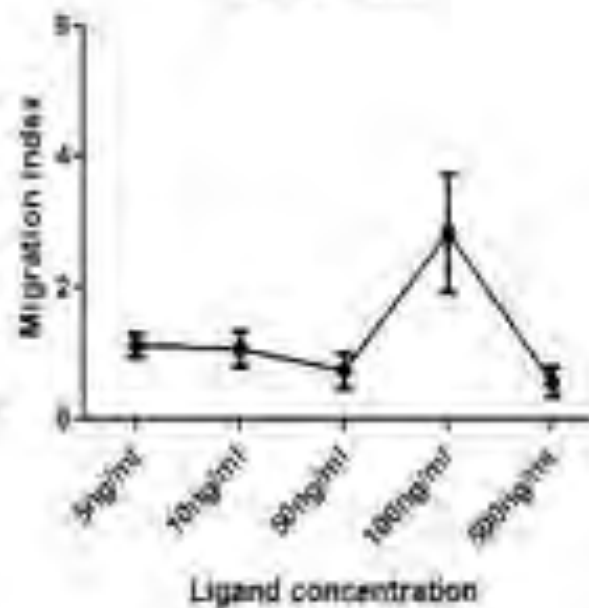
Migration of MSC to various chemokines titrated at 5, 10, 50, 100, 500ng/ml, assessed by Boyden Chamber assays, n=3. Data is expressed as Migration Index (cells/ field of view).



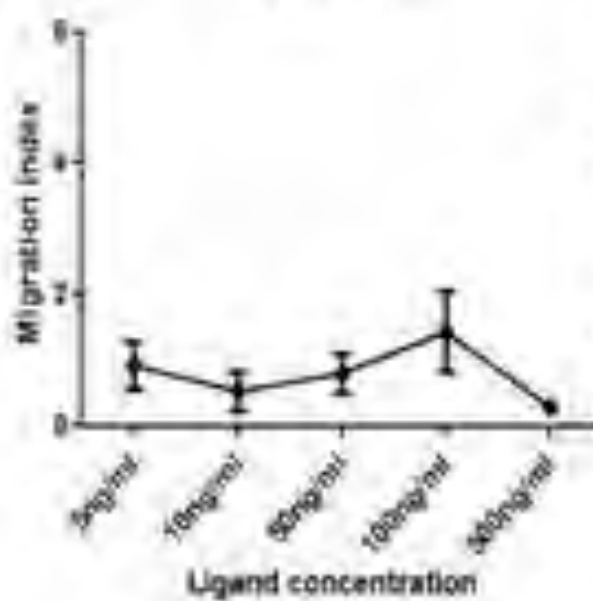
MCP1/ CCL2



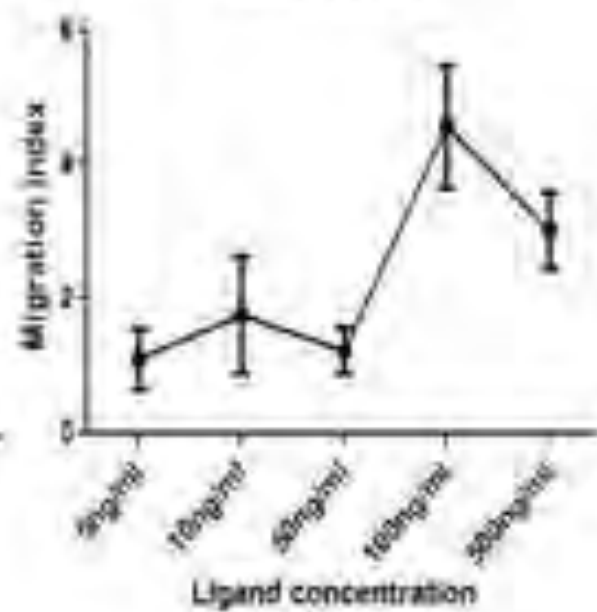
MCP2/ CCL8



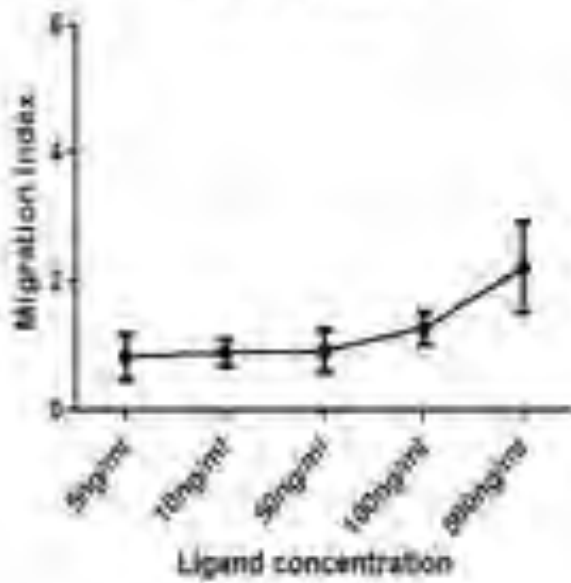
MIG/ CXCL9



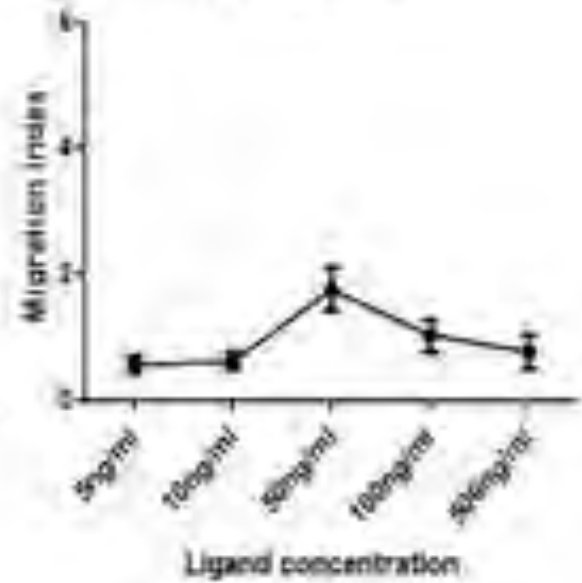
TECK/ CCL25



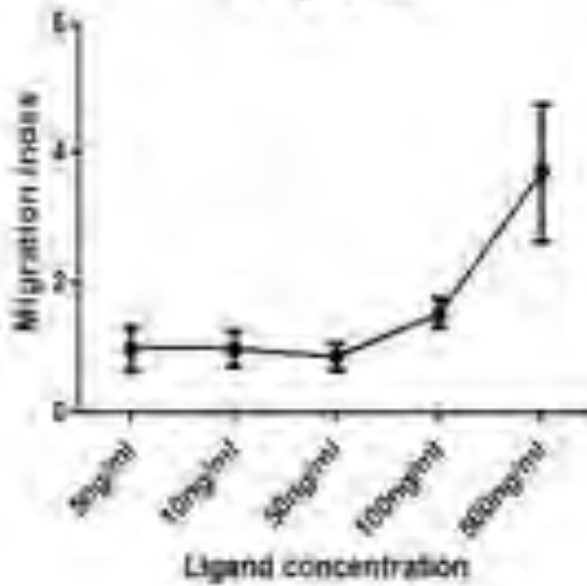
MDC/CCL22



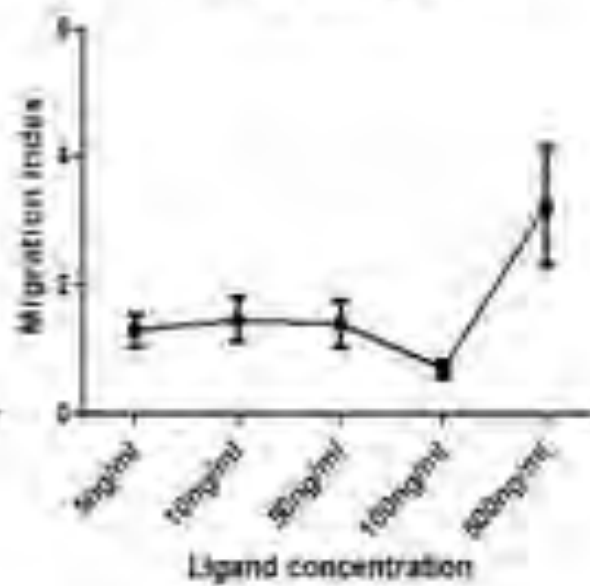
SDF1 $\alpha$ /CXCL12



MIP1 $\beta$ /CCL4

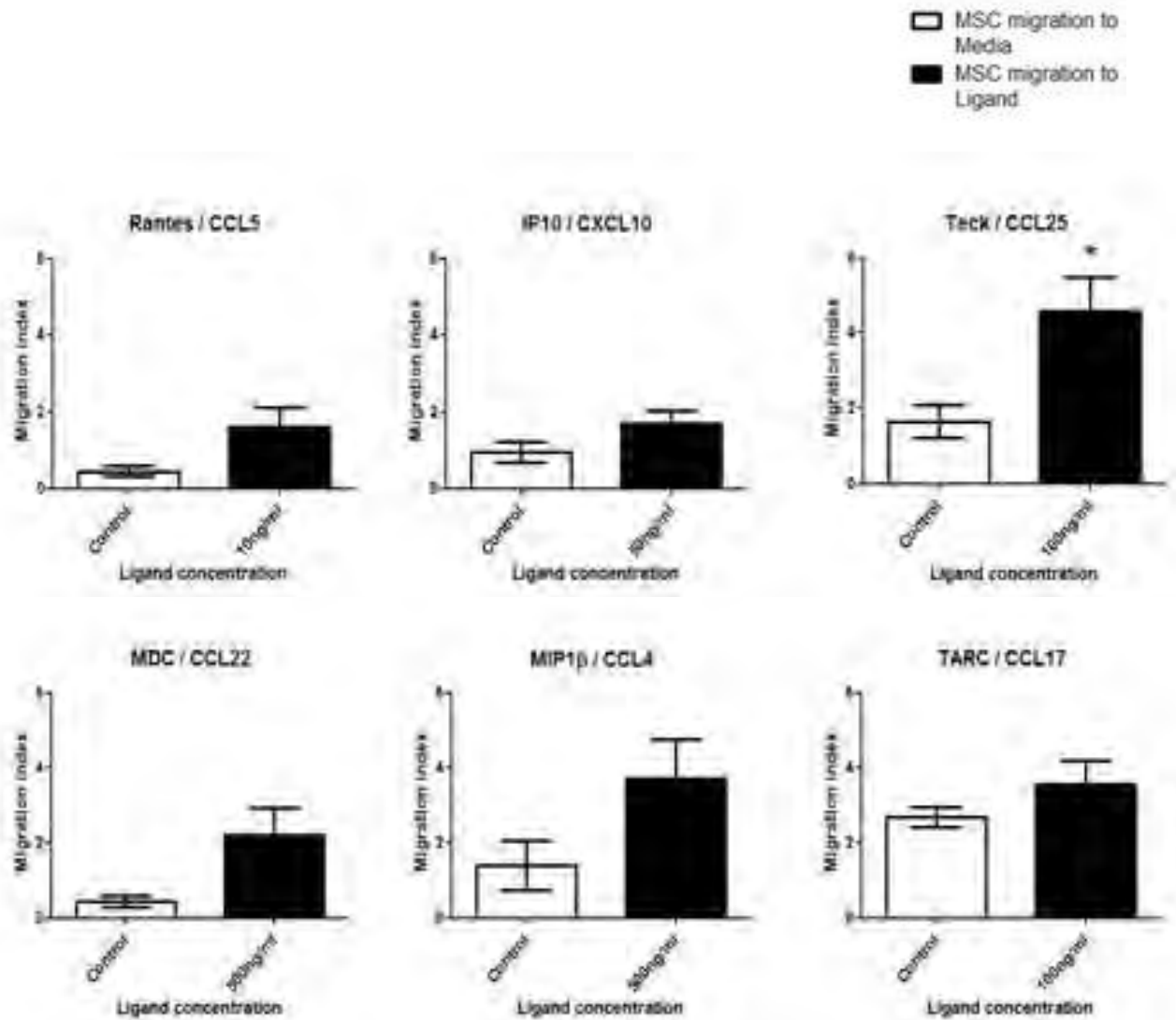


ITAC/CXCL11



**Figure 4.10: MSC migration to chemokine ligands.**

Selection of chemokine ligands (closed bars) compared with media only controls (open bars) to which there was significant migration of MSC which include SDF1 $\alpha$ / CXCL12, ITAC/ CXCL11, MCP-2/ CCL8, Teck/ CCL25. Other chemokines of interest to be investigated further include MDC/CCL22, MIP1 $\beta$ / CCL4, TARC/ CCL17, Rantes/ CCL5, IP10/ CXCL10. Data is expressed as Migration Index (cells/ field of view). Bars represent mean  $\pm$  SEM of n=3 donor samples.



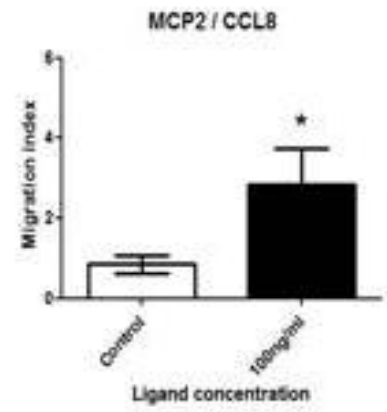
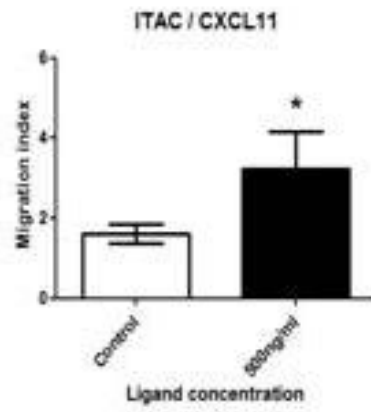
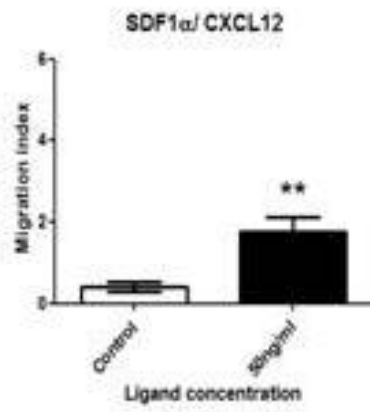
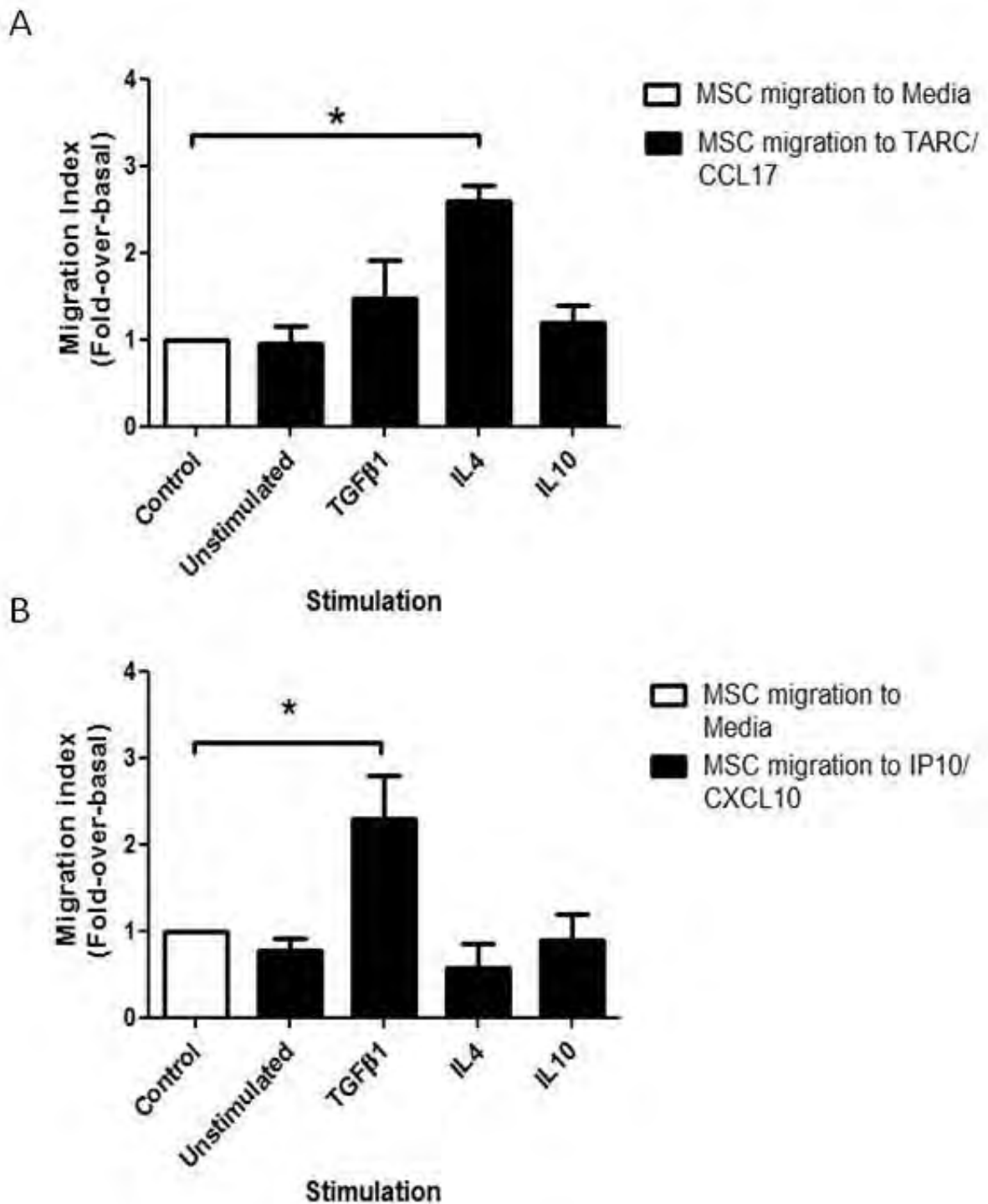


**Figure 4.11: Impact of TGFβ1, IL4 and IL10 stimulation on MSC migration to chemokine ligands.**

A: Migration of MSC to selected chemokines (closed bars) compared to media only controls (open bars) compared with TGFβ1, IL4 and IL10 stimulated MSC. B: Migration of unstimulated, TGFβ1, IL4 and IL10 stimulated MSC towards TARC/ CCL17 and IP-10/ CXCL10. Migration to ligand (closed bars) is expressed as fold change relative to migration of unstimulated MSC to media only control, defined as 1 (open bar). Bars represent mean ± SEM of n=3 donor samples. \*, p<0.05.



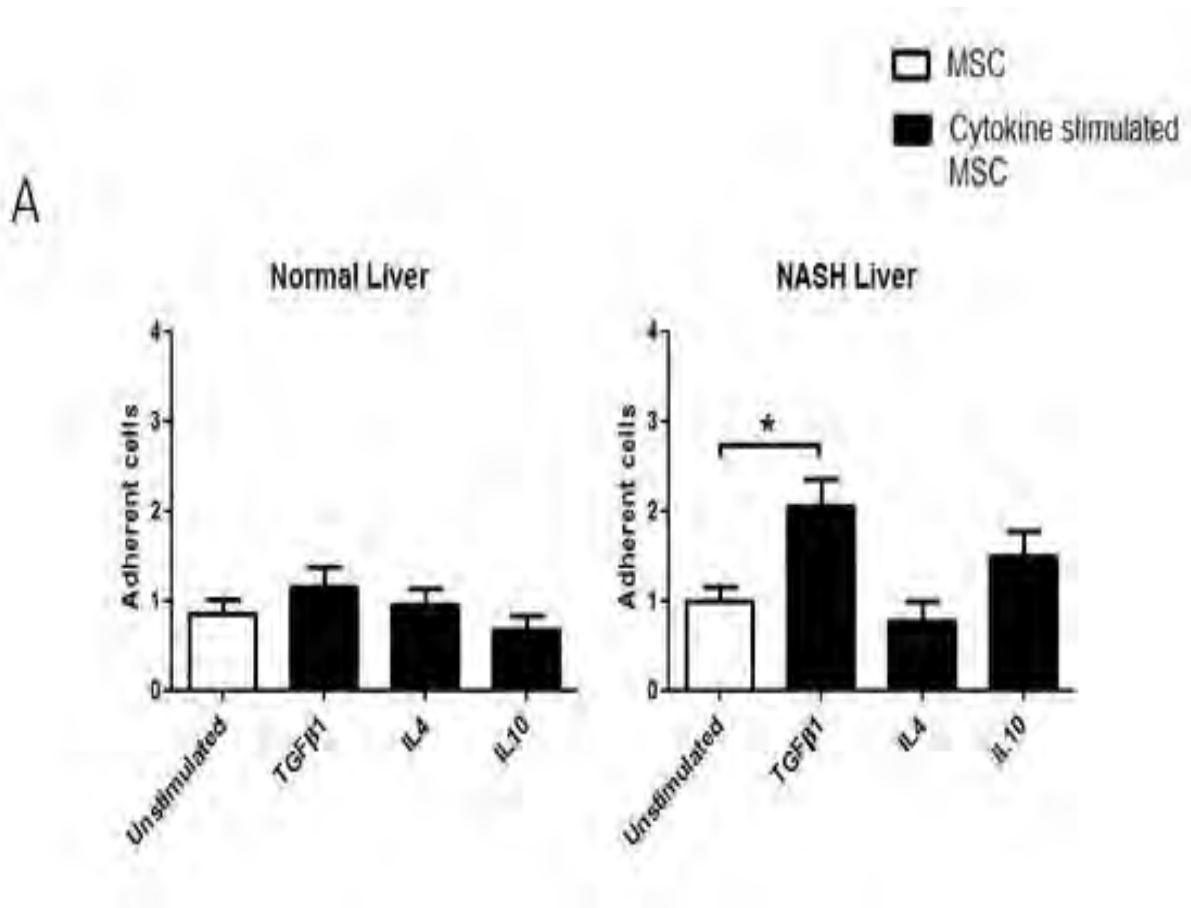
#### **4.2.4 TGFβ1 stimulated MSC show increased binding to hepatic sinusoidal endothelium in cirrhotic livers and in culture.**

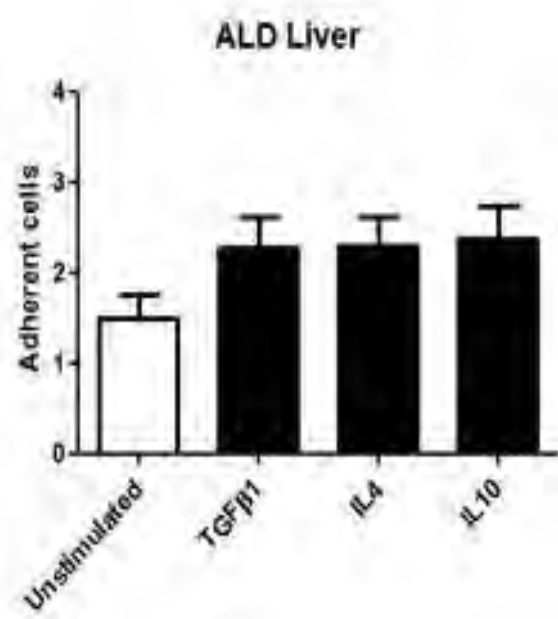
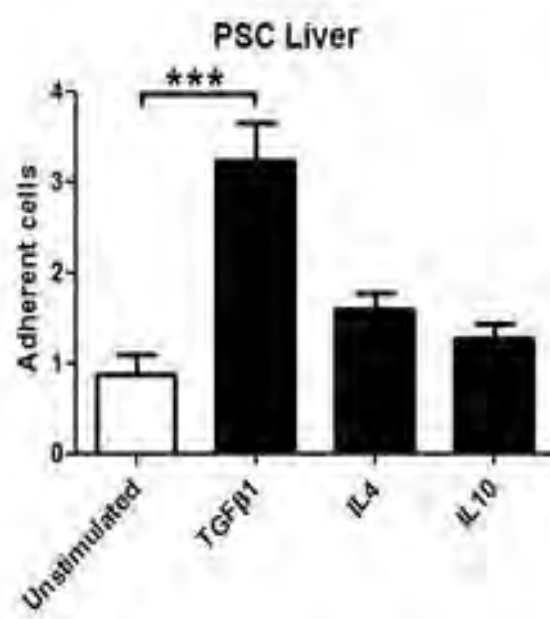
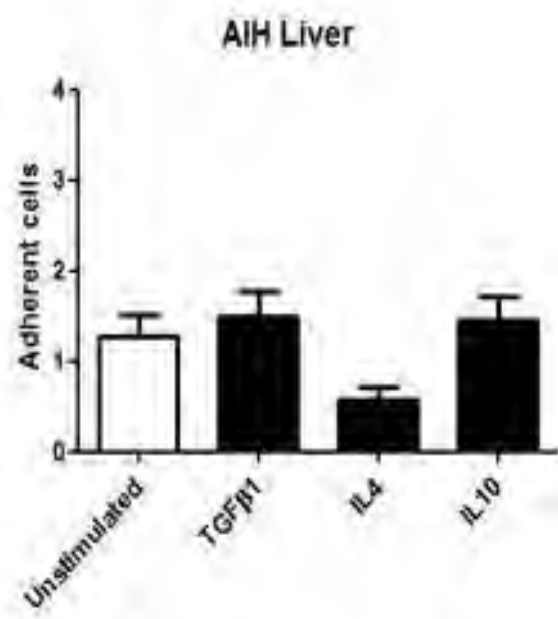
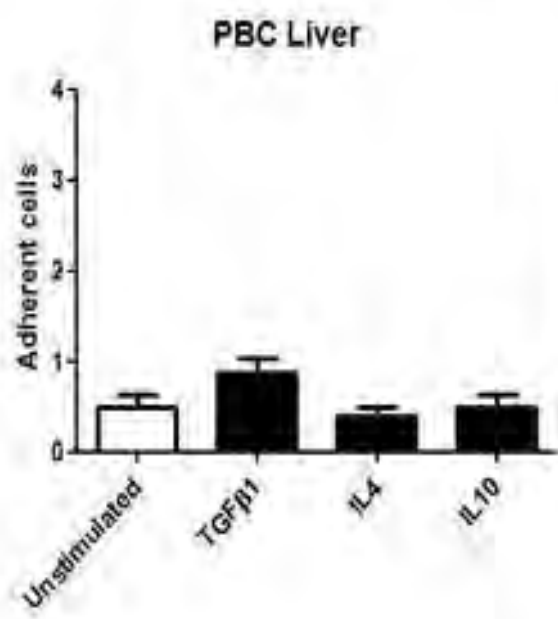
Modified Stamper Woodruff experiments were carried out with TGFβ1, IL4 and IL10 stimulated MSC and liver sections from explanted normal, NASH, PSC, PBC, AIH and ALD livers to test whether cytokine stimulations had an effect on MSC adhesion to these livers. TGFβ1 stimulated MSC were more adherent to NASH liver sections (unstimulated  $1.5 \pm 0.26$ , stimulated:  $2.28 \pm 0.35$ ;  $p < 0.05$ ) and PSC liver sections (unstimulated:  $0.88 \pm 0.21$ , stimulated:  $3.23 \pm 0.43$ ;  $p < 0.05$ ) (Figure 4.12A). TGFβ1 stimulated MSC were also used in modified adhesion assay experiments using HSEC, BEC and MF monolayers. TGFβ1 stimulated MSC were significantly more adherent to HSEC monolayers compared to unstimulated MSC (unstimulated:  $6.82 \pm 0.71$ , stimulated:  $9.5 \pm 0.65$ ;  $p < 0.05$ ) and compared with TGFβ1 stimulated BEC ( $4.65 \pm 0.39$ ;  $p < 0.05$ ) and MF ( $4.87 \pm 0.38$ ;  $p < 0.05$ ). HSEC monolayers were also stimulated with TNFα/IFNγ to mimic an injured environment. Once again TGFβ1 stimulated MSC ( $7.69 \pm 0.59$ ;  $p < 0.001$ ) exhibited increased adherence to stimulated HSEC compared with unstimulated MSC ( $4.18 \pm 0.66$ ;  $p < 0.001$ ) and also compared to adhesion with stimulated BEC ( $2.02 \pm 0.26$ ;  $p < 0.001$ ) and MF ( $1.97 \pm 0.2$ ;  $p < 0.001$ ) (Figure 4.12B).

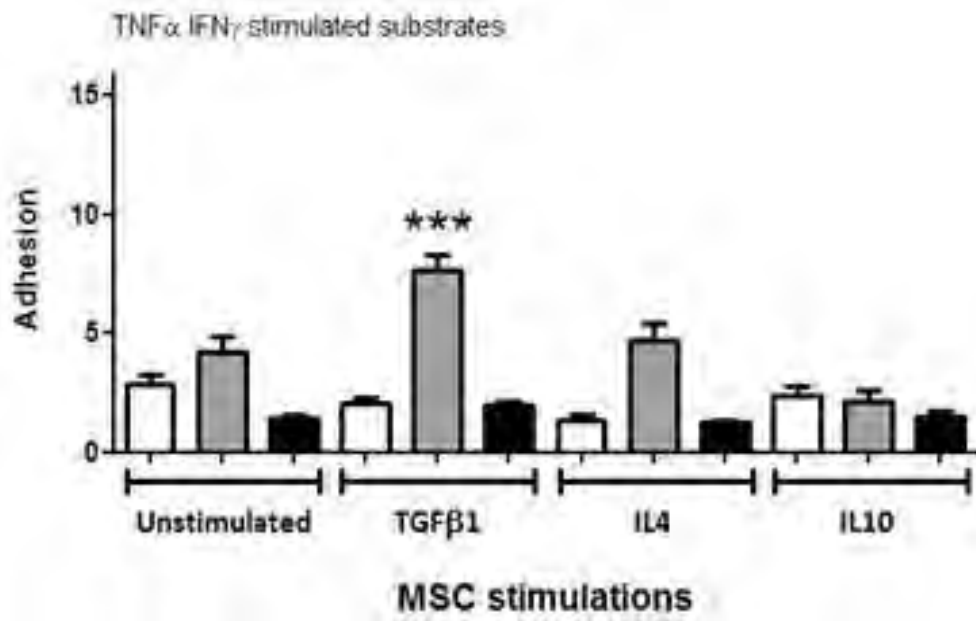
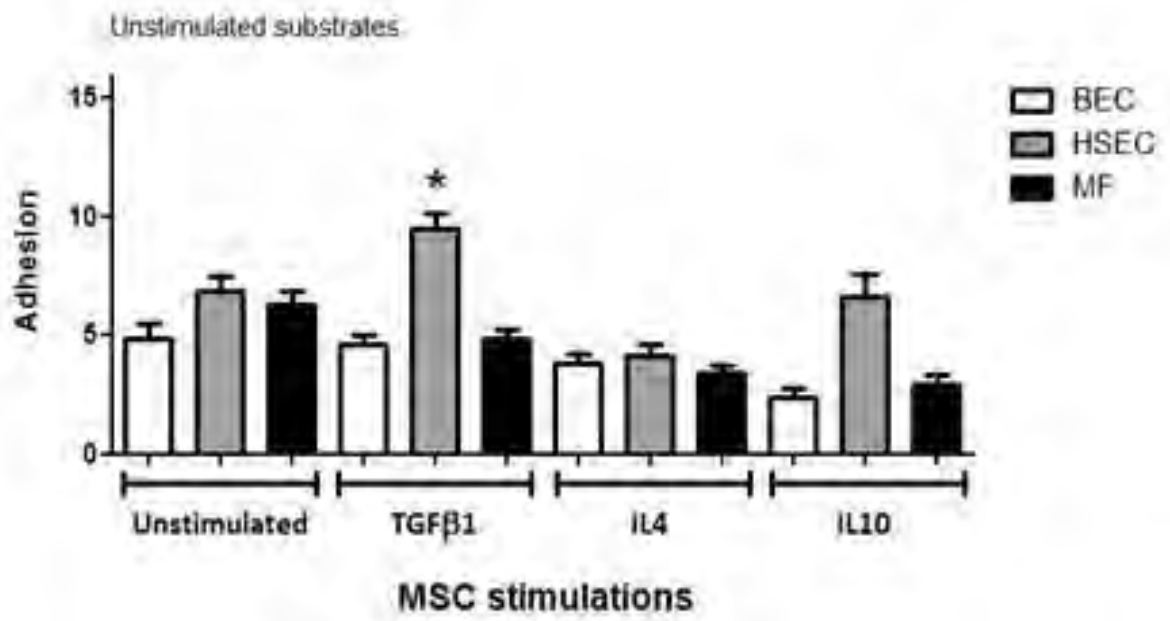


**Figure 4.12: Impact of cytokine stimulation on adhesion of MSC.**

A: Modified Stamper Woodruff assays showing basal adhesion of MSC (open bars) compared with TGF $\beta$ 1, IL4 and IL10 stimulated MSC adhesion (closed bars) to normal, Non alcoholic steatohepatitis (NASH), Primary sclerosing cholangitis (PSC), Primary biliary cirrhosis (PBC), Autoimmune hepatitis (AIH), Alcoholic liver disease (ALD) cirrhotic liver sections. B: Modified Stamper Woodruff assays showing basal adhesion of MSC (open bars) compared with TGF $\beta$ 1, IL4 and IL10 stimulated MSC (grey and closed bars) adhesion to unstimulated and TNF $\alpha$ /IFN $\gamma$  stimulated human liver cells including, hepatic sinusoidal endothelial cells (HSEC), biliary epithelial cells (BEC) and myofibroblast (MF) cell monolayers. Adhesion represents area fraction covered by adherent fluorescent MSC using Image J analysis. Bars represent mean  $\pm$  SEM cells/ field of view of n=3 liver donors and 3 MSC donors, \*, p<0.05; \*\*\*, p<0.001.







#### **4.2.5 Upregulation of cell surface CXCR3 modulates increased engraftment of TGFβ1 stimulated MSC in mice with carbon tetrachloride induced liver injury.**

We set up carbon tetrachloride induced liver injury experiments in two strains of mice. Liver injury was induced in Rag2<sup>-/-</sup>IL-2r<sup>γ</sup><sup>-/-</sup> mice after 12 weeks, with twice weekly intraperitoneal carbon tetrachloride injections compared with control/ sham injured mice. Figure 4.13A shows presence of injury confirmed by high levels of Van Gieson staining and Picrosirius red staining of collagen-1 depicting bridging fibrosis. Picrosirius red staining was quantified using Image J and we found significantly increased staining in injured mouse livers (1.17±0.23) compared to sham injured mouse livers (0.31±0.17) p<0.01 (Figure 4.13B). Liver injury was also induced in wild type C57BL/6 mice with 8 week, twice weekly intraperitoneal carbon tetrachloride compared with uninjured control mice. H and E staining shows tissue damage in injured mouse livers, as does increased Picrosirius red staining for collagen-1 (Figure 4.14A). Injured livers had characteristically higher levels of collagen-1 (6.26±0.49 fold; p<0.0001), αSMA (12.39±0.71; p<0.0001), serum bilirubin (control: 4.06±0.9 vs. injured: 3.26±0.11; p<0.0001) and reduced serum albumin (control: 0.1±0.004 vs. injured: 0.17±0.008; p<0.0001) (Figure 4.14B).

Modified Stamper Woodruff experiments were carried out with TGFβ1 stimulated MSC on liver sections from Rag2<sup>-/-</sup>IL-2r<sup>γ</sup><sup>-/-</sup> sham injured and carbon tetrachloride injured mice to test whether cytokine stimulations had an effect on MSC adhesion to these livers. TGFβ1 stimulated MSC were more adherent to sham injured liver sections (1.74±0.23 fold) compared to unstimulated MSC, (p<0.01), and there was a similar increase in binding (2.05±0.21 fold) of TGFβ1 stimulated MSC to carbon tetrachloride injured mouse Rag2<sup>-/-</sup>IL-2r<sup>γ</sup><sup>-/-</sup> livers

( $p < 0.001$ ) (Figure 4.15A). Similar experiments were also performed on liver sections from wild type C57BL/6 uninjured and carbon tetrachloride injured mice. Here TGF $\beta$ 1 stimulated MSC were  $1.56 \pm 0.19$  fold more adherent to carbon tetrachloride injured sections than unstimulated MSC ( $p < 0.05$ ) but there was no significant difference in binding of TGF $\beta$ 1 stimulated MSC to uninjured mouse C57BL/6 livers (Figure 4.15B).

To test adhesion and engraftment of MSC in injured liver *in vivo* we infused CFSE labelled MSC into carbon tetrachloride injured and uninjured C57BL/6 mice via the portal vein directly into the liver. MSC infused were either unstimulated, or stimulated with TGF $\beta$ 1, IL4 and IL10. We observed increased engraftment of TGF $\beta$ 1 stimulated CFSE labelled MSC in injured mouse livers compared to unstimulated MSC (Figure 4.15C). TGF $\beta$ 1 stimulated MSC engrafted  $2.29 \pm 0.08$  fold ( $p < 0.001$ ) more in injured mice, than unstimulated MSC, compared with IL4 and IL10 which showed no significant change in engraftment (Figure 4.15D). Figure 4.15E shows blocking CXCR3 (10 $\mu$ g/ml) on MSC has no significant effect on engraftment of MSC in injured C57BL/6 mouse livers, however the  $2.32 \pm 0.22$  fold increase of TGF $\beta$ 1 stimulated MSC engraftment ( $p < 0.001$ ) is significantly reduced after blocking CXCR3 on TGF $\beta$ 1 stimulated MSC ( $p < 0.001$ ). CXCR4 (10 $\mu$ g/ml) and CCR5 (10 $\mu$ g/ml) blockade had no significant effect on engraftment of MSC or TGF $\beta$ 1 stimulated MSC in injured mouse livers.

**Figure 4.13: Carbon tetrachloride induced liver injury in Rag2<sup>-/-</sup>IL-2r<sup>γ-/-</sup> mouse models.**

A: Representative 12 week, age matched sham/ mineral oil injured and carbon tetrachloride (CCl<sub>4</sub>) injured Rag2<sup>-/-</sup>IL-2r<sup>γ-/-</sup> mouse liver sections stained with Picosirius red for collagen-1 (red) and Van Gieson (purple/pink). Representative images of n=5 mice at x20 magnification.

B: Image J analysis of Picosirius red stained 12 week, age matched sham/ mineral oil injured and carbon tetrachloride (CCl<sub>4</sub>) injured Rag2<sup>-/-</sup>IL-2r<sup>γ-/-</sup> mouse liver sections. Data expressed as area fraction of Picosirius red staining in injured mouse livers (closed bars) relative to baseline control sham/ mineral oil injured livers. Bars represent mean ± SEM of n=5 mice, \*\*, p<0.01.

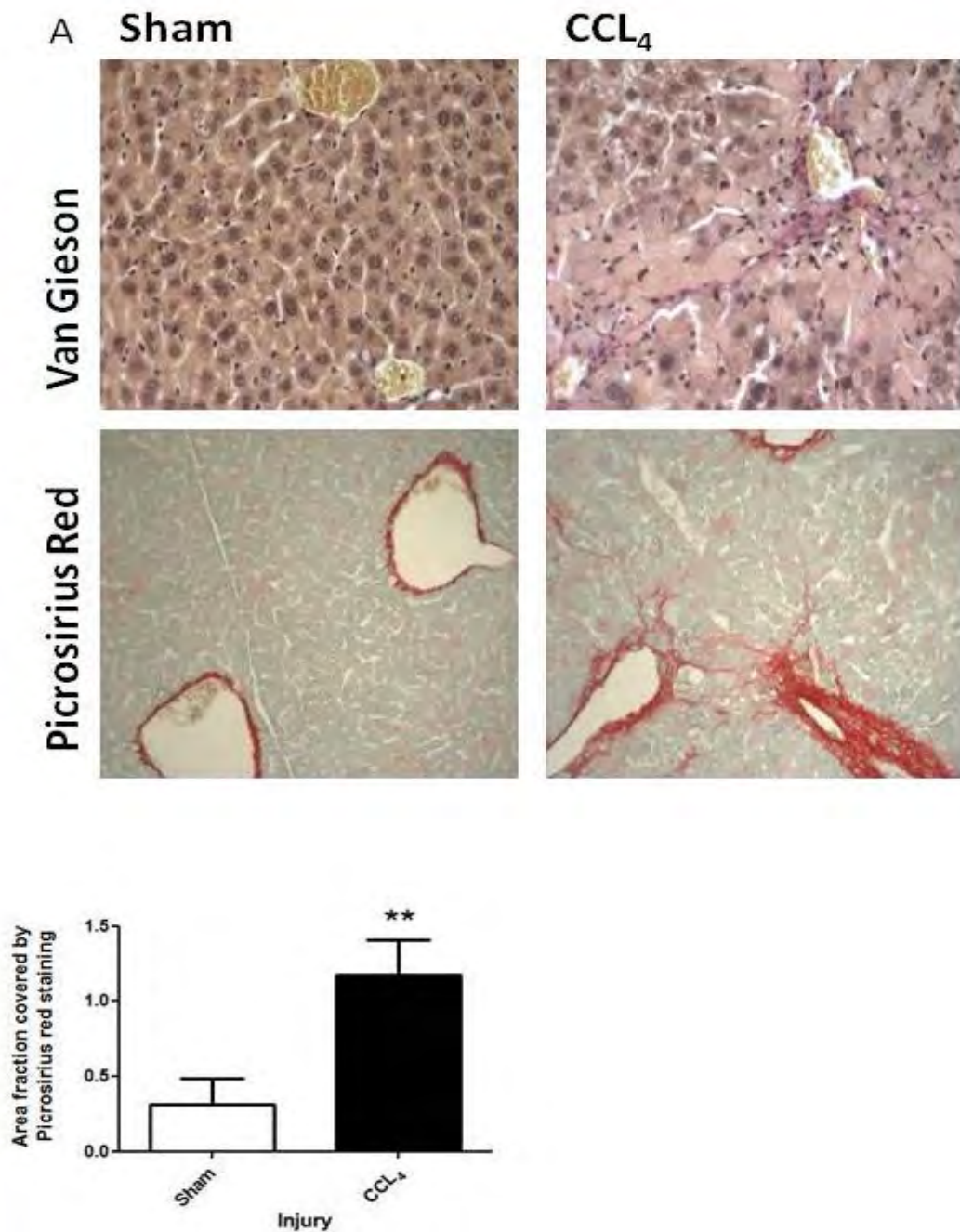
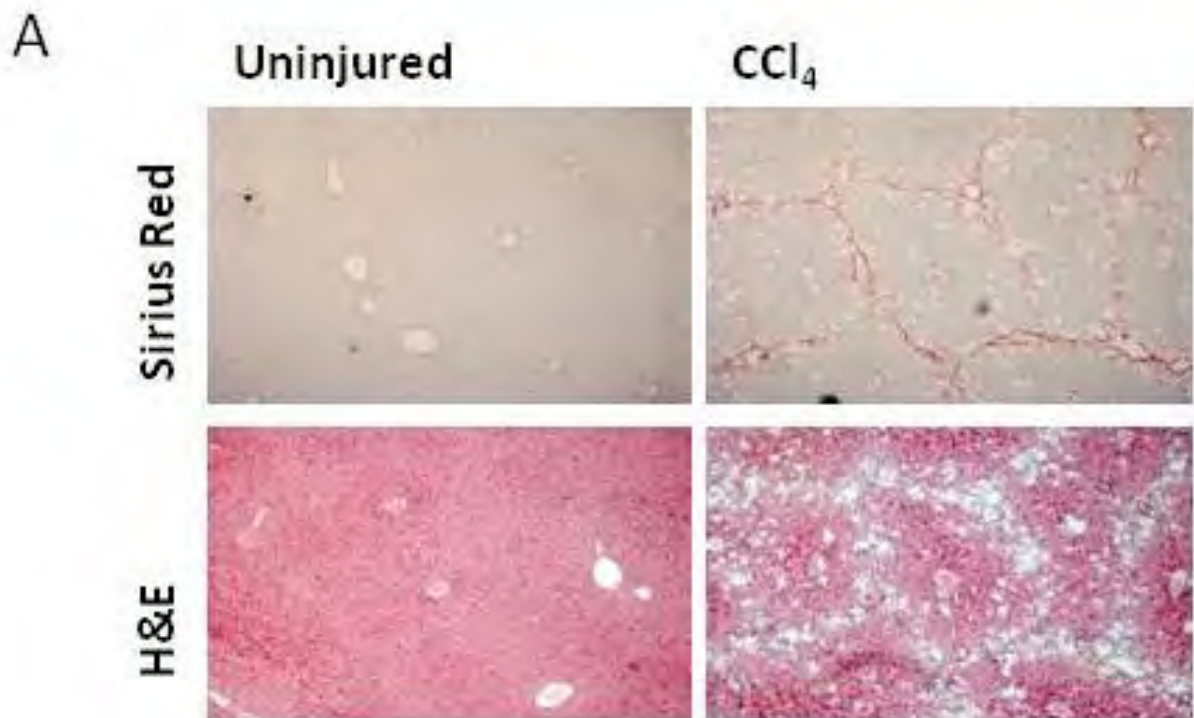


**Figure 4.14: Carbon tetrachloride induced liver injury in C57BL/6 mouse models.**

A: Representative 8 week, age matched uninjured and carbon tetrachloride (CCl<sub>4</sub>) injured C57BL/6 mouse liver sections stained for collagen with Picrosirius red (red) and to assess tissue histology with haematoxylin and eosin (H and E) staining. Representative images of n=5 mice at x20 magnification. B: Quantitative PCR analysis of 8 week, age matched uninjured and carbon tetrachloride (CCl<sub>4</sub>) injured C57BL/6 mouse livers for collagen1 $\alpha$ 1 and  $\alpha$ SMA mRNA. Injured liver gene levels relative to endogenous GAPDH levels (closed bars) were expressed as fold change over basal levels of genes in uninjured mice (open bars). The results were calculated by the comparative threshold cycle (Ct) method, with the Ct for GAPDH used to normalise the results. Expression of each gene was calculated with the difference in basal gene levels and endogenous level of GAPDH in uninjured mice defined as 1 (open bars). Bars represent mean  $\pm$  SEM of n=3 mice, performed in triplicate, \*, p<0.05. Serum albumin levels and serum bilirubin levels in CCl<sub>4</sub> injured and uninjured C57BL/6 mice measured by ELISA. Bars represent mean  $\pm$  SEM of n=3 different donor samples, performed in triplicate, \*, p<0.05.



B

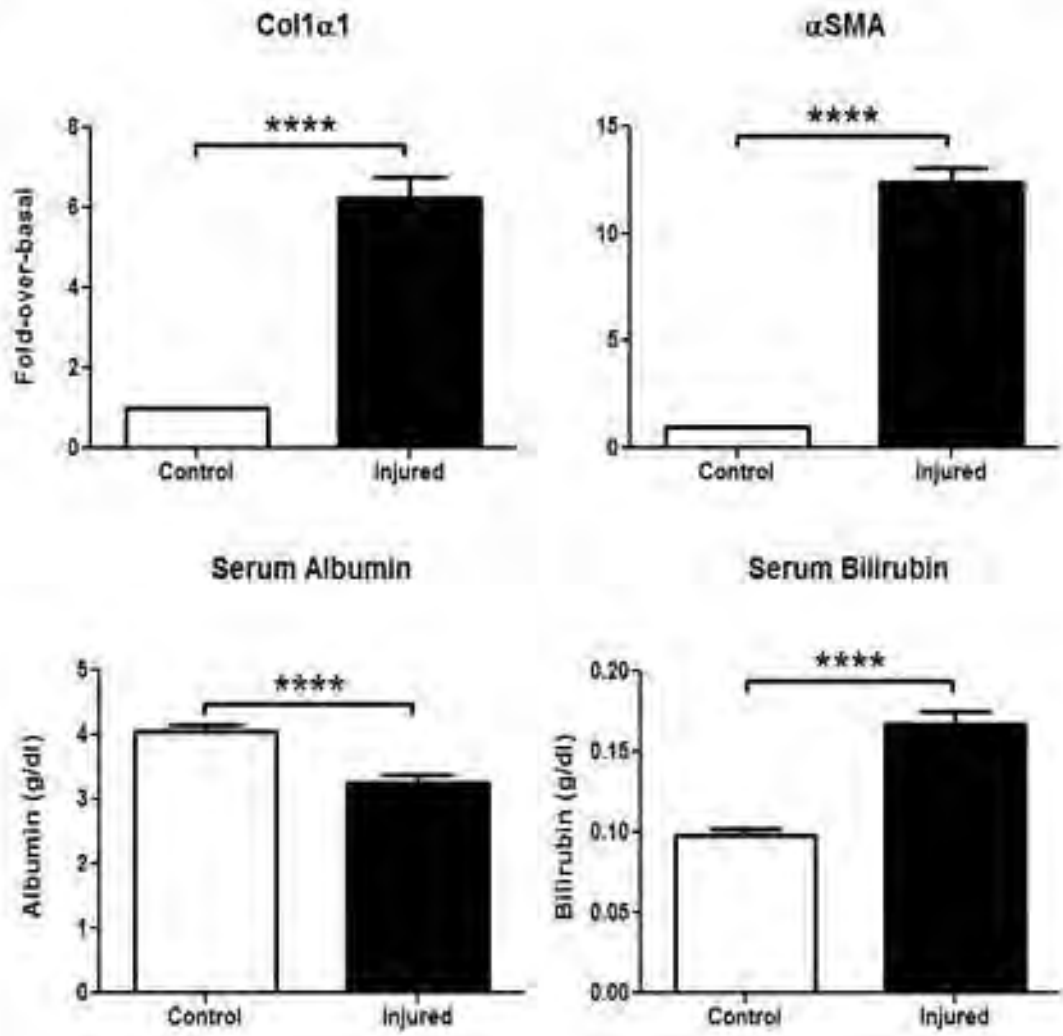
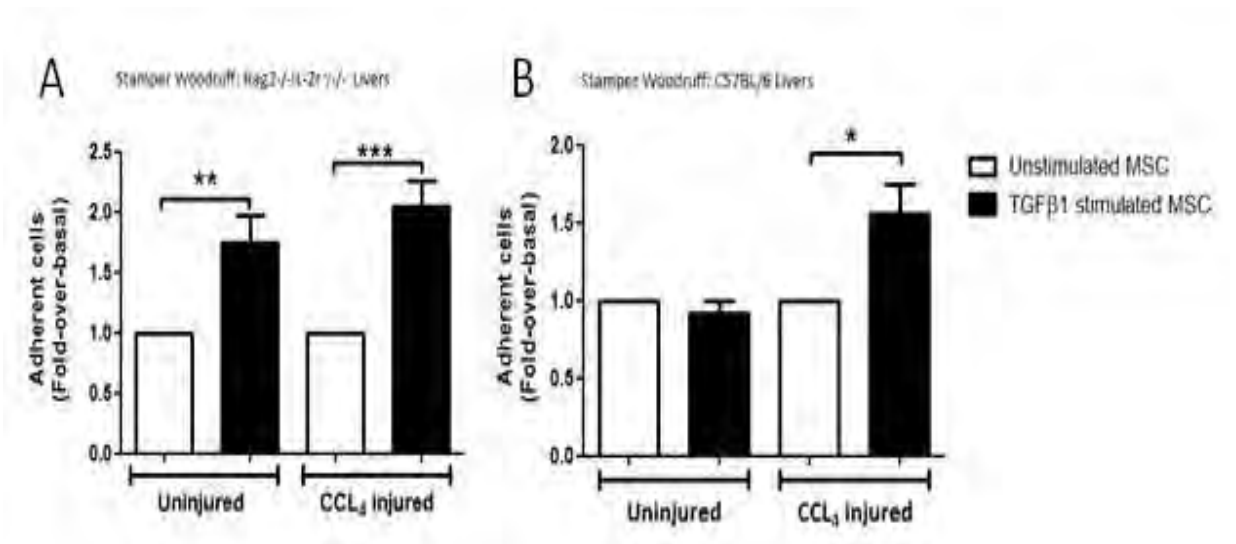


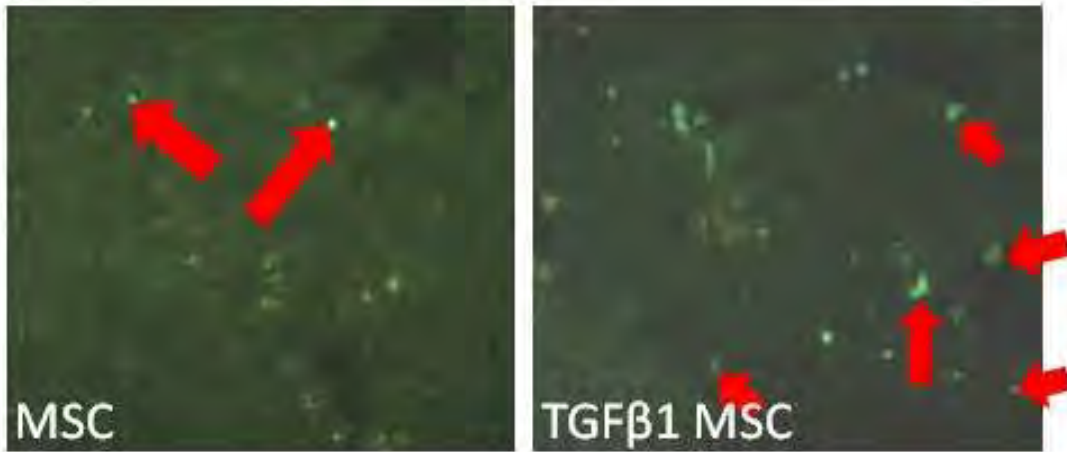


**Figure 4.15: Impact of TGFβ1 stimulation on MSC adhesion and engraftment.**

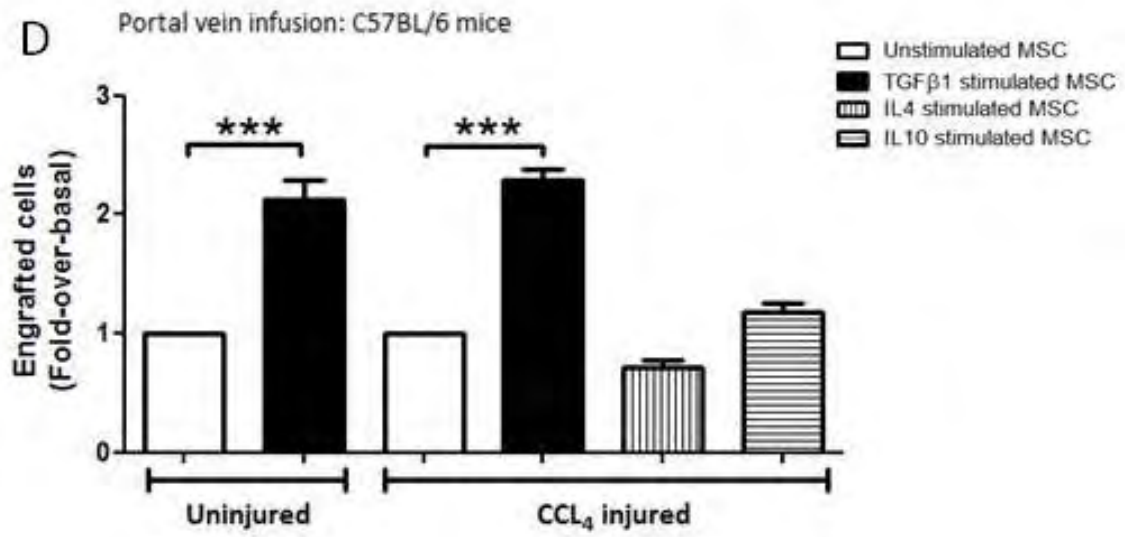
A: TGFβ1 stimulated MSC adhesion (closed bars) to sham injured and CCl<sub>4</sub> injured Rag2<sup>-/-</sup>IL-2r<sup>-/-</sup> mouse liver sections relative to basal adhesion of MSC (open bars), defined as 1. Bars represent mean ± SEM of n=3 samples, \*, p<0.05; \*\*, p<0.01; \*\*\*, p<0.001. B: TGFβ1 stimulated MSC adhesion (closed bars) to sham injured and CCl<sub>4</sub> injured C57BL/6 mouse liver sections relative to basal adhesion of MSC (open bars), defined as 1. Bars represent mean ± SEM of n=3 donors, \*, p<0.05; \*\*, p<0.01; \*\*\*, p<0.001. C: Representative images of CCl<sub>4</sub> injured C57BL/6 mouse liver sections after infusion of CFSE (green) labelled MSC and TGFβ1 stimulated MSC into liver via portal vein infusions and 15 minute incubation. Representative of n=3 mice at x20 magnification. D: TGFβ1 stimulated MSC engraftment in CCl<sub>4</sub> injured and uninjured C57BL/6 mice relative to baseline unstimulated MSC engraftment, defined as 1. MSC treated with IL4 and IL10 and infused into CCl<sub>4</sub> injured C57BL/6 mice as control cytokine stimulations. Data represents CFSE labelled MSC counted in 10 fields of view in four sections at four depths into the liver at x40 magnification. Bars represent mean ± SEM of n=3 donors, \*, p<0.05; \*\*, p<0.01; \*\*\*, p<0.001. E: The number of CFSE labelled MSC and TGFβ1 stimulated MSC that engraft in murine liver following portal vein injection was determined after treatment with function blocking antibodies to CXCR3 (10μg/ml), CXCR4 (10μg/ml), CCR5 (10μg/ml), and the relevant IgG control. Data is represented relative to IgG control labelled unstimulated MSC. Bars represent mean ± SEM of n=3 different donor samples, \*\*\*, p<0.001.

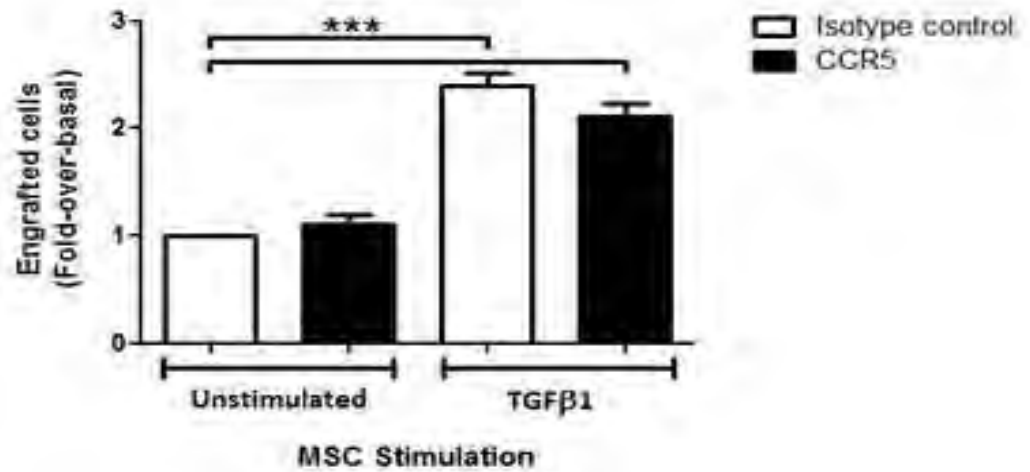
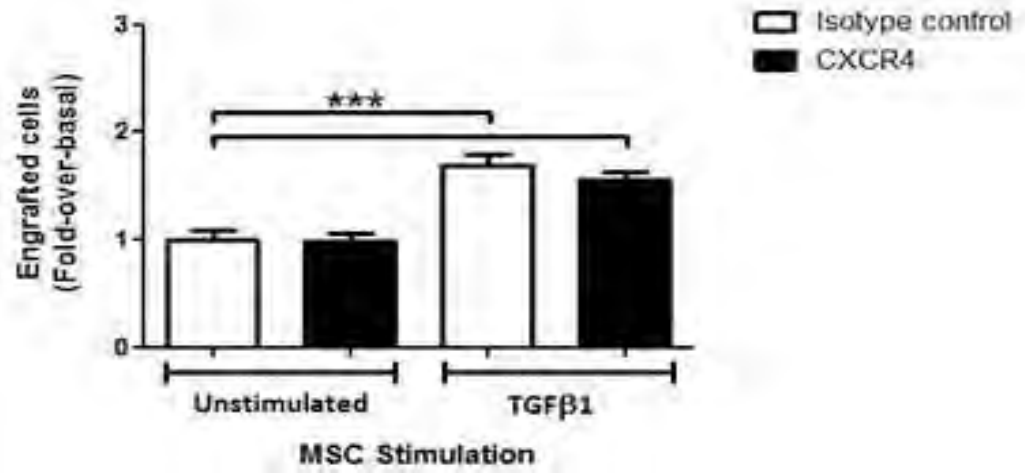
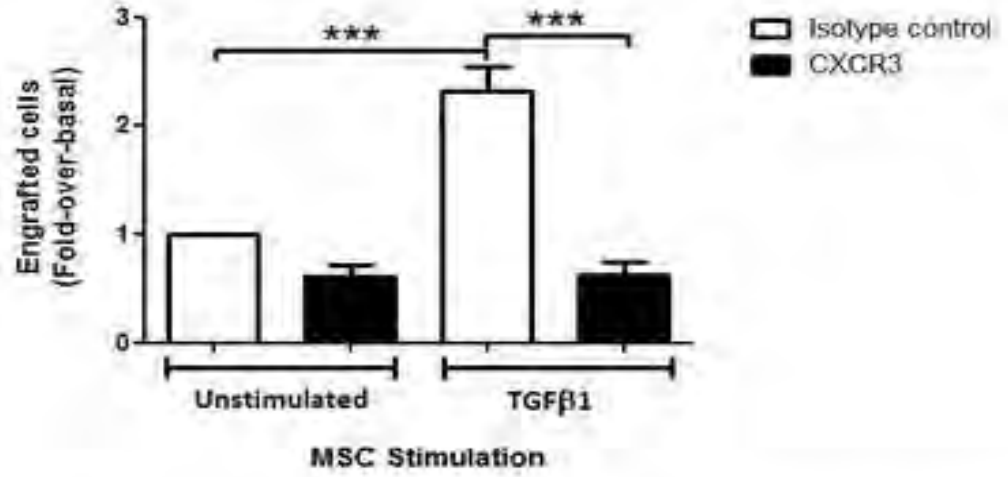


C



D



**E**Portal vein infusion: CCL<sub>4</sub> injured C57BL/6 mice

#### **4.2.6 TGFβ1 stimulation of MSC increases binding and engraftment of enzyme detached MSC to injured mouse livers**

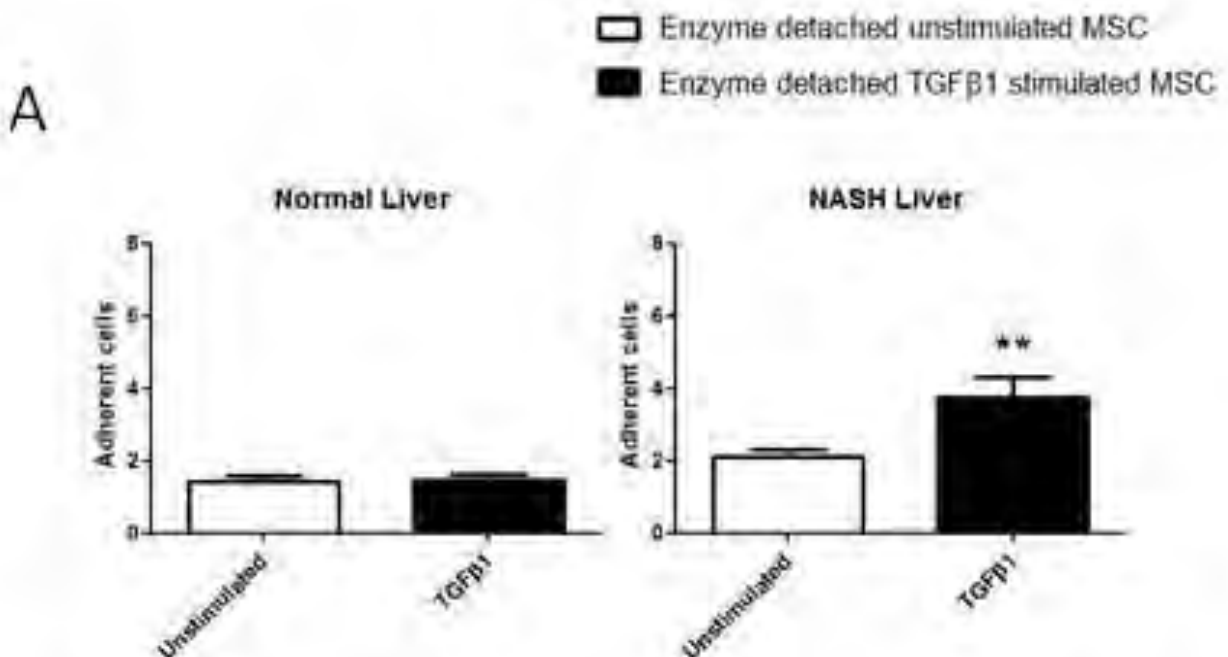
We repeated some of the studies above using enzymatically detached TGFβ1 stimulated MSC to compare effects with earlier experiments. There was no significant difference between binding of unstimulated or stimulated MSC to normal liver sections. However TGFβ1 stimulated MSC were significantly more adherent to NASH liver sections (unstimulated:  $2.09 \pm 0.21$ , stimulated:  $3.76 \pm 0.54$ ;  $p < 0.05$ ), PBC liver sections (unstimulated:  $1.03 \pm 0.13$ , stimulated:  $1.7 \pm 0.17$ ;  $p < 0.05$ ), AIH liver sections (unstimulated:  $2.58 \pm 0.26$ , stimulated:  $4.61 \pm 0.34$ ;  $p < 0.05$ ), PSC liver sections (unstimulated:  $1.22 \pm 0.17$ , stimulated:  $1.83 \pm 0.19$ ;  $p < 0.05$ ) and ALD liver sections (unstimulated:  $2.61 \pm 0.17$ , stimulated:  $3.26 \pm 0.2$ ;  $p < 0.05$ ) (Figure 4.16A). Enzymatically detached TGFβ1 stimulated MSC were  $1.49 \pm 0.13$  fold significantly more adherent to TNFα/IFNγ stimulated HSEC monolayers ( $p < 0.05$ ) but there was no significant change in TGFβ1 stimulated MSC binding to HSEC compared with unstimulated MSC (Figure 4.16B).

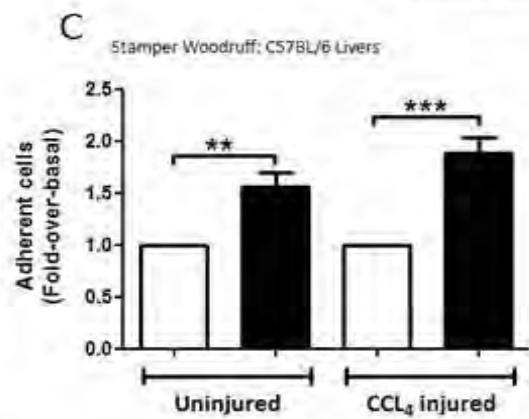
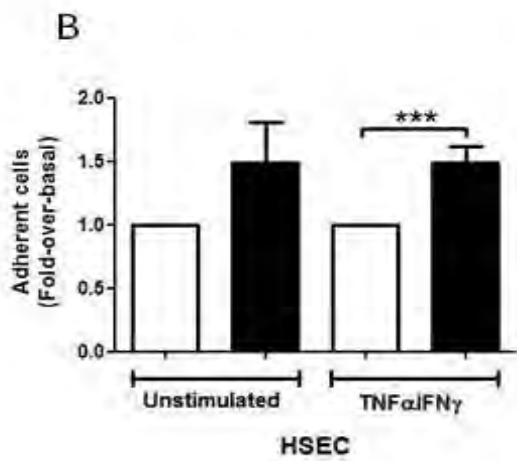
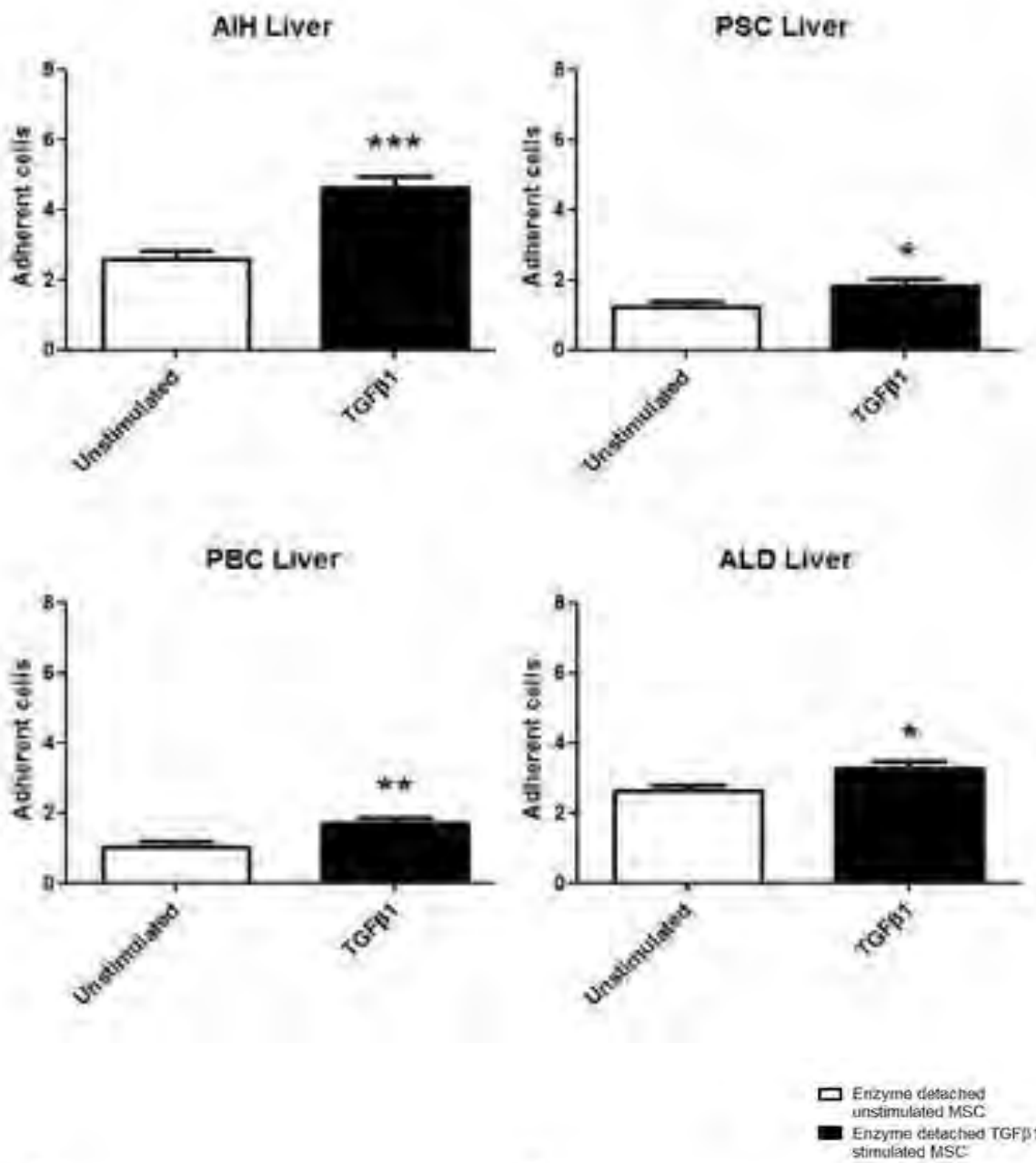
We observed  $2 \pm 0.19$  fold and  $1.89 \pm 0.17$  fold increases in binding of enzymatically detached TGFβ1 stimulated MSC to sham injured and carbon tetrachloride injured Rag2<sup>-/-</sup>IL-2r<sup>γ-/-</sup> mouse liver sections respectively ( $p < 0.001$ ) (Figure 4.16C). On uninjured and carbon tetrachloride injured C57BL/6 mouse liver sections there was  $1.56 \pm 0.14$  fold ( $p < 0.01$ ) and  $1.88 \pm 0.16$  fold ( $p < 0.001$ ), significantly increased binding, respectively, of TGFβ1 stimulated MSC (Figure 16D). Upon portal vein infusions of MSC into C57BL/6 mouse livers we observed significantly increased engraftment of TGFβ1 stimulated MSC in uninjured ( $2.12 \pm 0.17$  fold) ( $p < 0.001$ ) and carbon tetrachloride injured mouse livers ( $2.74 \pm 0.2$  fold) ( $p < 0.001$ ) compared

to unstimulated MSC or TNF $\alpha$  stimulated MSC which showed no significant change in engraftment of MSC (Figure 4.16E).

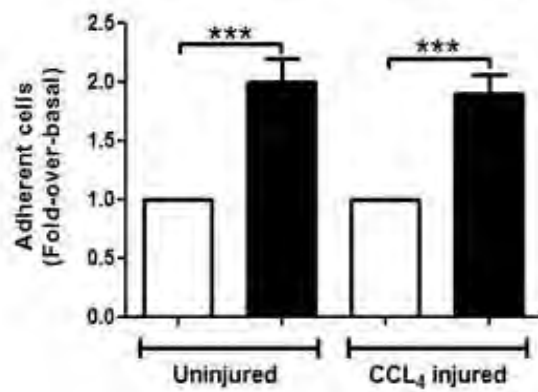
**Figure 4.16: Impact of TGFβ1 stimulation on MSC after enzymatic detachment.**

A: Modified Stamper Woodruff assays showing basal adhesion of enzyme detached MSC (open bars) compared with TGFβ1 stimulated enzyme detached MSC adhesion (closed bars) to normal, Non alcoholic steatohepatitis (NASH), Primary sclerosing cholangitis (PSC), Primary biliary cirrhosis (PBC), Autoimmune hepatitis (AIH), Alcoholic liver disease (ALD) cirrhotic liver sections. Bars represent mean  $\pm$  SEM cells/ field of view of n=3 samples, \*, p<0.05; \*\*\*, p<0.001. B: Modified Stamper Woodruff assays showing enzyme detached TGFβ1 stimulated MSC (closed bars) adhesion relative to basal adhesion of MSC (open bars), defined as 1, to unstimulated and TNFα/IFNγ stimulated human hepatic sinusoidal endothelial cells (HSEC). Bars represent n=3 samples, \*, p<0.05; \*\*\*, p<0.001. Enzyme detached TGFβ1 stimulated MSC adhesion (closed bars) to C: uninjured and injured C57BL/6, or D: sham injured and CCl<sub>4</sub> injured D: Rag2<sup>-/-</sup>IL-2<sup>r</sup>γ<sup>-/-</sup> mouse liver sections relative to basal adhesion of MSC (open bars), defined as 1. Bars represent mean  $\pm$  SEM of n=3 samples, \*, p<0.05; \*\*, p<0.01; \*\*\*, p<0.001. E: Enzyme detached TGFβ1 stimulated MSC engraftment in CCl<sub>4</sub> injured and uninjured C57BL/6 mice relative to baseline unstimulated MSC engraftment, defined as 1. MSC treated with TNFα and infused into CCl<sub>4</sub> injured C57BL/6 mice as control cytokine stimulations. Data represents CFSE labelled MSC counted in 10 fields of view in four sections at four depths into the liver at x40 magnification. Bars represent mean  $\pm$  SEM of n=3 donors, \*, p<0.05; \*\*, p<0.01; \*\*\*, p<0.001.

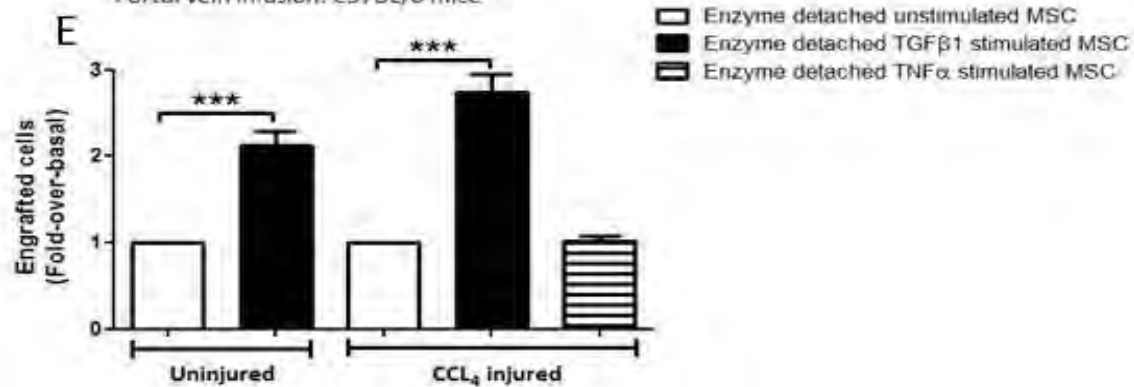




D Stamper Woodruff: Rag2<sup>-/-</sup>IL-2r<sup>γ</sup><sup>-/-</sup> Livers



Portal vein infusion: C57BL/6 mice



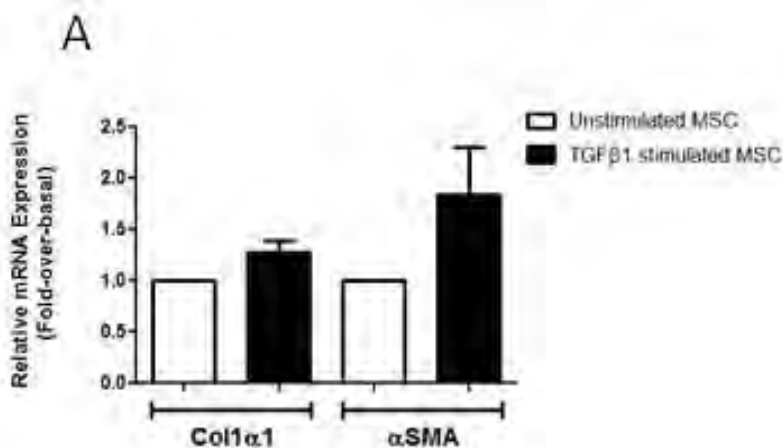


**4.2.7 TGFβ1 stimulation of MSC does not significantly alter tri-lineage differentiation of MSC and does not increase intracellular stress or the production of pro-fibrotic factors.**

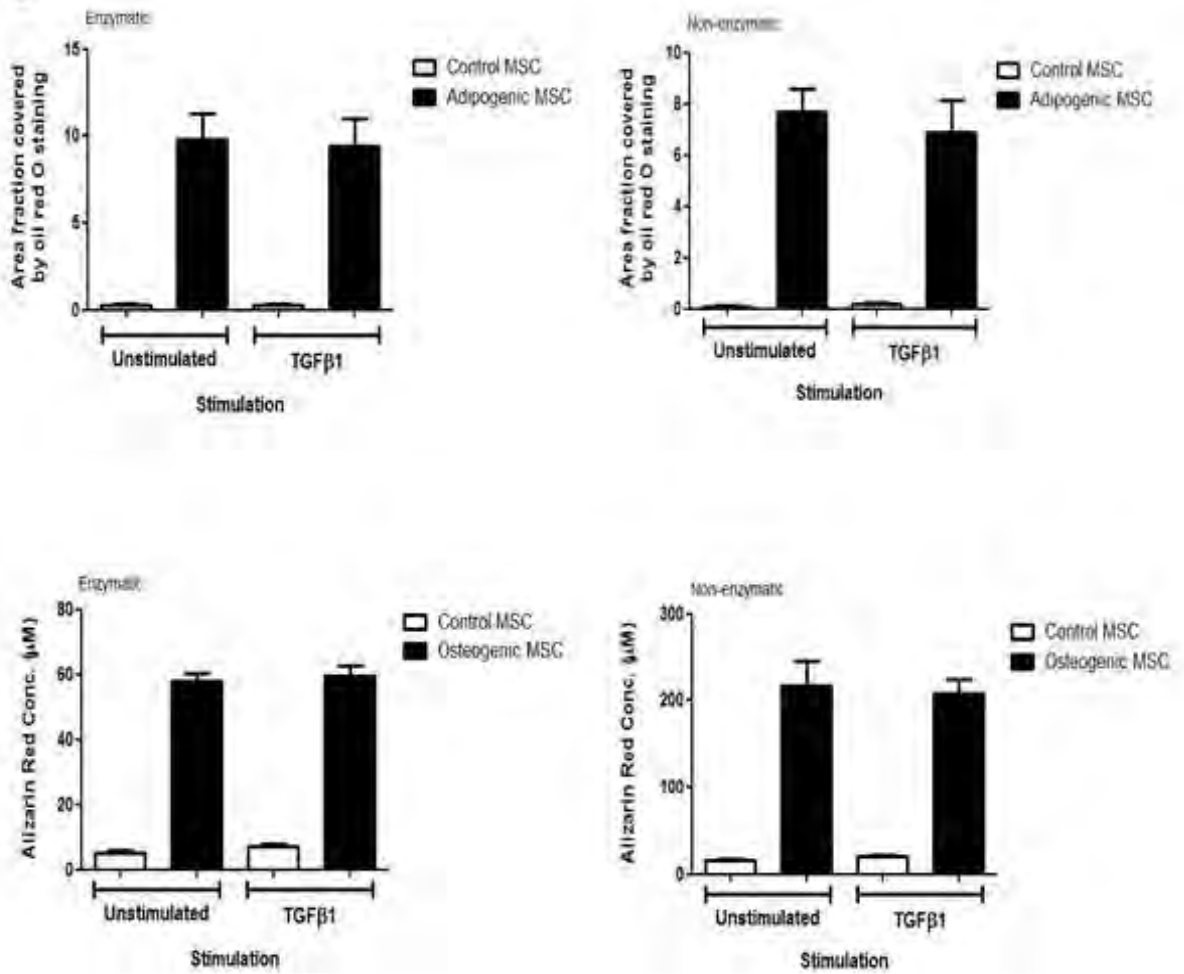
Using QPCR we measured mRNA levels of collagen-1 and αSMA in MSC after TGFβ1 stimulation of CDB detached MSC for 24 hours. There was no significant change in mRNA levels of collagen-1 or αSMA in TGFβ1 stimulated MSC (Figure 4.17A). Tri-lineage differentiation of MSC was maintained and there was no significant change in differentiation of enzymatically or non-enzymatically detached MSC into osteoblasts, adipocytes and chondrocytes after 24 hour TGFβ1 stimulation (Figure 4.17B and C). We also observed no indication of a difference in the presence of IROS, autophagy or MSC undergoing apoptosis or necrosis after TGFβ1 stimulation, regardless of the detachment method (Figure 4.17D).

**Figure 4.17: Effect of TGFβ1 stimulation on production of pro-fibrotic factors, tri-lineage differentiation and intracellular stress in MSC.**

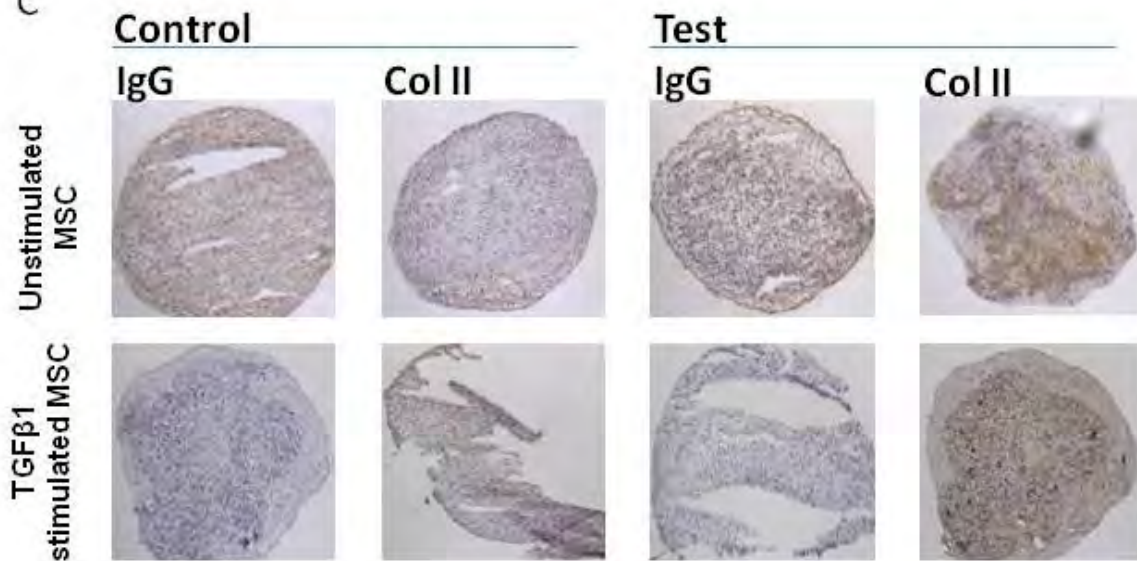
A: Quantitative analysis of total collagen-1 and αSMA gene levels in cytokine stimulated MSC, measured by Real Time Polymerase Chain Reaction (QPCR) analysis. Stimulated MSC gene levels relative to endogenous β-actin levels (closed bars) in stimulated MSC were expressed as fold change over basal levels of CCR in un-stimulated MSC (open bars). The results were calculated by the comparative threshold cycle (Ct) method, with the Ct for β-actin in cytokine treated and untreated MSC used to normalise the results. Expression of each gene was calculated with the difference in basal CCR levels and endogenous level of β-actin in untreated MSC defined as 1 (open bars). Bars represent mean ± SEM of n=3 different donor samples, performed in triplicate. B: Image J analysis of oil red O staining of enzyme and non enzyme detached TGFβ1 stimulated MSC differentiated into adipocytes. Bars represent oil red O stained mean area fraction ± SEM of n=3 samples. Alizarin red staining of enzyme and non enzyme detached TGFβ1 stimulated MSC differentiated into osteoblasts. Bars represent mean calcium concentration (μM) ± SEM of n=3 samples. C: Representative images, DAB staining of collagen II as a marker of chondrocyte differentiation. TGFβ1 stimulated MSC differentiated into chondrocytes at x20 magnification. MSC were cultured as pellets after detachment from tissue culture plastic and differentiated into chondrocytes. D: Levels of stress on TrypLE (enzymatic) and Cell Dissociation Buffer (CDB) (non enzymatic) detached, TGFβ1 stimulated cells. Table of CDB and TrypLE detached unstimulated MSC (red) and TGFβ1 stimulated MSC (black), labelled with IROS marker, 2',7'-dichlorofluorescein (DCF), autophagy marker, monodansylcadaverine (MDC), apoptosis marker, annexin V, D: Necrosis marker, 7AAD; with corresponding Median Fluorescent Intensity (MFI) values. Data represents mean ± SEM of n=3 different donors.



**B**



**C**



D

	IROS		Autophagy		Apoptosis		Necrosis	
	MSC	TGFβ1 MSC	MSC	TGFβ1 MSC	MSC	TGFβ1 MSC	MSC	TGFβ1 MSC
<b>Enzymatic</b>	162.84	157.06	21.54	19.33	7.29	8.42	8.12	7.84
<b>Non-enzymatic</b>	217.4	202.25	24.89	21.54	8.73	8.42	11.66	11.25

#### **4.2.8 TGFβ1 stimulation of MSC increases cell surface CD44 expression and secretion of CCL2 and IL-6**

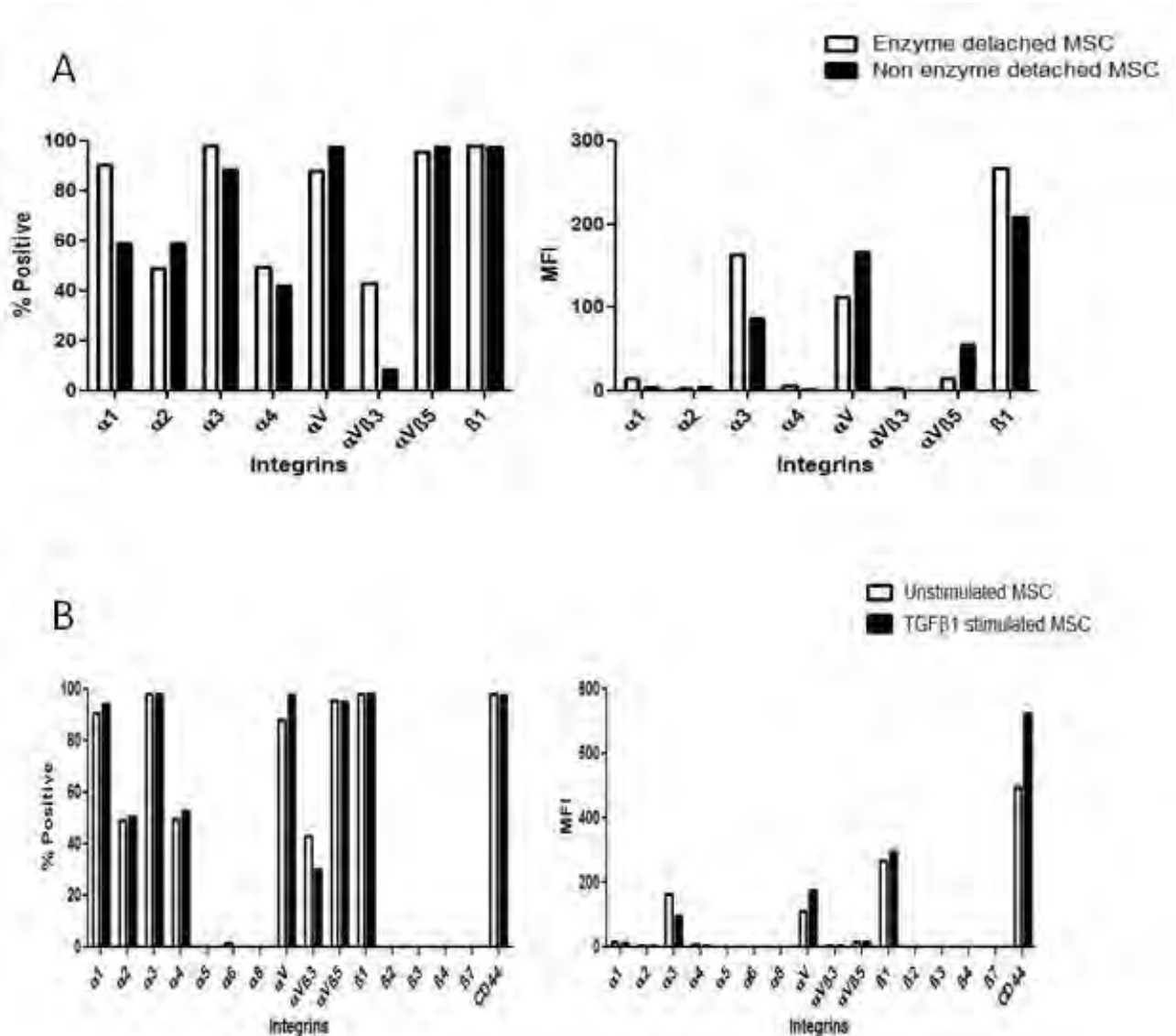
MSC were tested for differences in cell surface integrin expression after enzymatic and non enzymatic detachment. Based on preliminary experiments, integrin expression appeared to be preserved even after enzymatic detachment of MSC from tissue culture plastic so further experiments measuring surface integrin expression were carried out with enzyme detached MSC (Figure 4.18A). MSC expressed integrins  $\alpha$ 1-6,  $\alpha$ 8,  $\alpha$ v,  $\alpha$ v $\beta$ 3,  $\alpha$ v $\beta$ 5,  $\beta$ 1-4,  $\beta$ 7 and CD44 (Figure 4.18B) but there was no indication of a change in expression after stimulation. However this is based only on one experiment so could change based on further repeats. However there was an indication of a change in MFI for CD44 (Figure 4.18B and C). TGFβ1 stimulated MSC expressed higher levels of CD44 (MFI: 723.84) compared to unstimulated MSC (MFI: 496.37) but this could also change after repeat experiments (Figure 4.18B and C).

TGFβ1 stimulated MSC supernatants were tested using arrays for cytokine and angiogenic factor secretion. Supernatants from 24 hour TGFβ1 stimulated MSC contained significantly higher levels of MCP-1/ CCL2 (pixel density:  $2.05 \pm 0.21$  units) than unstimulated MSC supernatant (pixel density:  $0.2 \pm 0.1$  units) ( $p < 0.05$ ) (Figure 4.19A). There was also a trend towards an increase of IL6 in TGFβ1 stimulated MSC supernatant (pixel density:  $8.91 \pm 1.99$  units vs.  $4.72 \pm 0.05$  units in controls, Figure 4.19B). Unstimulated and TGFβ1 stimulated MSC supernatants showed no significant changes in levels of other cytokines that were present, including TGFβ1 (Figure 4.19A, B and C). Cell based ELISA was then used to measure the effects of supernatant from cytokine stimulated MSC on HSEC adhesion molecule expression. In general exposure of HSEC treated with TNFα/IFNγ to MSC

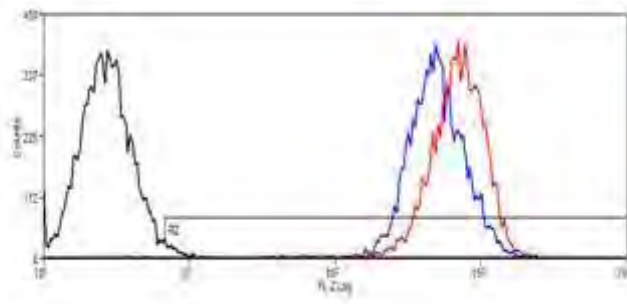
supernatant had no additional effects on expression. However, IL6 stimulated MSC conditioned media modestly increased ICAM-1 levels ( $9.97 \pm 0.63$  fold;  $p=0.09$ ) (Figure 4.20).

**Figure 4.18: TGFβ1 stimulated MSC surface integrin and adhesion molecule expression.**

A: Flow cytometry analysis for surface integrins and adhesion molecules as percentage positive MSC after enzymatic (open bars) and non-enzymatic detachment (closed bars) with, B: median fluorescence intensity (MFI). D: Flow cytometry analysis for surface integrins and adhesion molecules as enzyme detached percentage positive MSC (open bars) after TGF stimulation (closed bars) with, E: median fluorescence intensity (MFI). Bars represent n=1 sample. C: Representative cytometry histograms for enzymatic detached MSC (blue) and TGFβ1 stimulated MSC (blue) expression of CD44 compared with immunoglobulin matched control (IMC) (black) of n=1 sample.



C



- MFI of negative control
- MFI of TGFβ1 stimulated MSC
- MFI of unstimulated MSC



**Figure 4.19: Cytokines and angiogenic factors in TGFβ1 stimulated MSC supernatant.**

A: Supernatant collected from MSC stimulated with TGFβ1 for 24 hours was tested for various cytokines and angiogenic factors using an array for angiogenic factors, and for, B: cytokines. Bars represent mean ± SEM of n=2 different donors, \*, p<0.05. C: MSC were stimulated with TGFβ1 for 24 hours and cultured for a further 24 hours before supernatants were removed and TGFβ1 levels were measured using Sandwich ELISA. Bars represent mean ± SEM of n=3 different donors, \*, p<0.05.

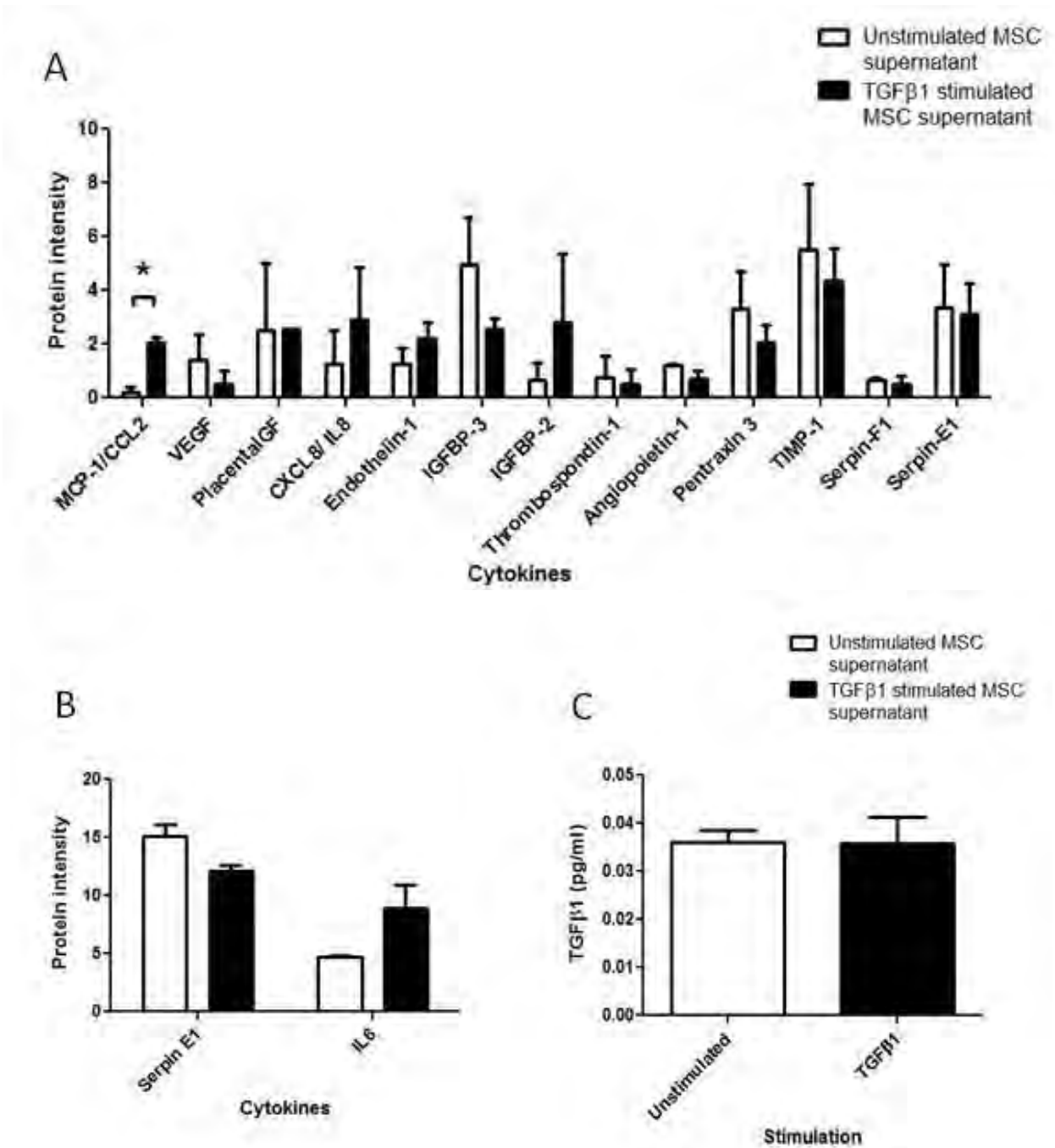
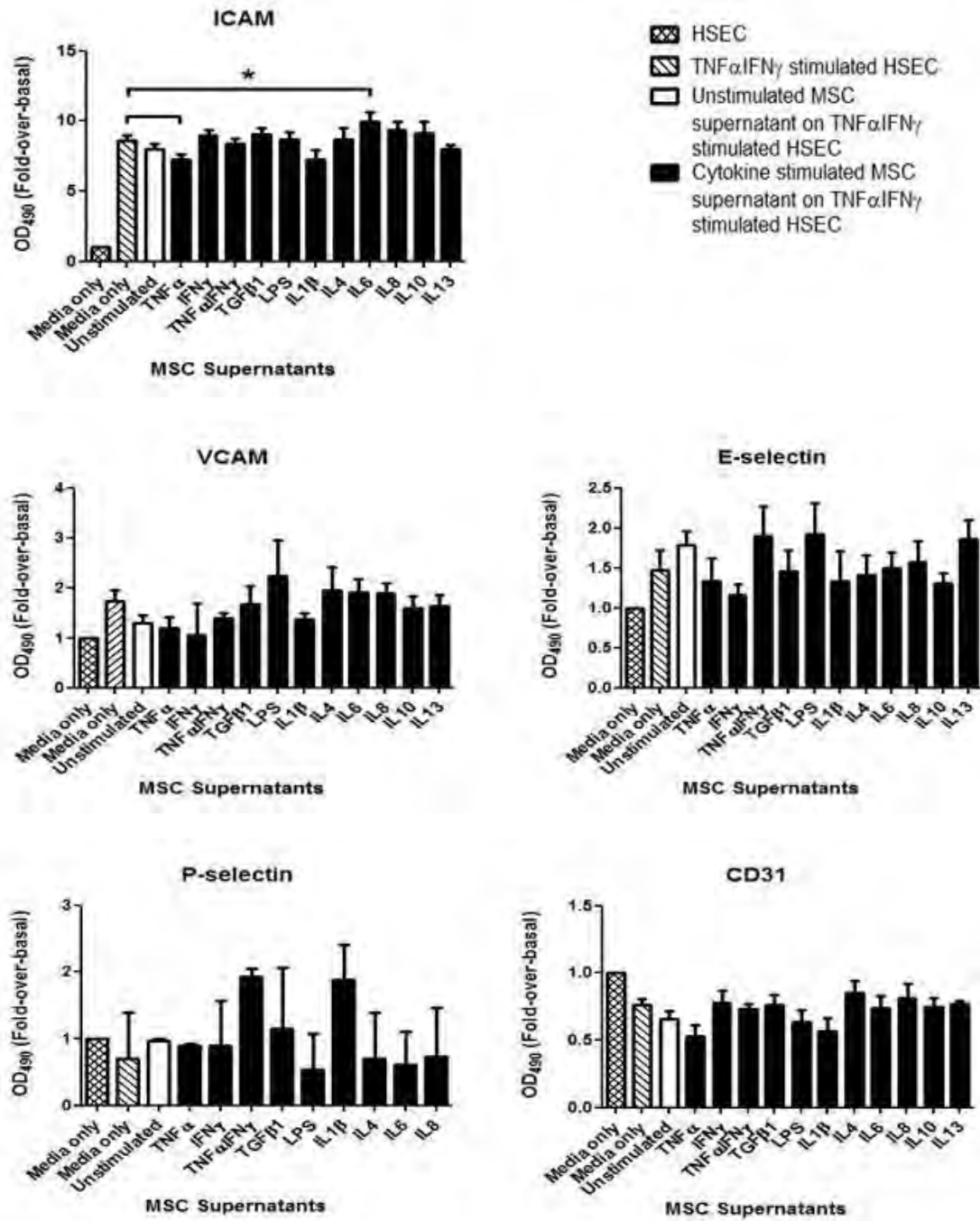


**Figure 4.20: Adhesion molecules on HSEC after culture with cytokine stimulated MSC supernatant.**

24 hour treatment of TNF $\alpha$ IFN $\gamma$  stimulated hepatic sinusoidal endothelial cells (HSEC) with supernatant from 24 hour cytokine stimulated MSC. Levels of adhesion molecules expressed on HSEC were tested with cell based ELISA relative to media only control on unstimulated HSEC, defined as 1. Bars represent mean  $\pm$  SEM of n=3 different donors.

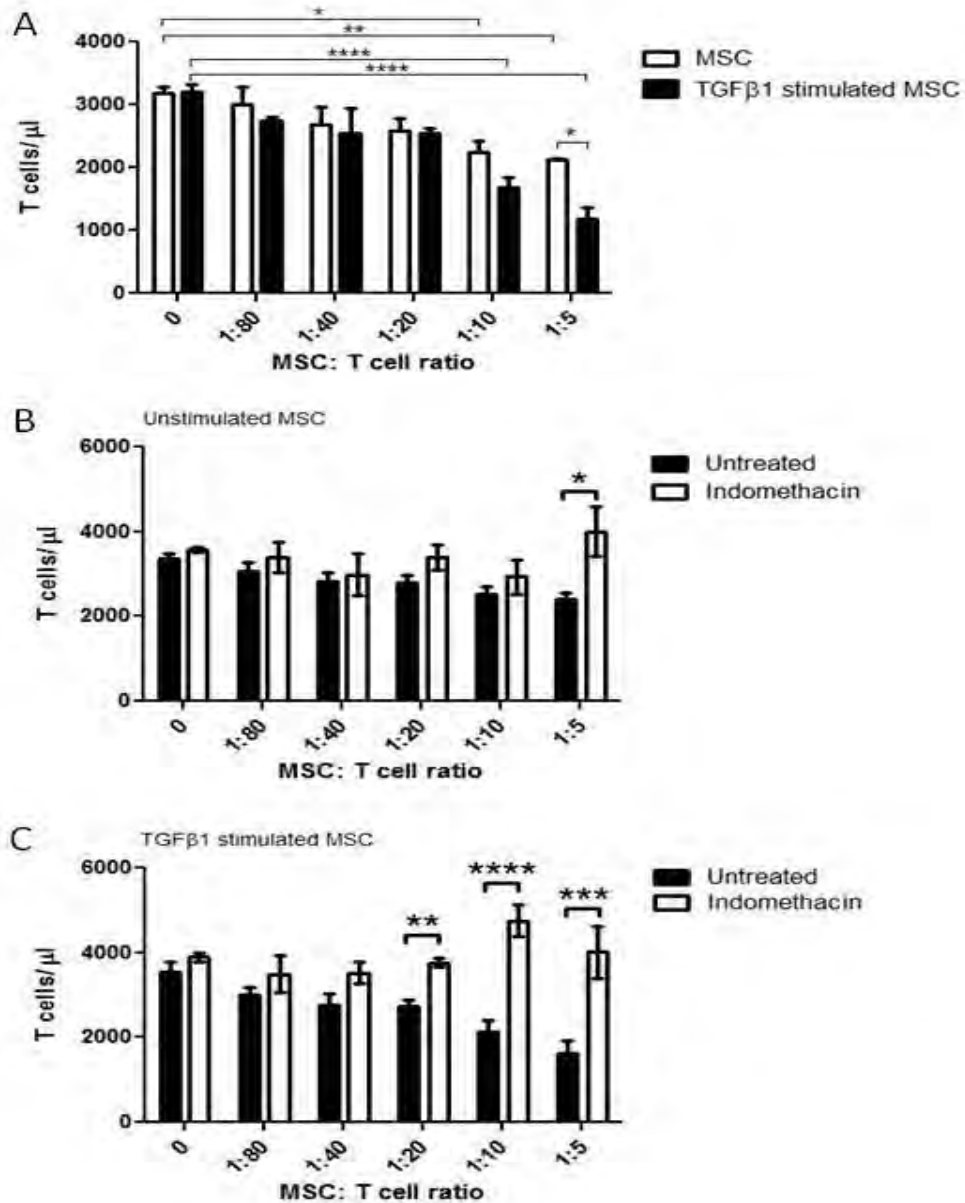


#### **4.2.9 TGFβ1 stimulated MSC exhibit increased suppression of CD4 T cell proliferation mediated by increased PGE2.**

MSC are able to suppress CD4 T cell proliferation from  $3176 \pm 117.2$  CD4 T cells/ $\mu$ l to  $2244 \pm 178.2$  cells/ $\mu$ l at a ratio of 1 MSC: 10 CD4 T cells/ $\mu$ l ( $p < 0.05$ ) and further to  $2131 \pm 11.39$  cells/ $\mu$ l at a ratio 1:5 ( $p < 0.01$ ) (Figure 4.21A). TGFβ1 stimulated MSC showed more potent suppression of total CD4 T cell proliferation ( $3207 \pm 108.5$  cells/ $\mu$ l) to  $1685 \pm 163$  cells/ $\mu$ l at a ratio of 1:10 ( $p < 0.0001$ ) and also to  $1184 \pm 185.5$  cells/ $\mu$ l at a ratio of 1: 5 ( $p < 0.0001$ ) (Figure 4.21A). There was a significant increase in suppression of CD4 T cell proliferation at a 1:5 ratio in TGFβ1 stimulated MSC compared to unstimulated MSC ( $p < 0.05$ ) (Figure 4.21A). Control and TGFβ1 stimulated MSC were treated with Indomethacin to block PGE2, a known suppressive agent produced by MSC. When treated with Indomethacin, control MSC lost all suppressive ability, with a significant increase in CD4 T cell proliferation ( $4004 \pm 571.9$  cells/ $\mu$ l) compared to untreated MSC ( $2394 \pm 164.7$  cells/ $\mu$ l) ( $p < 0.5$ ) (Figure 4.21B). Similarly TGFβ1 stimulated MSC treated with Indomethacin demonstrated a similar loss in immunosuppressive efficacy (Figure 4.21C).

**Figure 4.21: TGFβ1 stimulated MSC mediated suppression of CD4 T cell proliferation.**

Flow cytometry analysis of activated CD3<sup>+</sup>CD4<sup>+</sup>CD25<sup>-</sup> T effector cell proliferation labelled with CellTrace™ Violet and analysed with PE labelled Accucheck counting beads. A: MSC or B: TGFβ1 stimulated MSC were co-cultured with activated CD3<sup>+</sup>CD4<sup>+</sup>CD25<sup>-</sup> T effector cell, respectively and compared to CD3<sup>+</sup>CD4<sup>+</sup>CD25<sup>-</sup> T effector cell proliferation without MSC. C: Comparison of MSC and TGFβ1 stimulated MSC suppression of CD3<sup>+</sup>CD4<sup>+</sup>CD25<sup>-</sup> T effector cell proliferation at ratios of 1:5, 1:10, 1:20, 1:40, and 1:80. The number of CellTrace™ Violet labelled CD3<sup>+</sup>CD4<sup>+</sup>CD25<sup>-</sup> T effector cells after co-culture with, B: MSC, and C: TGFβ1 stimulated MSC, was determined after treatment with Indomethacin, a chemical blocker of Prostaglandin E2 (PGE2) at each ratio. Bars represent mean ± SEM of n=3 different donors, \*, p<0.05; \*\*, p<0.01; \*\*\*, p<0.001.



#### **4.2.10 Treatment of MSC with serum from cirrhotic ALD patients reduces cell surface CCR expression and increases levels of $\beta 1$ integrin.**

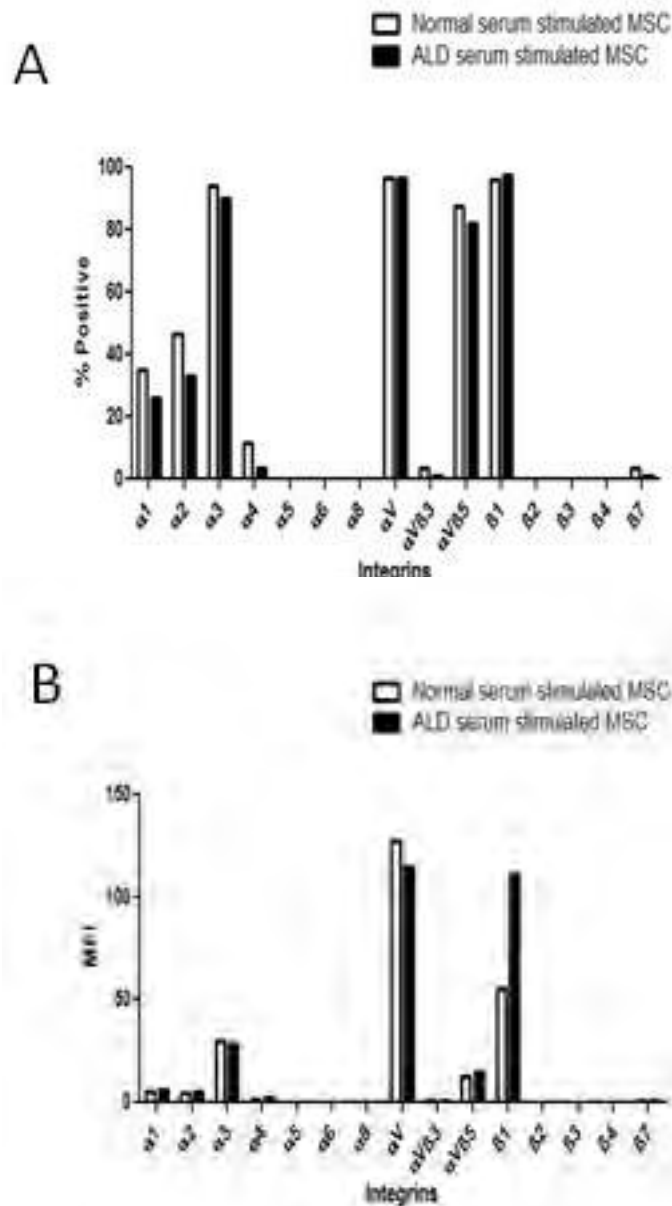
MSC integrin expression was preserved after enzymatic detachment (not shown) and so enzymatically detached MSC were exposed to patient serum. There was no change in the percentage of MSC expressing integrins  $\alpha 1-6$ ,  $\alpha 8$ ,  $\alpha v$ ,  $\alpha v\beta 3$ ,  $\alpha v\beta 5$ ,  $\beta 1-4$ ,  $\beta 7$  and CD44 after treatment (Figure 4.22A). However there was trend for increased integrin  $\beta 1$  expression (Figure 4.22B). ALD serum stimulated MSC express higher levels of  $\beta 1$  (MFI: 110.92) compared to unstimulated MSC (MFI: 55.92) (Figure 4.22C). There was also a suggestion of a decrease in percentage of MSC expressing cell surface CCR levels, CCR4 (ALD: 13.39%, Normal: 47.15%), CCR5 (ALD: 12.06%, Normal: 45.37%), CCR9 (ALD: 0%, Normal: 7.04%), CXCR3 (ALD: 3.76%, Normal: 40.31%), CXCR7 (ALD: 0 %, Normal: 3.63%) after ALD serum stimulation compared to control, respectively (Figure 22D). After ALD serum stimulation there was a decrease in the levels of MSC surface CCR4 (ALD: 2.04, Normal: 5.09), CCR5 (ALD: 1.83, Normal: 4.03), CCR9 (ALD: 0, Normal: 0.66), CXCR3 (ALD: 0.99, Normal: 2.71), CXCR7 (ALD: 0, Normal: 0.43). However, there was no detectable cell surface CXCR4 (Figure 4.12C and D). TGF $\beta 1$  levels were tested in normal and end stage cirrhosis ALD patient serum using sandwich ELISA. ALD patient serum ( $4.84 \pm 0.87$  pg/ml) had significantly lower levels of TGF $\beta 1$  levels than normal serum ( $7.57 \pm 0.33$  pg/ml) ( $p < 0.05$ ) (Figure 4.22E).

To determine whether this alteration in surface receptors had any functional relevance we carried out modified Stamper-Woodruff assays using normal and ALD serum stimulated MSC on normal and ALD liver tissue. Binding of ALD serum stimulated MSC ( $2.24 \pm 0.33$

cells/ field of view) was significantly reduced compared to normal serum stimulated MSC (5.36±0.73 cells/ field of view) ( $p<0.001$ ) on normal liver sections. Similarly on ALD liver sections, ALD serum stimulated MSC (2.18±0.27 cells/ field of view) were significantly less adherent compared with normal serum stimulated MSC (6.11±0.74 cells/ field of view) ( $p<0.001$ ) (Figure 4.23A)). Modified static adhesions were also performed on HSEC and TNF $\alpha$ IFN $\gamma$  stimulated HSEC monolayers using normal serum and ALD serum stimulated MSC. ALD serum stimulated MSC were significantly less adherent to unstimulated HSEC (1.48±0.28 cells/ field of view) and TNF $\alpha$ IFN $\gamma$  (1.98±0.25 cells/ field of view) stimulated HSEC compared with normal serum stimulated MSC (3.45±0.51, 4.16±0.4 cells/ field of view) on unstimulated and TNF $\alpha$ IFN $\gamma$  stimulated HSEC, respectively ( $p<0.001$ ) (Figure 4.23B).

**Figure 4.22: Impact of ALD serum on MSC surface receptor expression.**

A: Flow cytometry analysis for surface integrins and adhesion molecules as enzyme detached percentage positive normal serum stimulated MSC (open bars) and after ALD serum stimulation (closed bars) with, B: median fluorescence intensity (MFI). Bars represent n=1 samples. C: Flow cytometry analysis for surface CCR as percentage positive normal serum stimulated MSC (open bars) and after ALD serum stimulation (closed bars) with, D: median fluorescence intensity (MFI). Bars represent n=1 samples. E: TGF $\beta$ 1 levels in normal and ALD serum were measured using Sandwich ELISA. Bars represent mean  $\pm$  SEM of n=3 different donors, \*, p<0.05.



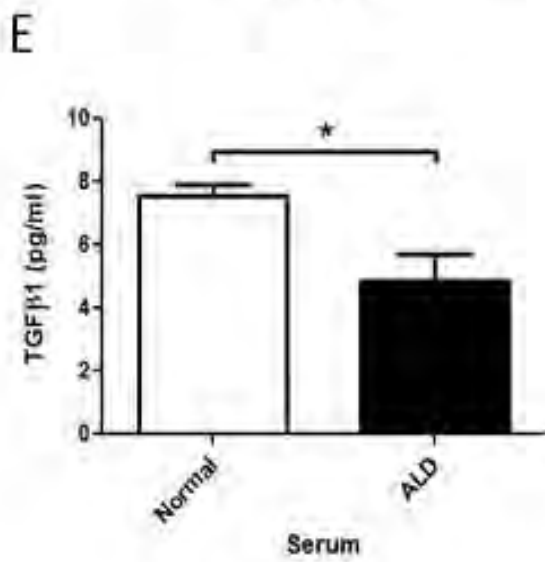
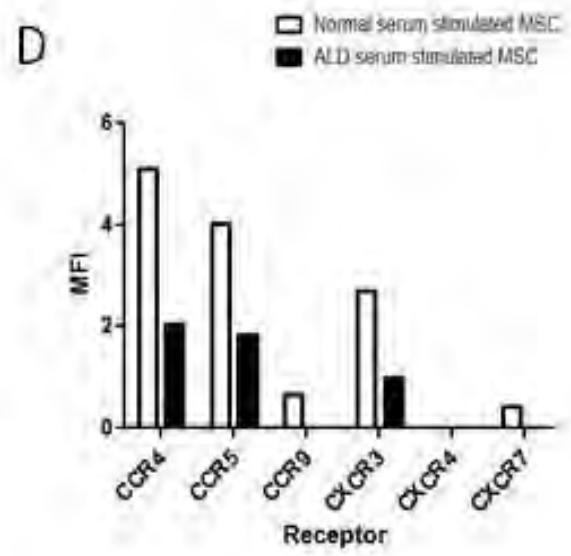
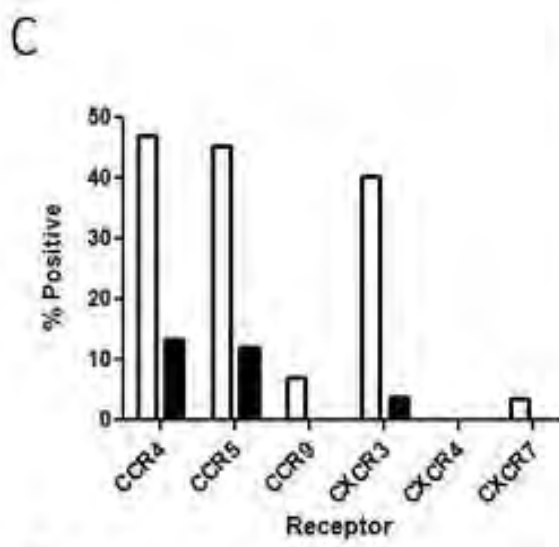
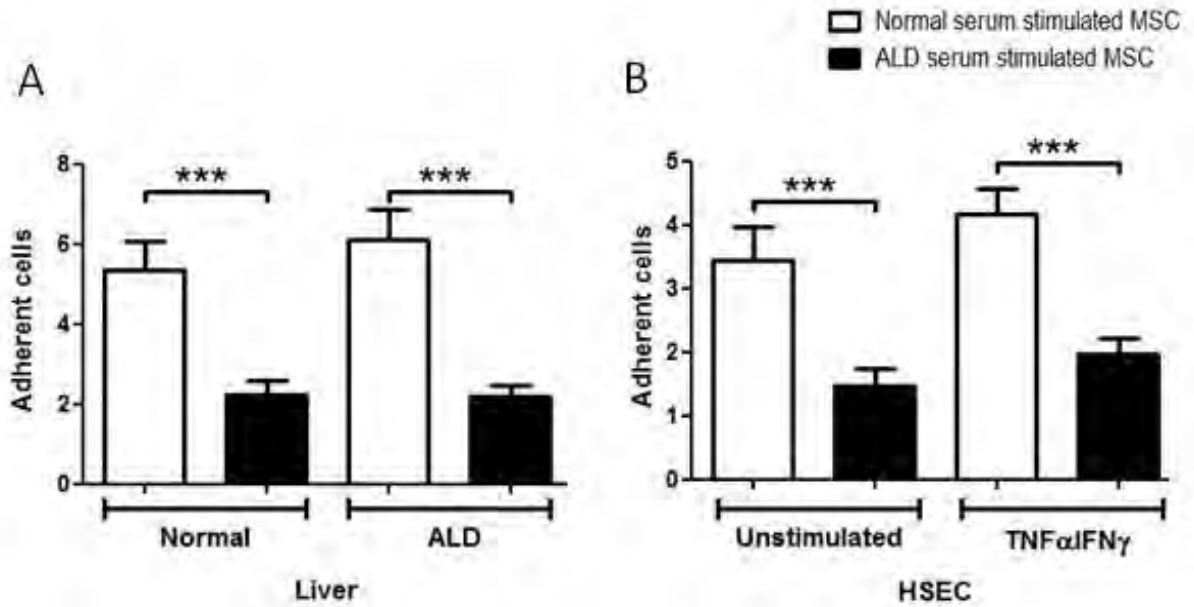




**Figure 4.23: Effect of ALD serum on MSC adhesion.**

A: Modified Stamper Woodruff assays showing adhesion of normal serum stimulated MSC (open bars) compared with ALD serum stimulated MSC (closed bars) adhesion to B: normal and ALD livers; and I: to unstimulated and TNF $\alpha$ IFN $\gamma$  stimulated human HSEC. Bars represent mean  $\pm$  SEM cells/ field of view of n=3 samples, \*, p<0.05; \*\*\*, p<0.001.



#### **4.2.11 Treatment of MSC with normal or end stage cirrhotic ALD patient serum can alter tri-lineage differentiation of the MSC without inducing intracellular stress**

There was no indication of a difference in the presence of IROS, autophagy or percentage of cells undergoing apoptosis or necrosis after normal or ALD serum stimulation, regardless of the detachment method (Figure 4.24). However cells treated with normal serum for 24 hours expressed increased levels of collagen II compared to ALD serum stimulated MSC (Figure 4.25A). It seems that stimulation with human serum induces some degree of chondrogenic differentiation. Culture of MSC in chondrogenic differentiation media (test) after serum stimulation induces expression of collagen II. Interestingly even culture of MSC in maintenance media (control) after stimulation with serum induces collagen II expression at low levels. There was no significant difference in adipogenic differentiation capability between Normal and ALD serum stimulated MSC (Figure 4.25B). However there was significantly increased osteogenic differentiation after MSC stimulation with ALD serum ( $46.86 \pm 1.19 \mu\text{M}$ ) compared to normal serum ( $36.03 \pm 1.79 \mu\text{M}$ ) as reported by higher levels of Alizarin red calcium staining ( $p < 0.05$ ) (Figure 4.25C).

**Figure 4.24: Effect of ALD serum on cellular stress.**

Levels of intracellular stress in normal and ALD serum stimulated MSC. Representative cytometry histogram for ALD serum stimulated MSC (red) and normal serum stimulated MSC (black), labelled with IROS marker, 2',7'-dichlorofluorescein (DCF), Autophagy marker, monodansylcadaverine (MDC), apoptosis marker, annexin V, D: Necrosis marker, 7AAD; with corresponding median fluorescent intensity (MFI) values. Data represents mean  $\pm$  SEM of n=1 donors.

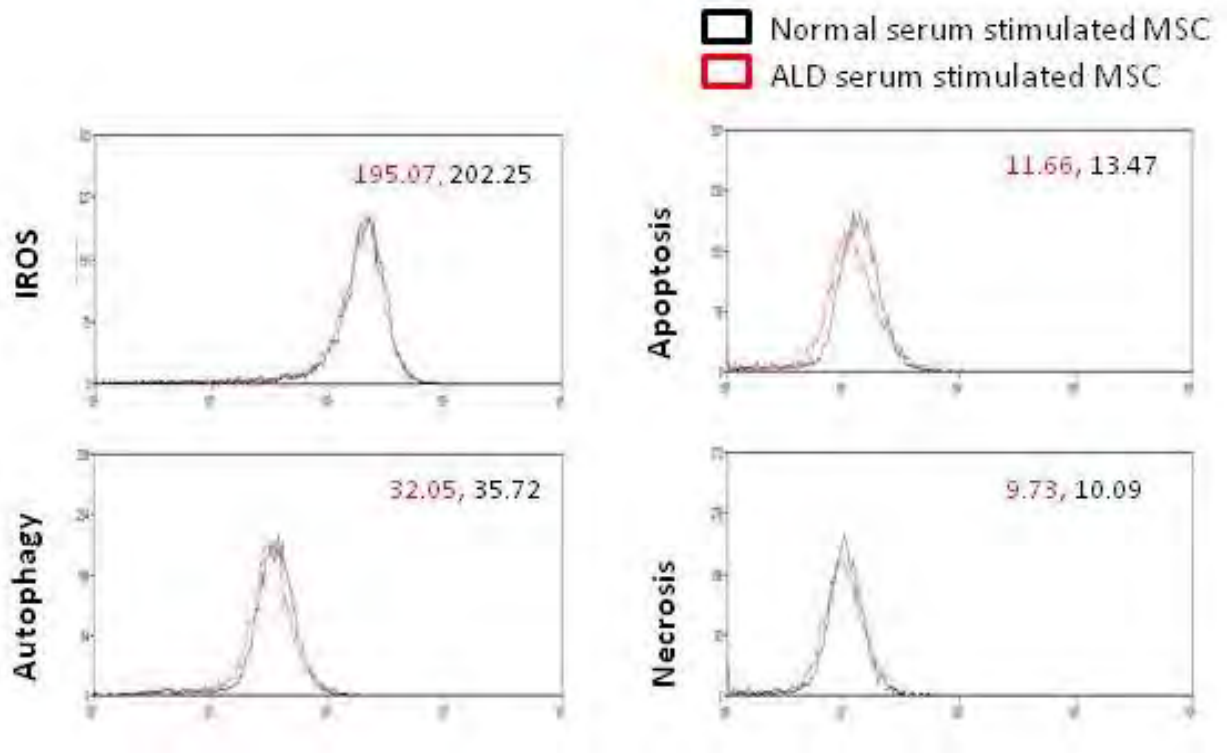
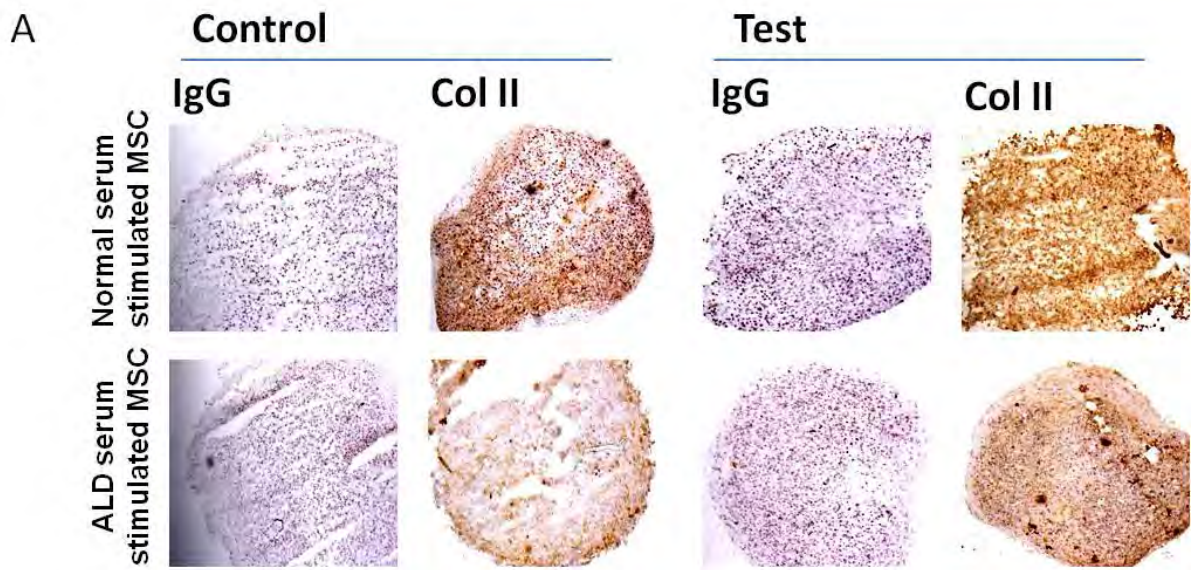
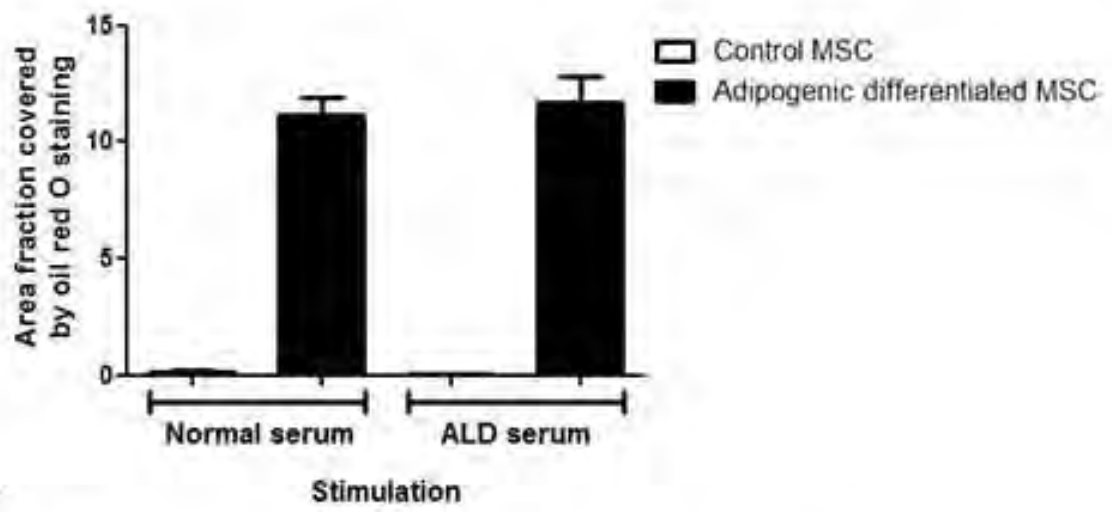


**Figure 4.25: Impact of ALD serum on tri-lineage differentiation.**

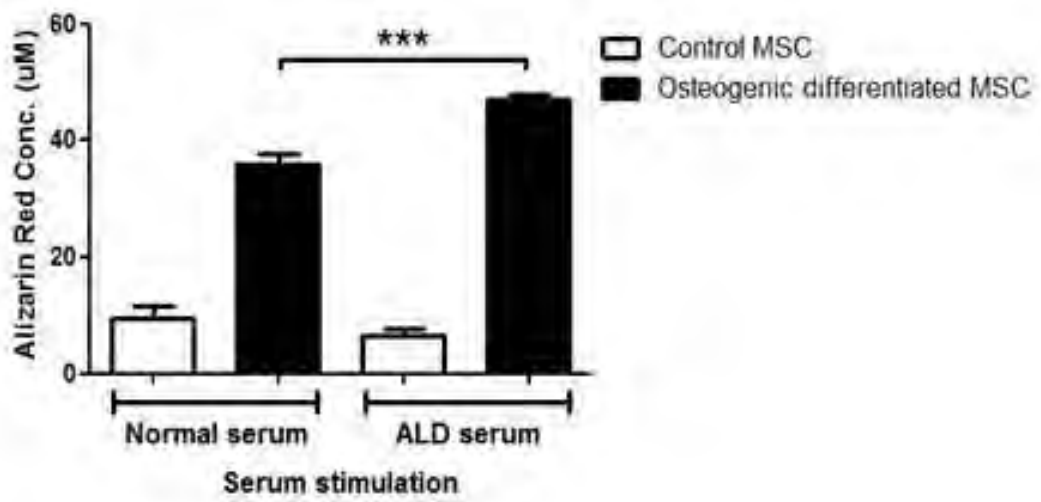
A: Representative images, DAB staining of collagen II as a marker of chondrocyte differentiation. ALD serum and normal stimulated MSC differentiated into chondrocytes at x20 magnification in maintenance media (control) and chondrogenic differentiation media (test). MSC were cultured as pellets after detachment from tissue culture plastic and differentiated into chondrocytes. B: Image J analysis of oil red O staining of normal and ALD stimulated MSC differentiated into adipocytes. Bars represent oil red O stained mean area fraction  $\pm$  SEM of n=3 samples. C: Alizarin red staining of normal and ALD serum stimulated MSC differentiated into osteoblasts. Bars represent mean calcium concentration ( $\mu$ M)  $\pm$  SEM of n=3 samples.



**B**



**C**



### 4.3 Discussion

The therapeutic effects of MSC when engrafted in the liver (Lin *et al.*, 2011, Popp *et al.*, 2009) are well established and MSC have even been used in clinical trials (Houlihan and Newsome, 2008). There are still limitations that exist in MSC therapy and these may lie with the transplant efficiency of MSC (Lin *et al.*, 2011). In order to overcome the impracticalities of expanding MSC to high numbers and to get maximal engraftment of infused cells the mechanism of MSC recruitment and engraftment needs to be elucidated and better understood so it can then be manipulated. In this chapter we have tried to utilise an important part of the cellular recruitment process by focussing our attention on MSC cell surface CCR. We have used cytokines commonly upregulated during liver injury to try and upregulate functional CCR which will likely play a major part in MSC migration to the site of injury. In this way we have tried to prime MSC for engraftment in the injured liver before exogenous administration.

The MSC CCR profile is still not established and has been inconsistent between reports from different groups (Honczarenko *et al.*, 2006, Ponte *et al.*, 2007, Ringe *et al.*, 2007, Sordi *et al.*, 2005). This may be due to a number of reasons, all of which we have tried to address in this chapter to ensure that we have found an accurate, reproducible and reliable profile of CCR on MSC. Firstly, there is no specific marker for MSC that can be used for prospective isolation; as a result, MSC populations are a variable heterogeneous mix of cells (Karp and Leng Teo, 2009). Any slight variations in isolation technique could drastically alter the MSC population that is obtained, so MSC populations could vary between groups. MSC are now commercially available and to avoid such issues we have purchased MSC. As a result, the repertoire of CCR

that we have identified is preserved and similar between every donor that we have analysed. Although there are some similarities with what other groups have found, the entire receptor profile we have observed has not been reported previously. To ensure the results we saw were not due to a defect with the antibodies we were using, we used them on PBMC as a control cell population. This population served as an adequate control for most of the CCR except for CCR3 and CCR8. This is of concern as CCR3 and CCR8 have previously been reported as present on MSC (Ponte *et al.*, 2007, Ringe *et al.*, 2007), but there are also reports of an absence of both CCR3 and CCR8 (Sordi *et al.*, 2005). Levels of CCR3 and CCR8 are variable between cell surface and intracellular expression suggesting that it is likely these antibodies are working as there is not a complete absence of expression.

Although all CCR warrant closer investigation we selected CCR4, CCR5, CCR9, CXCR3, CXCR4 and CXCR7 for further investigation based on a combination high levels of expression, upregulation of corresponding chemokine ligands in injured liver, and previous reports. CCR4 was expressed at the highest levels compared to other CCR. There is an upregulation during liver injury of CCR4 chemokine ligands, specifically, CCL2 (MCP-1), CCL4 (MIP-1 $\beta$ ), CCL5 (Rantes), CCL17 (TARC) and CCL22 (MDC) (Oo and Adams, 2010). Also there have been previous reports of CCR4 expression on MSC (Ponte *et al.*, 2007, Ringe *et al.*, 2007). CCR5 is also highly expressed on MSC, with an upregulation of corresponding ligands, CCL3 (MIP3 $\beta$ ), CCL4 (MIP1 $\beta$ ) and CCL5 (Rantes), in injured liver (Oo and Adams, 2010) and its presence on MSC has been observed in previous reports (Ponte *et al.*, 2007). Although CCR9 is expressed at intermediate levels, its presence on MSC has been reported in the past (Honczarenko *et al.*, 2006, Ringe *et al.*, 2007) and there are increased levels of its ligand CCL25 (Teck) on injured endothelium (Oo and Adams, 2010).

CXCR3 is highly expressed and appears in previous reports (Ringe *et al.*, 2007), with high levels of all its ligands in injured endothelium (Oo and Adams, 2010).

CXCR4 and CXCR7 are not expressed at very high levels but there are various reports suggesting the presence of CXCR4 on MSC (Ponte *et al.*, 2007, Ringe *et al.*, 2007, Son *et al.*, 2006, Sordi *et al.*, 2005). Equally there are also reports suggesting CXCR4 levels are absent or negligible (Phinney and Prockop, 2007, Ruster *et al.*, 2006, Sackstein *et al.*, 2008, Wynn *et al.*, 2004). Although most evidence for the significance of CXCR4 is based on migration towards CXCL12/ SDF1 $\alpha$  (Son *et al.*, 2006), there has been very little investigation into CXCR7. Although we see no cell surface CXCR4, there are smaller populations of MSC with intracellular CXCR4 expression. However we do not know if CXCR4 and CXCR7 are on the same cell population but this may be likely as CXCR4 and CXCR7 have been shown to work together to migrate towards SDF1 $\alpha$ / CXCL12 (Decaillot *et al.*, 2011, Levoye *et al.*, 2009). CXCR7 by itself is a scavenger receptor and there is little evidence to suggest it can solely mediate migration to SDF1 $\alpha$ / CXCL12. SDF1 $\alpha$ / CXCL12 levels are significantly increased during injury and could be a potent recruiter of MSC (Oo and Adams, 2010).

The selected panel of CCR was validated using immunohistochemistry and QPCR. Both methods supported our findings using flow cytometry, with receptors expressed at similar levels. However CXCR4 was not detectable either by QPCR or by immunohistochemistry, this may well be because of its presence in such a small population of cells. The techniques may not have been sensitive enough and to pick up such small levels in such small MSC populations.



Surface CCR levels were measured after stimulation using a panel of cytokines which are upregulated during most forms of liver injury. TGF $\beta$ 1, IL4, and IL10 were able to significantly upregulate CCR on the cell surface. TGF $\beta$ 1 was the most interesting as not only did it increase the proportion of MSC which expressed CXCR3, CCR4 and CCR5, but unlike IL10 and IL4, it was able to increase levels of CCR on the cell surface. As donor numbers were increased, increases in CCR expression became more apparent suggesting this was an accurate consistent and reproducible result. MSC were stimulated for 10 minutes with TGF $\beta$ 1 to investigate whether upregulation in receptor expression was happening at an earlier time point and then being sustained for the 24 hours. However this was not the case, MSC did not upregulate CCR at such early time points. This does not mean that upregulation occurs only after 24 hours. A more detailed time-course experiment needs to be carried out to identify exactly when this upregulation occurs.

Of note, the largest increases in proportions of cells expressing surface CCR occurred with receptors which had high intracellular stores. It has been shown that CCR can be re-expressed on the cell surface from intracellular stores, once they have internalised, and this may explain our observations (Borroni *et al.*, 2010). To prove this we analysed changes in mRNA levels of CCR after stimulation and found there was no significant changes after stimulation with these cytokines. This means the cell surface expression may be due to recycling CCR from intracellular stores back to the cell membrane. To ensure there were no false positive results we test for contaminants in the reagents by creating some cDNA samples with water rather than reverse transcriptase and running cDNA samples on gels after 18S rRNA PCR to ensure these samples were negative.

The migratory potential of the MSC to chemokine ligands was tested to determine which CCR were functional. Due to the multiple ligands for each CCR, there were many chemokine ligands for the selected CCR. Unstimulated MSC were titrated on over a range of concentrations from which certain ligands were selected based on whether there was significant migration towards that chemokine or if this was potentially a chemokine which could be highly expressed in injured liver. According to the chemokines that MSC migrated towards, it seemed that CCR5, CCR9, CXCR3 and CXCR4/ CXCR7 were all functional. However in experiments testing migration towards TARC/ CCL17 we saw very high levels of migration towards basal medium. This suggests there may have been some non-specific migration, or that CCR4 function was induced in some way. It is interesting that there was significant migration to SDF1 $\alpha$ / CXCL12 considering there were such low levels of its receptor. However, research suggests that migration towards SDF1 $\alpha$ / CXCL12 ligands may be regulated without CCR (Aldridge *et al.*, 2012, Sarkar *et al.*, 2008).

Comparisons of the migratory potential of stimulated MSC were analysed. TGF $\beta$ 1 significantly increased migration to IP-10/ CXCL10 and IL4 to TARC/ CCL17. Both TGF $\beta$ 1 and IL4 had also upregulated CXCR3 and CCR4 which may then have increased migration towards IP-10/ CXCL10 and TARC/ CCL17 respectively. This suggests that migration of a receptor towards a ligand may be dependent on the type of cytokine stimulus the receptor receives.

TGF $\beta$ 1 stimulation not only increased migration to IP-10/ CXCL10, but also made MSC more adherent to NASH cirrhotic and PSC explanted liver sections, compared to normal livers sections; and to unstimulated, IL4 and IL10 stimulated MSC. This effect of TGF $\beta$ 1 stimulated

MSC binding may be specific to the disease types such as NASH and PSC which have a high inflammatory component at the time of transplantation. However PBC and AIH patients may receive high doses of anti-inflammatory drugs, thus reducing the inflammatory component which may be responsible for increased binding of TGF $\beta$ 1 stimulated MSC. Inflammatory agents may reduce in ALD livers due to abstinence from alcohol before transplant. The MSC may be binding to inflammatory or fibrotic factors in NASH and PSC livers where anti-inflammatory drugs are not used before the liver is explanted. Alternatively this may be due to high baseline binding of cells in the control, as this assay has a high degree of variability when physically washing off unbound cells from adherent cells. PBC livers show a slight increase in binding of TGF $\beta$ 1 stimulated MSC but this is not statistically significant. Modified Stamper Woodruff assays were also performed with cytokine stimulated MSC on unstimulated and TNF $\alpha$ IFN $\gamma$  stimulated (to mimic injured conditions) HSEC, BEC and MF. TGF $\beta$ 1 stimulated MSC bound significantly more to HSEC in uninjured and injured conditions.

IFN $\gamma$  stimulated HSEC have been shown to increase ligand expression for CXCR3 receptors to recruit more leukocytes during inflammation and inflammatory diseases such as PBC have been shown to express higher levels of CXCR3 ligands (Curbishley *et al.*, 2005). As MSC bind indiscriminately to injured and uninjured HSEC, it is likely that increased binding could be due to increased receptors on the MSC surface rather than increased ligand in the cell monolayer, which would usually be the case when leukocyte recruitment occurs.

To investigate how TGF $\beta$ 1 stimulated MSC would behave in circulation in an *in vivo* model of liver injury, carbon tetrachloride liver injury was induced in C57BL/6 wild type mice.

Studies in these mice were to determine the initial binding and engraftment mechanisms employed by MSC and to determine whether TGF $\beta$ 1 stimulation of MSC could enhance engraftment in injured liver. Potentially for further long term studies, as a comparison to wild type mice, we set up a similar model in Rag2<sup>-/-</sup>IL-2 $\gamma$ <sup>-/-</sup> knockout immunocompromised mice. We found that TGF $\beta$ 1 stimulated MSC bound significantly more to frozen sections of livers from both strains of mice than unstimulated MSC. An obvious issue with these experiments was that we were using human MSC in mouse models. However such experiments have been carried out with human MSC in mice and even pigs, not only to investigate engraftment, but also to research the therapeutic effects of MSC in mouse and pig models of disease (Jung *et al.*, 2011b, Li *et al.*, 2012).

To infuse the MSC into circulation a number of methods can be employed. MSC can be infused through the tail vein or during intravital microscopy or other such procedures to investigate the early stages of adhesion and engraftment. However a problem specific to MSC is that administration through these routes means a significant number of cells become lodged in the lungs due to their large size (Gao *et al.*, 2001, Karp and Leng Teo, 2009). One of the ways around this has been by using a vasodilator sodium nitroprusside before intra arterial and intravenous MSC infusion which allowed more MSC to migrate to the liver and be cleared from the lungs, where they were previously becoming stuck (Gao *et al.*, 2001). Another way to overcome this is to infuse MSC through the portal vein. A major criticism is that this method is a highly invasive procedure that could lead to portal hypertension (Lin *et al.*, 2011). Eventually we will have to overcome this issue, one way may be to FACS sort MSC based on size before infusion, and then potentially infuse MSC via the tail vein. This may work as some cells do get to the liver albeit a small proportion. However experiments in

this chapter are investigating the interaction between MSC and mouse liver endothelium so are sufficient for this purpose.

Ideally we would have liked to carry out intravital microscopy experiments but because we employed portal vein infusions instead of infusion through the carotid, to administer cells, this did not leave enough time to view circulating and engrafting cells in the mouse liver. This meant that we had to cull mice after the procedure, freeze and section livers and count the number of CFSE pre-labelled MSC which had engrafted. Although this was not an ideal way of counting engrafted cells, sufficient measures were taken to ensure accurate and representative counting of engrafted cells. For future experiments we would need to develop a method to cannulate the portal vein, or collect the whole liver, homogenise to a single cell suspension and count the number of engrafted fluorescently labelled MSC using flow cytometry to give a more accurate result.

TGF $\beta$ 1 stimulated MSC engrafted into injured and uninjured mice at significantly higher levels than unstimulated MSC, IL4 and IL0 stimulated MSC which further proved this effect was TGF $\beta$ 1 specific. We then functionally blocked CXCR3 and CCR5 and CXCR4 with and without TGF $\beta$ 1 stimulation. Without stimulation of MSC there was no reduction in engraftment of MSC with any of the blocking antibodies. TGF $\beta$ 1 stimulation increased engraftment as we had previously observed but only blocking with CXCR3 blocking antibody was able to reduce the engraftment back to baseline levels. This suggests that the TGF $\beta$ 1 stimulation induces binding through CCR expression and without stimulation MSC CCR do not play a significant part in engraftment. This suggests that by preserving receptor expression, it may help in the study of MSC receptor profiles and we may even see increases

in their migratory function (as shown in the previous chapter) but there is limited functional effect on engraftment into livers without TGF $\beta$ 1 stimulation. Clearly not all CCR have been tested and further work needs to investigate the entire process of engraftment which may involve more chemokines and receptors than just CXCR3.

We hypothesised that even if MSC were detached from tissue culture plastic using enzymatic methods which we have shown can cleave CCR from the cell surface, TGF $\beta$ 1 stimulation should mobilise or prime internal MSC stores to a point where they can promptly come to the surface and significantly promote engraftment of MSC. The presence of surface receptors after CDB detachment could have been responsible for higher baseline levels of MSC binding to tissue. Enzymatic detachment would cleave receptors and so lower baseline binding was observed. This may have been why TGF $\beta$ 1 stimulated increases in binding would have appeared significant after enzymatic detachment. Similarly we saw significantly increased binding to mouse liver sections and HSEC monolayers. Infused TGF $\beta$ 1 stimulated MSC *in vivo* after enzymatic detachment also exhibited significantly increased engraftment, in both injured and uninjured mice compared with unstimulated and TNF $\alpha$  stimulated MSC which shows that the effect is specific to TGF $\beta$ 1. TGF $\beta$ 1 has been reported to upregulate CXCR3 on NK cells but the reasons behind why this happens were not pursued in the study (Inngjerdigen *et al.*, 2001).

Some studies suggest that TGF $\beta$ 1 stimulation can differentiate MSC towards a myofibroblast lineage and therefore a pro-fibrotic phenotype (Li *et al.*, 2009). We tested the MSC after TGF $\beta$ 1 stimulation for mRNA expression of collagen (coll1 $\alpha$ 1) and alpha smooth muscle actin ( $\alpha$ SMA) but observed no significant difference in expression from unstimulated MSC. Tri-

lineage differentiation of MSC was tested using both enzymatic and non enzymatic detachment methods. The reason for this was to investigate whether TGF $\beta$ 1 could alter its effects on the MSC depending on the way it had been detached. However we saw no difference in MSC tri-lineage differentiation after TGF $\beta$ 1 stimulation. Increased IROS has been implicated in stimulating MSC migration (Novo *et al.*, 2011). We hypothesised that TGF $\beta$ 1 may increase MSC migration or cause an upregulation in CCR expression through increased IROS. We tested MSC for IROS and for other stress related responses but saw no difference between unstimulated or TGF $\beta$ 1 stimulated MSC.

Recruitment of MSC to organs rarely occurs without the interaction of integrins (Karp and Leng Teo, 2009). To identify any obvious changes in integrin expression we began by testing enzymatic and non-enzymatic methods of detachment but saw no difference. This suggests that integrins are less susceptible to enzymatic cleavage than CCR. Interestingly we saw a marked increase in CD44 expression on TGF $\beta$ 1 stimulated MSC. Based on previous reports it is highly likely that this molecule increases MSC adhesion after being upregulated and therefore must be working in conjunction with CCR to increase engraftment (Aldridge *et al.*, 2012, Sarkar *et al.*, 2008). However this experiment has only been carried out once and further investigation will need to be done to elucidate the role of CD44 in this mechanism.

MSC have numerous and well characterised immunomodulatory properties including suppression of CD4 T cell proliferation (Newman *et al.*, 2009, Uccelli and Prockop, 2010). The suppressive effect exerted by MSC can be enhanced by cytokines including TNF $\alpha$  and IFN $\gamma$  (Prasanna *et al.*, 2010). We found that TGF $\beta$ 1 can also increase suppressive properties of MSC which they seem to exert through PGE2. PGE2 has been reported to be used by MSC

to suppress T cell proliferation (Newman *et al.*, 2009). TGF $\beta$ 1 may increase PGE2 expression by MSC and this in turn increases the potency of the MSC suppressive effect. We also found that TGF $\beta$ 1 stimulated MSC supernatants contain higher levels of IL6 although this is not statistically significant; which may be explained by low donor numbers that were tested. IL6 production by MSC has been implicated in inducing an increase in PGE2 levels secreted by MSC in an autocrine manner (Bouffi *et al.*, 2010). IL6 is an interesting cytokine as it has pro-fibrotic and pro-inflammatory properties as it has been implicated in increasing an increase in liver fibrosis and stimulating T cell proliferation, but it is also capable of inhibiting dendritic cell maturation and protects neutrophils from apoptosis (Newman *et al.*, 2009). This means that the point at which MSC are used as a therapy needs to be thoroughly evaluated when considered, for example, such cells would be more beneficial as a treatment of higher inflammatory periods than during high levels of fibrosis.

An important consideration in using TGF $\beta$ 1 stimulated MSC is the increased expression of MCP-1/ CCL2. Unfortunately this could add to the pro-fibrotic environment of the liver when there are already high levels of MCP-1/ CCL2 particularly during NASH and alcoholic liver disease where recruitment of neutrophils and macrophages could be promoted (Lalor *et al.*, 2007). MCP-1/ CCL2 expression by MSC has been previously reported (Honczarenko *et al.*, 2006) and mesenchymal stromal cells can use MCP-1/ CCL2 to recruit monocytes to sustain malignant B cell growth and set up a niche for the development of lymphomas (Guilloton *et al.*, 2012). There is equally compelling data which suggests that MCP-1/ CCL2 from mesenchymal stromal cells can suppress plasma cell immunoglobulin production and could potentially be used as a therapy for pathologic humoral responses (Rafei *et al.*, 2008). CCL2 stimulation of MSC has also been shown to induce MSC motility (Anton *et al.*, 2012) but at



the same time MSC have been shown not to migrate to MCP-1/ CCL2 (Ringe *et al.*, 2007). Higher MCP-1/ CCL2 levels could contribute to the increased migration we observe in TGF $\beta$ 1 stimulated MSC. MSC secreted MCP-1/ CCL2 has been shown to function in a paracrine way by promoting angiogenesis, increasing cell migration and preventing apoptosis, thus adding to the beneficial effects of stem cell therapy (Boomsma and Geenen, 2012).

We have seen MSC are able to bind to the endothelium, and to further investigate the effect of MSC in the surrounding environment we treated sinusoidal endothelium with cytokine stimulated MSC conditioned media and then measured levels of adhesion molecules on HSEC. There was no significant effect by this media. However there was a trend for ICAM-1 upregulation by IL6 stimulated MSC conditioned media, a significantly downregulation by TNF $\alpha$  stimulated MSC conditioned media and a slight downregulation by IL1 $\beta$ . This suggests using MSC in a highly inflammatory environment containing TNF $\alpha$  and IL1 $\beta$  (Greco and Rameshwar, 2008) could reduce inflammation by down regulating ICAM-1 and thus reducing recruitment of inflammatory cells. However in an environment with high levels of IL6, typical of most types of liver fibrosis, ICAM-1 expression on endothelium can be upregulated, suggesting this would promote inflammation. It is therefore important to delineate when MSC need to be used during liver disease to exhibit their most potent therapeutic effects.

To test the effects of TGF $\beta$ 1 in serum we used normal human serum and serum from end stage ALD patients to stimulate MSC for 24 hours. ALD disease patient serum has been reported to contain high levels of TGF $\beta$ 1 compared to normal serum (Grigorescu, 2006, Marek *et al.*, 2005). However we found the ALD serum to have lower levels of TGF $\beta$ 1 possibly as it was collected from patients after a period of alcohol abstinence and after a

lengthy course of anti-inflammatory drugs which would considerably reduce platelet levels in blood, which are a major source of TGF $\beta$ 1. As a result we observed significantly increased levels of surface CCR on MSC and there was increased binding of MSC to both frozen normal and ALD liver sections in modified Stamper Woodruff assays. A higher level of  $\beta$ 1 integrin was seen on the surface of MSC after ALD serum however this did not increase binding to tissue sections as we would expect. A reason for this could be that CCR have been implicated in integrin phosphorylation, so a lack of CCR may prevent phosphorylation of the integrins (Ley *et al.*, 2007) or that other receptors such as CD44 are more important in this context (Aldridge *et al.*, 2012).

Addition of serum did not seem to alter levels of stress in the cells as was measured by markers of IROS, autophagy, necrosis and apoptosis. Normal serum appeared to increase chondrogenic differentiation, which has been reported as a result of high levels of TGF $\beta$ 1, compared to ALD serum. There was no significant difference in adipogenic differentiation after stimulation of MSC with normal or diseased patient serum. There was a significant increase in osteogenic differentiation after stimulation by ALD patient serum and this could be due to lower levels of TNF $\alpha$  or IL1 $\beta$  which has been reported (Lacey *et al.*, 2009). The findings from experiments with ALD patient serum supported the results of TGF $\beta$ 1 and its effects on CCR expression. The results suggest that TGF $\beta$ 1 stimulation could play a significant part on binding of cells to liver tissue through the control of CCR.

The intracellular and cell surface CCR expression profile, of receptors (CCR1-10 and CXCR1-7) of MSC has been clearly described in this chapter. The effect of stimulation of a range of cytokines, typically upregulated during liver injury, on a select panel of receptors,

CCR4, CCR5, CCR9, CXCR3, CXCR4 and CXCR7 was investigated further. Distinct increases in CCR were observed, and of these, TGF $\beta$ 1 stimulation was able to induce an increase of CXCR3 surface expression and also an associated increase in CXCR3 function, both in terms of migration to IP-10/ CXCL10 and in binding to diseased human and mouse tissue. TGF $\beta$ 1 stimulation increased CXCR3 mediated engraftment of MSC into the liver of an *in vivo* model of CCl<sub>4</sub> induced liver injury. TGF $\beta$ 1 stimulation of MSC was not able to induce a pro-inflammatory phenotype on MSC or alter tri-lineage potential but increased immunosuppressive properties of MSC mediated via PGE<sub>2</sub>. In all this suggests that engraftment and immunomodulatory properties of MSC can be increased using TGF $\beta$ 1 stimulation without promoting any known negative effects, therefore our results warrant further research into the long term effects of TGF $\beta$ 1 stimulated MSC after engraftment in *in vivo* models of liver injury.

## **CHAPTER 5: FIBROCYTE ISOLATION AND PHENOTYPING**

## 5.1 Introduction

### 5.1.1 HSC derived fibrocytes

As demonstrated in the preceding chapters, MSC hold great promise as a cellular therapy in many clinical therapies for a range of diseases. Pro-inflammatory or pro-fibrotic haematopoietic populations (Ebihara *et al.*, 2006, LaRue *et al.*, 2006, Wilkins and Jones, 1996), namely fibrocytes within MSC populations may be responsible for much of the contradictory data reported regarding the effects of MSC (Auffray *et al.*, 2009, Baertschiger *et al.*, 2009, Carvalho *et al.*, 2008, Strieter *et al.*, 2009a). Hematopoietic stem cells (HSC) are multi-potent stem cells which give rise to all cell subsets from the myeloid and lymphoid lineages in the blood. HSC are a heterogeneous population of cells, which reside in the bone marrow of adults but can mobilise into the circulation. These cells are able to self renew and replenish blood cell types including monoblasts which further differentiate into monocytes (Auffray *et al.*, 2009).

Monocytes, dendritic cells and macrophages are involved in three major roles as part of the immune system including antigen presentation, phagocytosis of invading pathogens and the release of pro-inflammatory or anti-inflammatory cytokines to recruit more inflammatory cells (Geissmann *et al.*, 2010). Under normal conditions monocytes differentiate into different types of macrophages and dendritic cells in tissue as a means of immune surveillance but during injury and as part of an inflammatory response monocyte levels in circulation increase, with a subsequent increase in tissue recruitment and dendritic cells and macrophage differentiation to combat pathogens (Geissmann *et al.*, 2010). Monocytes exist as 3 major

subsets identified by their CD14 and CD16 surface receptor/ marker expression to generate CD14<sup>+</sup>CD16<sup>-</sup>, CD14<sup>+</sup>CD16<sup>+</sup> and CD14<sup>-</sup>CD16<sup>+</sup> subsets (Wong *et al.*, 2012).

Fibrocytes are a recently identified stromal cell type derived from monocytes (Shirai *et al.*, 2009) which possess monocyte-like immune cell attributes such as antigen presentation and cytokine production but are unable to phagocytose pathogens (Kisseleva *et al.*, 2011). Instead fibrocytes respond to bacteria by releasing extracellular traps formed by DNA fibres and containing the antimicrobial peptide cathelicidin (Kisseleva *et al.*, 2011). Fibrocytes are elongated, spindle shaped, cell culture plastic adherent cells found in healing wounds and fibrotic lesions (Wu *et al.*, 2007). All CD14<sup>+</sup> monocytes can contribute to the fibrocyte pool, although CD14<sup>+</sup>CD16<sup>-</sup> monocytes preferentially differentiate to fibrocytes (Abe *et al.*, 2001). Fibrocytes circulate in the blood as monocytes and differentiate to fibrocytes when they enter tissue (Bucala *et al.*, 1994), although some literature suggests that 'mature' fibrocytes can also exist in the circulation (Quan *et al.*, 2004) this has never been definitively proved (Bournazos *et al.*, 2009). When a monocyte differentiates into a fibrocyte it loses CD14 and CD16 expression, but retains CD45 and CXCR4 expression (Bellini and Mattoli, 2007). The fibrocyte also expresses low levels of collagen-1 and high levels of  $\alpha$ SMA once it has differentiated from a monocyte (Kisseleva *et al.*, 2006). Eventually in culture and in tissue due to chronic inflammatory and fibrotic stimuli, a fibrocyte can differentiate into a myofibroblast (Bellini and Mattoli, 2007). These myofibroblasts can completely lose CD45 expression and increase levels of collagen-1 and  $\alpha$ SMA expression, appearing phenotypically identical to tissue-resident myofibroblasts (Bellini and Mattoli, 2007, Iredale, 2008).

In the liver, resident myofibroblasts differentiate from hepatic stellate cells during liver injury. Myofibroblasts are responsible for laying down extracellular matrix and thus contribute to scar forming tissue in injured liver (Iredale, 2008). The ongoing inflammation concurrent with most forms of chronic fibrosis led to the hypothesis that monocyte derived fibrocytes of HSC origin could contribute to the hepatic myofibroblast population and thus to liver fibrosis (Kisseleva *et al.*, 2006). Subsequently, specific inflammatory and fibrotic stimuli responsible for monocyte differentiation to fibrocytes and then to myofibroblasts have been identified (Bellini and Mattoli, 2007).

### **5.1.2 Fibrocytes in diseased organs**

Fibrocytes have been identified in cardiac fibrosis, pancreatitis, pancreatic insulinomas, rheumatoid arthritis, Graves' disease, skin fibrosis, renal fibrosis, lung disease and the spleen (Direkze *et al.*, 2004, Douglas *et al.*, 2010, Galligan and Fish, 2012, Keeley *et al.*, 2009, Kisseleva *et al.*, 2011, Krenning *et al.*, 2010, Wada *et al.*, 2007, Wang *et al.*, 2008). In common with MSC, fibrocytes are very potent immunogenic cells. They play a role in antigen presentation and T cell priming (Chesney *et al.*, 1997), and are able to present antigen to CD4<sup>+</sup> and CD8<sup>+</sup> cytotoxic T cells (Balmelli *et al.*, 2005). Also, fibrocytes express both MHC class I and class II antigens and co-factors CD80 and CD86. The immunogenic potential of these cells suggests that should these enter the liver environment, possibly during inflammation, they could then contribute to the development of fibrosis (Scholten *et al.*, 2011).

The point at which fibrocytes appear in a diseased organ is still unclear, as is their specific role during this phase of injury. Due to their production of collagen and potential pro-fibrotic role it has been assumed they appear during active fibrogenesis. Furthermore in most forms of lung disease it has been shown that resident activated myofibroblasts, are responsible for driving fibrocyte recruitment (Gomperts and Strieter, 2007). Once recruited, fibrocytes can themselves differentiate into myofibroblasts and produce ECM molecules (Gomperts and Strieter, 2007), further stimulating new fibrocyte recruitment and fibrogenesis (Andersson-Sjoland *et al.*, 2011, Vannella *et al.*, 2007). It has also been suggested that autocrine and paracrine fibrocyte activation pathways encourage monocyte differentiation into fibrocytes (Vannella *et al.*, 2007). Recent data also suggests that fibrocytes retain some inflammatory cell features suggesting a bridging role between ongoing inflammation and concurrent fibrosis (Iwaisako *et al.*, 2012, Stramer *et al.*, 2007).



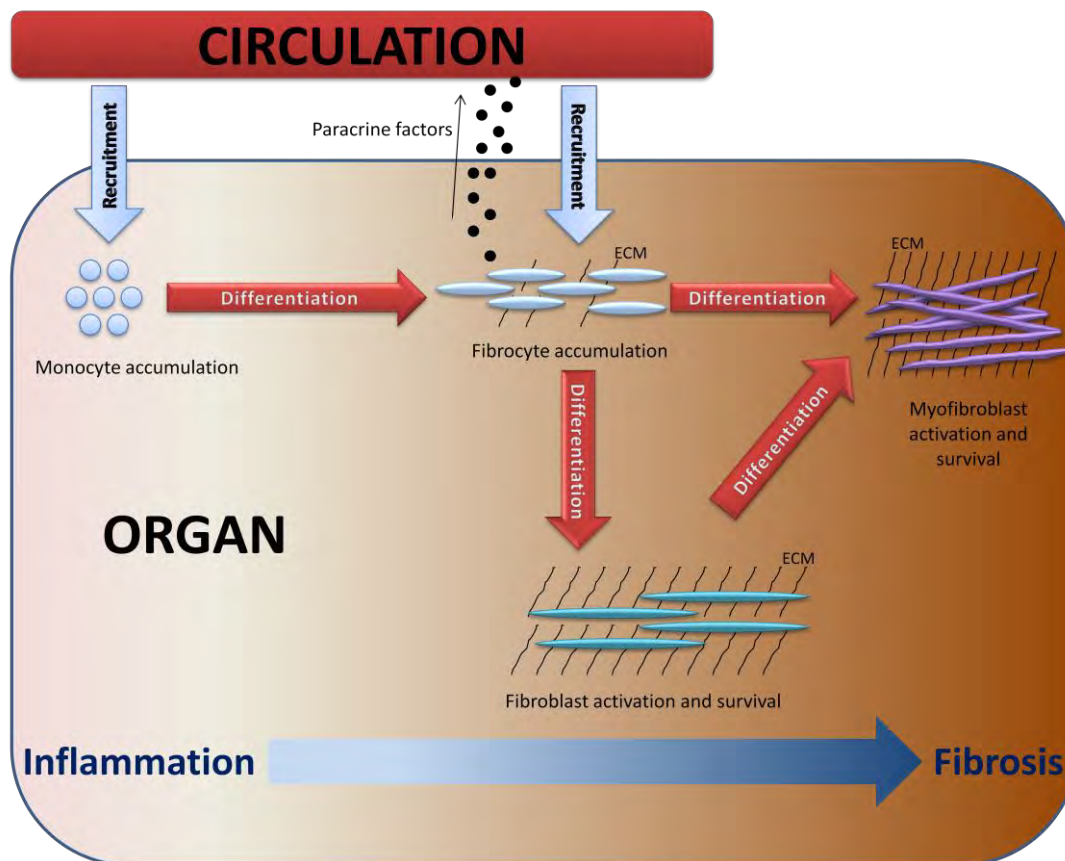


**Figure 5.1: Sources of fibrocytes, fibroblasts and myofibroblasts in inflammation and fibrosis.**

Blood borne fibrocytes and monocytes derived from the bone marrow enter the tissue where they may play roles in inflammation or elaborating matrix. Monocytes recruited during inflammation can also differentiate into fibrocytes in the tissue. Fibrocytes secrete paracrine factors to recruit more fibrocytes from the circulation. Fibrocytes retain inflammatory properties and take on low level fibrotic properties including low level ECM deposition during early stages of fibrosis. Finally resident fibroblasts are also capable of transdifferentiation into myofibroblasts, which exhibit both a contractile and matrix-producing phenotype. ECM = extracellular matrix.

It is also possible that specific monocytes may enter during long term inflammation and be retained in the tissue as a pro-fibrotic cell, thus switching from their original function and adapting to the fibrotic environment in the organ (Figure 5.1). This is supported by data showing that blockade of monocyte differentiation to fibrocytes reduced injury in models of

pulmonary and renal fibrosis (Nikam *et al.*, 2010, Nikam *et al.*, 2011, Sakai *et al.*, 2006, Song *et al.*, 2010, Tourkina *et al.*, 2011). In particular it has been suggested that increased serum amyloid protein (SAP) (Pilling *et al.*, 2003) and blocking Adenosine A<sub>2A</sub> receptor (Katebi *et al.*, 2008) on monocytes may reduce monocyte differentiation to fibrocytes in injured tissue and consequently reduce fibrosis in injured organs. Th1 cytokines have also been suggested to promote fibrocyte differentiation and Th2 cytokines inhibit fibrocyte differentiation suggesting a significant role of T cells in monocyte differentiation (Shao *et al.*, 2008), which is physiologically appropriate during chronic inflammation, leading to fibrosis. Cytokines such as TGFβ1 and IL4 have been shown to differentiate monocytes to collagen producing macrophages with antigen presenting abilities and reduced phagocytosis similar to fibrocytes (Gordon, 2003, Porcheray *et al.*, 2005), and there has been some discussion about fibrocytes being alternatively activated macrophages (Pilling *et al.*, 2009a, Reilkoff *et al.*, 2011). However, their pro-fibrotic phenotype and evidence from microarray analysis of these cells suggests that they constitute a discrete cell type from macrophages and dendritic cells (Curnow *et al.*, 2010).

### **5.1.3 The contribution of fibrocytes to liver disease**

Much of the research on fibrocytes in fibrotic organs has focussed on lung disease and models of lung injury. The presence of fibrocytes is well documented in various types of lung disease, including asthma (Schmidt *et al.*, 2003), idiopathic pulmonary fibrosis (Moeller *et al.*, 2009) and obliterative bronchiolitis (Andersson-Sjoland *et al.*, 2009), which have their own specific local niche that influences the fibrocyte phenotype (Andersson-Sjoland *et al.*, 2011). Migration of fibrocytes into the lung has been shown as dependent on CCR5 (Ishida *et al.*,

2007, van Deventer *et al.*, 2008), CXCR4 (Mehrad *et al.*, 2009, Phillips *et al.*, 2004), CCR2 (Ekert *et al.*, 2011, Ishida *et al.*, 2007, Moore *et al.*, 2005, Moore *et al.*, 2006, Sun *et al.*, 2011) and CCR7 (Keeley *et al.*, 2009) and the use of inhibitors or knockouts of CCR in mouse models has proved their involvement in fibrocyte recruitment to the lung (Ekert *et al.*, 2011, Keeley *et al.*, 2009, Song *et al.*, 2010, van Deventer *et al.*, 2008). Research into fibrocytes in lung disorders has identified fibrocyte differentiation from blood as a potential diagnostic tool as a clinical biomarker of lung disease.

In contrast there is significantly less research on the presence of fibrocytes in the liver and less still in human liver. The existence of fibrocytes in injured mouse liver has been demonstrated by Kisseleva *et al* (Kisseleva *et al.*, 2006) who transplanted bone marrow from transgenic mice with GFP-tagged collagen promoters into irradiated wild type mice, and then induced liver injury by bile duct ligation. Liver infiltrating cells were analysed and found to be positive for GFP, collagen producing cells, and expressed CD45. These cells were isolated, and after prolonged culture were found to take on a myofibroblast phenotype, with increasing collagen expression and loss of CD45 expression. It was found that the speed of differentiation to a myofibroblast was enhanced by the addition of TGF $\beta$ 1, a cytokine that is increased in fibrotic livers (Kisseleva *et al.*, 2006). Similarly in a model of CCL<sub>4</sub> injury in mice, fibrocytes were identified in the liver, (Kisseleva *et al.*, 2011). However Kisseleva *et al* went further to suggest fibrocyte migration was induced by TGF $\beta$ 1 and LPS, mediated by CCR1 and CCR2 which changed with age and therefore impaired fibrocyte recruitment. Fibrocytes were also described in the *Abcb4*<sup>-/-</sup> mouse model of Sclerosing Cholangitis and identified in fibrotic parenchyma where they infiltrated hepatic lobules from portal fields where stellate cell-derived myofibroblasts were absent (Roderfeld *et al.*, 2010).

However, the contribution of bone marrow derived fibrocytes to human liver disease is likely to be complex and may involve mechanisms similar to those described in other organs or organs in mice. The fate and impact of these cells in human liver is not clear and may be dependent on injury or even specific to mouse models. Although blocking fibrocyte recruitment could lead to reduced fibrosis, this seems only applicable in situations where the contribution of fibrocytes (as opposed to other cell populations) to fibrosis is significant. Also evidence confirming that fibrocytes can exist in normal or uninjured organs suggests that these cells may have key roles in normal organ homeostasis which could be impaired in the event of therapeutic intervention.

#### **5.1.4 Are fibrocytes likely to contaminate cultures of MSC?**

The current protocols used to isolate MSC from bone marrow involve plating bone marrow onto tissue culture plastic (Pittenger, 2008). A major flaw with this strategy is that it assumes MSC will outgrow and outlast all CD45<sup>+</sup> haematopoietic cells on tissue culture plastic, the majority of which will not adhere to the plastic. However, fibrocytes are CD45<sup>+</sup> and can acquire a MSC-like phenotype and over the period of time used for MSC isolation procedures, could lose their haematopoietic markers (Abe *et al.*, 2001). Interestingly over large periods of time, fibrocytes have been shown to acquire markers similar to MSC and share the tri-lineage differentiation potential thought to be unique to MSC (Choi *et al.*, 2010, Hong *et al.*, 2005). Thus conflicting experimental evidence describing pro- vs. anti-inflammatory effects of MSC may be linked to fibrocyte contamination (Wilkins and Jones, 1996). Thus, where MSC have been shown to possess anti-fibrotic and anti-inflammatory

properties, pro-fibrotic and potent inflammatory effects have been described for fibrocytes. Removal of fibrocytes from MSC populations may ensure a more potent population of MSC and would permit clearer understanding of the exact roles of MSC within tissue.

### **5.1.5 Current methodologies used to isolate and culture fibrocytes**

There has been much controversy over the optimal isolation and culture conditions for fibrocytes. Currently there are two different protocols used to isolate fibrocytes from blood. One method includes isolating fibrocytes from blood using negative selection and culture in serum media for 14 days (Phillips *et al.*, 2004), where Leukopheresis packs containing concentrated leukocytes are used, to yield a higher number of fibrocytes. An alternative protocol exists suggesting culture in media without serum for only 3 to 5 days (Pilling *et al.*, 2009b). Pilling *et al* suggest they isolate the same cell as Phillips *et al* and although some markers and receptors are similar between the two cells (Pilling *et al.*, 2003), an extensive comparison by Curnow *et al* suggests otherwise (Curnow *et al.*, 2010).

Phillips *et al* define fibrocytes as a circulating cell type but Pilling *et al* suggests that fibrocytes only appear in culture or in tissue, under low serum conditions, from a circulating monocyte precursor. Fibrocytes occurring in physiological conditions will most likely arise in an environment with serum, and for this reason we have focused on isolating cells obtained via the more established method of isolation by Bucala and then modified by Phillips *et al.* One component of serum thought responsible for inhibiting monocyte differentiation to fibrocytes was identified as serum amyloid protein (SAP) (Pilling *et al.*, 2003).

Importantly, recent work by Curnow *et al* suggests that different methods of isolation can result in inherently different populations of fibrocyte-like cells (Curnow *et al.*, 2010). This has been validated by work on isolated splenic fibrocytes which highlights unique features compared to other fibrocytes (Crawford *et al.*, 2010, Kisseleva *et al.*, 2011), and validates the hypothesis that fibrocytes differentiate according to their microenvironment.

It is important to phenotype and better understand the nature and functions of HSC-derived fibrocytes so measures can be taken to identify and exclude these cells from isolated MSC populations used therapeutically. Furthermore, although much of the existing research has utilised fibrocytes isolated from blood or from fibrotic organs, there is a distinct lack of convincing data showing the existence of fibrocytes in bone marrow or human diseased livers. In addition to this there is controversy in the literature regarding optimal culture and isolation procedures for fibrocytes.

Based on the current literature we hypothesise that fibrocytes can be isolated from blood using negative selection and plastic adherence. However the groups that have been able to do this reproducibly are limited and use only specific methods of phenotyping. It is also well documented that isolation is difficult and inconsistent among donors. Phenotyping of fibrocytes is also unresolved and for this reason we assume that isolation of fibrocytes will have its difficulties, including low cell number, donor variation and reproducibility among antibodies. Secondly there has been a lack of literature regarding presence of fibrocytes in human livers and I predict that fibrocyte presence may be mediated by a lack of serum amyloid protein (SAP) as has been shown in the lungs.

The aims of this chapter are:

- (i) To determine whether SAP may have a role in their occurrence in patients with liver disease, and to measure circulating SAP levels in patient serum
- (ii) To optimise protocols for isolation of fibrocytes from whole blood
- (iii) To address whether fibrocytes exist in circulation or are an artefact of culture conditions which can be manipulated to enhance their isolation.
- (iv) To identify whether fibrocytes are present in explanted cirrhotic livers

## 5.2 Results

### 5.2.1 Murine liver injury results in increased levels of Serum Amyloid Protein (SAP) levels in liver and serum.

SAP has been identified as a factor present in serum which may be responsible for inhibition of fibrocyte differentiation from monocytes in tissue. We measured levels of SAP in normal and patient serum by ELISA and showed no significant differences in serum from ALD patients ( $0.36 \pm 0.06$  ng/ml) compared with normal patients ( $0.2 \pm 0.01$  ng/ml) (Figure 5.2A). However there were significantly higher levels of SAP in serum from mice injured with carbon tetrachloride for 8 weeks ( $0.13 \pm 0.004$  ng/ml) compared with baseline uninjured SAP levels ( $0.03 \pm 0.005$  ng/ml) using ELISA (Figure 5.2B) ( $p < 0.0001$ ). In support of this, Western blot assays, confirmed mouse SAP levels in serum significantly increased  $2.02 \pm 0.35$  fold upon injury (Figure 5.2C) ( $p < 0.05$ ). Again, there was no significant difference in SAP level between human normal and ALD serum, (Figure 5.2D).

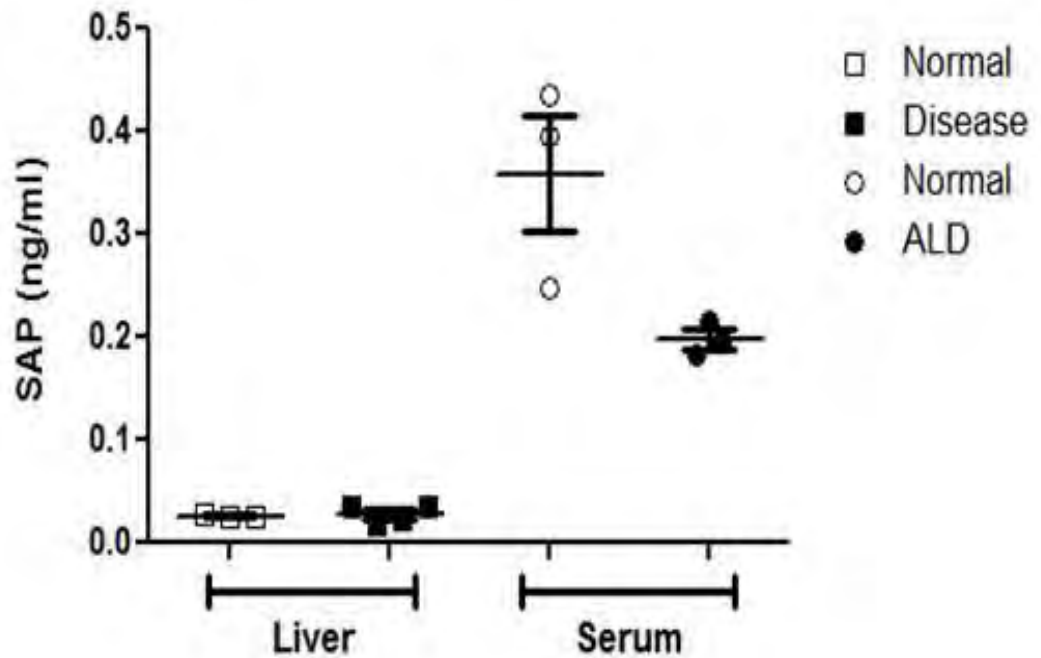
If whole liver lysates were analysed, no significant difference in SAP levels was observed in livers of humans and mice with or without liver injury using ELISA (Figure 5.2A, 5.2B and 5.2E). Human liver lysates were also measured for SAP levels using Western blot and showed significantly higher ( $149.2 \pm 49.9$  fold) levels in human diseased livers compared to normal human livers (Figure 5.2F) ( $p < 0.05$ ).



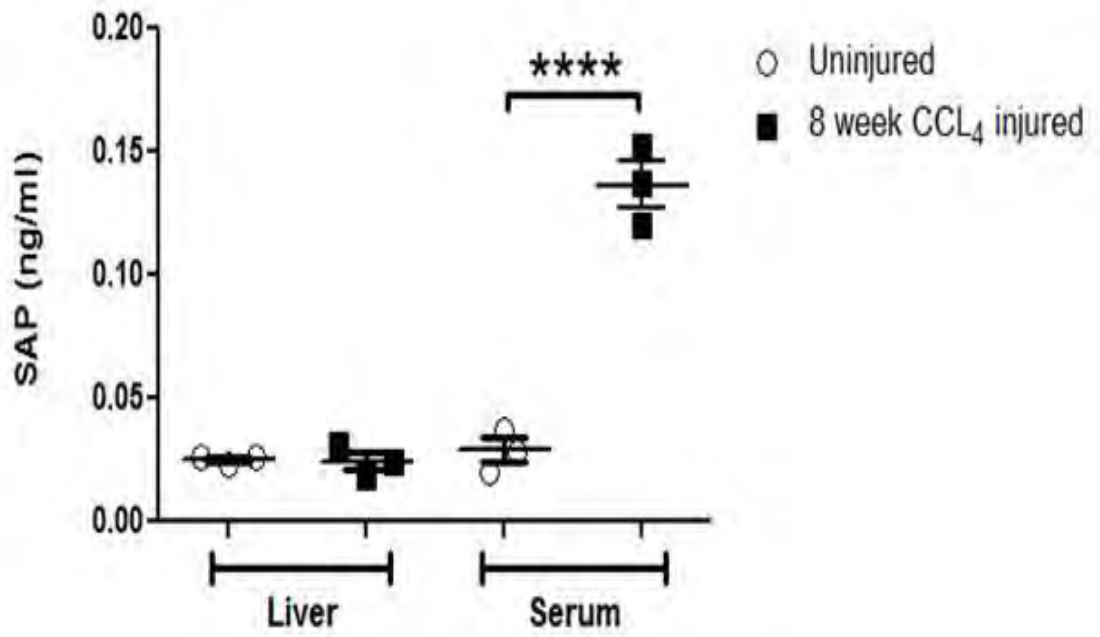
**Figure 5.2: SAP levels in serum and liver during liver injury.**

A: Sandwich ELISA to measure levels of SAP in normal human serum and serum from patients with end stage ALD liver cirrhosis. SAP levels in liver lysates of normal and other disease livers. B: Sandwich ELISA to measure levels of SAP in uninjured C57BL/6 mice serum and liver lysates, compared with 8 week carbon-tetrachloride injured C57BL/6 mice. Data represent SAP levels as mean  $\pm$  SEM in n=3 donors, \*\*\*\*, p<0.0001. C: Representative images of Western blot from 3 different donors to measure SAP levels in serum of uninjured and 8 week injured carbon tetrachloride injured mice, alongside a GAPDH endogenous control with quantification by densitometric analysis of replicate blots of mouse serum. D: Representative images of Western blot from 3 different donors to measure SAP levels in serum of normal and ALD patients alongside a GAPDH endogenous control with corresponding densitometric analysis of replicate blots of human serum. E: Representative images of Western blot and densitometric analysis from 3 different donors to measure SAP levels in liver lysates of uninjured and 8 week injured carbon tetrachloride injured mice, alongside a GAPDH endogenous control. F: Representative images of Western blot with corresponding densitometry from 3 different donors to measure SAP levels in liver lysates from normal and disease livers, alongside a GAPDH endogenous control. In all experiments data represent mean  $\pm$  SEM of relative intensity of at least n=3 donors compared to expression in normal/uninjured donors, \*, p<0.05.

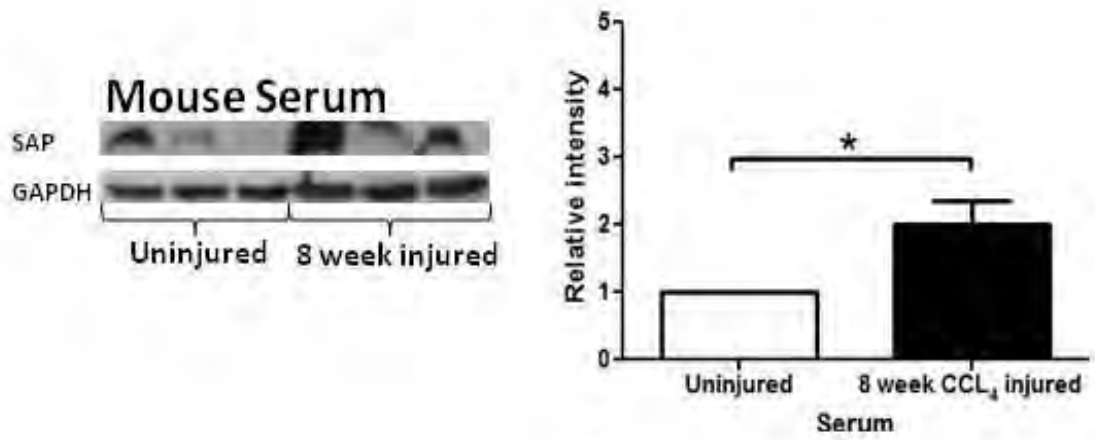
A



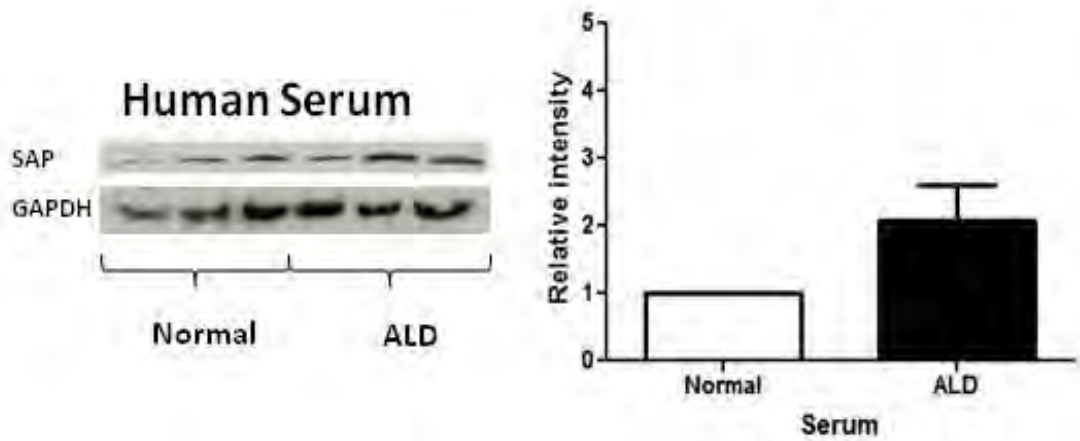
B



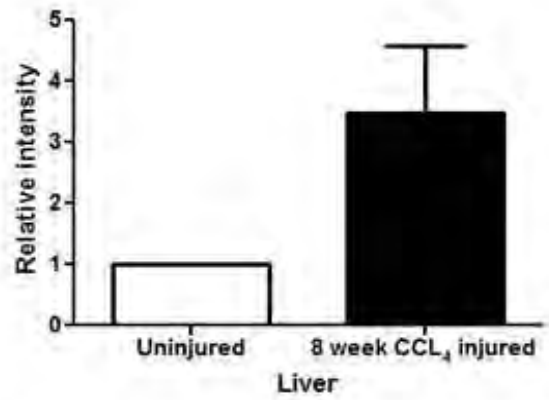
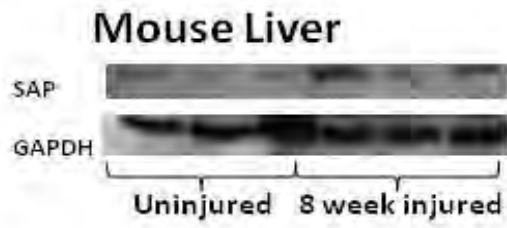
C



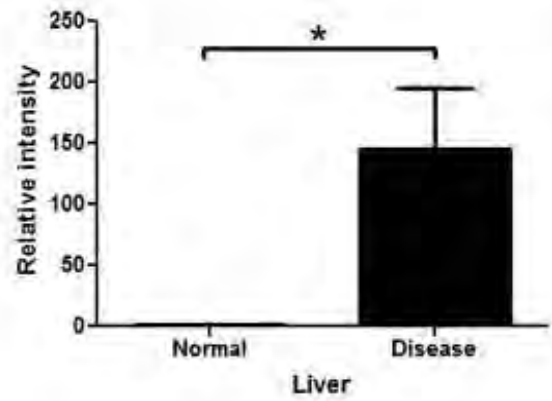
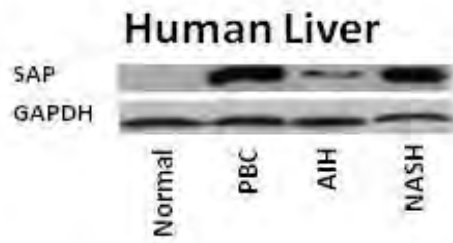
D



E



F

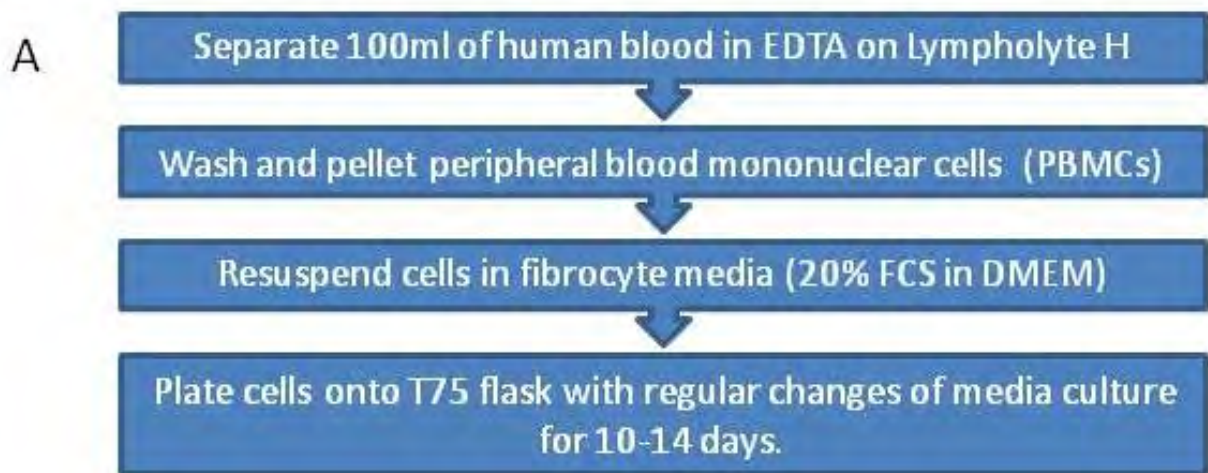


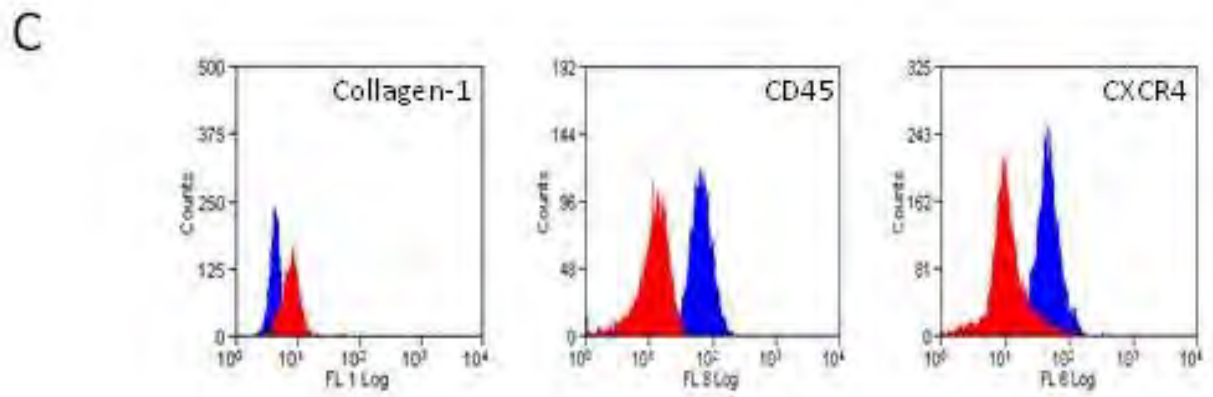
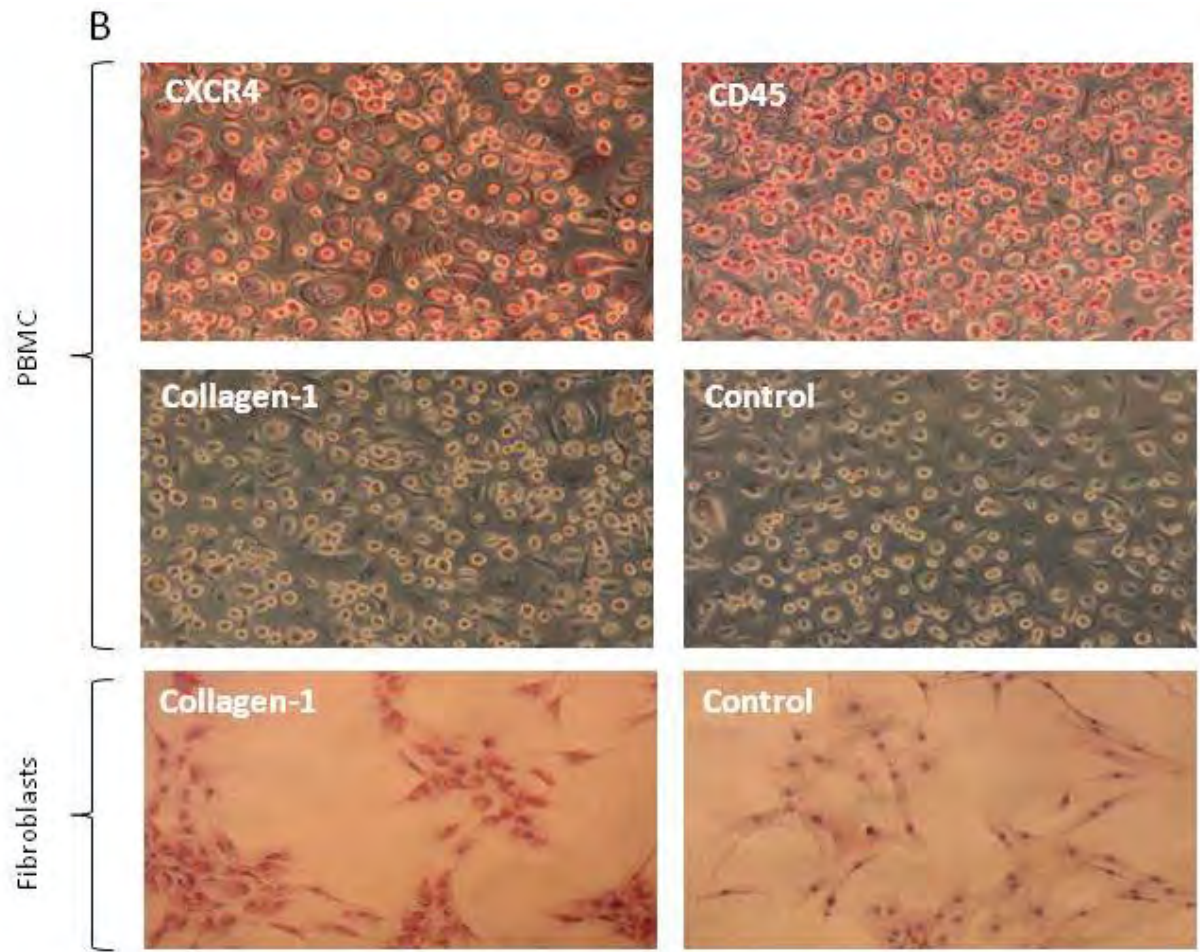
### **5.2.2 PBMC isolated from peripheral blood separated on Lympholyte-H gradient and grown on tissue culture plastic do not express a fibrocyte phenotype.**

PBMC were isolated using a standard leukocyte isolation method (Figure 5.3A) with separation on a Lympholyte-H gradient and cultured on tissue culture plastic in medium containing serum and therefore, SAP. Adherent cells were grown in culture for 10-14 days with regular media changes. Resulting cells were uniformly circular in appearance. Cells were tested for presence of the fibrocyte markers, CXCR4, CD45, collagen-1 and  $\alpha$ SMA using immunohistochemistry. Cells expressed high levels of CD45 and CXCR4, but no collagen-1 (Figure 5.3B) in contrast to positive control fibroblasts. These results were validated by flow cytometry, as shown in representative histograms, indicating an absence of collagen-1 but a distinct presence of CD45 and CXCR4 on these cells (Figure 5.3C).

**Figure 5.3:PBMC isolated from peripheral blood on Lympholyte-H.**

A: Protocol for isolation of human fibrocytes via a standard human PBMC isolation procedure using Lympholyte-H. B: Representative images at x20 magnification of Nova red immunohistochemical staining of isolated PBMC for fibrocyte markers. Images are representative from staining of cells from 3 different blood donors. C: Representative cytometry histograms showing isotype matched controls (red peak) and antibody labelled cells (blue peak) for cultured PBMC from 3 different donors for fibrocyte markers.



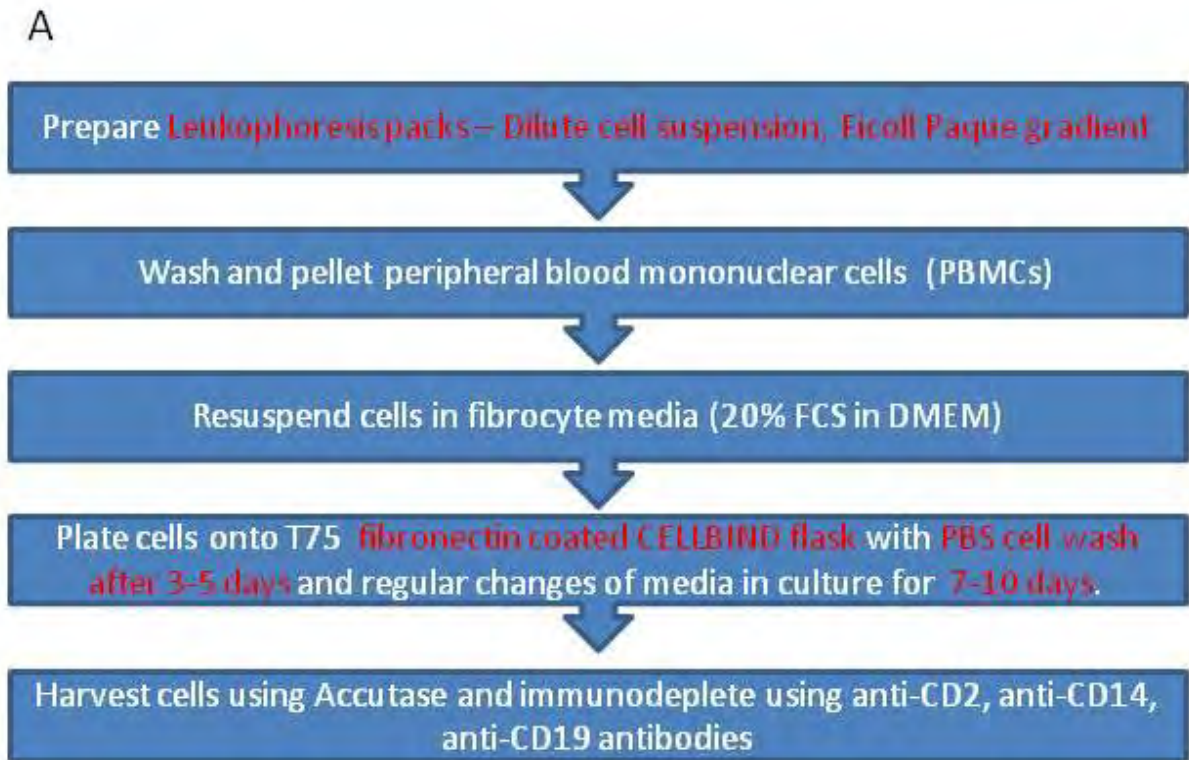


**5.2.3 PBMC isolated from peripheral blood separated on Ficoll-Paque gradient and grown on fibronectin coated Cell Bind tissue culture plastic vary between donors and on occasion small numbers of cells with a fibrocyte phenotype can be detected.**

PBMC were isolated according to a different, more reproducible, method which involved separation on a Ficoll-Paque gradient, and culture on fibronectin coated 'Cell Bind' tissue culture plastic in media containing serum (Figure 5.4A). The original published protocol suggested use of a high concentration of PBMC in the form of Leukopheresis packs, but a lack of a regular supply of this cell source meant we had to use large volumes of blood instead. Preparations using this method were inconsistent both in terms of cell number and morphology, from different donors (Figure 5.4B). Cells were detached using long incubations with Accutase and contaminating cells were removed using beads conjugated to anti-CD2, anti-CD14 and anti-CD19 antibodies. The resulting cell suspension was cytopun onto slides and stained for fibrocyte markers CD45 and collagen-1. Cells were strongly positive for CD45 expression, but contained only small numbers which expressed low levels of collagen-1 (Figure 5.4C). Of note this cell population was greatly reduced in cell number after negative selection with even fewer cells which expressed collagen-1 in the predominantly CD45<sup>+</sup> cell population.

**Figure 5.4: PBMC isolated from peripheral blood on Ficoll-Paque.**

A: Protocol for isolation of human fibrocytes using Ficoll-Paque. B: 3 representative images of isolated PBMC at x10 magnification using phase contrast microscopy, from 4 different blood donors. C: Representative images of APAAP immunohistochemical staining of isolated fibrocytes for fibrocyte markers. Images are representative from staining of cells from 3 different blood donors.





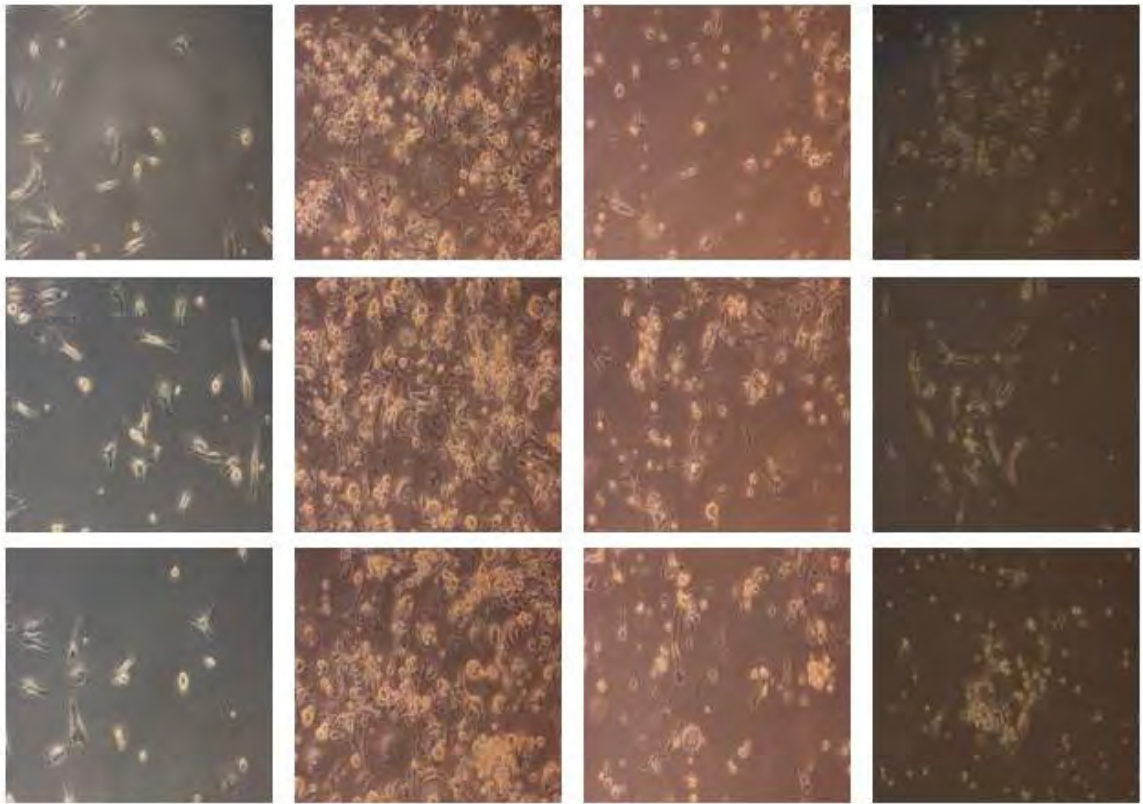
**B**

Donor 1

Donor 2

Donor 3

Donor 4

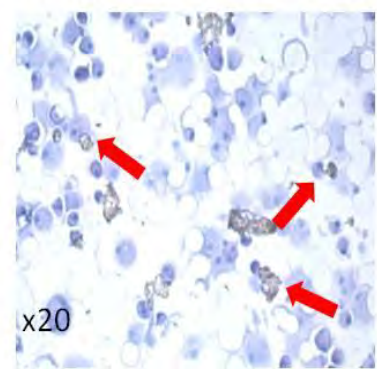
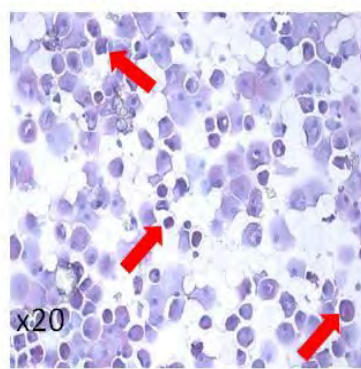
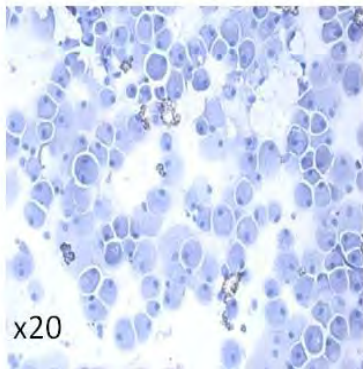
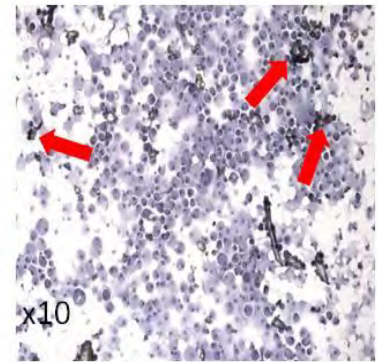
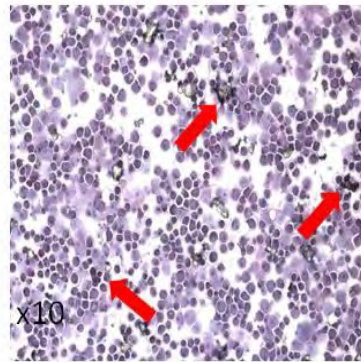
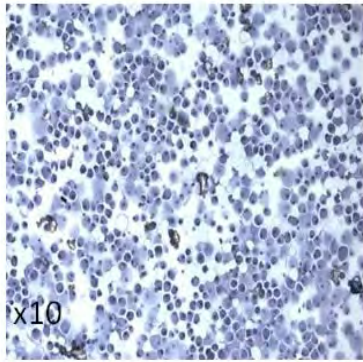


C

Control

CD45

Collagen 1

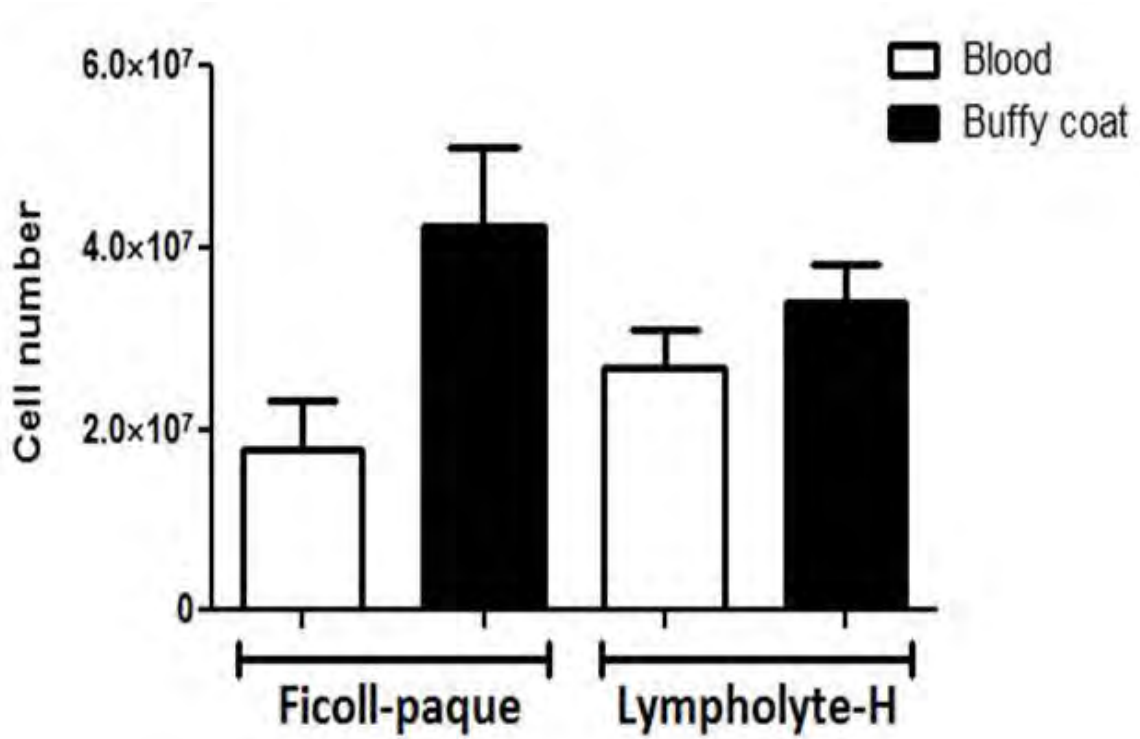


**5.2.4 PBMC isolated directly from blood or pre-prepared buffy coat using Ficoll-Paque or Lympholyte-H show no significant differences in cell number upon isolation.**

Different cell gradient preparations may be more efficient at cell isolation and thus yield a different number of fibrocytes. So we counted the number of cells isolated using Ficoll-Paque ( $1.77 \times 10^7 \pm 5.3 \times 10^6$  cells/ml) and Lympholyte-H ( $2.66 \times 10^7 + 4.26 \times 10^6$  cells/ml) from 500ml peripheral blood. Statistically there was no significant difference in cell number isolated using Ficoll-Paque or Lympholyte-H (Figure 5.5). To try and mimic the high concentration of cells achieved using Leukopheresis packs in some published protocols, we prepared buffy coat suspensions of peripheral blood prior to gradient centrifugation. The buffy coat preparation did show a trend towards an increase in cells recovered from both Lympholyte-H ( $3.38 \times 10^7 + 4.43 \times 10^6$  cells/ml) and Ficoll-Paque ( $4.22 \times 10^7 + 8.93 \times 10^6$  cells/ml) preparations compared to whole blood but the effect was not significant.

**Figure 5.5: Number of PBMC isolated from blood or pre-prepared buffy coat using Ficoll-Paque or Lympholyte-H.**

Human PBMC were prepared from whole blood or buffy coats placed onto indicated gradient preparation. Data is expressed as total cell number. Bars represent mean  $\pm$  SEM of n=4 donor samples.



### **5.2.5 The effect of culture substrate and cell seeding density on morphological appearance.**

As there was no significant difference in the number of cells obtained from either whole blood or buffy coats, we wanted to investigate the effect of using different separation gradients on the types of cells generated after culture based on morphology. Cells isolated using buffy coats and Ficoll-Paque gradients were cultured on fibronectin coated Cell Bind tissue culture plastic according to the protocol in Figure 5.4. Cell source (blood vs. buffy coat) and separation gradient used had no effect on morphology of cells from individual donors. However there was a clear difference between different donors. In the indicated images for example, Donor 2 seemed to yield a higher number of spindle shaped cells (Figure 5.6). However we noted there was a low total number of cells present from all donors after culture on fibronectin coated plastic. For this reason we next used buffy coats separated on Ficoll-Paque and investigated whether total numbers of cells binding and a change in morphology of cells was dependent upon a specific type of culture surface (Figure 5.7). Although again there was a clear difference in the behaviour of cells isolated from different donors, there was no significant difference in the morphology or binding of cells between different substrates. Next, PBMC isolated using buffy coats and Ficoll-Paque gradients were seeded and cultured at higher densities,  $8 \times 10^5$  cells/ml/cm<sup>2</sup> compared to  $6.67 \times 10^5$  cells/ml/cm<sup>2</sup>. The higher culture density seemed to reproducibly enhance binding of cells to tissue culture plastic and increase the number of spindle shaped cells in the final culture (Figure 5.8).

**Figure 5.6: PBMC isolated from blood or pre-prepared buffy coat using Ficoll-Paque or Lympholyte-H cultured on fibronectin coated Cell Bind tissue culture plastic.**

Representative images of human PBMC. Images were taken at x10 magnification using phase contrast microscopy, from 4 different blood donors.

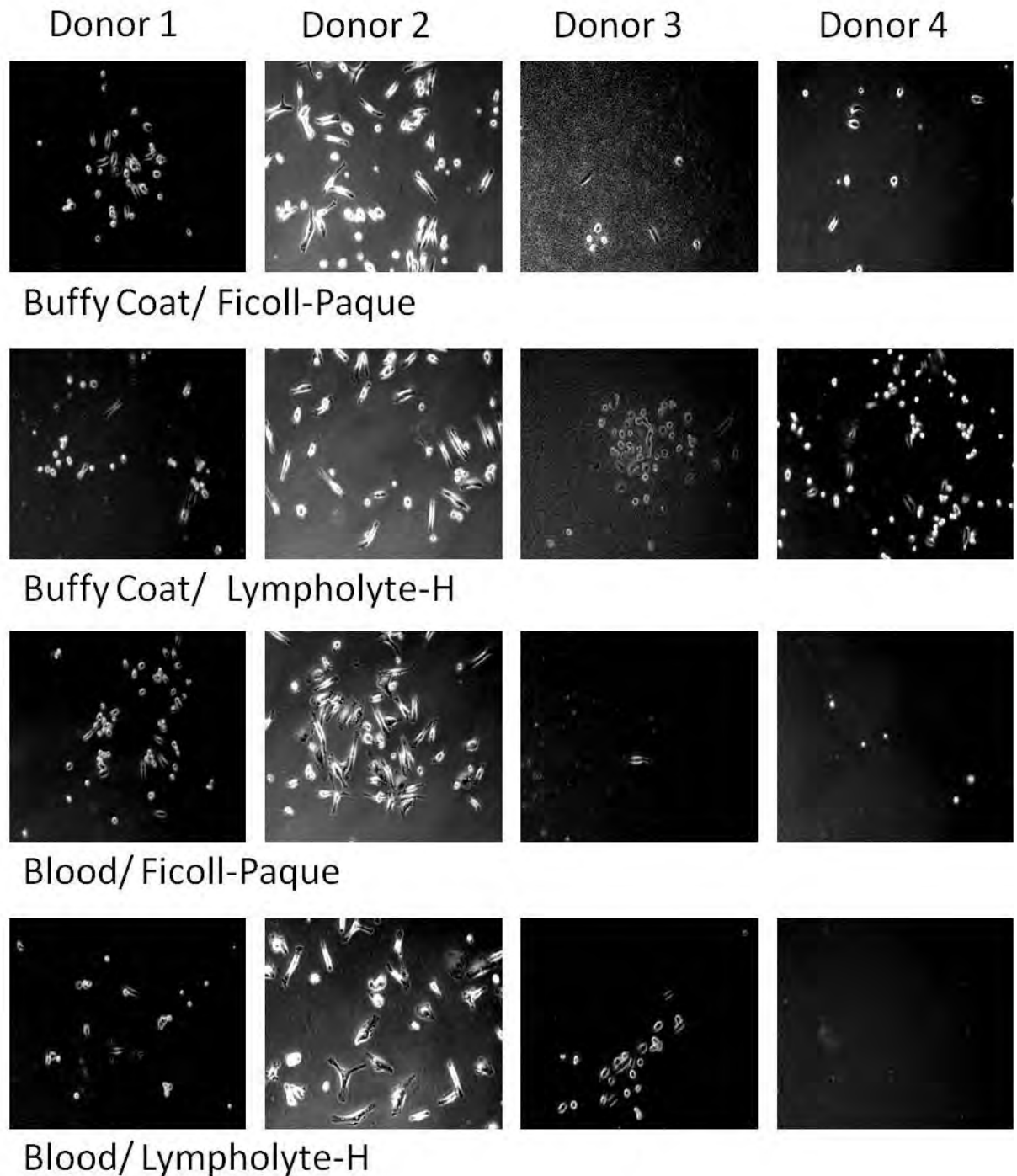


**Figure 5.7: PBMC isolated from buffy coat using Ficoll-Paque cultured on fibronectin, Cell Bind tissue culture plastic, or tissue culture plastic.**

Representative images of human PBMC isolated from buffy coat with Ficoll-Paque and cultured on Fibronectin coated Cell Bind, Cell Bind alone, fibronectin alone or untreated tissue culture plastic as indicated. Images were taken at x10 magnification using phase contrast microscopy, from 4 different blood donors.

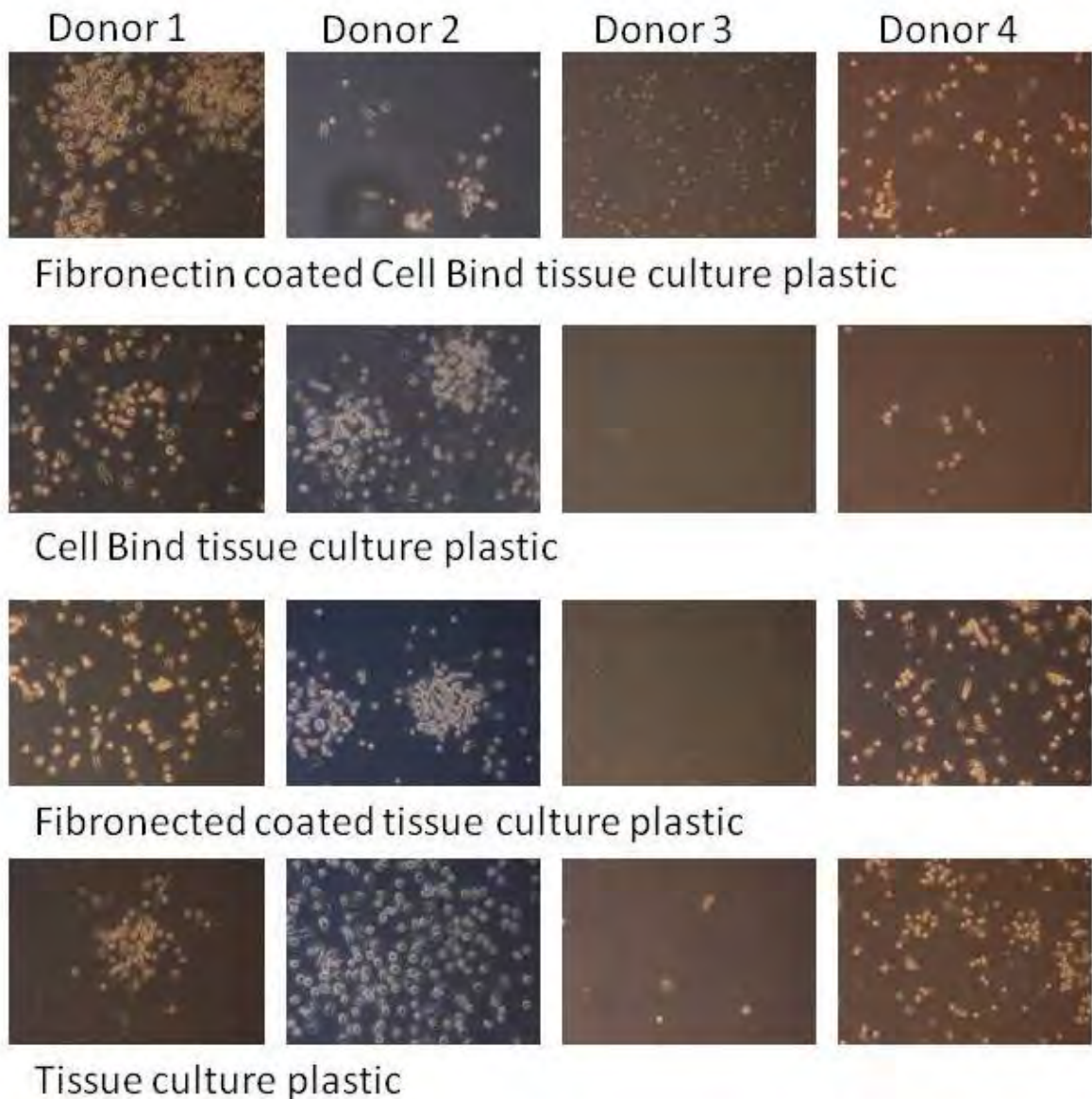
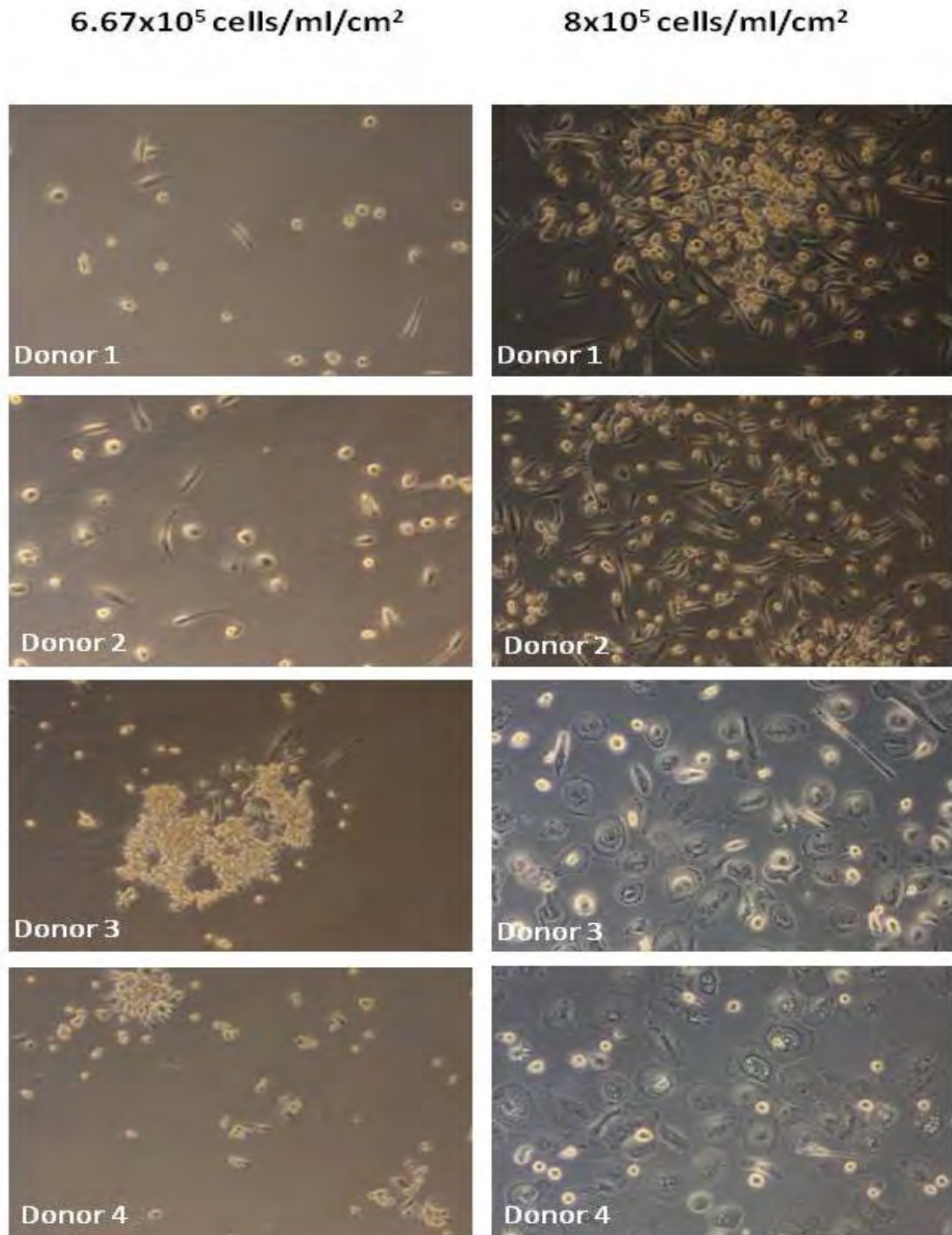


**Figure 5.8: PBMC isolated from buffy coat using Ficoll-Paque cultured on tissue culture plastic at low and high cell densities.**

Representative images of isolated human PBMC cultured at low density ( $6.67 \times 10^7$  cells/ml/cm<sup>2</sup>) and high density ( $8 \times 10^5$  cells/ml/cm<sup>2</sup>) at x10 magnification using phase contrast microscopy, from 4 different blood donors.





### **5.2.6 Significantly higher numbers of fibrocyte-like spindle shaped cells are observed when PBMC are cultured on tissue culture plastic.**

Next we specifically determined the effects of cell processing and culture on the numbers of cells which exhibited fibrocyte-like morphology (as opposed to total cell yields). Spindle shaped cells (Figure 5.9A) resembling a fibrocyte morphology were counted in PBMC cultures after isolation from blood or buffy coat and separation on a Lympholyte-H or Ficoll-Paque gradient as before.

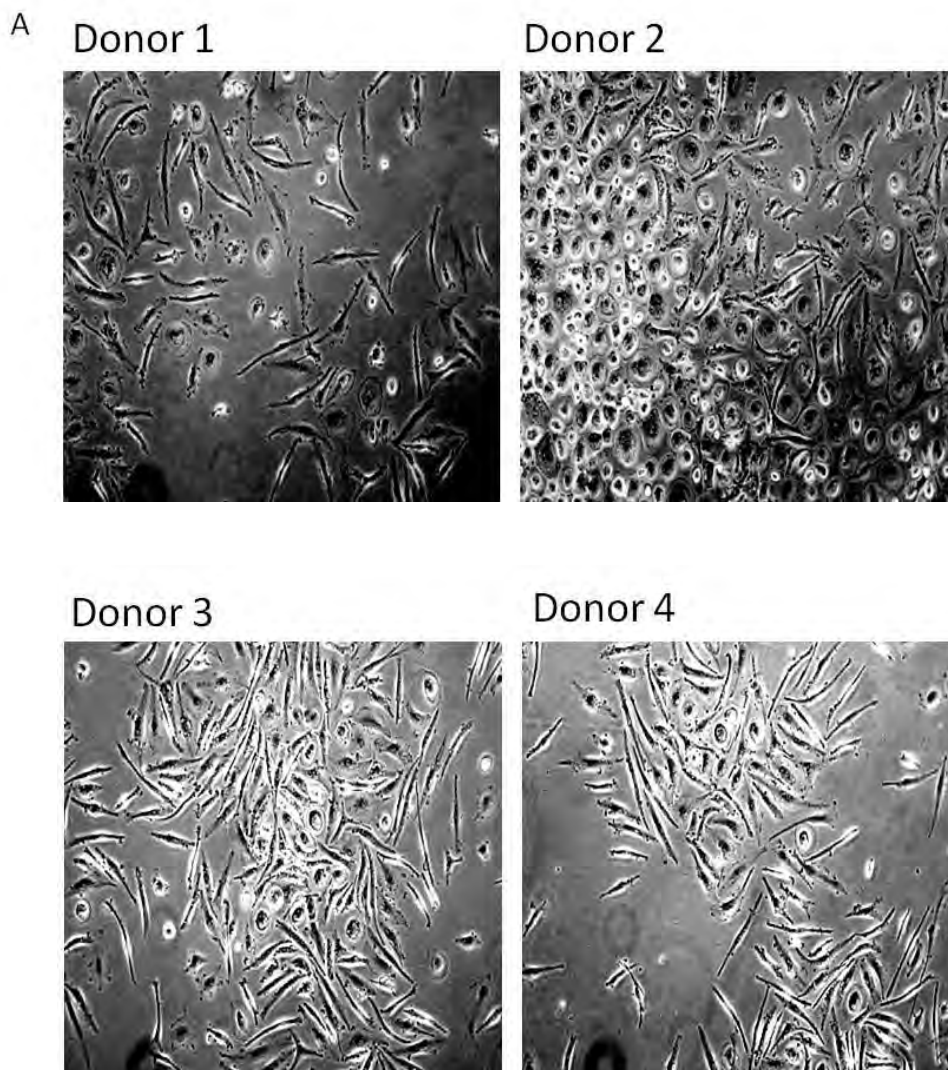
Figure 5.9B shows that there was no significant difference between number of spindle shaped cells due to the cell source or the gradient used to isolate PBMC. However, on normal tissue culture plastic, PBMC isolated from blood using Ficoll-Paque and Lympholyte-H yielded  $19.4 \pm 4.08$  cells/ field of view and  $20.07 \pm 1.85$  cells/ field of view respectively. This was the highest yield of any of the culture substrates, in contrast, PBMC isolated from buffy coat using Ficoll-Paque yielded  $12 \pm 1.69$  cells/field of view and Lympholyte-H,  $13.27 \pm 1.67$  cells/field of view. On fibronectin coated normal tissue culture plastic, Cell Bind tissue culture plastic and fibronectin coated Cell Bind tissue culture plastic, PBMC isolated from blood or buffy coat using Ficoll-Paque and Lympholyte-H yielded a similar low number of cells.

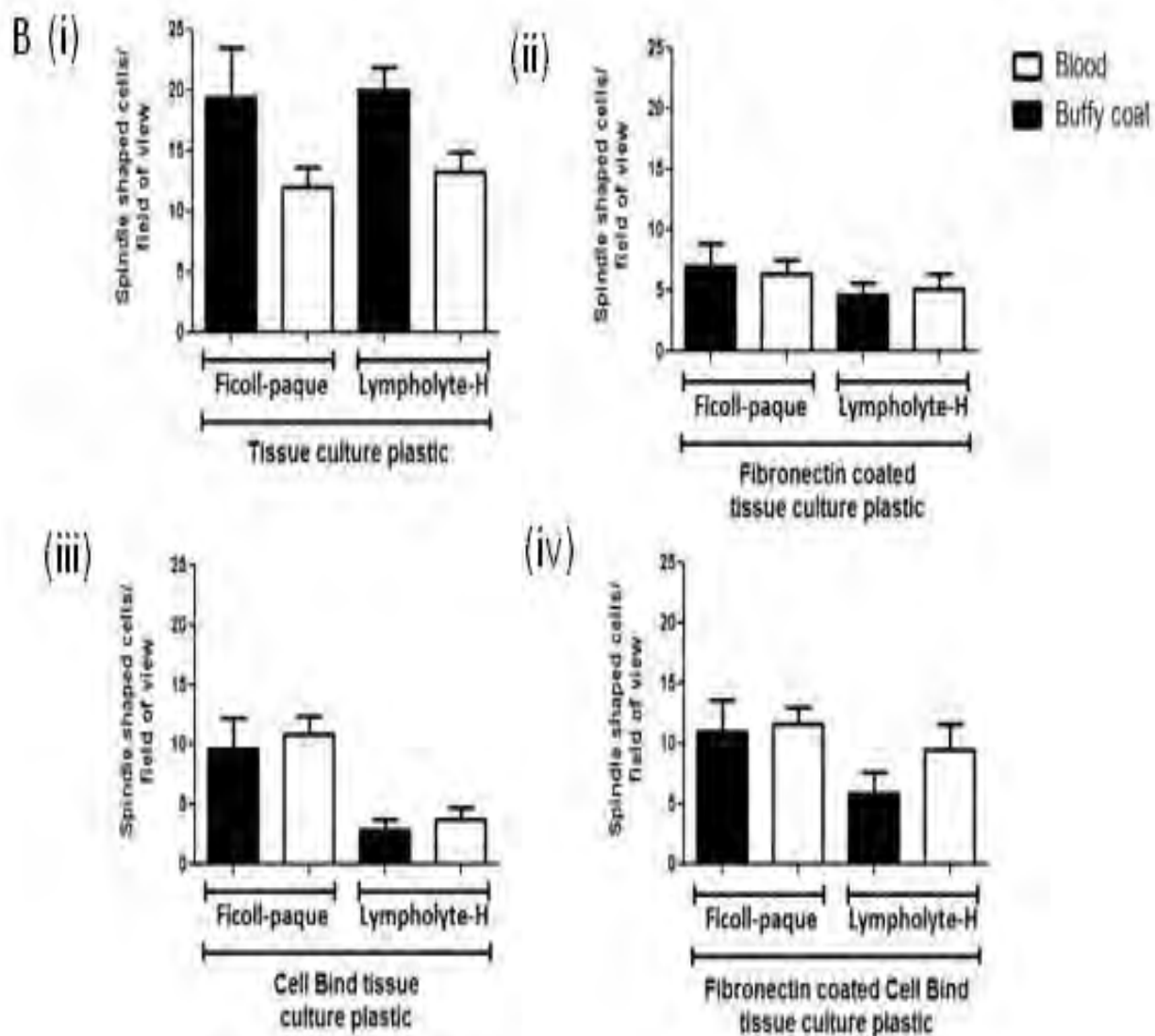
If the same data is compared based on the culture surface used (Figure 5.9C), rather than separation gradient (Figure 5.9C), it seems that PBMC isolated from blood separated on Ficoll-Paque, and seeded on normal tissue culture plastic yielded significantly higher numbers of spindle shaped cells,  $19.4 \pm 4.08$  cells/ field of view than on a fibronectin coated surface,  $7.07 \pm 1.9$  cells/ field of view. PBMC isolated from buffy coat separated on Ficoll-Paque, and

seeded on normal or fibronectin coated tissue culture plastic yielded  $20.07 \pm 1.85$  cells/ field of view and  $4.67 \pm 1.01$  cells/ field of view respectively. PBMC seeded on normal or fibronectin coated Cell Bind tissue culture plastic yielded  $2.93 \pm 0.78$  cells/field of view and  $5.87 \pm 1.83$  cells/ field of view respectively. PBMC isolated from blood separated on Lympholyte-H, and seeded on normal tissue culture plastic yielded  $12 \pm 1.69$  cells/ field of view, significantly higher, than any other surface. A similar effect is repeated in other isolations suggesting that a significantly higher number of spindle shaped PBMC are observed when cultured on normal tissue culture plastic compared to culture on any other type of surface (Figure 5.9C).

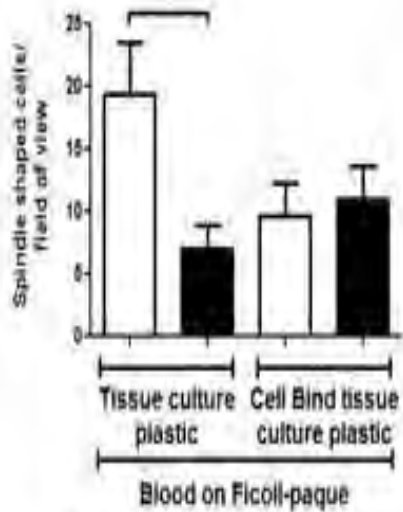
**Figure 5.9: Number of spindle shaped cells arising from PBMC isolated from blood or buffy coat using Ficoll-Paque or Lympholyte-H cultured on fibronectin, Cell Bind tissue culture plastic, or tissue culture plastic.**

A: Representative images of spindle shaped cells amongst human PBMC in culture. Images were taken at x10 magnification using phase contrast microscopy, from 4 different blood donors. B: Comparison of effect of cell source (blood or buffy coat) and separation gradient (Lympholyte-H and Ficoll-Paque) on occurrence of spindle shaped, fibrocyte-like cell numbers of among PBMC after culture on (i) tissue culture plastic, (ii) fibronectin coated tissue culture plastic, (iii) Cell Bind tissue culture plastic, and (iv) fibronectin coated tissue culture plastic. Bars represent mean  $\pm$  SEM of n=4 donor samples. C: Comparison of effect of tissue culture plastic (normal or Cell Bind) and surface matrix (none and fibronectin) on occurrence of spindle shaped, fibrocyte-like cell numbers of among PBMC after isolation from (i) blood on Ficoll-Paque (ii) blood on Lympholyte-H, (iii) buffy coat on Ficoll-Paque, and (iv) buffy coat on Lympholyte-H. Bars represent mean  $\pm$  SEM of n=4 donor samples, \*, p < 0.05; \*\*, p < 0.01; \*\*\*, p < 0.001; \*\*\*\*, p < 0.0001.

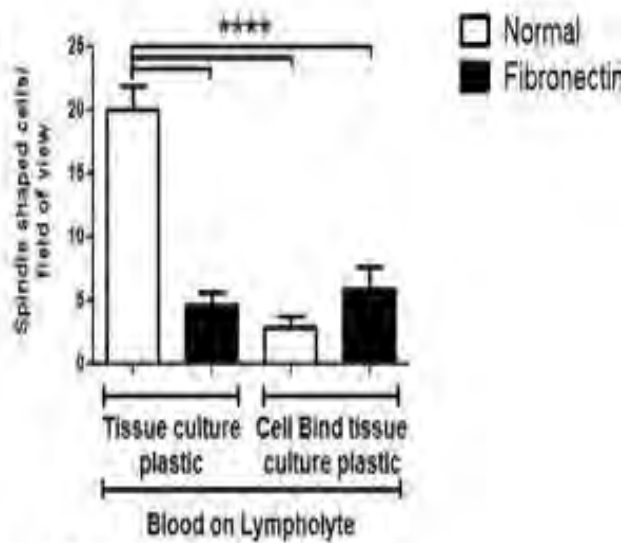




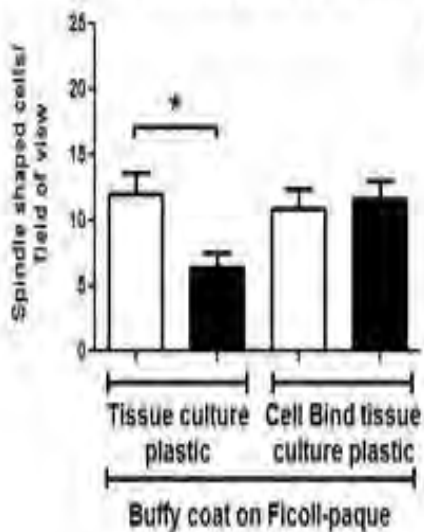
C (i)



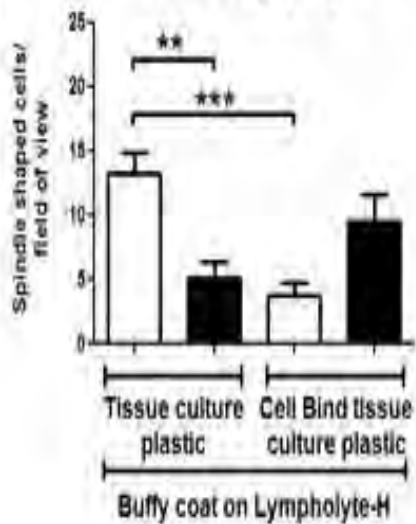
(ii)



(iii)



(iv)



### **5.2.7 Improvement in yield of fibrocytes using collagen-coated plastic and pre-selection of cells**

Since diverse extracellular matrix molecules including collagen are upregulated during fibrosis, we used collagen and fibronectin-coated plastic ware in culture experiments. Fibronectin has inconsistent effects on numbers of spindle shaped cells evident in culture (see images from donor 2 vs. others (Figure 5.10)). However use of collagen-coated tissue culture plastic seemed to consistently result in more fibrocyte shaped cells arising in culture (Figure 5.10). Again the different donors seem to have varying capabilities in forming fibrocyte like spindle shaped cells. Next we used unselected monocytes isolated from PBMC by allowing them to adhere to tissue culture plastic for 2 hours and washing off any remaining unbound cells, including lymphocytes. Over 2 weeks these cells acquired varying phenotypes on tissue culture plastic with a small proportion acquiring a fibrocyte like morphology. With these cells again, use of collagen coated plastic, increased the number of spindle shaped cells evident in culture (Figure 5.11). Finally we used positively selected CD14<sup>+</sup> cells as our source of fibrocytes. Here, spindle shaped fibrocyte-like cells seem to occur at high numbers among isolated CD14<sup>+</sup> cells but in contrast to unselected cells, use of matrix components during cell culture appeared to inhibit this process (Figure 5.12). If the non-adherent cells including lymphocytes were collected from adherent PBMC after 2 hours and plated on normal, fibronectin coated and collagen coated tissue culture plastic, these PBMC acquired a spindle shaped fibrocyte like appearance, significantly surpassing any number of spindle shaped cells seen before with any other isolation (Figure 5.13). This effect occurred in all conditions consistently among all 3 donors.

**Figure 5.10: PBMC cultured on normal, fibronectin coated and collagen coated tissue culture plastic.**

Representative images of human PBMC isolated from buffy coat with Ficoll-Paque and cultured on A: normal tissue culture plastic; B: fibronectin; or C: collagen coated tissue culture plastic. Images were taken at x10 magnification using phase contrast microscopy, from 3 different blood donors.

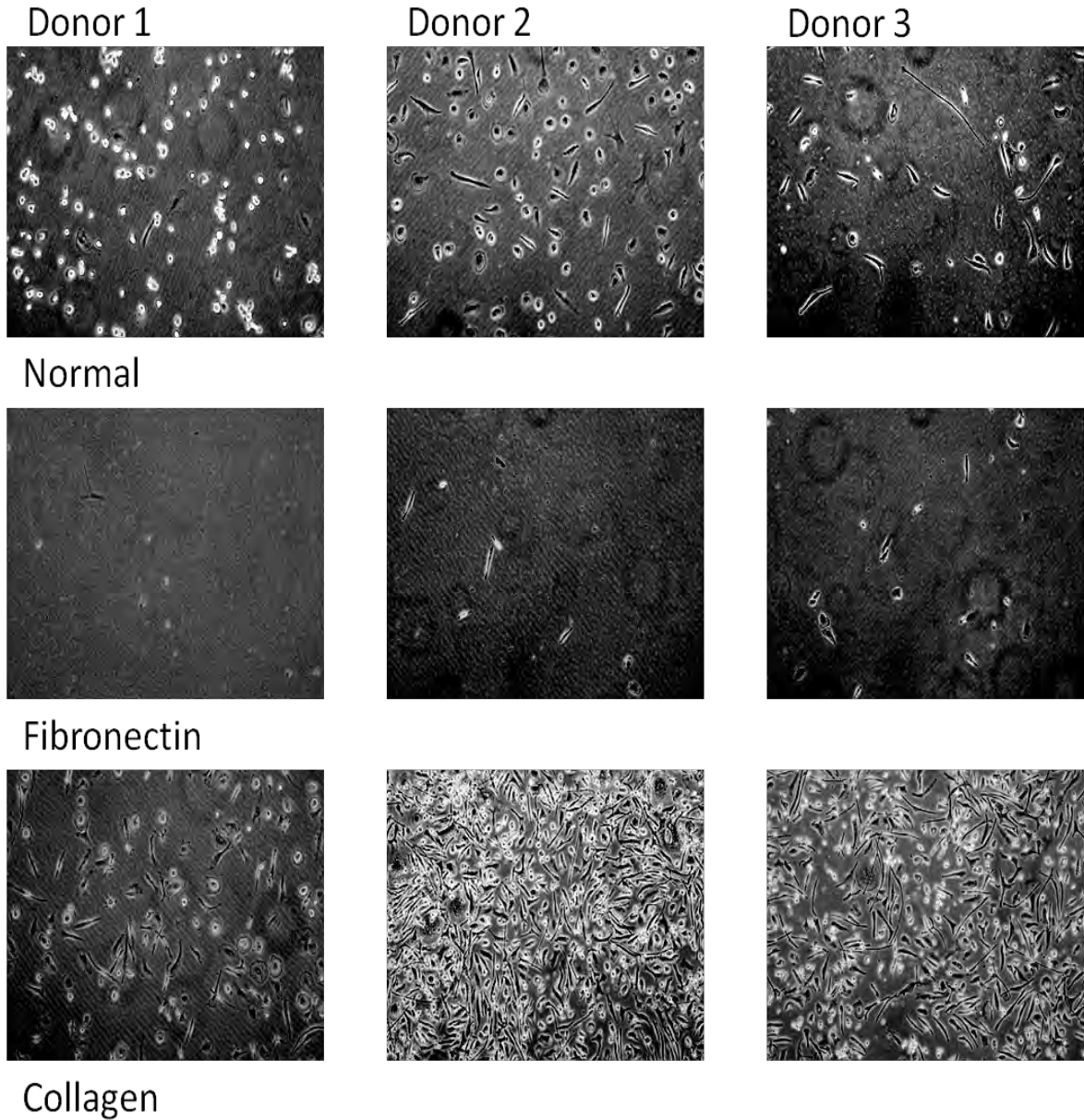


**Figure 5.11: Adherent PBMC cultured on normal, fibronectin coated and collagen coated tissue culture plastic.**

Representative images of adherent PBMC isolated from buffy coat with Ficoll-Paque and cultured on A: tissue culture plastic; B: fibronectin; or C: collagen coated tissue culture plastic. Images were taken at x10 magnification using phase contrast microscopy, from 3 different blood donors.

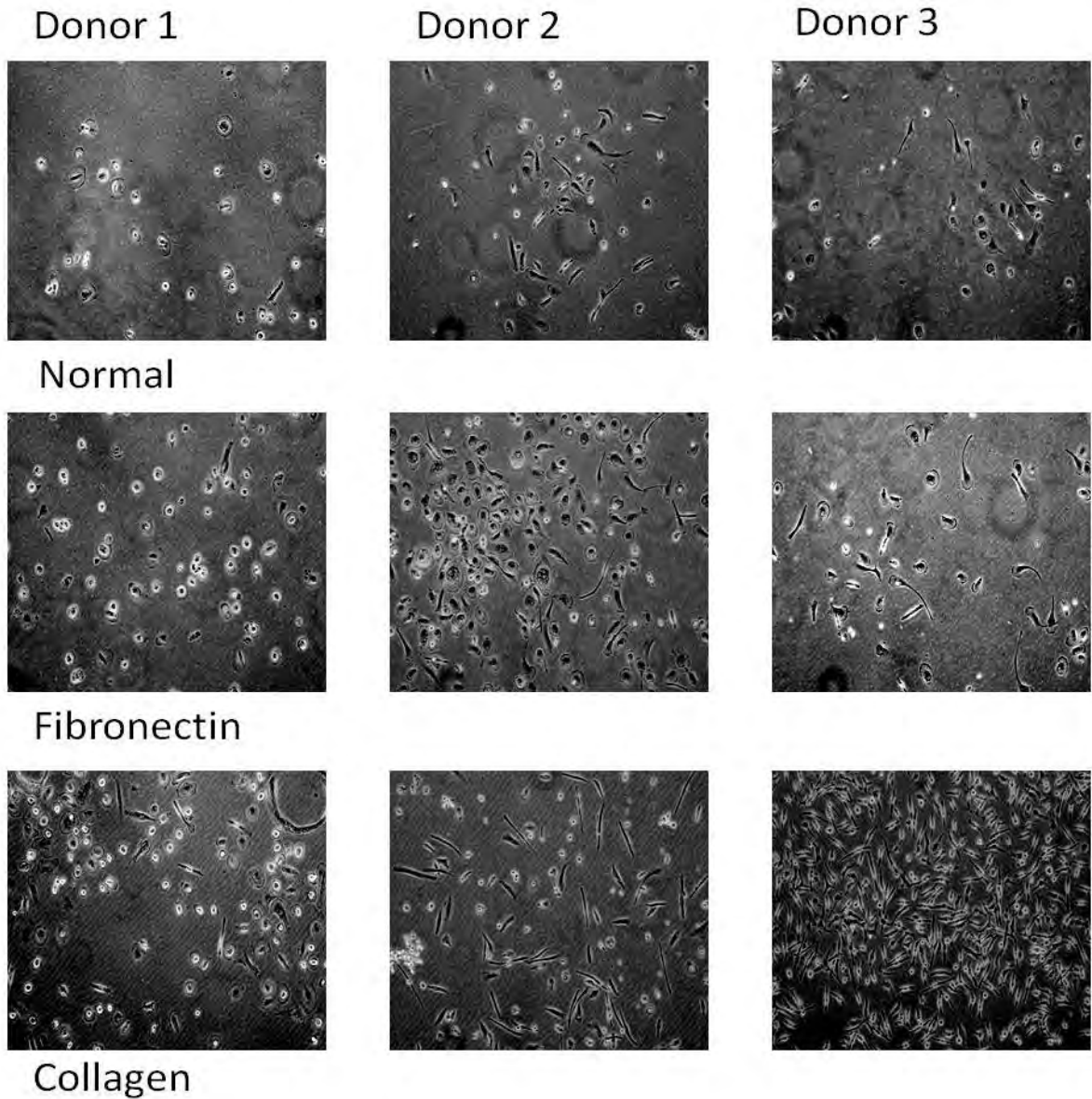




**Figure 5.12: CD14<sup>+</sup> and CD14<sup>-</sup> PBMC cultured on normal, fibronectin coated and collagen coated tissue culture plastic.**

A: Representative images of human CD14<sup>-</sup> PBMC isolated from buffy coat with Ficoll-Paque and cultured on tissue culture plastic. Representative images of CD14<sup>+</sup> bead selected PBMC isolated from buffy coat with Ficoll-Paque and cultured on B: normal tissue culture plastic; C: fibronectin; or D: collagen coated tissue culture plastic. Images were taken at x10 magnification using phase contrast microscopy, from 3 different blood donors.

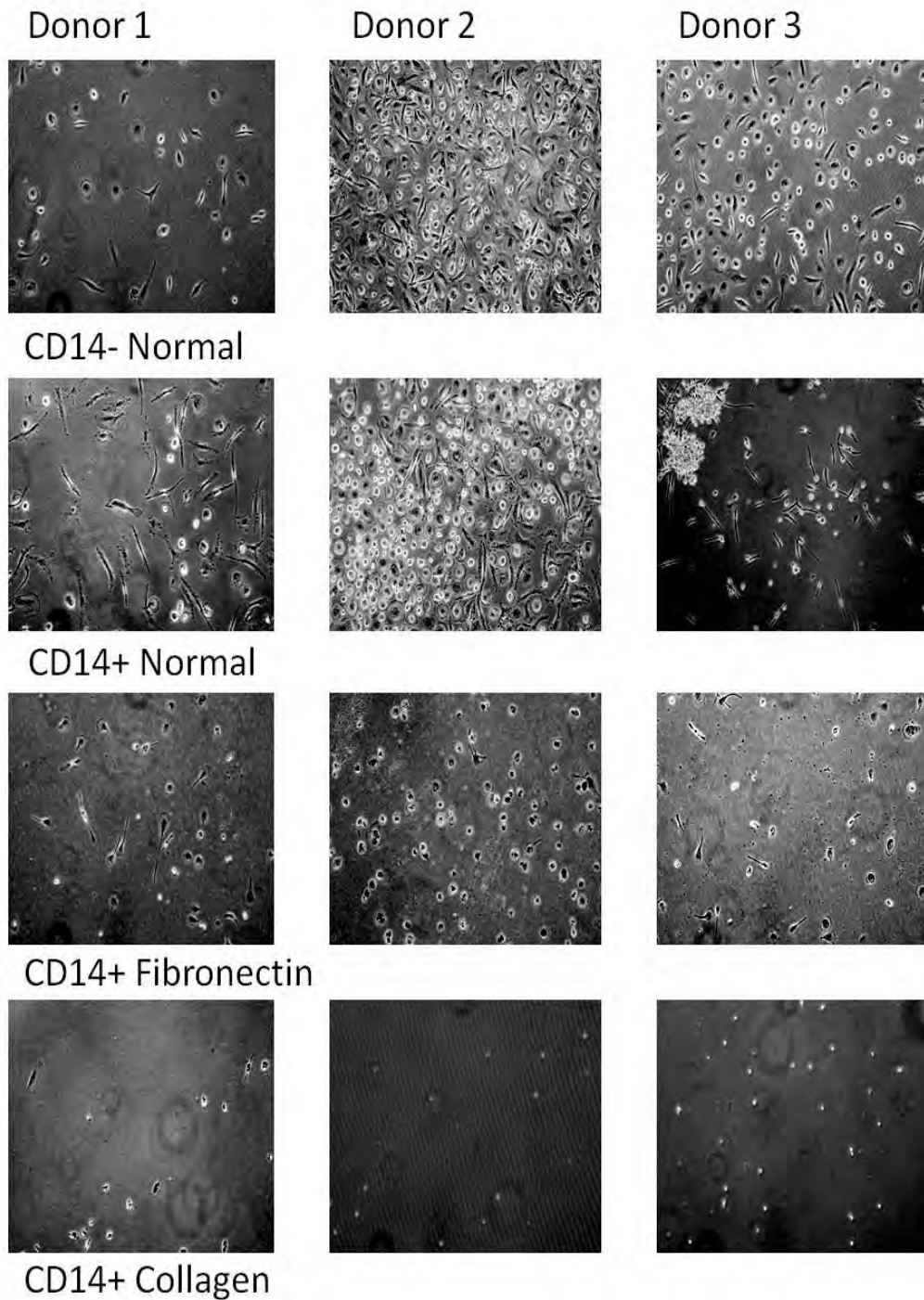
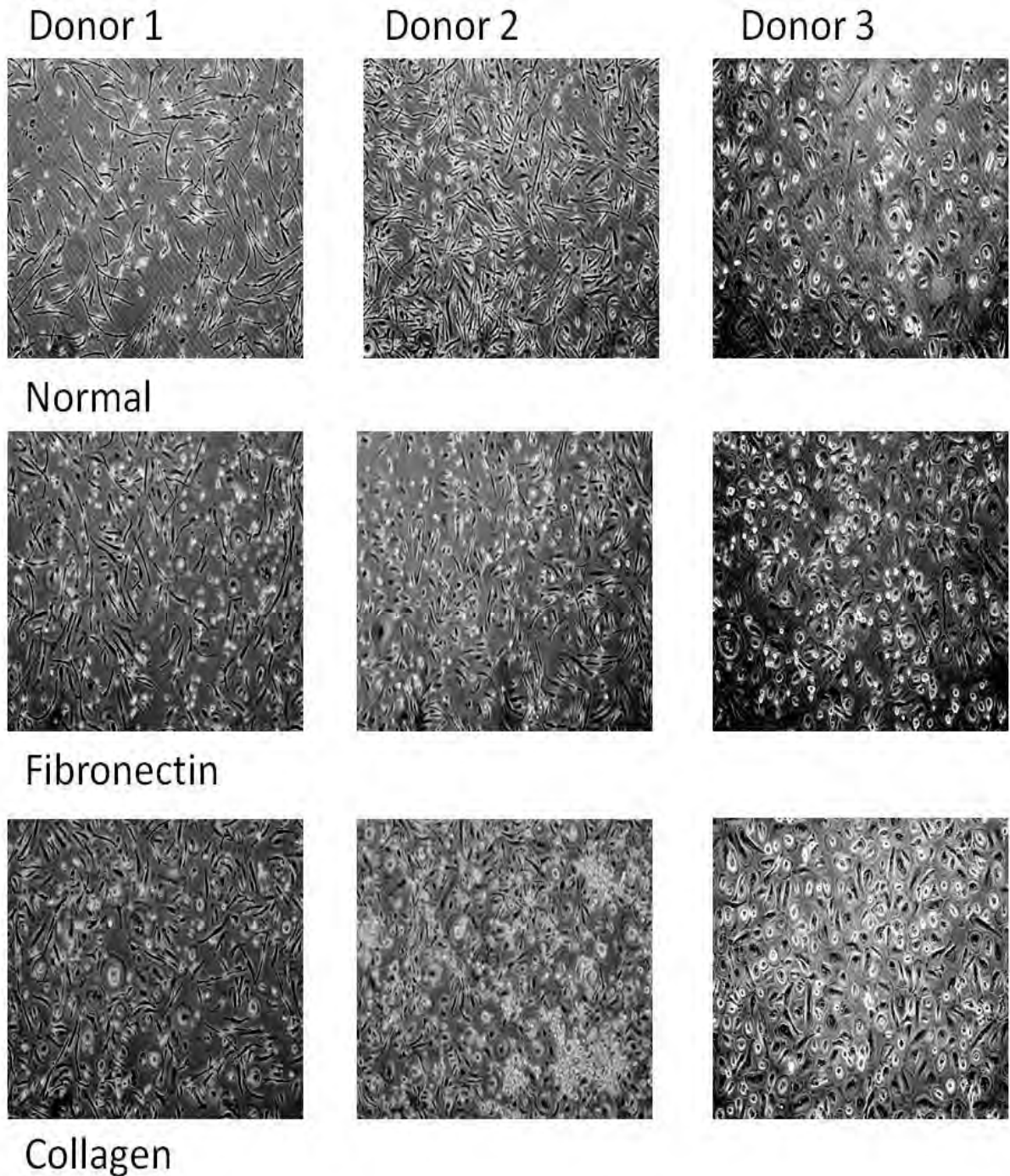


**Figure 5.13: Non adherent PBMC cultured on normal, fibronectin coated and collagen coated tissue culture plastic.**

Representative images of non adherent human PBMC isolated from buffy coat with Ficoll-Paque and cultured on A: tissue culture plastic; B: fibronectin; or C: collagen coated tissue culture plastic. Images were taken at x10 magnification using phase contrast microscopy, from 3 different blood donors.



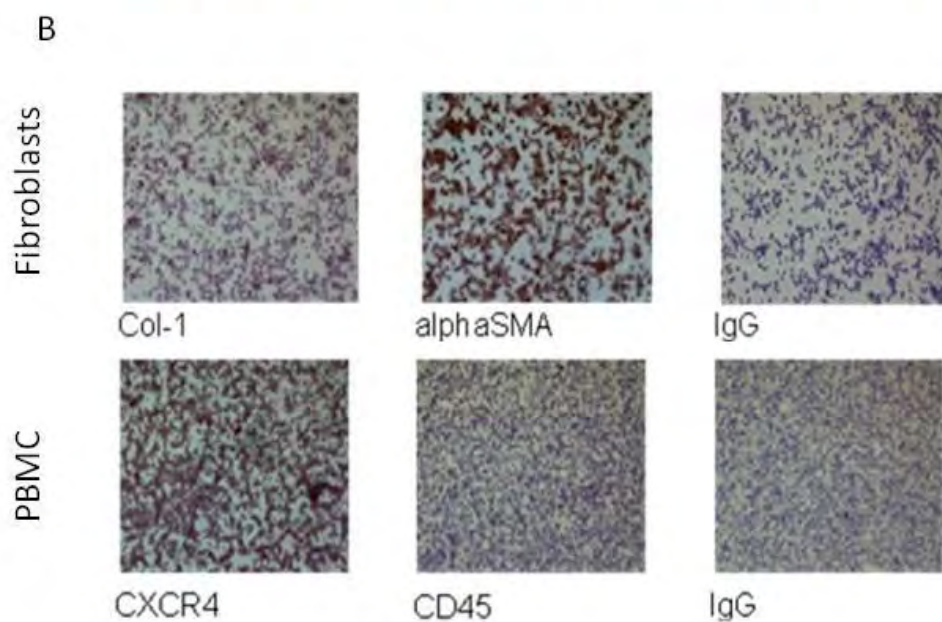
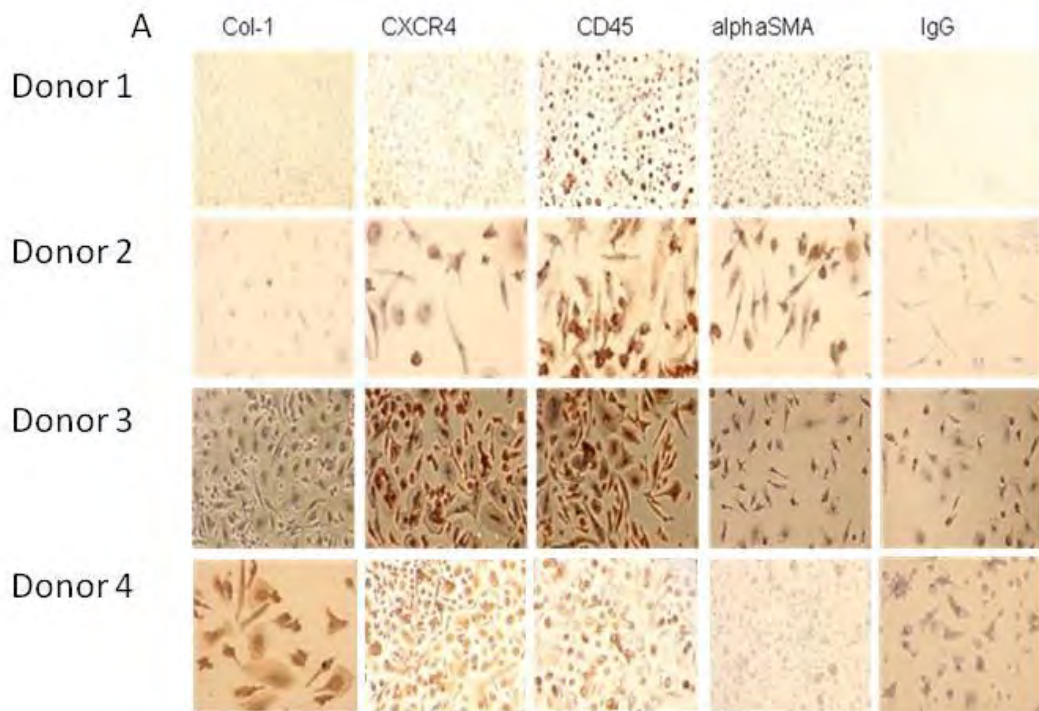
### **5.2.8 Spindle shaped-cells isolated from peripheral blood do not consistently express fibrocyte markers.**

We suspected that removal of contaminating blood cells after culture of fibrocytes resulted in a loss of remaining fibrocytes after treatment. Therefore we stained cells for fibrocyte markers without the negative selection step hoping to quantify cells positive for fibrocyte markers amongst the PBMC population in culture. PBMC isolated from buffy coat and cultured on normal tissue culture plastic consistently expressed CD45 and CXCR4. However expression of  $\alpha$ SMA was less uniform with samples from donors 1 and 2 only containing cells positive for  $\alpha$ SMA. Interestingly, the one donor (donor 4) positive for collagen-1 expression was negative for  $\alpha$ SMA expression (Figure 5.14A). Binding of the anti-collagen-1 and anti- $\alpha$ SMA antibodies was confirmed on cytopun fibroblast positive controls (Figure 5.14A) and anti-CXCR4 and anti-CD45 on cytopun lymphocytes (Figure 5.14B).

We confirmed that anti-procollagen-1 antibody stained CD90<sup>+</sup> synovial fibroblasts (Figure 5.15A) and was not expressed by lymphocytes using flow cytometry (Figure 5.15) and titrated optimal antibody concentration using fibroblasts. Procollagen-1 levels were then measured with optimised antibody dilutions (1:50) on monocytes before culture and on PBMC cultured on plastic with the optimised PBMC culture method. Figure 5.15E and F shows that both populations of cells had no detectable procollagen-1 expression before or after culture.

**Figure 5.14: Expression of fibrocyte markers on PBMC isolated from buffy coat and cultured on tissue culture plastic.**

A: Representative images at x10 and x20 magnification, of DAB immunohistochemical staining, of isolated human PBMC, for fibrocyte markers. B: (i) Positive controls for collagen-1,  $\alpha$ SMA, CD45 and CXCR4 as a positive control alongside an isotype matched negative control on cytopun cells. Images are representative from staining of cells from 4 different blood donors.



### 5.2.9 Expression of $\alpha$ SMA and collagen-1 by fibroblast populations

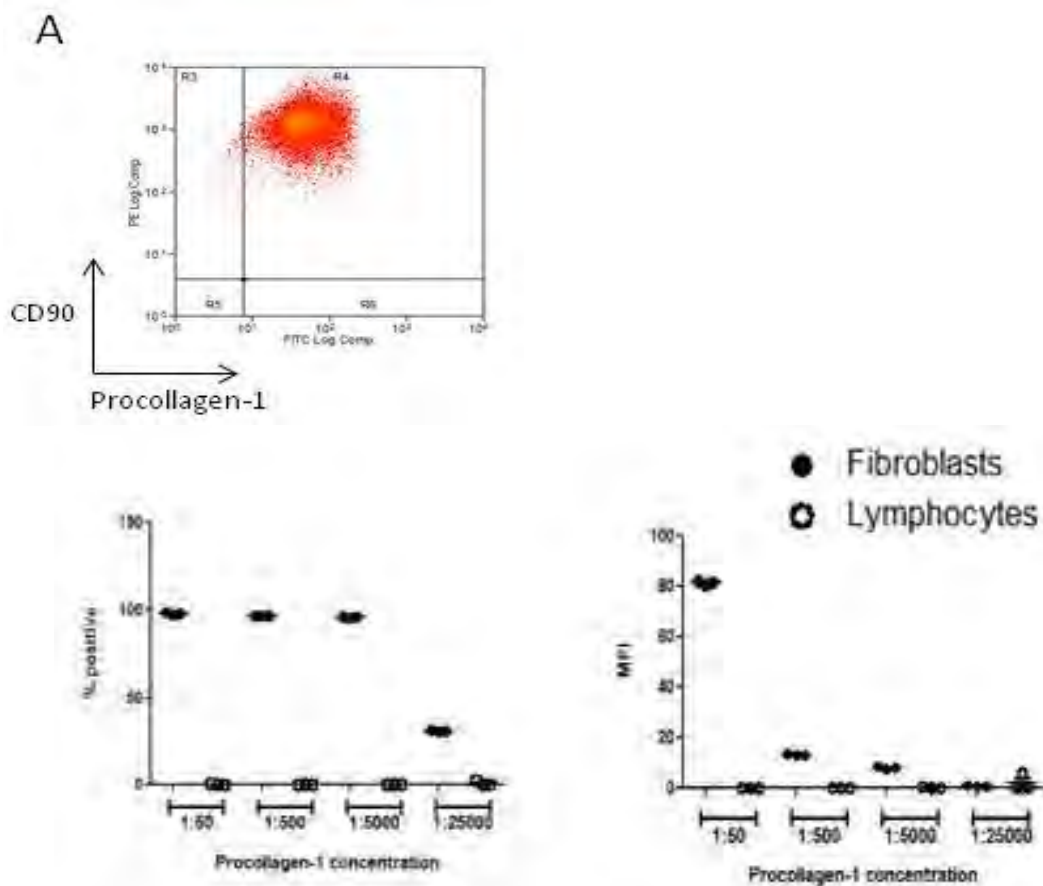
CD90<sup>+</sup> synovial fibroblasts (Figure 5.16A) were used to optimise anti-collagen-1 and anti- $\alpha$ SMA antibodies for dual staining with CD90 in flow cytometry and immunofluorescence. Cytometric analysis confirmed that CD90<sup>+</sup> cells were positive for collagen-1 and  $\alpha$ SMA (Figure 5.16B). Similarly although cytopins of synovial fibroblasts dual labelled positively using immunofluorescent anti- $\alpha$ SMA Texas red and anti-collagen-1 FITC antibodies (Figure 5.16B), staining for  $\alpha$ SMA was weak.

An alternative anti- $\alpha$ SMA antibody was then optimised on CD90<sup>+</sup> synovial fibroblasts using flow cytometry using lymphocytes as a negative control. We saw large differences between the intensity of staining using both antibodies (Figure 5.17) and observed that whilst both synovial fibroblasts and liver-derived myofibroblasts are positive for  $\alpha$ SMA, the intensity of expression varied ( $17.42 \pm 1.16$  vs.  $112.2 \pm 0.81$  MFI for synovial and liver fibroblasts respectively using R and D reagent). A similar pattern occurred with anti-collagen-1 antibodies from two suppliers (Figure 5.17), and again there were fewer collagen-1 expressing synovial fibroblasts compared to PBC liver-derived myofibroblasts (Figure 5.17).

We then performed dual staining of human normal and diseased liver sections for CD45 (red) and collagen-1 (green) co-expression using immunofluorescence techniques (Figure 5.18A). Total collagen-1 was increased in diseased liver compared to normal livers accompanied by an increase in CD45<sup>+</sup> cells. Of note cells co-expressing fibrocyte markers (yellow) were only detectable in some diseased livers (PSC, AIH and ALD) although this effect was dependent on the antibody used (Figure 5.19B).

**Figure 5.15: Expression of procollagen-1 on PBMC isolated from buffy coat obtained from peripheral blood.**

A: Representative flow cytometric plots, including i-dots in quadrant R4 representing CD90<sup>+</sup> human synovial fibroblasts positive for procollagen-1. Flow cytometry plots represent results from n=3 different donors. Anti-procollagen-1 antibody titration for flow cytometry on synovial fibroblasts (positive control) and peripheral blood lymphocytes (negative control). Data represents mean  $\pm$  SEM of percentage positive and MFI of cells expressing procollagen-1 from n=3 samples. B: Representative flow cytometric plots, of human lymphocytes in gate R1 with representative histogram of isotype labelled control cells (black) and procollagen-1 labelled cells (red). Plots represent results from n=3 different donors. C: Representative flow cytometric plots, of monocytes in gate R1 with representative histogram of isotype labelled control cells (black) and procollagen-1 labelled cells (red). D: Representative flow cytometry plot of PBMC cultured for human fibrocyte isolation and labelled for fibrocyte marker procollagen-1, where, gate R1 includes only monocytes but no lymphocytes, from n=9 different donors, with representative histogram of isotype labelled control cells (black) and procollagen labelled cells (red). E: Representative flow cytometry plot of PBMC labelled for fibrocyte marker procollagen-1, where, gate R1 includes only lymphocytes but not monocytes, from n=9 different donors, with representative histogram of isotype labelled control cells (black) and procollagen labelled cells (red).



 Control  
Procollagen-1

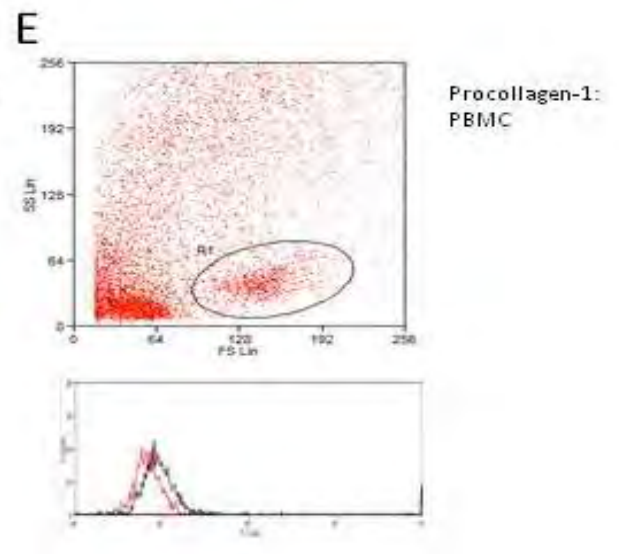
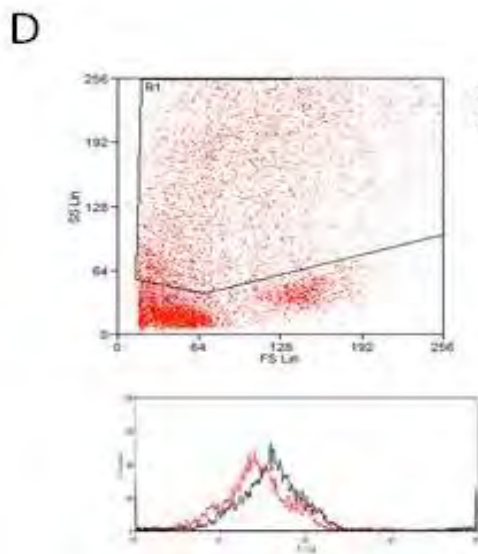
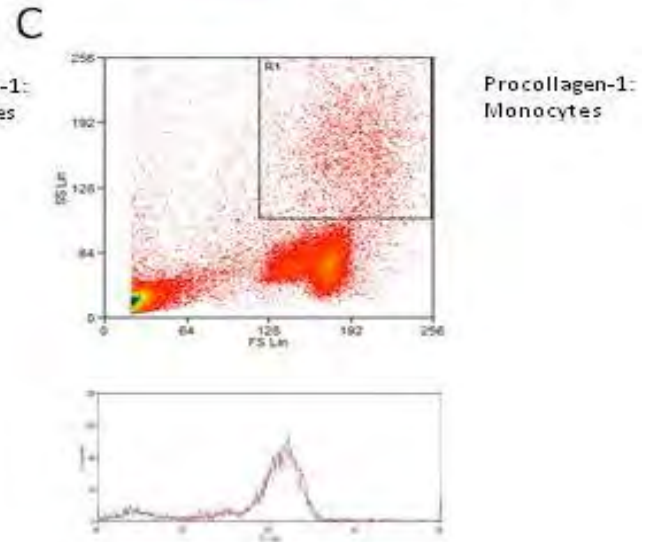
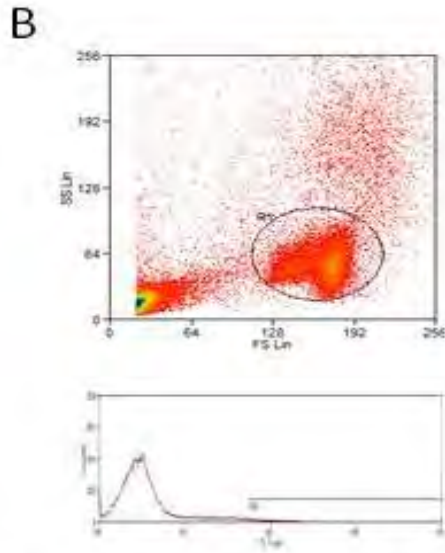
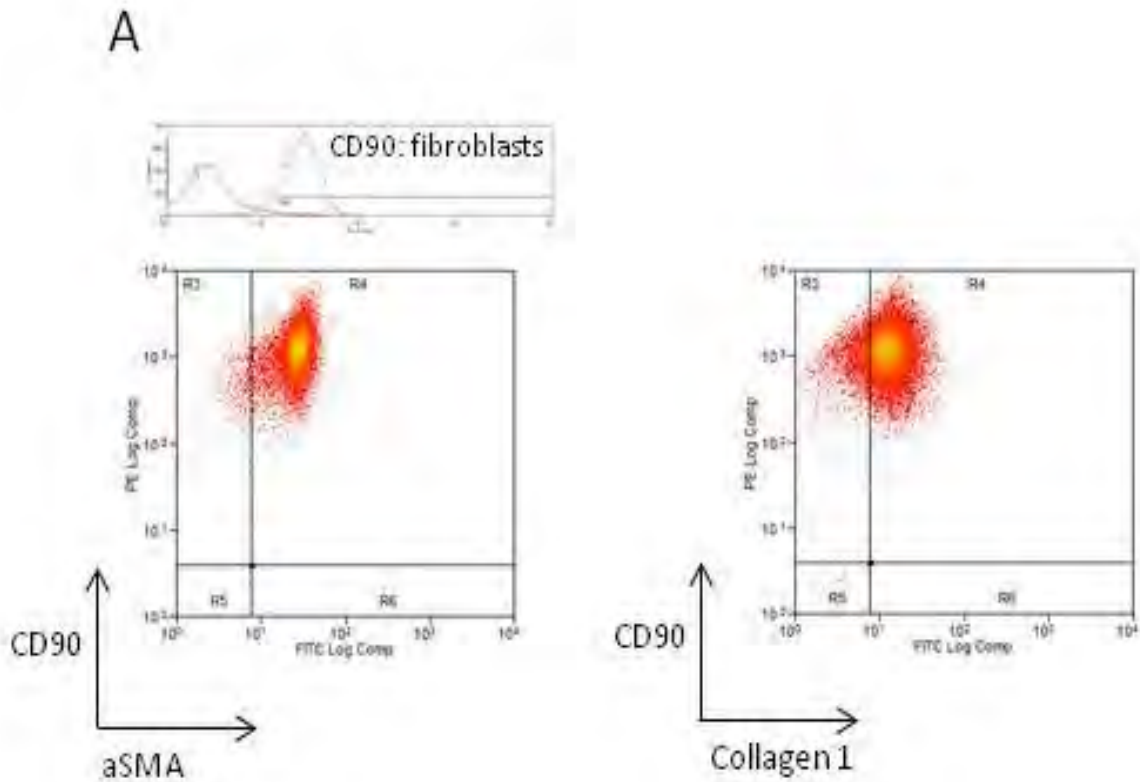


**Figure 5.16: Collagen-1 and  $\alpha$ SMA expression on CD90<sup>+</sup> synovial fibroblasts.**

A: A representative flow cytometry histogram stained with CD90 (red) against isotype matched control labelled cells (black). CD90 and  $\alpha$ SMA, CD90 and collagen-1 dual labelled human fibroblasts. B: Representative images at x10 magnification of cytopun lymphocytes for collagen-1 (green) and  $\alpha$ SMA (red). Images are representative from staining of cells from 3 different blood donors





B

## Fibroblasts

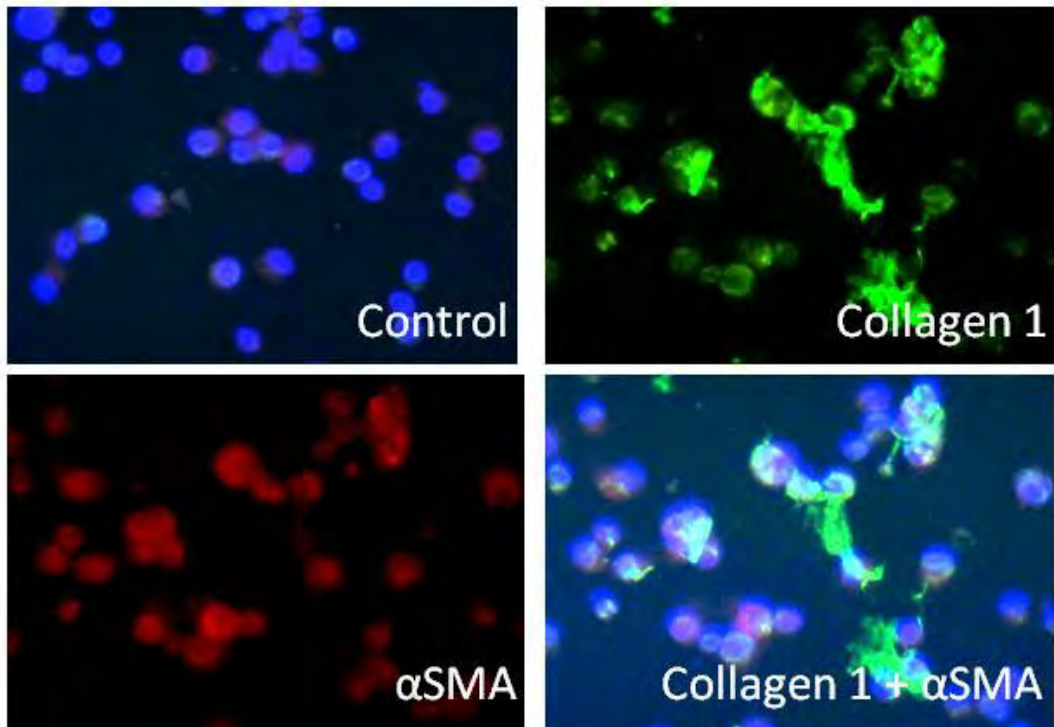


**Figure 5.17: Collagen-1 and  $\alpha$ SMA expression on CD90<sup>+</sup> synovial fibroblasts and PBC liver derived myofibroblasts.**

Flow cytometry analysis using anti- $\alpha$ SMA antibody (R and D systems), anti- $\alpha$ SMA antibody (Dako), anti-collagen-1 antibody (Sigma) and anti-collagen-1 antibody (Rockland) on human synovial and PBC liver derived fibroblasts expressed as percentage cells positive for surface CCR expression, median fluorescence intensity (MFI) of cells. Bars represent mean  $\pm$  SEM of n=3 donor samples, \*\*\*\*, p<0.0001.

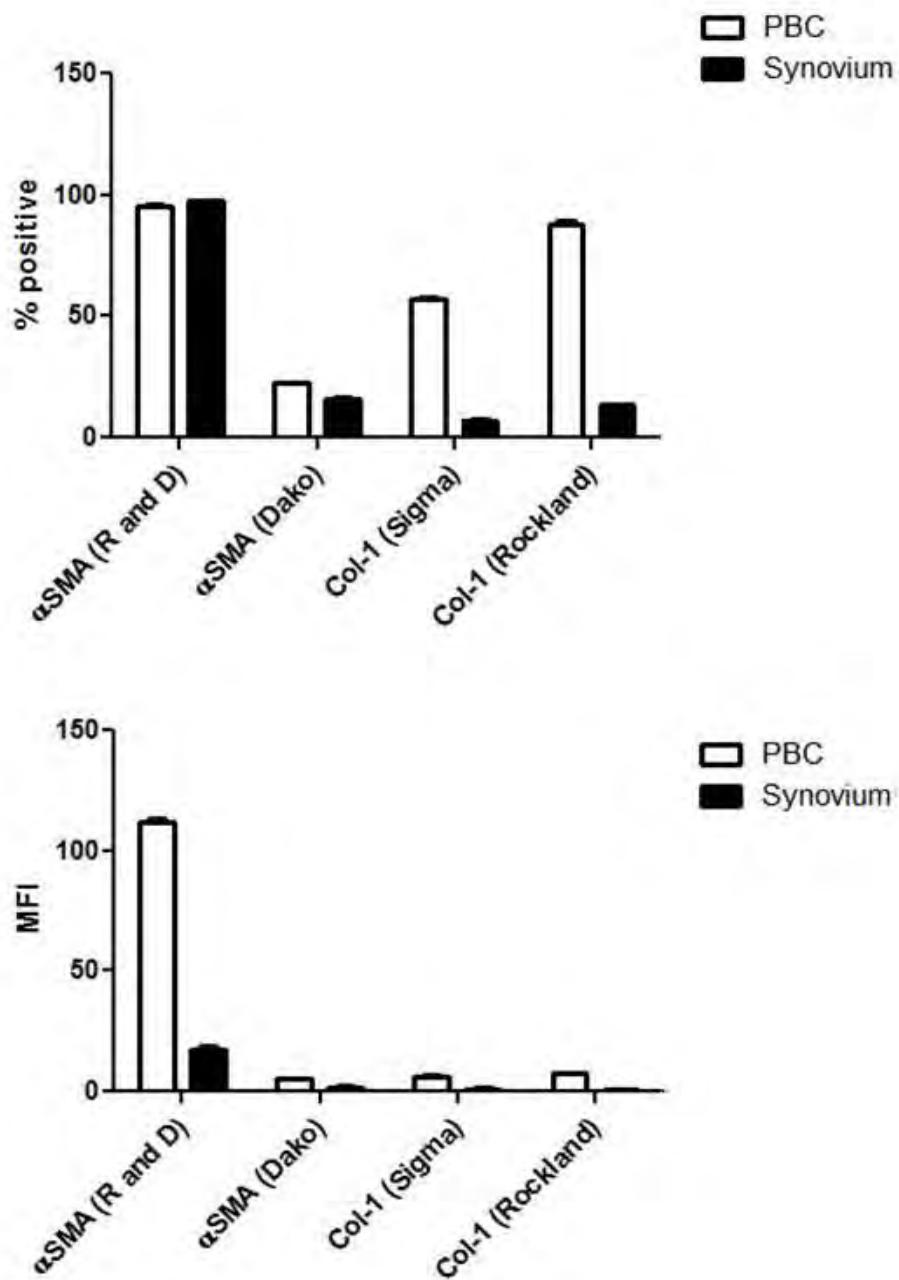
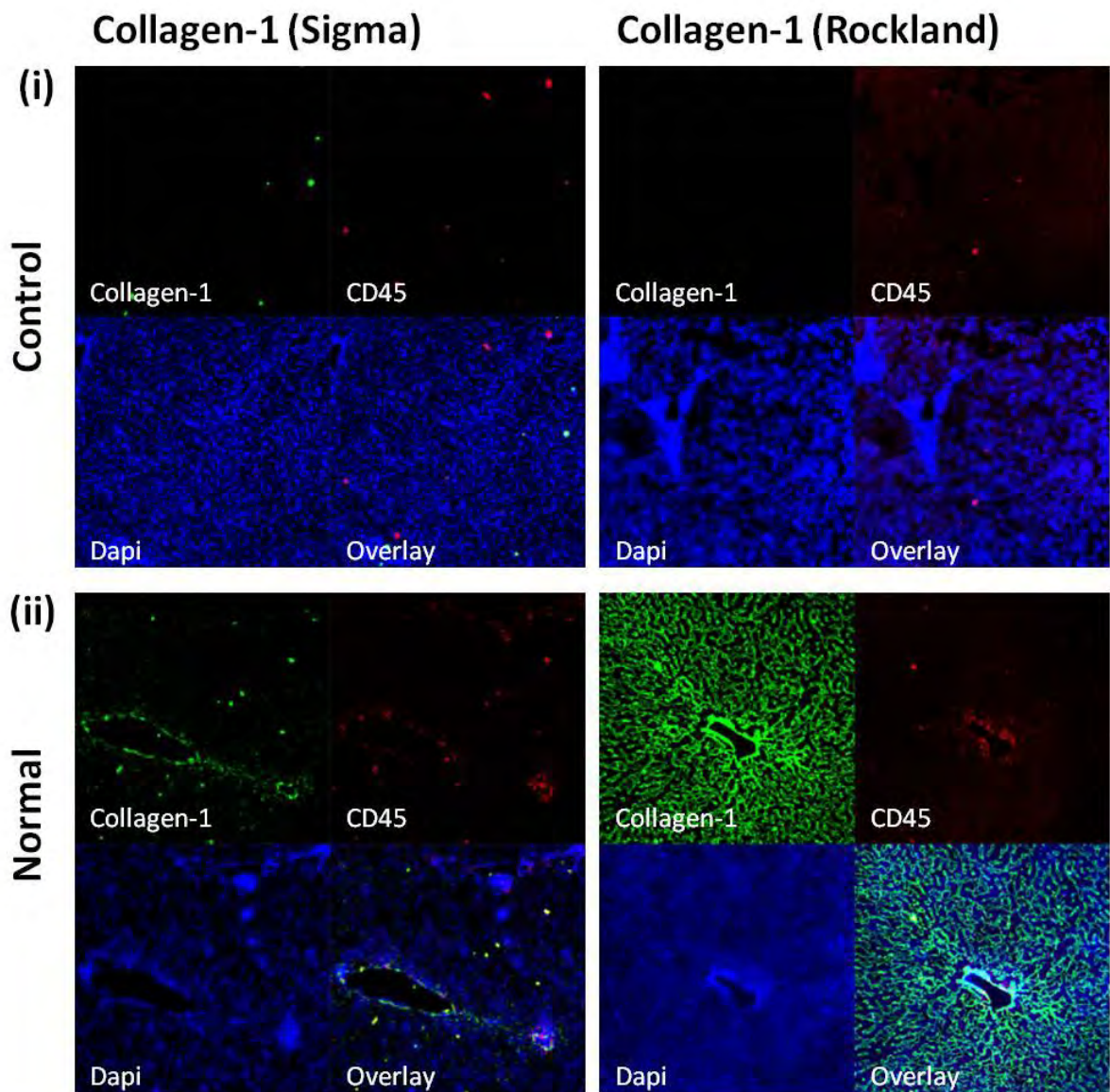


**Figure 5.18: CD45 and collagen-1 co-expression in human liver injury.**

Representative images of human liver sections labelled for co-expression (yellow) of CD45 (red), DAPI (blue) and collagen-1 (Sigma) (green), or collagen-1 (Rockland) (green). A: Representative images of, (i) isotype matched negative controls vs (ii) normal livers. B: Representative images of (i) ALD livers, (ii) AIH livers, (iii) NASH livers, (iv) PBC livers, (v) PSC livers. Images are representative of n=3 donors at x10 magnification.

**A**

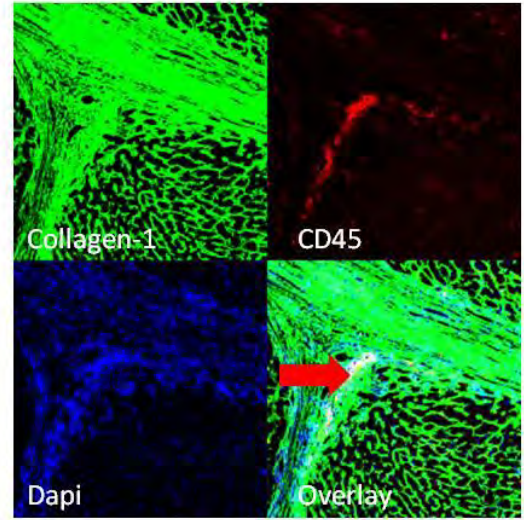
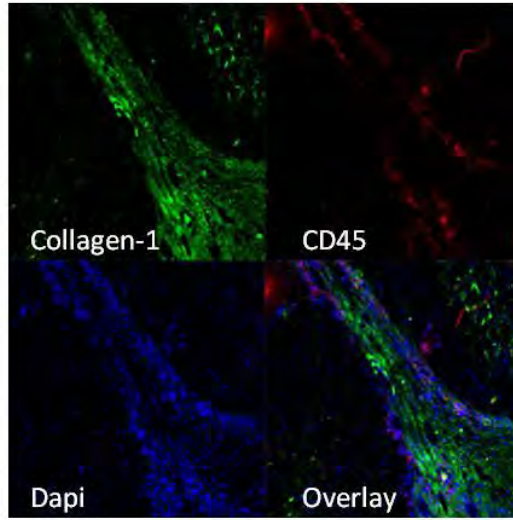


B

Collagen-1 (Sigma)

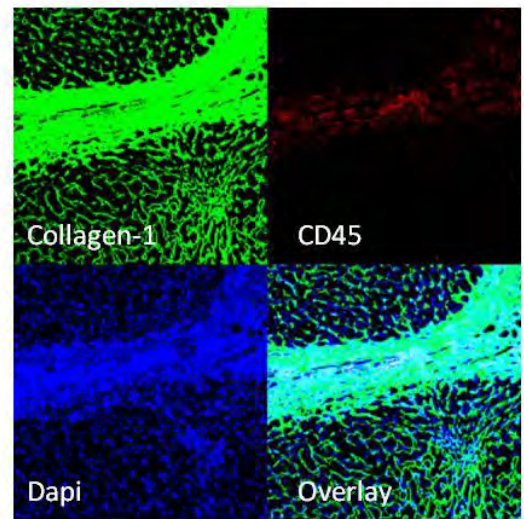
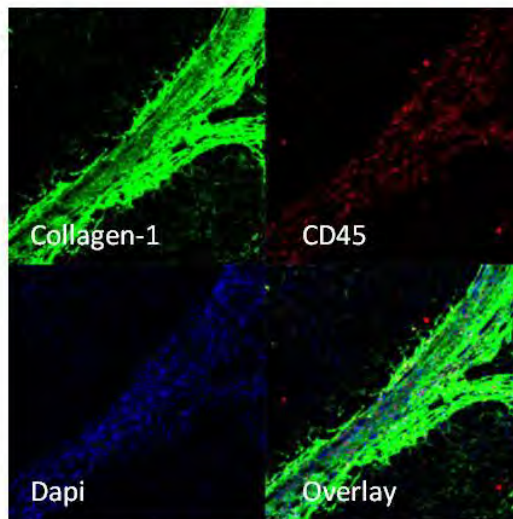
Collagen-1 (Rockland)

(i)



AIH

(ii)

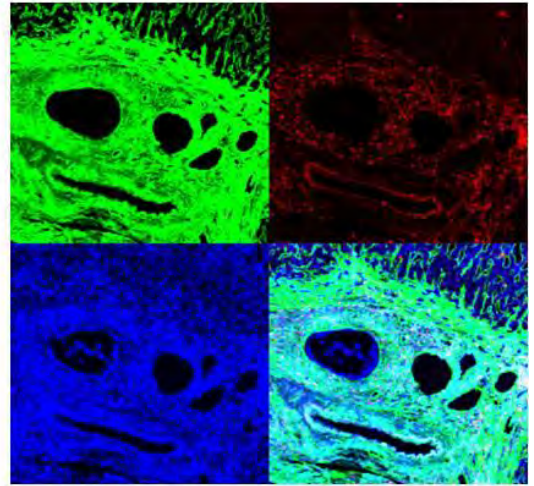
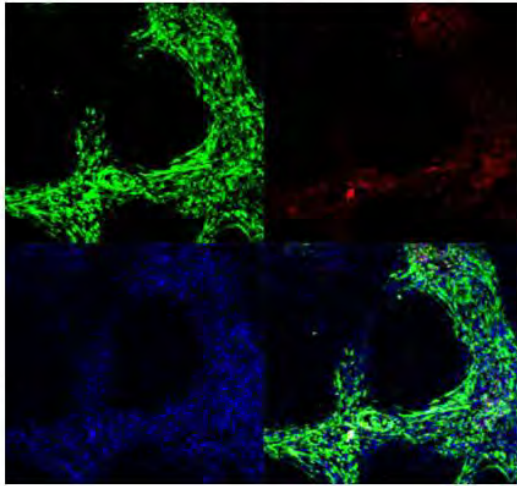


NASH

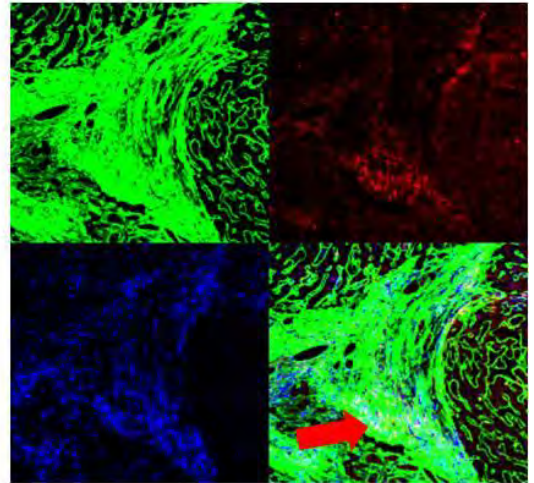
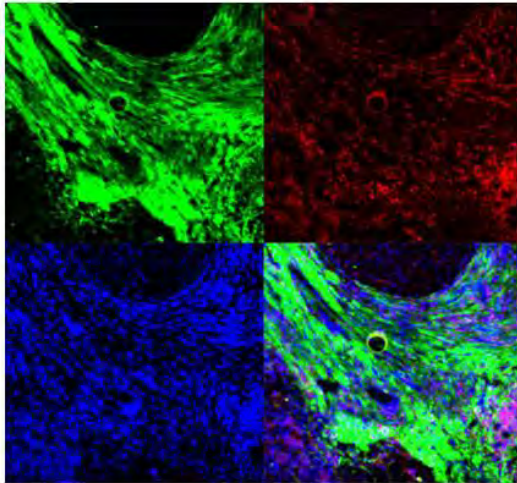
Collagen-1 (Sigma)

Collagen-1 (Rockland)

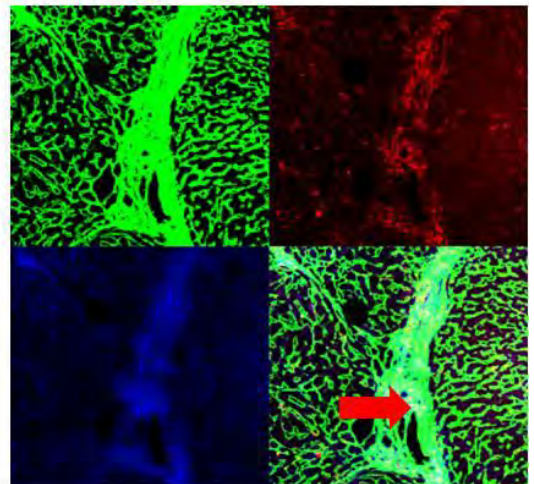
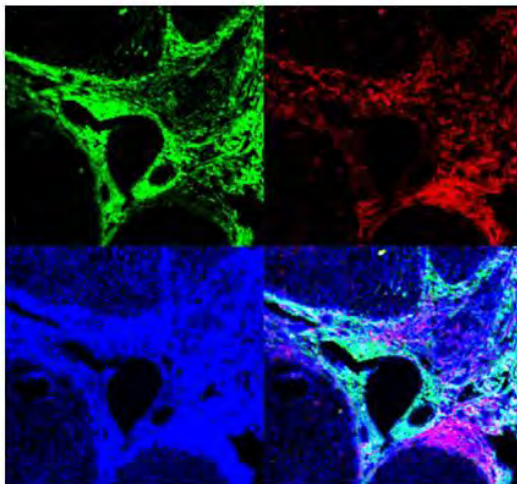
(iii)



(iv)



(v)

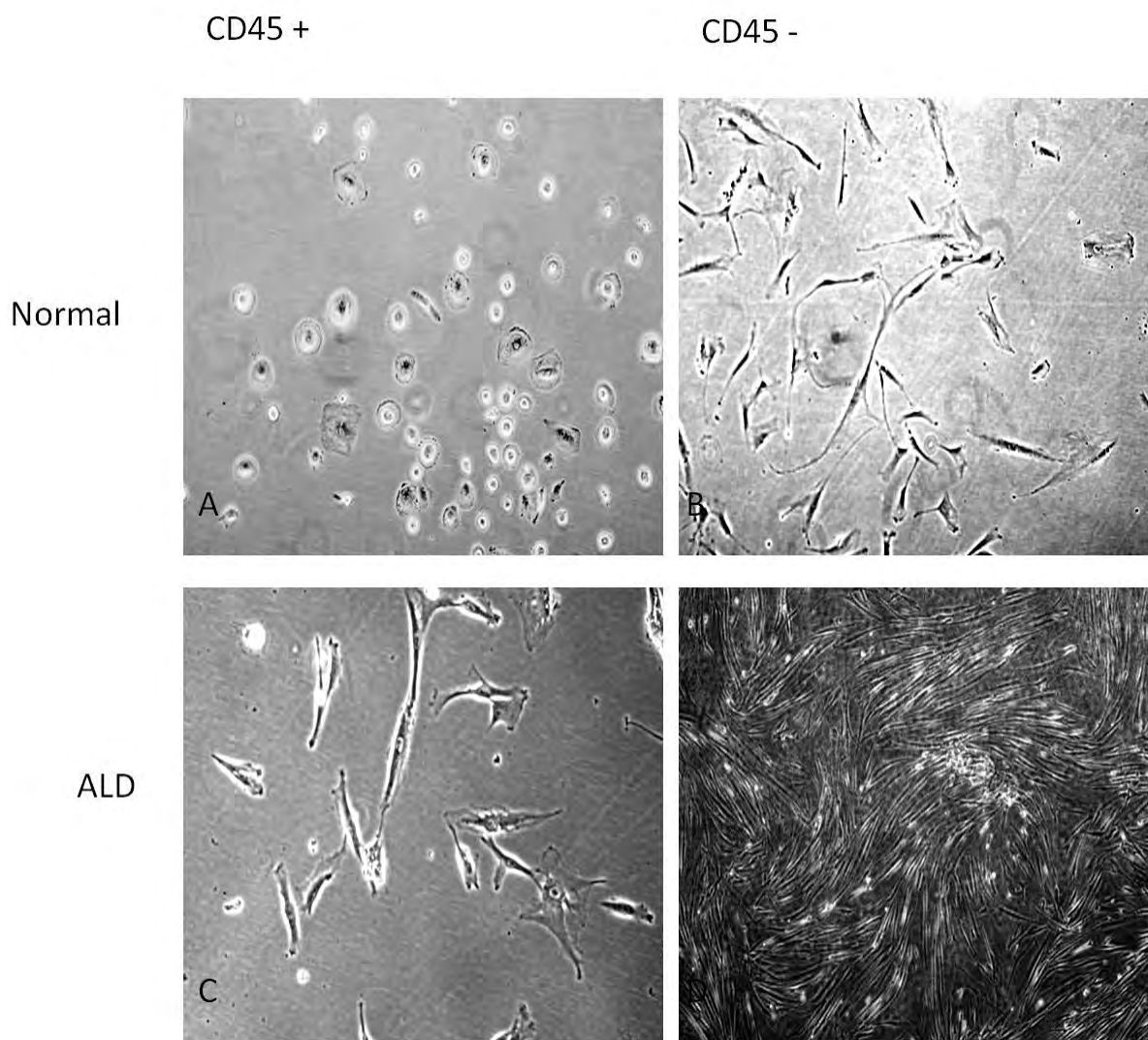


#### **5.2.10 CD45<sup>+</sup> cells isolated from HSEC isolation waste from ALD livers have a spindle shaped fibrocyte-like phenotype compared to normal livers.**

We routinely use human liver slices to isolate hepatic cell populations (see earlier chapters). As our staining data indicated that a population of CD45<sup>+</sup>/αSMA<sup>+</sup> cells is present in injured human livers we decided to try and isolated these cells. Thus waste taken from HSEC and BEC isolations from liver was immunomagnetically selected with anti-CD45 antibodies. In culture, cells from normal livers took on a circular shape similar to macrophages (Figure 5.19A) compared to CD45<sup>+</sup> cells from ALD livers which took on a more spindle shaped fibrocyte-like morphology (Figure 5.19C). CD45<sup>-</sup> cells from both livers adopted a spindle shaped myofibroblast like morphology as expected (Figure 5.19B and D).

**Figure 5.19: CD45<sup>+</sup> selected cells from HSEC and BEC depleted, digested liver slices.**

Representative images of cells selected from HSEC and BEC depleted liver slice waste. A: CD45<sup>+</sup> cells, B: CD45<sup>-</sup> cells from normal liver slices. A: CD45<sup>+</sup> cells, B: CD45<sup>-</sup> cells from ALD liver slices. Images were taken at x10 magnification using phase contrast microscopy, from 2 different liver donors.



### 5.3 Discussion

It is difficult to remove fibrocytes from MSC isolations because fibrocytes express both stromal and hematopoietic markers (Wilkins and Jones, 1996). Fibrocytes lose the latter in culture (Abe *et al.*, 2001), retention of stromal markers means that the two cell types are indistinguishable in culture. The method of MSC isolation commonly used is plastic adherence, due to the lack of a specific marker for MSC positive selection (Pittenger, 2008). Most hematopoietic stem cells are non-adherent and lost during culture, fibrocytes are tissue culture plastic adherent and express most of the markers used to identify MSC as well as possessing a MSC-like tri-lineage potential (Choi *et al.*, 2010, Hong *et al.*, 2005, Sera *et al.*, 2009, Strieter *et al.*, 2009b). Thus hematopoietic stem cell derived fibrocytes could contaminate MSC during isolations from bone marrow (Wilkins and Jones, 1996), and this impact upon downstream functions of cells used as a cellular therapy. Fibrocytes have been shown to promote fibrosis and inflammation (Keeley *et al.*, 2010). This could explain why some data show that MSC promote fibrosis and inflammation (Ogawa *et al.*, 2006), and some studies suggest no significant effect which contradicts most MSC research suggesting that MSC have anti-inflammatory and anti-fibrotic roles. Given the increased number of ongoing clinical trials with therapeutic MSC, and potential for fibrocyte contamination, we feel it is important to phenotype and characterise HSC derived fibrocytes, so measures can be taken to remove them from clinical MSC preparations.



### 5.3.1 SAP in fibrocyte differentiation

Fibrocytes can be isolated in two ways, with and without culture in media containing serum (Curnow *et al.*, 2010), but both methods yield different subsets of fibrocytes. Fibrocytes cultured in serum arise after 12-14 days of culture and fibrocytes without serum can appear 3 days (Curnow *et al.*, 2010). Curnow *et al* show that both types of fibrocytes appear morphologically similar and express similar stromal and hematopoietic markers. However, they are distinctly different in the way they differentiate from monocytes as part of a PBMC population and from purified CD14<sup>+</sup> monocytes. PBMC give rise to higher numbers of fibrocytes in serum free conditions whereas greater numbers of fibrocytes appear from CD14<sup>+</sup> monocytes in serum. Curnow *et al* go further to show that when serum is added to fibrocytes which arise in serum free conditions, the cells lose their characteristic spindle shaped morphology and become rounded but retain hematopoietic and stromal markers. If serum is removed from fibrocytes in serum, there is no change to their morphology or phenotype. Extensive microarray carried out by Curnow *et al* with the two fibrocyte types suggests that they differ in no less than 5144 genes. Microarray data also suggests that fibrocytes isolated in serum are closely related to macrophages, with upregulation of genes involved in immune and inflammatory response pathways, chemotaxis, RNA processing and lipid metabolism. Curnow *et al* suggest that serum free fibrocytes are a distinct population of cells likely to have a different function during fibrosis. Therefore in our choice of preparation procedure, we had to consider the type of fibrocyte that would likely contaminate bone marrow MSC isolations.

Since most MSC isolation procedures require serum we concentrated on fibrocytes that may arise in media supplemented with serum. However there is evidence to suggest that fibrocytes

which arise in serum-free cultures do so due to a lack of SAP (Pilling *et al.*, 2003). In support of this, SAP deficiencies have been observed in patients and mouse models with lung injury, particularly during resolution of inflammation and a corresponding increase in fibrocyte differentiation is seen from the blood of lung disease patients or models of lung injury. Reconstitution of SAP has alleviated levels of fibrosis in bleomycin induced lung injury (Pilling *et al.*, 2003, 2007a, Pilling *et al.*, 2007b). SAP has been shown to block differentiation through the FC $\gamma$ R receptor on fibrocytes and to inhibit fibrosis (Crawford *et al.*, 2012). Evidence suggests that the anti-fibrotic effects of SAP in differentiation may relate to inhibition of macrophages rather than monocytes (Castano *et al.*, 2009). Given the large numbers of liver-resident macrophages with the potential to differentiate into fibrocytes, we wanted to investigate whether human liver disease is associated with low levels of SAP as shown in lung disease. Thus as one of our specific aims for this chapter we measured SAP levels in normal and disease human serum and liver lysates and repeated this in a mouse model of carbon tetrachloride induced liver injury. Importantly we found there was either a significant increase or at times no significant difference in SAP levels after injury, and so fibrocytes in liver disease would arise in an environment with normal or higher SAP levels.

We found that there was a significantly higher level of serum in mouse injured livers and more strikingly in injured mouse serum compared to uninjured livers. There are three reasons for such a substantial increase in SAP levels in the liver. Firstly, during injury and in the early stages of repair, there is a loss of tissue integrity and increased endothelial permeability (Curnow *et al.*, 2010). The second reason is more specific to the liver, in mice, SAP is an acute phase protein synthesised by hepatocytes (Hutchinson *et al.*, 1994). Mouse hepatocytes have been shown to increase SAP secretion during an acute phase response, like CCl<sub>4</sub> injury,

*in vivo* and *in vitro*, this increase is mediated by activated macrophages which may occur during inflammation and fibrosis or by IL1 and IL6, typically upregulated cytokines during liver injury (Le and Mortensen, 1984a, b, Lin *et al.*, 1990). Lastly, mouse hepatocytes are responsible for the removal of SAP (Hutchinson *et al.*, 1994), and CCl<sub>4</sub> injury drastically reduces the number of functioning hepatocytes, thus impairing the ability of the liver to catabolise SAP. However data suggests processes involved in increased synthesis of SAP are bigger factors for increased levels of serum SAP than a reduced rate of SAP removal and processing (Baltz *et al.*, 1985). SAP does not behave like an acute phase protein in humans as shown in SLE patients (Bijl *et al.*, 2004, Levo *et al.*, 1986) so this may be why there is not a similar effect to what we observe in mice.

Although we saw a significant increase of SAP in human liver disease compared with normal livers, NASH and PBC livers had strikingly higher levels of SAP compared with AIH, which showed a small but significant increase in SAP, and we did not see any significant changes in serum SAP levels from ALD patients. This can be explained as ALD serum was taken from end stage cirrhotic patients, who were likely to be abstinent from alcohol. Stopping the disease causing stimuli could reduce the hepatocyte stress and cell death therefore returning SAP levels to normal. During resolution of injury, tissue integrity would eventually be restored and endothelial permeability reduced, coupled with reduced inflammatory stimuli responsible for macrophage activation, would result in reduced SAP levels, both in explanted livers and in serum. Similar to what we have observed in human serum and human livers, circulating levels of SAP would most likely reduce back to normal first, followed then by SAP levels at the source of SAP synthesis in the liver. Earlier experiments by Levo *et al* suggest SAP levels significantly decrease in patient serum with liver disease, this could be

true particularly as the cohort of donors for their study was larger and we have only measured serum in ALD patients whereas they considered a range of diseases (Levo *et al.*, 1982). Thus our results may be limited by low donor numbers and potentially by the disease type we have tested.

Curnow *et al.*, suggest fibrocytes can arise in both serum and non serum conditions but both cells can be classed as fibrocytes due to the expression of hematopoietic and stromal markers, these fibrocytes are functionally distinct and serum may be what regulates this change (Curnow *et al.*, 2010). Thus fibrocytes present during early and late stages of repair are different and may fulfill different functional roles. Curnow *et al.* also suggest that although this change could be regulated by SAP they found no evidence to support this, but other studies have shown the influence of various other cytokines in fibrocyte differentiation suggesting the regulation of fibrocyte differentiation may not solely regulated by SAP (Maharjan *et al.*, 2010, 2011, Niedermeier *et al.*, 2009, Shao *et al.*, 2008). Alternatively, fibrocytes differentiated by proteins other than SAP, could yield further, functionally distinct subsets which may come under the umbrella term of fibrocytes. Subsequent research by Tennent *et al.* has been highly critical of the findings of Pilling *et al.* regarding decreased levels of SAP and has shown that normal levels of SAP are sustained in patients with systemic sclerosis (Tennent *et al.*, 2007).

### **5.3.2 Isolation of fibrocytes from whole blood**

Although fibrocytes originate from cell populations in human bone marrow, most research is based upon fibrocytes isolated directly from blood. Thus we attempted to isolate fibrocytes

from blood and phenotype them to identify markers we could later use to identify contaminating fibrocytes in MSC isolations. Much of our research centres on using MSC as a cellular therapy in liver disease, so we also wanted to see if it is possible to identify fibrocytes in liver tissue as a step towards gauging their fibrotic and inflammatory potential. A common method of isolating fibrocytes from blood involves isolating PBMC and culturing them for 4 days before washing and culturing for a further 10 days in serum<sup>+</sup> media (Bucala *et al.*, 1994, Phillips *et al.*, 2004). We initially attempted this using a Lympholyte-H density gradient. However, we did not observe any spindle shaped cells in these isolations, and no cells expressed fibrocyte markers. Next, by necessity we isolated PBMC from blood rather than Leukophoresis packs (Phillips *et al.*, 2004) using Ficoll-Paque and then depleted cells which did not express fibrocyte markers. The cells were then cytopun onto slides and labelled for fibrocyte markers. The cells were CD45<sup>+</sup> as expected but at best only weakly positive for collagen-1. Of note, we saw no collagen-1 staining if we used Lympholyte-H gradients.

The number of PBMC we isolated after 14 days of culture was small, leaving fewer fibrocytes available after the depletion of contaminating cells. This was disappointing and likely reflects the fact that the original protocol used Leukophoresis packs, which are a far more concentrated leukocyte cell suspension compared to blood. Due to a lack of available Leukophoresis packs for our study, we attempted to mimic this highly concentrated, leukocyte preparation using buffy coats. This strategy did not have the desired effect and due to the low number of fibrocyte precursors in circulation it seems that Leukophoresis packs are an essential part of this protocol and must be acquired for future studies. However we continued to use buffy coat rather than whole blood as this significantly reduced the time the leukocytes

were kept on the separation gradient, and sped up the process so PBMC could be isolated without them being too stressed.

Since we found differences in final yield of fibrocytes dependent on gradient and material used for culture, we tested whether cell recovery differed with Lympholyte-H and Ficoll-Paque. However we found no significant difference in initial cell yield or morphology of fibrocytes at the end of the culture protocol. Ficoll-Paque seems to be the preferred gradient to isolate fibrocytes, and although it shares a similar density with Lympholyte-H, it seems there must be a toxic effect that Lympholyte-H may have on the mononuclear cells isolated, this may be why the percentage viability of mononuclear cells isolated from Lympholyte-H has not been specified but the mononuclear cell population isolated using Ficoll-Paque should yield  $95\pm 5\%$  mononuclear cells. Although it is difficult to say what may cause this suspected high toxicity, the presence of Edetate Calcium Disodium in Ficoll-Paque could prevent the aggregation of PBMC during separation, but Lympholyte-H has no such chemical. Aggregated leukocytes can become activated, and via oxygen free radicals and proteolytic enzymes can lead to increased aggregation of red blood cells but decreased deformability and partitioning. Contaminating aggregated RBC can therefore create an environment where isolation of PBMC is distorted (Baskurt and Meiselman, 1998).

The use of blood or buffy coat with Ficoll-Paque or Lympholyte-H did not cause a significant difference in the amount of spindle shaped cells that arose but the surface on which the cells were plated and cultured seemed to be the determining factor. Uncoated tissue culture plastic seemed to produce a significantly greater number of spindle shaped PBMC although the number varied between donors. This was an unexpected result as the literature suggests

fibronectin coating tissue culture plastic should yield more fibrocyte like cells. An explanation for this could be that papers citing this protocol often use a large number of cells in the form of Leukophoresis packs as their cell source (Phillips *et al.*, 2004). Due to the comparatively low number of cells available to us, it can be suggested that fibronectin may have enhanced binding of contaminating cells, in support of this we saw that when we increased the density of PBMC, they gave rise to more spindle shaped cells when grown on fibronectin coated tissue culture plastic. The low number of fibrocyte precursors in such an active environment could have negatively affected fibrocyte differentiation.

One possible factor which has been reported to influence the outcome of fibrocyte cultures grown in the absence of serum is the density at which the cells are cultured, specifically  $2.5$  to  $5 \times 10^5$  cells/ml (Pilling *et al.*, 2009b), and as these were in 96 well plates the approximate density per well was  $3.2 \times 10^5$ /ml/cm<sup>2</sup>. Interestingly we observed an increased number of cells bound and in cells which morphologically resembled fibrocyte-like spindle shaped at higher cell densities,  $8 \times 10^5$  cells/ml/cm<sup>2</sup>. At such higher densities coating plates with fibronectin increased the appearance of fibrocyte-like spindle shaped cells. This may well be because there is increased cell contact between a higher number of fibrocyte precursors. Although increased binding to fibronectin via integrin or adhesion molecule ligation similar to binding shown to Hyaluronic acid via CD44 (Maharjan *et al.*, 2011), would occur, a higher density of cells may promote an environment where fibrocytes would not only adhere but also survive for longer periods on fibronectin. We need to take into consideration that like, hyaluronic acid, fibronectin may also influence the differentiation of the fibrocyte (Maharjan *et al.*, 2011).

When we tried to phenotype these PBMC, only 1 out of 4 donors had cells that expressed collagen-1, interestingly this donor did not express  $\alpha$ SMA but the other 3 donors expressed  $\alpha$ SMA and not collagen-1. This inconsistency in fibrocyte isolation is well documented in the literature as some donors have been shown to yield little or no fibrocytes (Pilling *et al.*, 2009b). This may be due to the variability in proportions of fibrocyte differentiation factors found in different donors, but equally may be due to how these PBMC subsets fare in culture conditions.

### **5.3.3 Fibrocytes in circulation and effects of cell culture conditions**

The definitive method for identifying fibrocytes is collagen-1 expression, the literature suggests fibrocytes express very low levels of collagen-1 (Kisseleva *et al.*, 2006) so we used flow cytometry which is a more sensitive and quantitative assay than immunohistochemistry. Also we measured procollagen-1, a pre-cursor of PBMC rather than collagen-1 to try and identify any cells with the potential to express mature collagen-1 or those that expressed collagen-1 at very low levels. In 9 donors we did not see any procollagen-1 positivity in freshly isolated PBMC in the lymphocyte or monocyte fractions, which although expected had not previously been tested, and suggests the term “circulating” fibrocytes is inappropriate for these cells. Also we observed no expression of pro-collagen-1 in any of the isolated and cultured PBMC in both the lymphocyte or monocyte fractions from 9 donors. This was a highly unusual result as most papers show presence of dual positive cells using flow cytometry (Phillips *et al.*, 2004), however this is a true result as we have tested procollagen-1 staining and it has worked well in flow cytometry experiments using collagen-1 producing fibroblasts as a control. A key difference in our work compared with others is in the antibody



used. Commonly an anti-collagen-1 biotinylated antibody (Rockland) is used for these experiments. However if a cell expresses collagen-1 it is highly likely that it will express procollagen-1. The only instance where collagen-1 but not procollagen-1 can be observed is in macrophages which phagocytose collagen producing cells (Roderfeld *et al.*, 2010). The cells identified as fibrocytes could be macrophages, which, based on how closely they are related, is a strong possibility, Western blot analysis for collagen-1 and procollagen-1 could be used to validate this date, but ideally mRNA levels of collagen-1 need to be identified in these cells, as was done in work by Chesney *et al* (Chesney *et al.*, 1998) but with stronger negative controls. This suggests there is either inconsistency among antibodies used by different groups and/ or the cells that we and other groups have seen are not fibrocytes.

A reason for such inconsistencies between our findings and those in the literature could be the affinity of the antibodies used. For this reason we tested the anti-collagen-1 antibody (Sigma) and anti- $\alpha$ SMA (Dako), which we used initially, against anti-collagen-1 (Rockland) and anti- $\alpha$ SMA (R and D Systems). Notably anti-collagen-1 antibody (Rockland) is the antibody commonly used to identify fibrocytes (Curnow *et al.*, 2010, Phillips *et al.*, 2004). Comparisons using these antibodies were made using synovial and PBC liver myofibroblasts. Interestingly there was a clear difference between the anti- $\alpha$ SMA and anti-collagen-1 expression with antibodies from different companies and this coupled with the inherent high variability between donors could be a reason why we did not identify fibrocytes to the same extent or reproducibility as other groups. Currently from this data, with no procollagen-1 expression alongside morphology alone, one can only infer these are not fibrocytes. Further experiments identifying characteristic pro-inflammatory cytokine secretion, reduced

phagocytic ability, T cell priming, tri-lineage differentiation and differentiation into myofibroblasts will tell us if these cells are actually fibrocytes but do not express collagen-1.

We wanted to assess what effect the fibrotic environment may have on the appearance of spindle shaped fibrocyte-like cells among PBMC in culture. The aim was to investigate the effect of the niche on the fibrocyte differentiation and also to harness this effect to try to enhance the number of fibrocyte-like cells we could isolate. Culturing PBMC on collagen coated tissue culture plastic increased the number of spindle shaped fibrocyte-like cells among PBMC in all donors. This is consistent with fibrocyte research in lung disease which suggests myofibroblasts or fibroblasts, which express high levels of collagen, from areas of fibrosis recruit fibrocytes (Andersson-Sjoland *et al.*, 2011). A subset of PBMC may then come into contact with the high levels of collagen and differentiate into a fibrocyte like phenotype (Andersson-Sjoland *et al.*, 2011). Similar to collagen, hyaluronic acid has also been implicated in serum<sup>-</sup> fibrocyte differentiation, regulated through CD44 (Maharjan *et al.*, 2011). There is evidence that PBMC differentiate into fibrocytes depending on their recruitment to a particular niche (Andersson-Sjoland *et al.*, 2011) and this could account for the range of fibrocyte subsets as shown by the different roles when isolated from the spleen (Kisseleva *et al.*, 2011) and skin during wound healing (Wang *et al.*, 2008).

It is well documented that fibrocytes differentiate from CD14<sup>+</sup> monocytes (Curnow *et al.*, 2010), therefore CD14<sup>+</sup> monocytes were isolated from PBMC before culture and selected using CD14 conjugated Dynabeads. CD14<sup>+</sup> monocytes only differentiated into spindle shaped fibrocyte-like cells on normal tissue culture plastic. Surprisingly we noticed that culturing PBMC without CD14<sup>+</sup> monocytes on tissue culture plastic had a similar effect but gave rise to

a higher number of spindle shaped cells. Unfortunately the purity of the CD14<sup>-</sup> PBMC fraction was not tested so there may have been a contamination of CD14<sup>+</sup> monocytes. We proposed then that a higher proportion of CD14<sup>-</sup> PBMC (predominantly lymphocytes) is able to cause spindle shaped fibrocyte like cells to differentiate from CD14<sup>+</sup> PBMC (predominantly monocytes).

To investigate our hypothesis further, monocytes were depleted from PBMC by using plastic adherence for 2 hours and the non adherent fraction was collected and cultured separately. Interestingly over a longer period of time in culture we saw PBMC binding from the non adherent fraction. We found that the adhered PBMC fraction differentiated into the highest number of spindle shaped cells on collagen coated plastic however the non adherent fraction which would have far fewer monocytes in proportion to lymphocytes was able to give rise to larger numbers of spindle shaped cells regardless of the condition PBMC were cultured. This suggested that lymphocytes or their associated cytokines played a large part in causing monocytes to differentiate into spindle shaped fibrocyte like cells. It has been shown that cytokines, like TGFβ1, IL4 and IL13, produced by T cells are able to promote, while IFNγ and IL12 inhibit serum<sup>-</sup> fibrocyte differentiation, but the effect is not as dominant as SAP (Shao *et al.*, 2008). However, serum<sup>+</sup> fibrocytes from mice are inhibited by IL2, TNF, IFNγ and IL4 (Niedermeier *et al.*, 2009). It seems that fibrocytes may differentiate as a result of their niche in fibrotic conditions; similarly this may be why fibrocytes arise in culture.

Spindle shaped fibrocyte-like cells may arise due to disproportionately high lymphocyte numbers compared to monocytes and also, less significantly, due to high levels of collagen. A hierarchical effect of conditions can be deduced due to a lack of fibrocyte-like cells

developing from CD14 monocytes on collagen. This could be because the presence of the non CD14<sup>-</sup> PBMC fraction is essential for spindle shaped cells to develop from CD14<sup>+</sup> monocytes on collagen in long term culture conditions. Collagen may adversely affect CD14<sup>+</sup> monocytes in long term culture when they are isolated from other PBMC subsets, hence why we saw no cells on collagen coated plastic after 14 days. However the adherent PBMC on normal tissue culture plastic, and the non adherent PBMC fraction on all culture surface conditions, may give rise to different subsets of fibrocytes. Most inflammatory fibrotic disorders are usually composed of high lymphocyte levels and high levels of collagen in an environment shared by monocytes. Although we have not considered low SAP levels in this report, this may still be a factor in bringing about a different subset of fibrocytes; this report focuses on a fibrocyte subset which arises in areas of high collagen or disproportionately high lymphocytes and under high SAP levels.

#### **5.3.4 Fibrocytes presence in explanted cirrhotic livers**

To identify fibrocytes in human livers we tested the two collagen antibodies on sections from normal and disease livers. There was no CD45 and collagen-1 co-expression in any cells in normal or diseased livers using anti-collagen-1 (Sigma) but using anti-collagen-1 (Rockland) a higher number of CD45 and collagen-1 expressing fibrocytes were detected in injured liver sections, particularly in PSC, ALD and AIH livers. However, compared with anti-collagen-1 (Sigma), anti-collagen-1 (Rockland) staining in normal livers was unusually high and there seemed to be higher staining of the parenchyma even in normal livers which is unusual and uncharacteristic collagen-1 expression. As there is high non-specific binding of the antibody which we do not see with the control, this could mean anti-collagen-1 (Rockland) is

specifically staining more than just collagen-1, perhaps cross reacting with a different type of collagen. If the anti-collagen-1 (Rockland) staining is accurate, it seems that ALD livers express fibrocytes in fibrotic scar regions. There is also an increase in ALD serum and diseased liver SAP levels, suggesting fibrocytes can arise in a high SAP environment contrary to existing research. However, fibrocytes have previously been identified in mouse liver fibrotic parenchyma and not in scar areas (Roderfeld *et al.*, 2010). This could mean that mouse liver fibrocytes are found in a different area to human liver fibrocytes, alternatively, the fibrocytes in human livers may not be real and this may be an effect of the antibody.

Although fibrocytes have been identified and isolated from fibrotic mouse livers (Kisseleva *et al.*, 2006, Roderfeld *et al.*, 2010, Scholten *et al.*, 2011), this has yet not been done in human livers. A common method of isolating myofibroblasts from explanted human livers is to culture liver waste from HSEC and BEC isolations (Holt *et al.*, 2009). Often a large number of macrophages are seen in these populations but they are lost with time in culture. We wanted to isolate CD45<sup>+</sup> cells from this waste in the hope of isolating fibrocytes, or fibrocyte-like cells among macrophages. We cultured the CD45<sup>-</sup> waste which would have been a purer myofibroblast population fraction alongside CD45<sup>+</sup> cells. Interestingly, we identified some clear differences between the CD45<sup>+</sup> population from the normal liver waste and from ALD liver waste. CD45<sup>+</sup> selected cells from normal livers appeared uniformly circular and had the typical “fried egg” macrophage shape. However, CD45<sup>+</sup> cells isolated from the ALD diseased liver were far more spindle shaped and irregular, and they appeared to be spindle shaped fibrocyte-like cells. The myofibroblasts from both populations were very similar and but ALD myofibroblasts grew to confluence much faster than their normal counterparts probably as a property of a more activated phenotype.

### 5.3.5 Similarities between macrophages and fibrocytes

Macrophages, like fibrocytes, differentiate from monocytes, and studies have shown that splenic fibrocytes can differentiate into macrophages and dendritic cells (Kisseleva *et al.*, 2011). Fibrocytes may be a subtype of macrophages, perhaps even representing an activated form of macrophages (Reilkoff *et al.*, 2011). The plasticity of macrophages has been investigated in detail and under certain conditions these cells can take on a fibrocyte-like morphology (Porcheray *et al.*, 2005). Macrophage plasticity can be dictated by cytokines to take on a spindle shaped fibrocyte-like morphology, particularly TGF $\beta$ RI, IFN $\gamma$ , IL10, TNF $\alpha$  and M-CSF (Porcheray *et al.*, 2005), and this may go some way to explain why certain donors may yield fibrocytes and certain donors do not. PBMC are cultured for 3-5 days, in a mixture of cells which can vary greatly in number and proportion between patients. Culturing PBMC for 3-5 days can also mean there are different levels and proportions of cytokines, which may have variable effects on the adherent monocytes.

IL4, IL13 and TGF $\beta$  have been shown to alternatively activate macrophages (Gordon, 2003, Gordon and Martinez, 2010), causing them to adopt a spindle shaped fibrocyte-like morphology and also yield a subtype which has lower phagocytic properties, increased inflammatory cytokine secretion, but sustained antigen presenting capabilities (Varin *et al.*, 2010) similar to fibrocytes. More recently, macrophages have been shown to express collagen-1 (Pilling *et al.*, 2009a). This suggests that the fibrocytes we observe could be alternatively activated macrophages. Spindle shaped fibrocyte-like cells can arise from macrophages, this suggests macrophages are a very plastic cell type (Porcheray *et al.*, 2005). However this does not suggest that fibrocytes are the same cell as macrophages. In fact there is evidence to suggest plasticity between macrophages and dendritic cells, which are

considered a different but related cell type. It can be suggested that fibrocytes are a subtype of macrophages with a different functional role as these are far more closely related to macrophages than dendritic cells (Curnow *et al.*, 2010).

### 5.3.6 Conclusion

In this project we set out to investigate the phenotype of fibrocytes which arise in high serum environments to permit future incorporation of a fibrocyte exclusion step in the MSC isolation procedure. We also wanted to identify fibrocytes and understand their pro-fibrotic potential in the liver. However it is clear that fibrocyte research is still in its early stages with many unanswered questions. The isolation of fibrocytes is highly variable and markers for fibrocyte expression are not as robust as they should be. We could not reproduce fibrocyte isolation between donors, although we found cell-cell contact is a major factor as higher densities from similar donors yield more spindle shaped fibrocyte-like cells. Higher numbers of fibrocytes are seen in diseased compared to normal livers but this varies between different antibodies used, bringing into question some of the methods and antibodies used to identify fibrocytes.

We have found that altering conditions of PBMC culture can drastically alter the spindle shaped fibrocyte-like morphology of the cell populations we obtain, and that the niche can influence differentiation of spindle shaped fibrocyte-like cells, similar to what has been observed *in vivo*. In particular we have found that high proportions of lymphocytes at a high ratio to monocytes can influence fibrocyte differentiation which can be further supported by high levels of collagen in the matrix. This suggests that the high degree of variability of fibrocyte differentiation observed is because isolation of fibrocytes comes from a very crude

method of fibrocyte isolation involving a 5 day culture of PBMC, thus fibrocyte differentiation is dependent on the mixture of cytokines and cell proportions exists at highly variable proportions in different donors, that we do not control.

We have also found that we can identify a population of cells from diseased liver which resembles fibrocytes in morphology but the same population from normal livers resembles a macrophage-like morphology bringing into question whether fibrocytes are alternatively activated macrophages. However with reference to the high degree of plasticity of macrophages and the overlap which is inherent between cell types such as macrophages and dendritic cells, it is clear that fibrocytes may be a subtype of macrophages with a different phenotype and potentially a different role to macrophages. Of particular importance is that fibrocytes are able to phenotypically resemble MSC at some stage, but at the same time possess the opposite functional effect. This is a cause for concern in MSC research, particularly as we move towards using MSC as a therapy in a clinical setting. To properly address this question, efforts must be focussed on identifying and isolating fibrocytes from bone marrow, but clearly more pertinent questions need to be answered regarding fibrocyte existence and function before this can happen.

Further work is required to identify optimum cell culture methods for fibrocyte isolation, particularly using negative depletion to remove lymphocytes and then gradually re-introducing lymphocytes to elucidate the effects of lymphocytes and the cytokines they release. Fibrocytes then need to be identified and isolated from bone marrow and compared to myofibroblasts to identify markers that are common and differ aside from hematopoietic cells. Furthermore antibodies need to be tested extensively to use the most accurate antibodies to



identify fibrocytes. To confirm whether fibrocytes do actually exist in diseased human livers, it would be ideal to investigate fibrocyte presence in explanted livers from liver transplant patients with gender mismatched bone marrow transplant using fluorescence in situ hybridisation and co staining with collagen-1. To further investigate the fibrotic effect of fibrocytes, their presence and comparison of markers in lung and liver biopsies from patients with diseases in both organs can be assessed.

Finally, robust experiments have been carried out in this chapter to identify and phenotype fibrocytes particularly with commonly used antibodies, specifically anti-collagen-1 (Rockland). These antibodies have been used extensively in fibrocyte research. We have identified major flaws with this antibody, in regard to non specific staining and differences in staining compared with other anti-collagen-1 antibodies. We have on a rare occasion identified CD45<sup>+</sup> and collagen-1 cells indicating these cells are real and present, but this brings into question much of the existing fibrocyte research.

We have only been able to identify such cells as an artefact of culture from peripheral blood and although they may exist in the lungs it is unlikely these cells exist in human liver or bone marrow. The data that exists on fibrocytes in mouse liver injury is limited to the findings of one group who have reported limited influence of fibrocytes on fibrosis. Our experiments have identified some serious flaws in existing fibrocyte research. The future of research into fibrocytes in liver injury is limited and this is demonstrated by the drastic fall in new research from the field in the last few years. Fibrocyte research will continue to be hazy unless appropriate experiments are done to answer some very important questions regarding fibrocyte phenotype, *in vitro* and *in vivo* using robust, proven and tested reagents. We have

come to the conclusion that there is such a lack of robust fibrocyte data, that in MSC research, it would be of greater value to try and identify markers which could be used to sort MSC directly from bone marrow rather than using techniques such as plastic adherence to isolate MSC which could harbour fibrocyte contaminants in culture.

## **CHAPTER 6: FINAL REMARKS**

## **6.1 Cell dissociation buffer (CDB) mediated preservation of surface CCR expression after MSC detachment**

CCR were preserved on MSC after non-enzymatic detachment from tissue culture plastic. Although highest levels of viability were maintained by enzymatic detachment, as previously reported, we saw almost complete loss of surface CCR expression using these methods and so CDB was the best alternative. In chapter 4 we also tested the effects of methods of detachment on integrin expression and saw no difference (Figure 4.18). This suggests that integrins have a different response to enzyme detachment compared to CCR, making integrins less resistant to enzymatic cleavage (Taubenberger *et al.*, 2007). After re-plating cells which had been detached by non-enzymatic methods we observed the greatest recovery in cell viability with MSC detached by CDB. The method of cell survival appears to rely on MSC entering autophagy (Levine and Yuan, 2005) which could lead to more MSC recovered compared to other non-enzymatic detachment methods (Figure 3.7-3.9).

In chapter 3 we confirmed that preserved expression of MSC surface CCR is functionally relevant and showed increased migration towards corresponding ligands (Figure 3.6). We were also able to show consistent surface CCR expression on MSC among multiple donors (Chapter 4, Figure 4.1). We demonstrated that addition of serum improved viability of non-enzymatically dissociated cells, in agreement with studies of increased survival when bound to ECM or serum proteins (Yang *et al.*, 2012, Yu *et al.*, 2012). However levels were not restored to those observed with enzymatic detachment methods (Figure 3.10). Importantly we also tested effects of dissociation strategies upon downstream functions of MSC in the form of tri-lineage differentiation and suppression of T cell proliferation. Interestingly CDB

seemed to reduce but not prevent adipogenic differentiation (Figure 3.12). This may be due to a loss of receptors like PDGR $\alpha$ , important for promoting adipogenic differentiation. However it is more likely that those cells with adipogenic potential are reduced by cell death upon detachment. Certainly it has previously been reported that there are fewer cells with adipogenic potential in an MSC population which might suggest a loss in viability will effect this population more than cells with osteogenic potential (Russell *et al.*, 2010). Differences in chondrogenic differentiation were difficult to assess as it was not possible to quantify levels reliably but chondrogenic differentiation was preserved with CDB detachment (Figure 3.12).

CDB detached MSC were able to suppress T cell proliferation but with significantly less potency compared with TrypLE detached MSC (Figure 3.14). Although cell numbers were similar in both conditions, higher numbers of autophagic cells were present after CDB detachment suggesting they were not functioning at their optimum (Figure 3.9). This may also suggest that soluble mediators are not as influential in immunomodulation as CDB detachment would preserve any surface receptor but could reduce the secretion of soluble mediators. Also an important fact is that although we have used equal numbers of viable cells in these assays from TrypLE or CDB detached MSC, CDB detached MSC contain a higher proportion of dead cells and factors produced by these dead cells. This may have an effect on the immunomodulatory properties of the existing cells. A soluble factor implicated in suppression of T cells is PGE2 (Vercammen and Ceuppens, 1987). In chapter 4 MSC were shown to mediate their suppressive actions through PGE2 which has previously been reported (Bouffi *et al.*, 2010), and a reduction in PGE2 may result from CDB mediated detachment (Figure 4.21). PGE2 receptors are trypsin sensitive (Lord and Ziboh, 1979) and as PGE2 has

been linked with cell apoptosis (Priatelj *et al.*, 2011), this seems to be avoided by cleavage of receptors in MSC detached by TrypLE, promoting the survival of MSC.

We have shown that surface CCR which can play a major role in engraftment are cleaved with an associated loss of function with commonly used enzymatic detachment protocols. Use of MSC with preserved chemokine expression could enhance the efficiency and efficacy of engraftment in clinical trials whilst retaining significant immunosuppressive properties. However although we could promote engraftment, the issue of reduced levels of viability which could lead to reduced immunosuppressive properties needs to be addressed. We have shown there are methods to increase viability of MSC and have shown significant improvement of viability by using serum in the cell washing process post detachment. This raises the need to use autologous serum from patients as this increases the potential of infusing serum into the patient along with MSC. Serum can be collected and stored and we show significant improvements with low levels of 1% serum, this would still place increased demands on the patient and could potentially lead to more discomfort. It is important to elucidate what mechanism may be responsible for maintaining viability so that alternative methods may be determined.

Direct infusion of MSC to diseased livers in a clinical setting may cause more damage than any therapeutic benefit the cells may have. Non-invasive methods would be the method of choice in such a scenario. The prospect of maintaining high levels of surface receptor expression on MSC would serve to increase the migration along a chemokine gradient which is often present in patients with liver injury. Preserving surface receptor expression makes recruitment of cells after non-invasive methods a more likely prospect. We go further in this

project to use an intraportal vein infusion method to investigate engraftment. Further work would investigate migration of MSC along a chemokine gradient set up in circulation of liver injury models and would employ less invasive methods such as intravenous infusions which would more likely be attributable to a clinical setting.

We also observe reduced adipogenic differentiation after detachment with CDB. At first this may appear to alter the MSC tri-lineage potential by either pushing the cells to a progenitor cell type or eliminating adipogenic progenitors from the MSC population, as detailed earlier in this chapter. However immunosuppressive properties are still retained by the MSC and adipogenic differentiation is less likely to be important in the context of repairing fibrotic liver injury. However, such a reduction in adipogenic differentiation properties coupled with immunosuppression could encourage the prospect of introducing a cell into diseases such as NASH where there is already a heavy load of fatty tissue. Adipogenic differentiation may add to this load and cause a net increase on inflammation negating any anti-inflammatory properties the cell might initially have had. To further this work it would be important to test whether the effects of serum can restore tri-lineage differentiation and immunosuppressive properties of the MSC can be restored with viability.

In summary we have identified that methods of MSC detachment from tissue culture plastic need to be carefully considered depending on what downstream function of an MSC is being studied or utilised. It is important to note that our strategies which preserve receptor expression and therefore may increase the delivery of cells, which is the main focus of this project, do not completely eliminate the beneficial properties of the cell. Although at reduced levels, the MSC detached by CDB maintain tri-lineage potential and immunosuppressive

properties compared with TrypLE detached MSC. In essence we have identified a method to preserve the migratory capabilities of MSC once detached and in suspension, the challenge now is to reverse or minimise some of the associated effects of this method. In this study we have proved that viability even after CDB can be maintained by modifying the preparation procedure to include serum. We would suggest that to maintain high viability, tri-lineage differentiation, and immunosuppressive abilities, MSC need to be detached with TrypLE. Importantly, if CCR expression, with associated migration, is the main focus then detachment with CDB needs to be adopted. Further work needs to investigate temperature sensitive methods of detachment on CCR expression, as this method has been reported to preserve viability at higher levels than enzyme detachment methods (Yang *et al.*, 2012).

## **6.2 Increased engraftment in injured liver via TGF $\beta$ 1 up-regulated MSC surface CXCR3 expression**

Once we had demonstrated successful detachment of functionally competent MSC we next investigated their ability to adhere to and engraft within the liver environment. Here we found that TGF $\beta$ 1 significantly increased levels of CXCR3 surface expression on MSC and engraftment of MSC in injured liver (Figure 4.15). Engraftment was found to be dependent on TGF $\beta$ 1 regulated CXCR3 expression since functional blockade of CXCR3 reduced MSC engraftment to baseline levels after TGF $\beta$ 1 stimulation but had no effect on binding of unstimulated MSC (Figure 4.15). We have yet to define the mechanisms which underlie this observation but it agrees with the TGF $\beta$ 1 stimulated increase in CXCR3 surface expression previously reported on NK cells (Inngjerdingen *et al.*, 2001).



There is evidence for the interaction of TGF $\beta$ 1 with cytokine receptor expression on human airway fibroblast cell surfaces. TGF $\beta$ 1 appears to be able to regulate cytokine receptor expression. TGF $\beta$ 1 has been linked to the regulation of IL13 signalling by reducing IL13R $\alpha$  expression via the MEK/ERK pathway (Zhou *et al.*, 2012). However TGF $\beta$ 1 does not alter CXCR3 mRNA levels (Figure 4.8), and coupled with high intracellular stores of CXCR3 (Figure 4.1) in MSC it seems likely that CXCR3 recycling to the cell surface is enhanced after TGF $\beta$ 1 stimulation. Recycling of CCR has previously been reported, in particular for CCR5, due to its relevance in HIV research (Mueller *et al.*, 2002). Although recycling of CCR occurs at a baseline level for some CCR, CXCR3 has been reported to be degraded after internalisation (Meiser *et al.*, 2008). The mechanism of CXCR3 upregulation on MSC cell surface is unlikely to be dependent on SMAD signalling as we see no increase of cell surface CXCR3 after MSC stimulation with TGF $\beta$ 1. TGF $\beta$ 1 seems to be able to activate the Rab4 pathway. TGF $\beta$ R also recycles via a Rab11 dependent pathway and this could affect the other ligands passing through a similar pathway after TGF $\beta$ 1 ligand binding (Miaczynska *et al.*, 2004). It is possible that this mechanism exists in MSC in order to mobilise them during fibrosis. TGF $\beta$ 1 allows cells to remain responsive to migratory stimuli. Allowing the CCR to be degraded will stop the migration of the cells. Recycling CCR continually to the surface induces migration across a chemokine gradient. During fibrosis there is an increase in TGF $\beta$ 1 inducing mesenchymal cell mobilisation, proliferation and migration, in order to provide a stromal platform for recruited inflammatory or immune cells (Kershenovich Stalnikowitz and Weissbrod, 2003). To understand the mechanism involved in the observed MSC recruitment to the injured liver via CXCR3 we could consider the findings of Sahin *et al.* They show a fibrogenic dependent increase in CXCL9 expression in the livers of CCL<sub>4</sub> injured Wild Type

C57BL/6 mice. They observed that recruitment of CXCR3<sup>+</sup> cells to the liver played a significant role in preventing fibrosis progression using CXCR3<sup>-/-</sup> mice (Sahin *et al.*, 2012).

We have previously shown that low levels of engraftment of unstimulated MSC into injured tissue occurs independently of a role for CCR (Aldridge *et al.*, 2012). Indeed we observed a similar effect in the current study but also observed that stimulation with TGFβ1 caused CXCR3 to become functional and involved in the engraftment process. TGFβ1 stimulation significantly increases the number of MSC that bind to injured liver (Figure 4.15). Due to the heterogeneous sizes of MSC, 5μm to 50μm in culture, physical entrapment can cause cells to arrest in the vasculature rather than physical engagement of receptors. However our previous study suggests that MSC actively engraft in injured liver as there was no significant increase in number of larger cells which engrafted. The focus of this study is on the effect of chemokines in MSC engraftment and effects of chemokines are observed after arrest or adhesion to endothelium. Although it would be interesting to identify if engraftment via CCR is linked with size, and if TGFβ1 can increase the size of MSC, it was not pertinent for this study. Although we cannot identify whether binding is due to active or passive methods in this study we can assume that regardless of method of initial binding in the vasculature, the method of extravasation which would involve CCR is enhanced with TGFβ1 stimulation as blocking the function of CXCR3 significantly reduced engraftment of MSC. When we observe sections from transplanted livers the engrafted cells were located within the parenchyma, suggesting MSC had migrated into the tissue.

Although it cannot be overlooked that higher levels of surface expression could increase baseline engraftment, enzymatic cleavage of receptors after TGFβ1 stimulation suggests that

CCR function is dependent on its internalisation and subsequent recycling (Figure 4.16) which enables the cell to move across a particular gradient (Neel *et al.*, 2005). Such a mechanism suggests that we could maintain high levels of viability and immunosuppressive potential while still maintaining an increased migratory potential, allowing the use of non invasive methods of infusion.

Based on our findings we propose that internalised stores of CXCR3 not only avoid degradation after TGF $\beta$ 1 stimulation and upon recognition of ligand also enter a rapid recycling pathway rather than the slow recycling pathway, which is otherwise utilised by receptors at base line levels (Neel *et al.*, 2005). This would in effect increase engraftment and migration towards a CXCR3 ligand. Indeed we observed increased migration of TGF $\beta$ 1 stimulated MSC to the CXCR3 ligand IP-10/ CXCL10 (Figure 4.11) and furthermore observed significantly higher levels of binding to HSEC which have previously been reported to express high levels of IP-10/ CXCL10 (Curbishley *et al.*, 2005) (Figure 4.12). CXCR3 has been reported to mediate T cell recruitment to the liver during injury through interaction with CXCR3 ligands on HSEC (Curbishley *et al.*, 2005, Oo *et al.*, 2012, Oo *et al.*, 2010). Thus it may be postulated that TGF $\beta$ 1 increases MSC engraftment into injured liver through binding to HSEC via its association with IP-10/ CXCL10, with a potential role for CD44. CD44 expression was also increased on TGF $\beta$ 1 stimulated MSC but was not investigated further in this project. We have previously shown that  $\beta$ 1 integrin and CD44 are used by MSC to roll and firmly adhere, respectively, to injured HSEC (Aldridge *et al.*, 2012). CD44 has also been implicated in playing an integral role in recruitment of HSC to injured liver with an associated role of CCR (Crosby *et al.*, 2009). We observed increased CD44 expression on MSC after TGF $\beta$ 1 stimulation and this may also enhance MSC engraftment in a chemokine mediated

way (Aldridge *et al.*, 2012). Cellular transplantation has been reported to cause local ischemia, and could influence adhesion of MSC but this can take 1-4 hours to develop. Our experiments were shorter than this (15 minutes) but our previous work has reported no increase in hepatic MSC adhesion in a murine model of hepatic reperfusion injury (Aldridge *et al.*, 2012).

Cytokine stimulation of MSC has been reported to affect tri-lineage potential and immunosuppressive capabilities (Lacey *et al.*, 2009, Liu *et al.*, 2011b). However we report no effect on MSC tri-lineage differentiation after TGF $\beta$ 1 stimulation but we see increased potency of T cell suppression by stimulated MSC (Figure 4.21). As reported in the literature, PGE2 was identified as the mediator of this suppression (Aggarwal and Pittenger, 2005) and TGF $\beta$ 1 may enhance PGE2 expression or add to the suppression via other factors. Although we cannot rule out other factors may also suppress T cell proliferation after TGF $\beta$ 1 stimulation, including IDO, we can rule out direct effects of IL10 and TGF $\beta$ 1 on immune cells since these were undetected or detected at negligible levels, respectively, in our MSC supernatants. In clinical therapy, infusion of MSC into an injured liver environment with high levels of T cell infiltration will serve to reduce the impact of inflammation on liver and resultant fibrosis. We have shown increased binding of TGF $\beta$ 1 stimulated MSC to livers from patients with NASH and PSC (Figure 4.12). In these diseases chronic inflammation is a common feature. Thus enhanced binding in these livers and increased suppression of inflammation could act to halt the progression of injury and encourage resolution. Similarly this type of therapy can also be utilised post-transplant to protect from rejection or diseases such as graft-versus host (Hong *et al.*, 2009). The use of a cellular therapy that not only engrafts to the area of injury but promotes stronger local immunosuppressive effects can

potentially stop the use of immunosuppressive or anti-inflammatory drugs which deliver a systemic loss of immunity, potentially paving the way for higher incidence of infections or in worst cases, the development of tumours.

A major concern for TGF $\beta$ 1 stimulation of MSC before exogenous administration for liver therapy is that such treatment may promote a myofibroblastic phenotype of MSC (Li *et al.*, 2009). However our findings suggest that there is no significant difference in production of pro-fibrotic factors such as collagen-1 and  $\alpha$ SMA after TGF $\beta$ 1 stimulation (Figure 4.17). Future long-term experiments would need to determine whether infusion of TGF $\beta$ 1 stimulated MSC into injured environments where there are already high levels of TGF $\beta$ 1 would differentiate into a pro-fibrotic phenotype with detrimental results. Alternatively, MSC could take on a myofibroblastic phenotype and push the liver further towards cirrhosis cancelling out any beneficial effects the MSC might have. Alternately infusion of such cells could reduce inflammation thereby reducing fibrosis and have a negligible contribution to fibrosis by adopting a myofibroblastic phenotype. These outcomes can only be determined by long term engraftment experiments in liver injury models, perhaps with repeat infusions of MSC, which would likely be the case in clinical treatments, and assessing how MSC may progress or reduce fibrosis. The advantage of such animal models makes it possible to infuse MSC at different stages in disease development and resolution. Furthermore cell tracking experiments could also be used to track the fate of such cells in the liver, identifying whether or not these cells have taken on a myofibroblastic phenotype.

MSC can engraft into injured liver when infused via the portal vein and this engraftment is enhanced with TGF $\beta$ 1 pre-stimulation of MSC by increased surface recycling of CXCR3.

This implies that the migratory capacity of MSC can be enhanced with TGF $\beta$ 1 stimulation as can the immunosuppressive potential serving as a potential strategy in MSC therapy in liver disease. Cytokine treatment of MSC is a relatively low cost way of enhancing MSC engraftment and could easily be incorporated into protocols to enhance the efficacy of this treatment. Increased engraftment of infused cells with increased immunomodulatory capacity could lead to the use of fewer cells requiring less expansion and passaging in culture, therefore altering the intrinsic therapeutic capabilities of MSC. This also implies a faster application of these cells in therapy. Using fewer cells to maximum effect could mean a shorter time frame in which cells can be prepared for therapy. T cell infiltration is responsible for a large proportion of the damage done during chronic inflammation and resultant fibrosis (Fernandez-Cruz *et al.*, 1978). By increasing the potency of the MSC immunomodulatory effect, TGF $\beta$ 1 stimulation could also increase suppression of T cell proliferation during hepatic inflammation. The crucial next step is to investigate the effect of these cells in pre-clinical models of disease after increased engraftment. Future research needs to focus on the therapeutic effect of TGF $\beta$ 1 stimulated MSC in long term engraftment in models of liver injury, the fate of the cells, the method, time and number of infusions need to all be considered and investigated in detail.

### **6.3 Unsuccessful isolation and identification of fibrocytes with current protocols, markers and antibodies**

In the final section of the thesis I attempted to phenotype fibrocytes from peripheral blood. The central focus of this project was to increase the therapeutic potential of MSC. Previous sections explored increasing engraftment but in this section we tried to identify markers which could be used to select and deplete pro-inflammatory and pro-fibrotic fibrocytes from cultured bone marrow MSC isolates. This approach was taken with a view to enhancing therapeutic potential of the typically heterogeneous population of MSC by concentrating MSC into a purer MSC population.

Fibrocytes could go undetected due to similar marker expression and reported tri-lineage differentiation potential to MSC (H. Peng and Herzog, 2012). Fibrocytes could thus contaminate MSC isolations competing with them for space and oxygen in bioreactors making conditions highly unfavourable for MSC. Furthermore in clinical applications any beneficial anti-fibrotic and immunosuppressive properties of MSC could be reduced or even reversed by contaminating fibrocytes. Although fibrocytes have been reported in the bone marrow (Ogawa *et al.*, 2006), recent literature has identified them in peripheral blood with comprehensive isolation methods (Phillips *et al.*, 2004).

The isolation of fibrocytes from blood proved to be challenging in our hands since fibrocytes expressing procollagen-1 were not identified in blood before or after culture (Figure 5.14). Attempts to isolate fibrocytes from peripheral blood mononuclear cells (PBMC) yielded fibrocyte-like, spindle shaped cells which were not consistently positive for stromal and

hematopoietic markers, collagen-1 and CD45 respectively (Figure 5.15). We then attempted to increase numbers of spindle shaped cells in an effort to increase numbers of fibrocytes, assuming that the low cell number was making it difficult to identify them. Increasing cell density was successful in increasing spindle shaped cells (Figure 5.8). We also observed that growing both PBMC and isolated monocytes on collagen increased the presence of spindle shaped cells (Figure 5.10). Surprisingly we discovered that if we depleted monocytes from PBMC, conditions most favoured the development of spindle shaped fibrocyte like cells (Figure 5.13). T cell cytokines have been proven to increase fibrocyte differentiation from monocytes and a high proportion of contaminating lymphocytes in our cultures could have caused this result (Shao *et al.*, 2008). In support of this, monocytes with depleted lymphocyte populations can only differentiate to fibrocyte-like cells on collagen.

However we were not able to consistently identify the existence of fibrocytes among these spindle shaped cells from peripheral blood with collagen-1 expression (Figure 5.15). On further investigation we found inconsistent staining between multiple, commonly used antibodies for collagen-1 and  $\alpha$ SMA using control cells (Figure) and fibrocytes with high levels of non specific labelling (Figure 5.17). We next moved to staining tissue since fibrocytes have been reported in CCl<sub>4</sub> injured livers in mice (Scholten *et al.*, 2011). In our efforts to identify human fibrocytes we labelled sections from multiple diseased livers but only observed collagen-1 and CD45 dual staining using a collagen-1 antibody we considered unreliable (Figure 5.18). Finally we digested tissue samples in an attempt to collect fibrocytes, and whilst fibrocyte-like spindle shaped cells were identified in the adherent CD45<sup>+</sup> fraction from diseased liver (Figure 5.18), normal livers processed the same way yielded cells



resembling macrophages. This is not surprising and could lend support to the hypothesis that fibrocytes are alternatively activated macrophages (Reilkoff *et al.*, 2011).

Other groups have used what we believe to be an unreliable anti-collagen-1 antibody specifically in phenotyping isolated fibrocytes and have not phenotyped these cells in tissue (Curnow *et al.*, 2010, Phillips *et al.*, 2004). We have shown through staining for fibrocytes in liver tissue that this antibody may non-specifically detect other types of collagen which are not type 1 collagen. Using this antibody to phenotype cells, the presence of collagen-1 could be falsely detected as a range of cells can commonly express other forms of collagen. Cells co-expressing collagen-1 and CD45 were observed in areas of scarring where there are a large number of CD45<sup>+</sup> cells and collagen-1<sup>+</sup> myofibroblastic cells (Figure 5.18). The localisation of fibrocytes in these areas where other collagen-1 cells are present increases the likelihood of misidentification of cells. Furthermore we have shown there are apparent inconsistencies between staining with different antibodies for  $\alpha$ SMA. Use of diffusely expressed cytoskeletal and ECM proteins for cell identification increases the possibility of erroneous or non specific identification in contrast to more robust discrete membrane markers. There is a necessity for identification a more robust specific cell membrane marker to identify these cells.

SAP, a major contributor to the suppression of fibrocyte differentiation (Pilling *et al.*, 2003), was significantly increased or showed no change in injured or diseased serum or livers in mice and humans (Figure 5.2). This may be because the SAP has different roles in mice and humans. SAP is an acute phase protein in mice and reacts to inflammatory and fibrotic stimuli (Baltz *et al.*, 1985), whereas this is commonly the role for another protein, CRP in humans (Steel and Whitehead, 1994). Therefore, contrary to existing reports of decreased SAP levels

in mice with lung injury, fibrocytes reported to exist in mice with liver injury must not be mediated by low levels of SAP (Pilling *et al.*, 2003). This could mean that the reported cells are different and perhaps different from the fibrocytes observed from blood. These cells may come about from a similar precursor but the conditions they encounter in different organs could influence their differentiation into very different cell subtypes with different functions. We therefore propose that to term these cells fibrocytes is misleading when in essence these could all be different subtypes of monocytes, shaped by disease or culture conditions.

To conclude, our data suggest it is of little value to phenotype fibrocytes in order to deplete them from MSC isolates. The phenotyping strategy to identify fibrocytes is unreliable and irreproducible. Although it has been reported that this is due to an inherent variability among donors, it seems the use of unreliable antibodies for non specific markers of fibrocytes could be a more obvious reason. Development of these cells seem to be influenced by culture conditions which can vary between experiments particularly as we have shown, if these cells are dependent on the mixture of cells in culture which can depend on donor variability and researcher error. Rather, we feel it will be more sensible to identify markers on MSC which could help isolate purer populations of MSC with high immunosuppressive and therapeutic properties. Importantly fibrocytes from humans are not as robust a cell type as the literature may suggest, and the drastically reduced research into fibrocytes in recent years appropriately reflects the unreliable and inconsistent identification and culture procedures for this unlikely subtype of cells.

## 6.4 Future perspectives

We have found that MSC can be manipulated with TGF $\beta$ 1 stimulation to increase therapeutic properties and engraftment in models of liver injury. We can learn from these experiments and take our findings closer to preclinical development in a translational setting by pursuing this investigation in the immediate future and developing our findings in the long term in the following ways:

### 6.4.1 Immediate experiments.

Based on the findings of this report, the experiments I feel would be important to address in the immediate future would include a closer investigation of the migratory properties to chemokine ligands utilized by receptors these MSC express. Although we potentially saw the migration of MSC to a range of chemokines the high degree of variability which exists within Boyden chamber experiments meant certain effects of cytokine stimulated increases in MSC migration could potentially be masked and overlooked. We have also not addressed the effects of multiple chemokines in combination which would recreate likely patterns of expression *in vivo* and may demonstrate hierarchical functionality. For example we report for the first time, the presence of high levels of CXCR7 expression and negligible CXCR4 levels, with high levels of migration of MSC towards SDF1 $\alpha$ / CXCL12. Due to recent reports focusing on CXCR7 and CXCR4 co-operation being involved in migration towards SDF1 $\alpha$ / CXCL12, we feel this could prove the existence of a mechanism of migration of MSC expressing apparently negligible levels of CXCR4 to the CXCR4/ CXCR7 ligand which has not previously been reported. It would also be important to consider measurement of

migration responses under conditions of shear stress *in vitro* as blood flow is known to be important as a stimulator of leukocyte migration and similar mechanisms may operate for MSC.

#### **6.4.2 Longterm experiments**

A key experiment to validate our findings would be to investigate the effects of increased MSC engraftment and immunosuppressive properties on liver injury. The therapeutic effect of TGF $\beta$ 1 stimulated MSC can be measured in short term *in vivo* experiments investigating effects on immune cell infiltration and by measuring early markers of fibrosis. It would be interesting to investigate the effect MSC can have on infiltrating cell types in once engrafted in the liver. Here we could phenotype the immune component of the engrafted livers or consider utilizing flow based assays to observe the effect of MSC on recruitment of immune cell subtypes across endothelial monolayers. In particular we would investigate the well characterized immunomodulatory properties of MSC via the recruitment of immunosuppressive T regulatory cells.

Long term engraftment studies with MSC infusions in mouse liver injury models can provide us with information regarding the long term efficacy of TGF $\beta$ 1 stimulated MSC, and allow assessment of effects across the time-course of disease progression and resolution. The effect of MSC infusions on inflammation could be investigated after initial insult and subsequent fibrosis in the liver. Intravenous delivery needs to be investigated as a method of MSC infusion in this setting with regard to migration to the liver, with repeat infusions of MSC and investigation of effects at multiple time points. Such studies could also focus on retention in

the injured liver and infusion of MSC at a specific stage of injury, particularly with easily controlled and characterized models of liver injury and resolution induced by CCl<sub>4</sub>. Long term experiments should also address important safety issues raised with regard to reported cancer promoting properties and pro-fibrotic potential of MSC in models of liver injury. Such issues need to be carefully addressed before MSC can be utilized to their full potential as a means of clinical therapy for liver disease.

## LIST OF REFERENCES

- Abdel aziz, M.T., El Asmar, M.F., Atta, H.M., et al. (2011) Efficacy of mesenchymal stem cells in suppression of hepatocarcinogenesis in rats: possible role of Wnt signaling. **J Exp Clin Cancer Res**, 30: 49.
- Abe, R., Donnelly, S.C., Peng, T., et al. (2001) Peripheral blood fibrocytes: differentiation pathway and migration to wound sites. **J Immunol**, 166: (12): 7556-7562.
- Achyut, B.R. and Yang, L. (2011) Transforming growth factor-beta in the gastrointestinal and hepatic tumor microenvironment. **Gastroenterology**, 141: (4): 1167-1178.
- Aggarwal, S. and Pittenger, M.F. (2005) Human mesenchymal stem cells modulate allogeneic immune cell responses. **Blood**, 105: (4): 1815-1822.
- Aldridge, V., Garg, A., Davies, N., et al. (2012) Human mesenchymal stem cells are recruited to injured liver in a beta1-integrin and CD44 dependent manner. **Hepatology**, 56: (3): 1063-1073.
- Amado, L.C., Saliaris, A.P., Schuleri, K.H., et al. (2005) Cardiac repair with intramyocardial injection of allogeneic mesenchymal stem cells after myocardial infarction. **Proc Natl Acad Sci U S A**, 102: (32): 11474-11479.
- Andersson-Sjoland, A., Erjefalt, J.S., Bjermer, L., et al. (2009) Fibrocytes are associated with vascular and parenchymal remodelling in patients with obliterative bronchiolitis. **Respir Res**, 10: 103.
- Andersson-Sjoland, A., Nihlberg, K., Eriksson, L., et al. (2011) Fibrocytes and the tissue niche in lung repair. **Respir Res**, 12: 76.
- Anton, K., Banerjee, D. and Glod, J. (2012) Macrophage-associated mesenchymal stem cells assume an activated, migratory, pro-inflammatory phenotype with increased IL-6 and CXCL10 secretion. **PLoS One**, 7: (4): e35036.
- Asari, S., Itakura, S., Ferreri, K., et al. (2009) Mesenchymal stem cells suppress B-cell terminal differentiation. **Exp Hematol**, 37: (5): 604-615.
- Askari, J.A., Buckley, P.A., Mould, A.P., et al. (2009) Linking integrin conformation to function. **J Cell Sci**, 122: (Pt 2): 165-170.
- Auffray, C., Sieweke, M.H. and Geissmann, F. (2009) Blood monocytes: development, heterogeneity, and relationship with dendritic cells. **Annu Rev Immunol**, 27: 669-692.
- Baertschiger, R.M., Serre-Beinier, V., Morel, P., et al. (2009) Fibrogenic potential of human multipotent mesenchymal stromal cells in injured liver. **PLoS One**, 4: (8): e6657.
- Balmelli, C., Ruggli, N., McCullough, K., et al. (2005) Fibrocytes are potent stimulators of anti-virus cytotoxic T cells. **J Leukoc Biol**, 77: (6): 923-933.
- Baltz, M.L., Dyck, R.F. and Pepys, M.B. (1985) Studies of the in vivo synthesis and catabolism of serum amyloid P component (SAP) in the mouse. **Clin Exp Immunol**, 59: (1): 235-242.
- Banas, A., Teratani, T., Yamamoto, Y., et al. (2008) IFATS collection: in vivo therapeutic potential of human adipose tissue mesenchymal stem cells after transplantation into mice with liver injury. **Stem Cells**, 26: (10): 2705-2712.
- Baskurt, O.K. and Meiselman, H.J. (1998) Activated polymorphonuclear leukocytes affect red blood cell aggregability. **J Leukoc Biol**, 63: (1): 89-93.
- Bataller, R. and Brenner, D.A. (2005) Liver fibrosis. **J Clin Invest**, 115: (2): 209-218.
- Batista, U., Garvas, M., Nemec, M., et al. (2010) Effects of different detachment procedures on viability, nitroxide reduction kinetics and plasma membrane heterogeneity of V-79 cells. **Cell Biol Int**, 34: (6): 663-668.
- Belema-Bedada, F., Uchida, S., Martire, A., et al. (2008) Efficient homing of multipotent adult mesenchymal stem cells depends on FROUNT-mediated clustering of CCR2. **Cell Stem Cell**, 2: (6): 566-575.

Bellini, A. and Mattoli, S. (2007) The role of the fibrocyte, a bone marrow-derived mesenchymal progenitor, in reactive and reparative fibroses. **Lab Invest**, 87: (9): 858-870.

Bensidhoum, M., Chapel, A., Francois, S., et al. (2004) Homing of in vitro expanded Stro-1- or Stro-1+ human mesenchymal stem cells into the NOD/SCID mouse and their role in supporting human CD34 cell engraftment. **Blood**, 103: (9): 3313-3319.

Berres, M.L., Koenen, R.R., Rueland, A., et al. (2010) Antagonism of the chemokine Ccl5 ameliorates experimental liver fibrosis in mice. **J Clin Invest**, 120: (11): 4129-4140.

Bhogal, R.H., Weston, C.J., Curbishley, S.M., et al. (2012) Autophagy: A cyto-protective mechanism which prevents primary human hepatocyte apoptosis during oxidative stress. **Autophagy**, 8: (4).

Bijl, M., Bootsma, H., Van Der Geld, Y., et al. (2004) Serum amyloid P component levels are not decreased in patients with systemic lupus erythematosus and do not rise during an acute phase reaction. **Ann Rheum Dis**, 63: (7): 831-835.

Bocker, W., Docheva, D., Prall, W.C., et al. (2008) IKK-2 is required for TNF-alpha-induced invasion and proliferation of human mesenchymal stem cells. **J Mol Med (Berl)**, 86: (10): 1183-1192.

Boomsma, R.A. and Geenen, D.L. (2012) Mesenchymal stem cells secrete multiple cytokines that promote angiogenesis and have contrasting effects on chemotaxis and apoptosis. **PLoS One**, 7: (4): e35685.

Borroni, E.M., Mantovani, A., Locati, M., et al. (2010) Chemokine receptors intracellular trafficking. **Pharmacol Ther**, 127: (1): 1-8.

Bouffi, C., Bony, C., Courties, G., et al. (2010) IL-6-dependent PGE2 secretion by mesenchymal stem cells inhibits local inflammation in experimental arthritis. **PLoS One**, 5: (12): e14247.

Bournazos, S., Fahim, A. and Hart, S.P. (2009) Identification of fibrocytes in peripheral blood. **Am J Respir Crit Care Med**, 180: (12): 1279; author reply 1279.

Boxall, S.A. and Jones, E. (2012) Markers for characterization of bone marrow multipotential stromal cells. **Stem Cells Int**, 2012: 975871.

Brazelton, T.R., Rossi, F.M., Keshet, G.I., et al. (2000) From marrow to brain: expression of neuronal phenotypes in adult mice. **Science**, 290: (5497): 1775-1779.

Bucala, R., Spiegel, L.A., Chesney, J., et al. (1994) Circulating fibrocytes define a new leukocyte subpopulation that mediates tissue repair. **Mol Med**, 1: (1): 71-81.

Buhring, H.J., Treml, S., Cerabona, F., et al. (2009) Phenotypic characterization of distinct human bone marrow-derived MSC subsets. **Ann N Y Acad Sci**, 1176: 124-134.

Burst, V.R., Gillis, M., Putsch, F., et al. (2010) Poor cell survival limits the beneficial impact of mesenchymal stem cell transplantation on acute kidney injury. **Nephron Exp Nephrol**, 114: (3): e107-116.

Buzzard, J.J., Gough, N.M., Crook, J.M., et al. (2004) Karyotype of human ES cells during extended culture. **Nat Biotechnol**, 22: (4): 381-382; author reply 382.

Cao, H., Yang, J., Yu, J., et al. (2012) Therapeutic potential of transplanted placental mesenchymal stem cells in treating Chinese miniature pigs with acute liver failure. **BMC Med**, 10: 56.

Carrero, R., Cerrada, I., Lledo, E., et al. (2012) IL1beta Induces Mesenchymal Stem Cells Migration and Leucocyte Chemotaxis Through NF-kappaB. **Stem Cell Rev**, 8: (3): 905-916.

Carter, D.R., Blenman, P.R. and Beaupre, G.S. (1988) Correlations between mechanical stress history and tissue differentiation in initial fracture healing. **J Orthop Res**, 6: (5): 736-748.

Carvalho, A.B., Quintanilha, L.F., Dias, J.V., et al. (2008) Bone marrow multipotent mesenchymal stromal cells do not reduce fibrosis or improve function in a rat model of severe chronic liver injury. **Stem Cells**, 26: (5): 1307-1314.

Castano, A.P., Lin, S.L., Surowy, T., et al. (2009) Serum amyloid P inhibits fibrosis through Fc gamma R-dependent monocyte-macrophage regulation in vivo. **Sci Transl Med**, 1: (5): 5ra13.

Chamberlain, G., Fox, J., Ashton, B., et al. (2007) Concise review: mesenchymal stem cells: their phenotype, differentiation capacity, immunological features, and potential for homing. **Stem Cells**, 25: (11): 2739-2749.

Chamberlain, G., Smith, H., Rainger, G.E., et al. (2011) Mesenchymal stem cells exhibit firm adhesion, crawling, spreading and transmigration across aortic endothelial cells: effects of chemokines and shear. **PLoS One**, 6: (9): e25663.

Chamberlain, G., Wright, K., Rot, A., et al. (2008) Murine mesenchymal stem cells exhibit a restricted repertoire of functional chemokine receptors: comparison with human. **PLoS One**, 3: (8): e2934.

Chavakis, E., Urbich, C. and Dimmeler, S. (2008) Homing and engraftment of progenitor cells: a prerequisite for cell therapy. **J Mol Cell Cardiol**, 45: (4): 514-522.

Che, N., Li, X., Zhou, S., et al. (2012) Umbilical cord mesenchymal stem cells suppress B-cell proliferation and differentiation. **Cell Immunol**, 274: (1-2): 46-53.

Chen, Y., Xiang, L.X., Shao, J.Z., et al. (2010) Recruitment of endogenous bone marrow mesenchymal stem cells towards injured liver. **J Cell Mol Med**, 14: (6B): 1494-1508.

Chesney, J., Bacher, M., Bender, A., et al. (1997) The peripheral blood fibrocyte is a potent antigen-presenting cell capable of priming naive T cells in situ. **Proc Natl Acad Sci U S A**, 94: (12): 6307-6312.

Chesney, J., Metz, C., Stavitsky, A.B., et al. (1998) Regulated production of type I collagen and inflammatory cytokines by peripheral blood fibrocytes. **J Immunol**, 160: (1): 419-425.

Chiesa, S., Morbelli, S., Morando, S., et al. (2011) Mesenchymal stem cells impair in vivo T-cell priming by dendritic cells. **Proc Natl Acad Sci U S A**, 108: (42): 17384-17389.

Chivu, M., Dima, S.O., Stancu, C.I., et al. (2009) In vitro hepatic differentiation of human bone marrow mesenchymal stem cells under differential exposure to liver-specific factors. **Transl Res**, 154: (3): 122-132.

Choi, Y.H., Burdick, M.D. and Strieter, R.M. (2010) Human circulating fibrocytes have the capacity to differentiate osteoblasts and chondrocytes. **Int J Biochem Cell Biol**, 42: (5): 662-671.

Ciuculescu, F., Giesen, M., Deak, E., et al. (2011) Variability in chemokine-induced adhesion of human mesenchymal stromal cells. **Cytotherapy**, 13: (10): 1172-1179.

Covas, D.T., Panepucci, R.A., Fontes, A.M., et al. (2008) Multipotent mesenchymal stromal cells obtained from diverse human tissues share functional properties and gene-expression profile with CD146+ perivascular cells and fibroblasts. **Exp Hematol**, 36: (5): 642-654.

Crawford, J.R., Pilling, D. and Gomer, R.H. (2010) Improved serum-free culture conditions for spleen-derived murine fibrocytes. **J Immunol Methods**, 363: (1): 9-20.

Crawford, J.R., Pilling, D. and Gomer, R.H. (2012) FcγRIIb mediates serum amyloid P inhibition of fibrocyte differentiation. **J Leukoc Biol**.

Crosby, H.A., Lalor, P.F., Ross, E., et al. (2009) Adhesion of human haematopoietic (CD34+) stem cells to human liver compartments is integrin and CD44 dependent and modulated by CXCR3 and CXCR4. **J Hepatol**, 51: (4): 734-749.

Curbishley, S.M., Eksteen, B., Gladue, R.P., et al. (2005) CXCR 3 activation promotes lymphocyte transendothelial migration across human hepatic endothelium under fluid flow. **Am J Pathol**, 167: (3): 887-899.

Curnow, S.J., Fairclough, M., Schmutz, C., et al. (2010) Distinct types of fibrocyte can differentiate from mononuclear cells in the presence and absence of serum. **PLoS One**, 5: (3): e9730.

Cuthbert, R., Boxall, S.A., Tan, H.B., et al. (2012) Single-platform quality control assay to quantify multipotential stromal cells in bone marrow aspirates prior to bulk manufacture or direct therapeutic use. **Cytotherapy**, 14: (4): 431-440.

Dambly-Chaudiere, C., Cubedo, N. and Ghysen, A. (2007) Control of cell migration in the development of the posterior lateral line: antagonistic interactions between the chemokine receptors CXCR4 and CXCR7/RDC1. **BMC Dev Biol**, 7: 23.

Danese, S. and Gao, B. (2010) Interleukin-6: a therapeutic Jekyll and Hyde in gastrointestinal and hepatic diseases. **Gut**, 59: (2): 149-151.

Decailot, F.M., Kazmi, M.A., Lin, Y., et al. (2011) CXCR7/CXCR4 heterodimer constitutively recruits beta-arrestin to enhance cell migration. **J Biol Chem**, 286: (37): 32188-32197.



- Delorme, B., Chateauvieux, S. and Charbord, P. (2006) The concept of mesenchymal stem cells. **Regen Med**, 1: (4): 497-509.
- Dexter, T.M., Moore, M.A. and Sheridan, A.P. (1977) Maintenance of hemopoietic stem cells and production of differentiated progeny in allogeneic and semiallogeneic bone marrow chimeras in vitro. **J Exp Med**, 145: (6): 1612-1616.
- di Bonzo, L.V., Ferrero, I., Cravanzola, C., et al. (2008) Human mesenchymal stem cells as a two-edged sword in hepatic regenerative medicine: engraftment and hepatocyte differentiation versus profibrogenic potential. **Gut**, 57: (2): 223-231.
- Di Ianni, M., Del Papa, B., De Ioanni, M., et al. (2008) Mesenchymal cells recruit and regulate T regulatory cells. **Exp Hematol**, 36: (3): 309-318.
- Ding, Y., Xu, D., Feng, G., et al. (2009) Mesenchymal stem cells prevent the rejection of fully allogenic islet grafts by the immunosuppressive activity of matrix metalloproteinase-2 and -9. **Diabetes**, 58: (8): 1797-1806.
- Direkze, N.C., Hodivala-Dilke, K., Jeffery, R., et al. (2004) Bone marrow contribution to tumor-associated myofibroblasts and fibroblasts. **Cancer Res**, 64: (23): 8492-8495.
- Docheva, D. (2008) Mesenchymal Stem Cells and their Cell surface Receptors. **Current Rheumatology Reviews**, 2008, 4, 000-000, (4).
- Dominici, M., Le Blanc, K., Mueller, I., et al. (2006) Minimal criteria for defining multipotent mesenchymal stromal cells. The International Society for Cellular Therapy position statement. **Cytotherapy**, 8: (4): 315-317.
- Dong, X.J., Zhang, H., Pan, R.L., et al. (2010) Identification of cytokines involved in hepatic differentiation of mBM-MSCs under liver-injury conditions. **World J Gastroenterol**, 16: (26): 3267-3278.
- Douglas, R.S., Afifiyan, N.F., Hwang, C.J., et al. (2010) Increased generation of fibrocytes in thyroid-associated ophthalmopathy. **J Clin Endocrinol Metab**, 95: (1): 430-438.
- Duffield, J.S., Forbes, S.J., Constandinou, C.M., et al. (2005) Selective depletion of macrophages reveals distinct, opposing roles during liver injury and repair. **J Clin Invest**, 115: (1): 56-65.
- Ebihara, Y., Masuya, M., Larue, A.C., et al. (2006) Hematopoietic origins of fibroblasts: II. In vitro studies of fibroblasts, CFU-F, and fibrocytes. **Exp Hematol**, 34: (2): 219-229.
- Ekert, J.E., Murray, L.A., Das, A.M., et al. (2011) Chemokine (C-C motif) ligand 2 mediates direct and indirect fibrotic responses in human and murine cultured fibrocytes. **Fibrogenesis Tissue Repair**, 4: (1): 23.
- English, K., Barry, F.P., Field-Corbett, C.P., et al. (2007) IFN-gamma and TNF-alpha differentially regulate immunomodulation by murine mesenchymal stem cells. **Immunol Lett**, 110: (2): 91-100.
- Ezquer, M., Ezquer, F., Ricca, M., et al. (2011) Intravenous administration of multipotent stromal cells prevents the onset of non-alcoholic steatohepatitis in obese mice with metabolic syndrome. **J Hepatol**, 55: (5): 1112-1120.
- Faint, J.M., Tuncer, C., Garg, A., et al. (2011) Functional consequences of human lymphocyte cryopreservation: implications for subsequent interactions of cells with endothelium. **J Immunother**, 34: (8): 588-596.
- Fernandez-Cruz, E., Escartin, P., Bootello, A., et al. (1978) Hepatocyte damage induced by lymphocytes from patients with chronic liver diseases, as detected by LDH release. **Clin Exp Immunol**, 31: (3): 436-442.
- Forbes, S.J., Russo, F.P., Rey, V., et al. (2004) A significant proportion of myofibroblasts are of bone marrow origin in human liver fibrosis. **Gastroenterology**, 126: (4): 955-963.
- Forte, G., Minieri, M., Cossa, P., et al. (2006) Hepatocyte growth factor effects on mesenchymal stem cells: proliferation, migration, and differentiation. **Stem Cells**, 24: (1): 23-33.
- Fox, J.M., Chamberlain, G., Ashton, B.A., et al. (2007) Recent advances into the understanding of mesenchymal stem cell trafficking. **Br J Haematol**, 137: (6): 491-502.

Friedenstein, A.J., Chailakhjan, R.K. and Lalykina, K.S. (1970) The development of fibroblast colonies in monolayer cultures of guinea-pig bone marrow and spleen cells. **Cell Tissue Kinet**, 3: (4): 393-403.

Friedenstein, A.J., Chailakhyan, R.K., Latsinik, N.V., et al. (1974) Stromal cells responsible for transferring the microenvironment of the hemopoietic tissues. Cloning in vitro and retransplantation in vivo. **Transplantation**, 17: (4): 331-340.

Friedman, S.L. (1993) Seminars in medicine of the Beth Israel Hospital, Boston. The cellular basis of hepatic fibrosis. Mechanisms and treatment strategies. **N Engl J Med**, 328: (25): 1828-1835.

Frith, J.E., Thomson, B. and Genever, P.G. (2010) Dynamic three-dimensional culture methods enhance mesenchymal stem cell properties and increase therapeutic potential. **Tissue Eng Part C Methods**, 16: (4): 735-749.

Galligan, C.L. and Fish, E.N. (2012) Circulating fibrocytes contribute to the pathogenesis of arthritis. **Arthritis Rheum**.

Gao, J., Dennis, J.E., Muzic, R.F., et al. (2001) The dynamic in vivo distribution of bone marrow-derived mesenchymal stem cells after infusion. **Cells Tissues Organs**, 169: (1): 12-20.

Garcia, M.G., Bayo, J., Bolontrade, M.F., et al. (2011) Hepatocellular carcinoma cells and their fibrotic microenvironment modulate bone marrow-derived mesenchymal stromal cell migration in vitro and in vivo. **Mol Pharm**, 8: (5): 1538-1548.

Geissmann, F., Manz, M.G., Jung, S., et al. (2010) Development of monocytes, macrophages, and dendritic cells. **Science**, 327: (5966): 656-661.

Ghannam, S., Pene, J., Torcy-Moquet, G., et al. (2010) Mesenchymal stem cells inhibit human Th17 cell differentiation and function and induce a T regulatory cell phenotype. **J Immunol**, 185: (1): 302-312.

Gieling, R.G., Wallace, K. and Han, Y.P. (2009) Interleukin-1 participates in the progression from liver injury to fibrosis. **Am J Physiol Gastrointest Liver Physiol**, 296: (6): G1324-1331.

Girdlestone, J., Limbani, V.A., Cutler, A.J., et al. (2009) Efficient expansion of mesenchymal stromal cells from umbilical cord under low serum conditions. **Cytotherapy**, 11: (6): 738-748.

Gomperts, B.N. and Strieter, R.M. (2007) Fibrocytes in lung disease. **J Leukoc Biol**, 82: (3): 449-456.

Gordon, S. (2003) Alternative activation of macrophages. **Nat Rev Immunol**, 3: (1): 23-35.

Gordon, S. and Martinez, F.O. (2010) Alternative activation of macrophages: mechanism and functions. **Immunity**, 32: (5): 593-604.

Greco, S.J. and Rameshwar, P. (2008) Microenvironmental considerations in the application of human mesenchymal stem cells in regenerative therapies. **Biologics**, 2: (4): 699-705.

Grigorescu, M. (2006) Noninvasive biochemical markers of liver fibrosis. **J Gastrointest Liver Dis**, 15: (2): 149-159.

Gronthos, S., Zannettino, A.C., Hay, S.J., et al. (2003) Molecular and cellular characterisation of highly purified stromal stem cells derived from human bone marrow. **J Cell Sci**, 116: (Pt 9): 1827-1835.

Guilloton, F., Caron, G., Menard, C., et al. (2012) Mesenchymal stromal cells orchestrate follicular lymphoma cell niche through the CCL2-dependent recruitment and polarization of monocytes. **Blood**, 119: (11): 2556-2567.

Hemeda, H., Jakob, M., Ludwig, A.K., et al. (2010) Interferon-gamma and tumor necrosis factor-alpha differentially affect cytokine expression and migration properties of mesenchymal stem cells. **Stem Cells Dev**, 19: (5): 693-706.

Heng, B.C., Cowan, C.M. and Basu, S. (2009) Comparison of enzymatic and non-enzymatic means of dissociating adherent monolayers of mesenchymal stem cells. **Biol Proced Online**, 11: 161-169.

Higashiyama, R., Inagaki, Y., Hong, Y.Y., et al. (2007) Bone marrow-derived cells express matrix metalloproteinases and contribute to regression of liver fibrosis in mice. **Hepatology**, 45: (1): 213-222.

Higashiyama, R., Moro, T., Nakao, S., et al. (2009) Negligible contribution of bone marrow-derived cells to collagen production during hepatic fibrogenesis in mice. **Gastroenterology**, 137: (4): 1459-1466 e1451.

- Holt, A.P., Haughton, E.L., Lalor, P.F., et al. (2009) Liver myofibroblasts regulate infiltration and positioning of lymphocytes in human liver. **Gastroenterology**, 136: (2): 705-714.
- Honczarenko, M., Le, Y., Swierkowski, M., et al. (2006) Human bone marrow stromal cells express a distinct set of biologically functional chemokine receptors. **Stem Cells**, 24: (4): 1030-1041.
- Hong, K.M., Burdick, M.D., Phillips, R.J., et al. (2005) Characterization of human fibrocytes as circulating adipocyte progenitors and the formation of human adipose tissue in SCID mice. **FASEB J**, 19: (14): 2029-2031.
- Hong, Z.F., Huang, X.J., Yin, Z.Y., et al. (2009) Immunosuppressive function of bone marrow mesenchymal stem cells on acute rejection of liver allografts in rats. **Transplant Proc**, 41: (1): 403-409.
- Horiuti, Y., Nakamura, T. and Ichihara, A. (1982) Role of serum in maintenance of functional hepatocytes in primary culture. **J Biochem**, 92: (6): 1985-1994.
- Houlihan, D.D. and Newsome, P.N. (2008) Critical review of clinical trials of bone marrow stem cells in liver disease. **Gastroenterology**, 135: (2): 438-450.
- Humphries, J.D., Byron, A. and Humphries, M.J. (2006) Integrin ligands at a glance. **J Cell Sci**, 119: (Pt 19): 3901-3903.
- Hutchinson, W.L., Noble, G.E., Hawkins, P.N., et al. (1994) The pentraxins, C-reactive protein and serum amyloid P component, are cleared and catabolized by hepatocytes in vivo. **J Clin Invest**, 94: (4): 1390-1396.
- Imai, T., Chantry, D., Raport, C.J., et al. (1998) Macrophage-derived chemokine is a functional ligand for the CC chemokine receptor 4. **J Biol Chem**, 273: (3): 1764-1768.
- Inngjerdigen, M., Damaj, B. and Maghazachi, A.A. (2001) Expression and regulation of chemokine receptors in human natural killer cells. **Blood**, 97: (2): 367-375.
- Ip, J.E., Wu, Y., Huang, J., et al. (2007) Mesenchymal stem cells use integrin beta1 not CXC chemokine receptor 4 for myocardial migration and engraftment. **Mol Biol Cell**, 18: (8): 2873-2882.
- Iredale, J. (2008) Defining therapeutic targets for liver fibrosis: exploiting the biology of inflammation and repair. **Pharmacol Res**, 58: (2): 129-136.
- Ishida, Y., Kimura, A., Kondo, T., et al. (2007) Essential roles of the CC chemokine ligand 3-CC chemokine receptor 5 axis in bleomycin-induced pulmonary fibrosis through regulation of macrophage and fibrocyte infiltration. **Am J Pathol**, 170: (3): 843-854.
- Ivaska, J. and Heino, J. (2011) Cooperation between integrins and growth factor receptors in signaling and endocytosis. **Annu Rev Cell Dev Biol**, 27: 291-320.
- Iwaisako, K., Brenner, D.A. and Kisseleva, T. (2012) What's new in liver fibrosis? The origin of myofibroblasts in liver fibrosis. **J Gastroenterol Hepatol**, 27 Suppl 2: 65-68.
- Ji, J.F., He, B.P., Dheen, S.T., et al. (2004) Interactions of chemokines and chemokine receptors mediate the migration of mesenchymal stem cells to the impaired site in the brain after hypoglossal nerve injury. **Stem Cells**, 22: (3): 415-427.
- Jiang, X.X., Zhang, Y., Liu, B., et al. (2005) Human mesenchymal stem cells inhibit differentiation and function of monocyte-derived dendritic cells. **Blood**, 105: (10): 4120-4126.
- Jiang, Y., Jahagirdar, B.N., Reinhardt, R.L., et al. (2002) Pluripotency of mesenchymal stem cells derived from adult marrow. **Nature**, 418: (6893): 41-49.
- Jung, E.M., Kwon, O., Kwon, K.S., et al. (2011a) Evidences for correlation between the reduced VCAM-1 expression and hyaluronan synthesis during cellular senescence of human mesenchymal stem cells. **Biochem Biophys Res Commun**, 404: (1): 463-469.
- Jung, K.H., Song, S.U., Yi, T., et al. (2011b) Human bone marrow-derived clonal mesenchymal stem cells inhibit inflammation and reduce acute pancreatitis in rats. **Gastroenterology**, 140: (3): 998-1008.
- Kanazawa, H., Fujimoto, Y., Teratani, T., et al. (2011) Bone marrow-derived mesenchymal stem cells ameliorate hepatic ischemia reperfusion injury in a rat model. **PLoS One**, 6: (4): e19195.

- Karp, J.M. and Leng Teo, G.S. (2009) Mesenchymal stem cell homing: the devil is in the details. **Cell Stem Cell**, 4: (3): 206-216.
- Katebi, M., Fernandez, P., Chan, E.S., et al. (2008) Adenosine A2A receptor blockade or deletion diminishes fibrocyte accumulation in the skin in a murine model of scleroderma, bleomycin-induced fibrosis. **Inflammation**, 31: (5): 299-303.
- Kavanagh, H. and Mahon, B.P. (2011) Allogeneic mesenchymal stem cells prevent allergic airway inflammation by inducing murine regulatory T cells. **Allergy**, 66: (4): 523-531.
- Keeley, E.C., Mehrad, B. and Strieter, R.M. (2009) The role of circulating mesenchymal progenitor cells (fibrocytes) in the pathogenesis of fibrotic disorders. **Thromb Haemost**, 101: (4): 613-618.
- Keeley, E.C., Mehrad, B. and Strieter, R.M. (2010) Fibrocytes: bringing new insights into mechanisms of inflammation and fibrosis. **Int J Biochem Cell Biol**, 42: (4): 535-542.
- Kershenovich Stalnikowitz, D. and Weissbrod, A.B. (2003) Liver fibrosis and inflammation. A review. **Ann Hepatol**, 2: (4): 159-163.
- Kim, Y.S., Park, H.J., Hong, M.H., et al. (2009) TNF-alpha enhances engraftment of mesenchymal stem cells into infarcted myocardium. **Front Biosci**, 14: 2845-2856.
- Kirovski, G., Gabele, E., Dorn, C., et al. (2010) Hepatic steatosis causes induction of the chemokine RANTES in the absence of significant hepatic inflammation. **Int J Clin Exp Pathol**, 3: (7): 675-680.
- Kisseleva, T., Uchinami, H., Feirt, N., et al. (2006) Bone marrow-derived fibrocytes participate in pathogenesis of liver fibrosis. **J Hepatol**, 45: (3): 429-438.
- Kisseleva, T., von Kockritz-Blickwede, M., Reichart, D., et al. (2011) Fibrocyte-like cells recruited to the spleen support innate and adaptive immune responses to acute injury or infection. **J Mol Med (Berl)**, 89: (10): 997-1013.
- Kopp, H.G., Avecilla, S.T., Hooper, A.T., et al. (2005) The bone marrow vascular niche: home of HSC differentiation and mobilization. **Physiology (Bethesda)**, 20: 349-356.
- Krampera, M., Cosmi, L., Angeli, R., et al. (2006) Role for interferon-gamma in the immunomodulatory activity of human bone marrow mesenchymal stem cells. **Stem Cells**, 24: (2): 386-398.
- Krampera, M., Pasini, A., Rigo, A., et al. (2005) HB-EGF/HER-1 signaling in bone marrow mesenchymal stem cells: inducing cell expansion and reversibly preventing multilineage differentiation. **Blood**, 106: (1): 59-66.
- Krenning, G., Zeisberg, E.M. and Kalluri, R. (2010) The origin of fibroblasts and mechanism of cardiac fibrosis. **J Cell Physiol**, 225: (3): 631-637.
- Kuo, T.K., Hung, S.P., Chuang, C.H., et al. (2008) Stem cell therapy for liver disease: parameters governing the success of using bone marrow mesenchymal stem cells. **Gastroenterology**, 134: (7): 2111-2121, 2121 e2111-2113.
- Lacey, D.C., Simmons, P.J., Graves, S.E., et al. (2009) Proinflammatory cytokines inhibit osteogenic differentiation from stem cells: implications for bone repair during inflammation. **Osteoarthritis Cartilage**, 17: (6): 735-742.
- Lalor, P.F., Faint, J., Aarbodem, Y., et al. (2007) The role of cytokines and chemokines in the development of steatohepatitis. **Semin Liver Dis**, 27: (2): 173-193.
- LaRue, A.C., Masuya, M., Ebihara, Y., et al. (2006) Hematopoietic origins of fibroblasts: I. In vivo studies of fibroblasts associated with solid tumors. **Exp Hematol**, 34: (2): 208-218.
- Le Blanc, K., Frassoni, F., Ball, L., et al. (2008) Mesenchymal stem cells for treatment of steroid-resistant, severe, acute graft-versus-host disease: a phase II study. **Lancet**, 371: (9624): 1579-1586.
- Le, P.T. and Mortensen, R.F. (1984a) In vitro induction of hepatocyte synthesis of the acute phase reactant mouse serum amyloid P-component by macrophages and IL 1. **J Leukoc Biol**, 35: (6): 587-603.
- Le, P.T. and Mortensen, R.F. (1984b) Mouse hepatocyte synthesis and induction of the acute phase reactant: serum amyloid P-component. **In Vitro**, 20: (6): 505-511.

Lee, K.D., Kuo, T.K., Whang-Peng, J., et al. (2004) In vitro hepatic differentiation of human mesenchymal stem cells. **Hepatology**, 40: (6): 1275-1284.

Lee, R.H., Seo, M.J., Pulin, A.A., et al. (2009) The CD34-like protein PODXL and alpha6-integrin (CD49f) identify early progenitor MSCs with increased clonogenicity and migration to infarcted heart in mice. **Blood**, 113: (4): 816-826.

Lehoux, G., Le Gouill, C., Stankova, J., et al. (2003) Upregulation of expression of the chemokine receptor CCR5 by hydrogen peroxide in human monocytes. **Mediators Inflamm**, 12: (1): 29-35.

Levine, B. and Yuan, J. (2005) Autophagy in cell death: an innocent convict? **J Clin Invest**, 115: (10): 2679-2688.

Levo, Y., Shalit, M. and Tur-Kaspa, R. (1982) Serum amyloid P-component as a marker of liver disease. **Am J Gastroenterol**, 77: (6): 427-430.

Levo, Y., Wollner, S. and Treves, A.J. (1986) Serum amyloid P-component levels in patients with malignancy. **Scand J Immunol**, 24: (2): 147-151.

Levoye, A., Balabanian, K., Baleux, F., et al. (2009) CXCR7 heterodimerizes with CXCR4 and regulates CXCL12-mediated G protein signaling. **Blood**, 113: (24): 6085-6093.

Ley, K., Laudanna, C., Cybulsky, M.I., et al. (2007) Getting to the site of inflammation: the leukocyte adhesion cascade updated. **Nat Rev Immunol**, 7: (9): 678-689.

Li, C., Kong, Y., Wang, H., et al. (2009) Homing of bone marrow mesenchymal stem cells mediated by sphingosine 1-phosphate contributes to liver fibrosis. **J Hepatol**, 50: (6): 1174-1183.

Li, H., Zhang, B., Lu, Y., et al. (2011) Adipose tissue-derived mesenchymal stem cell-based liver gene delivery. **J Hepatol**, 54: (5): 930-938.

Li, J. and Li, L. (2012) Immediate intraportal transplantation of human bone marrow mesenchymal stem cells prevents death from fulminant hepatic failure in pigs. **Hepatology**.

Li, J., Zhang, L., Xin, J., et al. (2012) Immediate intraportal transplantation of human bone marrow mesenchymal stem cells prevents death from fulminant hepatic failure in pigs. **Hepatology**, 56: (3): 1044-1052.

Liaskou, E., Wilson, D.V. and Oo, Y.H. (2012) Innate immune cells in liver inflammation. **Mediators Inflamm**, 2012: 949157.

Lin, B.F., Ku, N.O., Zahedi, K., et al. (1990) IL-1 and IL-6 mediate increased production and synthesis by hepatocytes of acute-phase reactant mouse serum amyloid P-component (SAP). **Inflammation**, 14: (3): 297-313.

Lin, H., Xu, R., Zhang, Z., et al. (2011) Implications of the immunoregulatory functions of mesenchymal stem cells in the treatment of human liver diseases. **Cell Mol Immunol**, 8: (1): 19-22.

Liu, F., Akiyama, Y., Tai, S., et al. (2008) Changes in the expression of CD106, osteogenic genes, and transcription factors involved in the osteogenic differentiation of human bone marrow mesenchymal stem cells. **J Bone Miner Metab**, 26: (4): 312-320.

Liu, Y., Jiang, X., Zhang, X., et al. (2011a) Dedifferentiation-reprogrammed mesenchymal stem cells with improved therapeutic potential. **Stem Cells**, 29: (12): 2077-2089.

Liu, Y., Wang, L., Kikuri, T., et al. (2011b) Mesenchymal stem cell-based tissue regeneration is governed by recipient T lymphocytes via IFN-gamma and TNF-alpha. **Nat Med**, 17: (12): 1594-1601.

Loebinger, M.R., Eddaoudi, A., Davies, D., et al. (2009) Mesenchymal stem cell delivery of TRAIL can eliminate metastatic cancer. **Cancer Res**, 69: (10): 4134-4142.

Loetscher, P., Pellegrino, A., Gong, J.H., et al. (2001) The ligands of CXC chemokine receptor 3, I-TAC, Mig, and IP10, are natural antagonists for CCR3. **J Biol Chem**, 276: (5): 2986-2991.

Lord, J.T. and Ziboh, V.A. (1979) Specific binding of prostaglandin E2 to membrane preparations from human skin: receptor modulation by UVB-irradiation and chemical agents. **J Invest Dermatol**, 73: (5): 373-377.

Louis, H., Van Laethem, J.L., Wu, W., et al. (1998) Interleukin-10 controls neutrophilic infiltration, hepatocyte proliferation, and liver fibrosis induced by carbon tetrachloride in mice. **Hepatology**, 28: (6): 1607-1615.

- Lubis, A.M., Sandhow, L., Lubis, V.K., et al. (2011) Isolation and cultivation of mesenchymal stem cells from iliac crest bone marrow for further cartilage defect management. **Acta Med Indones**, 43: (3): 178-184.
- Maccario, R., Podesta, M., Moretta, A., et al. (2005) Interaction of human mesenchymal stem cells with cells involved in alloantigen-specific immune response favors the differentiation of CD4+ T-cell subsets expressing a regulatory/suppressive phenotype. **Haematologica**, 90: (4): 516-525.
- Maharjan, A.S., Pilling, D. and Gomer, R.H. (2010) Toll-like receptor 2 agonists inhibit human fibrocyte differentiation. **Fibrogenesis Tissue Repair**, 3: 23.
- Maharjan, A.S., Pilling, D. and Gomer, R.H. (2011) High and low molecular weight hyaluronic acid differentially regulate human fibrocyte differentiation. **PLoS One**, 6: (10): e26078.
- Maltby, J., Wright, S., Bird, G., et al. (1996) Chemokine levels in human liver homogenates: associations between GRO alpha and histopathological evidence of alcoholic hepatitis. **Hepatology**, 24: (5): 1156-1160.
- Marek, B., Kajdaniuk, D., Mazurek, U., et al. (2005) TGF-beta1 mRNA expression in liver biopsy specimens and TGF-beta1 serum levels in patients with chronic hepatitis C before and after antiviral therapy. **J Clin Pharm Ther**, 30: (3): 271-277.
- Mareschi, K., Rustichelli, D., Comunanza, V., et al. (2009) Multipotent mesenchymal stem cells from amniotic fluid originate neural precursors with functional voltage-gated sodium channels. **Cytotherapy**, 11: (5): 534-547.
- Mehrad, B., Burdick, M.D. and Strieter, R.M. (2009) Fibrocyte CXCR4 regulation as a therapeutic target in pulmonary fibrosis. **Int J Biochem Cell Biol**, 41: (8-9): 1708-1718.
- Meiser, A., Mueller, A., Wise, E.L., et al. (2008) The chemokine receptor CXCR3 is degraded following internalization and is replenished at the cell surface by de novo synthesis of receptor. **J Immunol**, 180: (10): 6713-6724.
- Miaczynska, M., Pelkmans, L. and Zerial, M. (2004) Not just a sink: endosomes in control of signal transduction. **Curr Opin Cell Biol**, 16: (4): 400-406.
- Mitalipova, M.M., Rao, R.R., Hoyer, D.M., et al. (2005) Preserving the genetic integrity of human embryonic stem cells. **Nat Biotechnol**, 23: (1): 19-20.
- Moeller, A., Gilpin, S.E., Ask, K., et al. (2009) Circulating fibrocytes are an indicator of poor prognosis in idiopathic pulmonary fibrosis. **Am J Respir Crit Care Med**, 179: (7): 588-594.
- Mohamadnejad, M., Namiri, M., Bagheri, M., et al. (2007) Phase 1 human trial of autologous bone marrow-hematopoietic stem cell transplantation in patients with decompensated cirrhosis. **World J Gastroenterol**, 13: (24): 3359-3363.
- Mohamadnejad, M., Sohail, M.A., Watanabe, A., et al. (2010) Adenosine inhibits chemotaxis and induces hepatocyte-specific genes in bone marrow mesenchymal stem cells. **Hepatology**, 51: (3): 963-973.
- Mohanty, S., Bose, S., Jain, K.G., et al. (2011) TGFbeta1 contributes to cardiomyogenic-like differentiation of human bone marrow mesenchymal stem cells. **Int J Cardiol**.
- Moore, B.B., Kolodsick, J.E., Thannickal, V.J., et al. (2005) CCR2-mediated recruitment of fibrocytes to the alveolar space after fibrotic injury. **Am J Pathol**, 166: (3): 675-684.
- Moore, B.B., Murray, L., Das, A., et al. (2006) The role of CCL12 in the recruitment of fibrocytes and lung fibrosis. **Am J Respir Cell Mol Biol**, 35: (2): 175-181.
- Moore, K.A. (2004) Recent advances in defining the hematopoietic stem cell niche. **Curr Opin Hematol**, 11: (2): 107-111.
- Moore, K.A. and Lemischka, I.R. (2006) Stem cells and their niches. **Science**, 311: (5769): 1880-1885.
- Mougiakakos, D., Jitschin, R., Johansson, C.C., et al. (2011) The impact of inflammatory licensing on heme oxygenase-1-mediated induction of regulatory T cells by human mesenchymal stem cells. **Blood**, 117: (18): 4826-4835.
- Mueller, A., Kelly, E. and Strange, P.G. (2002) Pathways for internalization and recycling of the chemokine receptor CCR5. **Blood**, 99: (3): 785-791.

Murdoch, C. and Finn, A. (2000) Chemokine receptors and their role in inflammation and infectious diseases. **Blood**, 95: (10): 3032-3043.

Naumann, U., Cameroni, E., Pruenster, M., et al. (2010) CXCR7 functions as a scavenger for CXCL12 and CXCL11. **PLoS One**, 5: (2): e9175.

Neel, N.F., Schutyser, E., Sai, J., et al. (2005) Chemokine receptor internalization and intracellular trafficking. **Cytokine Growth Factor Rev**, 16: (6): 637-658.

Nelson, D.R., Lauwers, G.Y., Lau, J.Y., et al. (2000) Interleukin 10 treatment reduces fibrosis in patients with chronic hepatitis C: a pilot trial of interferon nonresponders. **Gastroenterology**, 118: (4): 655-660.

Nemeth, K., Keane-Myers, A., Brown, J.M., et al. (2010) Bone marrow stromal cells use TGF-beta to suppress allergic responses in a mouse model of ragweed-induced asthma. **Proc Natl Acad Sci U S A**, 107: (12): 5652-5657.

Nemeth, K., Leelahavanichkul, A., Yuen, P.S., et al. (2009) Bone marrow stromal cells attenuate sepsis via prostaglandin E(2)-dependent reprogramming of host macrophages to increase their interleukin-10 production. **Nat Med**, 15: (1): 42-49.

Newman, R.E., Yoo, D., LeRoux, M.A., et al. (2009) Treatment of inflammatory diseases with mesenchymal stem cells. **Inflamm Allergy Drug Targets**, 8: (2): 110-123.

Niedermeier, M., Reich, B., Rodriguez Gomez, M., et al. (2009) CD4+ T cells control the differentiation of Gr1+ monocytes into fibrocytes. **Proc Natl Acad Sci U S A**, 106: (42): 17892-17897.

Niess, H., Bao, Q., Conrad, C., et al. (2011) Selective targeting of genetically engineered mesenchymal stem cells to tumor stroma microenvironments using tissue-specific suicide gene expression suppresses growth of hepatocellular carcinoma. **Ann Surg**, 254: (5): 767-774; discussion 774-765.

Nikam, V.S., Schermuly, R.T., Dumitrescu, R., et al. (2010) Treprostinil inhibits the recruitment of bone marrow-derived circulating fibrocytes in chronic hypoxic pulmonary hypertension. **Eur Respir J**, 36: (6): 1302-1314.

Nikam, V.S., Wecker, G., Schermuly, R., et al. (2011) Treprostinil inhibits the adhesion and differentiation of fibrocytes via the cyclic adenosine monophosphate-dependent and Ras-proximate protein-dependent inactivation of extracellular regulated kinase. **Am J Respir Cell Mol Biol**, 45: (4): 692-703.

Novo, E., Busletta, C., Bonzo, L.V., et al. (2011) Intracellular reactive oxygen species are required for directional migration of resident and bone marrow-derived hepatic pro-fibrogenic cells. **J Hepatol**, 54: (5): 964-974.

Ogawa, M., LaRue, A.C. and Drake, C.J. (2006) Hematopoietic origin of fibroblasts/myofibroblasts: Its pathophysiological implications. **Blood**, 108: (9): 2893-2896.

Oo, Y.H. and Adams, D.H. (2010) The role of chemokines in the recruitment of lymphocytes to the liver. **J Autoimmun**, 34: (1): 45-54.

Oo, Y.H., Banz, V., Kavanagh, D., et al. (2012) CXCR3-dependent recruitment and CCR6-mediated positioning of Th-17 cells in the inflamed liver. **J Hepatol**.

Oo, Y.H., Weston, C.J., Lalor, P.F., et al. (2010) Distinct roles for CCR4 and CXCR3 in the recruitment and positioning of regulatory T cells in the inflamed human liver. **J Immunol**, 184: (6): 2886-2898.

Oswald, J., Boxberger, S., Jorgensen, B., et al. (2004) Mesenchymal stem cells can be differentiated into endothelial cells in vitro. **Stem Cells**, 22: (3): 377-384.

Pan, R.L., Wang, P., Xiang, L.X., et al. (2011) Delta-like 1 serves as a new target and contributor to liver fibrosis down-regulated by mesenchymal stem cell transplantation. **J Biol Chem**, 286: (14): 12340-12348.

Parekkadan, B., van Poll, D., Megeed, Z., et al. (2007a) Immunomodulation of activated hepatic stellate cells by mesenchymal stem cells. **Biochem Biophys Res Commun**, 363: (2): 247-252.

Parekkadan, B., van Poll, D., Suganuma, K., et al. (2007b) Mesenchymal stem cell-derived molecules reverse fulminant hepatic failure. **PLoS One**, 2: (9): e941.

- Patel, S.A., Meyer, J.R., Greco, S.J., et al. (2010) Mesenchymal stem cells protect breast cancer cells through regulatory T cells: role of mesenchymal stem cell-derived TGF-beta. **J Immunol**, 184: (10): 5885-5894.
- Peng, H. and Herzog, E.L. (2012) Fibrocytes: emerging effector cells in chronic inflammation. **Curr Opin Pharmacol**, 12: (4): 491-496.
- Peng, L., Xie, D.Y., Lin, B.L., et al. (2011) Autologous bone marrow mesenchymal stem cell transplantation in liver failure patients caused by hepatitis B: short-term and long-term outcomes. **Hepatology**, 54: (3): 820-828.
- Phillips, R.J., Burdick, M.D., Hong, K., et al. (2004) Circulating fibrocytes traffic to the lungs in response to CXCL12 and mediate fibrosis. **J Clin Invest**, 114: (3): 438-446.
- Phinney, D.G. and Prockop, D.J. (2007) Concise review: mesenchymal stem/multipotent stromal cells: the state of transdifferentiation and modes of tissue repair--current views. **Stem Cells**, 25: (11): 2896-2902.
- Pilling, D., Buckley, C.D., Salmon, M., et al. (2003) Inhibition of fibrocyte differentiation by serum amyloid P. **J Immunol**, 171: (10): 5537-5546.
- Pilling, D., Buckley, C.D., Salmon, M., et al. (2007a) Serum amyloid P and fibrosis in systemic sclerosis: comment on the article by Tennent et al. **Arthritis Rheum**, 56: (12): 4229; author reply 4229-4230.
- Pilling, D., Fan, T., Huang, D., et al. (2009a) Identification of markers that distinguish monocyte-derived fibrocytes from monocytes, macrophages, and fibroblasts. **PLoS One**, 4: (10): e7475.
- Pilling, D., Roife, D., Wang, M., et al. (2007b) Reduction of bleomycin-induced pulmonary fibrosis by serum amyloid P. **J Immunol**, 179: (6): 4035-4044.
- Pilling, D., Vakil, V. and Gomer, R.H. (2009b) Improved serum-free culture conditions for the differentiation of human and murine fibrocytes. **J Immunol Methods**, 351: (1-2): 62-70.
- Piryaei, A., Valojerdi, M.R., Shahsavani, M., et al. (2011) Differentiation of bone marrow-derived mesenchymal stem cells into hepatocyte-like cells on nanofibers and their transplantation into a carbon tetrachloride-induced liver fibrosis model. **Stem Cell Rev**, 7: (1): 103-118.
- Pittenger, M.F. (2008) Mesenchymal stem cells from adult bone marrow. **Methods Mol Biol**, 449: 27-44.
- Pittenger, M.F., Mackay, A.M., Beck, S.C., et al. (1999) Multilineage potential of adult human mesenchymal stem cells. **Science**, 284: (5411): 143-147.
- Polchert, D., Sobinsky, J., Douglas, G., et al. (2008) IFN-gamma activation of mesenchymal stem cells for treatment and prevention of graft versus host disease. **Eur J Immunol**, 38: (6): 1745-1755.
- Ponte, A.L., Marais, E., Gallay, N., et al. (2007) The in vitro migration capacity of human bone marrow mesenchymal stem cells: comparison of chemokine and growth factor chemotactic activities. **Stem Cells**, 25: (7): 1737-1745.
- Popp, F.C., Renner, P., Eggenhofer, E., et al. (2009) Mesenchymal stem cells as immunomodulators after liver transplantation. **Liver Transpl**, 15: (10): 1192-1198.
- Porcheray, F., Viaud, S., Rimaniol, A.C., et al. (2005) Macrophage activation switching: an asset for the resolution of inflammation. **Clin Exp Immunol**, 142: (3): 481-489.
- Prasanna, S.J., Gopalakrishnan, D., Shankar, S.R., et al. (2010) Pro-inflammatory cytokines, IFN-gamma and TNF-alpha, influence immune properties of human bone marrow and Wharton jelly mesenchymal stem cells differentially. **PLoS One**, 5: (2): e9016.
- Prevosto, C., Zancolli, M., Canevali, P., et al. (2007) Generation of CD4+ or CD8+ regulatory T cells upon mesenchymal stem cell-lymphocyte interaction. **Haematologica**, 92: (7): 881-888.
- Prigione, I., Benvenuto, F., Bocca, P., et al. (2009) Reciprocal interactions between human mesenchymal stem cells and gamma-delta T cells or invariant natural killer T cells. **Stem Cells**, 27: (3): 693-702.
- Prijatelj, M., Celhar, T. and Mlinaric-Rascan, I. (2011) Prostaglandin EP4 receptor enhances BCR-induced apoptosis of immature B cells. **Prostaglandins Other Lipid Mediat**, 95: (1-4): 19-26.



Puglisi, M.A., Tesori, V., Lattanzi, W., et al. (2011) Therapeutic implications of mesenchymal stem cells in liver injury. **J Biomed Biotechnol**, 2011: 860578.

Quan, T.E., Cowper, S., Wu, S.P., et al. (2004) Circulating fibrocytes: collagen-secreting cells of the peripheral blood. **Int J Biochem Cell Biol**, 36: (4): 598-606.

Quirici, N., Soligo, D., Bossolasco, P., et al. (2002) Isolation of bone marrow mesenchymal stem cells by anti-nerve growth factor receptor antibodies. **Exp Hematol**, 30: (7): 783-791.

Rafei, M., Hsieh, J., Fortier, S., et al. (2008) Mesenchymal stromal cell-derived CCL2 suppresses plasma cell immunoglobulin production via STAT3 inactivation and PAX5 induction. **Blood**, 112: (13): 4991-4998.

Raport, C.J., Gosling, J., Schweickart, V.L., et al. (1996) Molecular cloning and functional characterization of a novel human CC chemokine receptor (CCR5) for RANTES, MIP-1beta, and MIP-1alpha. **J Biol Chem**, 271: (29): 17161-17166.

Rattigan, Y., Hsu, J.M., Mishra, P.J., et al. (2010) Interleukin 6 mediated recruitment of mesenchymal stem cells to the hypoxic tumor milieu. **Exp Cell Res**, 316: (20): 3417-3424.

Ray, P., Mihalko, L.A., Coggins, N.L., et al. (2012) Carboxy-terminus of CXCR7 regulates receptor localization and function. **Int J Biochem Cell Biol**, 44: (4): 669-678.

Reilkoff, R.A., Bucala, R. and Herzog, E.L. (2011) Fibrocytes: emerging effector cells in chronic inflammation. **Nat Rev Immunol**, 11: (6): 427-435.

Ren, G., Zhang, L., Zhao, X., et al. (2008) Mesenchymal stem cell-mediated immunosuppression occurs via concerted action of chemokines and nitric oxide. **Cell Stem Cell**, 2: (2): 141-150.

Ringe, J., Strassburg, S., Neumann, K., et al. (2007) Towards in situ tissue repair: human mesenchymal stem cells express chemokine receptors CXCR1, CXCR2 and CCR2, and migrate upon stimulation with CXCL8 but not CCL2. **J Cell Biochem**, 101: (1): 135-146.

Roderfeld, M., Rath, T., Voswinckel, R., et al. (2010) Bone marrow transplantation demonstrates medullar origin of CD34+ fibrocytes and ameliorates hepatic fibrosis in Abcb4-/- mice. **Hepatology**, 51: (1): 267-276.

Russell, K.C., Phinney, D.G., Lacey, M.R., et al. (2010) In vitro high-capacity assay to quantify the clonal heterogeneity in trilineage potential of mesenchymal stem cells reveals a complex hierarchy of lineage commitment. **Stem Cells**, 28: (4): 788-798.

Russo, F.P., Alison, M.R., Bigger, B.W., et al. (2006) The bone marrow functionally contributes to liver fibrosis. **Gastroenterology**, 130: (6): 1807-1821.

Ruster, B., Gottig, S., Ludwig, R.J., et al. (2006) Mesenchymal stem cells display coordinated rolling and adhesion behavior on endothelial cells. **Blood**, 108: (12): 3938-3944.

Ryan, J.M., Barry, F.P., Murphy, J.M., et al. (2005) Mesenchymal stem cells avoid allogeneic rejection. **J Inflamm (Lond)**, 2: 8.

Sackstein, R., Merzaban, J.S., Cain, D.W., et al. (2008) Ex vivo glycan engineering of CD44 programs human multipotent mesenchymal stromal cell trafficking to bone. **Nat Med**, 14: (2): 181-187.

Sahin, H., Borkham-Kamphorst, E., Kuppe, C., et al. (2012) Chemokine Cxcl9 attenuates liver fibrosis-associated angiogenesis in mice. **Hepatology**, 55: (5): 1610-1619.

Sakai, N., Wada, T., Yokoyama, H., et al. (2006) Secondary lymphoid tissue chemokine (SLC/CCL21)/CCR7 signaling regulates fibrocytes in renal fibrosis. **Proc Natl Acad Sci U S A**, 103: (38): 14098-14103.

Sarkar, D., Vemula, P.K., Teo, G.S., et al. (2008) Chemical engineering of mesenchymal stem cells to induce a cell rolling response. **Bioconjug Chem**, 19: (11): 2105-2109.

Sarkar, D., Vemula, P.K., Zhao, W., et al. (2010) Engineered mesenchymal stem cells with self-assembled vesicles for systemic cell targeting. **Biomaterials**, 31: (19): 5266-5274.

Savarin-Vuaillet, C. and Ransohoff, R.M. (2007) Chemokines and chemokine receptors in neurological disease: raise, retain, or reduce? **Neurotherapeutics**, 4: (4): 590-601.

Schmidt, M., Sun, G., Stacey, M.A., et al. (2003) Identification of circulating fibrocytes as precursors of bronchial myofibroblasts in asthma. **J Immunol**, 171: (1): 380-389.

Scholten, D., Reichart, D., Paik, Y.H., et al. (2011) Migration of fibrocytes in fibrogenic liver injury. **Am J Pathol**, 179: (1): 189-198.

Schweichel, J.U. and Merker, H.J. (1973) The morphology of various types of cell death in prenatal tissues. **Teratology**, 7: (3): 253-266.

Secchiero, P., Zorzet, S., Tripodo, C., et al. (2010) Human bone marrow mesenchymal stem cells display anti-cancer activity in SCID mice bearing disseminated non-Hodgkin's lymphoma xenografts. **PLoS One**, 5: (6): e11140.

Segers, V.F., Van Riet, I., Andries, L.J., et al. (2006) Mesenchymal stem cell adhesion to cardiac microvascular endothelium: activators and mechanisms. **Am J Physiol Heart Circ Physiol**, 290: (4): H1370-1377.

Selmani, Z., Naji, A., Zidi, I., et al. (2008) Human leukocyte antigen-G5 secretion by human mesenchymal stem cells is required to suppress T lymphocyte and natural killer function and to induce CD4<sup>+</sup>CD25<sup>high</sup>FOXP3<sup>+</sup> regulatory T cells. **Stem Cells**, 26: (1): 212-222.

Sera, Y., LaRue, A.C., Moussa, O., et al. (2009) Hematopoietic stem cell origin of adipocytes. **Exp Hematol**, 37: (9): 1108-1120, 1120 e1101-1104.

Shao, D.D., Suresh, R., Vakil, V., et al. (2008) Pivotal Advance: Th-1 cytokines inhibit, and Th-2 cytokines promote fibrocyte differentiation. **J Leukoc Biol**, 83: (6): 1323-1333.

Sheng, H., Wang, Y., Jin, Y., et al. (2008) A critical role of IFN $\gamma$  in priming MSC-mediated suppression of T cell proliferation through up-regulation of B7-H1. **Cell Res**, 18: (8): 846-857.

Shi, M., Li, J., Liao, L., et al. (2007) Regulation of CXCR4 expression in human mesenchymal stem cells by cytokine treatment: role in homing efficiency in NOD/SCID mice. **Haematologica**, 92: (7): 897-904.

Shinagawa, K., Kitadai, Y., Tanaka, M., et al. (2010) Mesenchymal stem cells enhance growth and metastasis of colon cancer. **Int J Cancer**, 127: (10): 2323-2333.

Shirai, K., Sera, Y., Bulkeley, W., et al. (2009) Hematopoietic stem cell origin of human fibroblasts: cell culture studies of female recipients of gender-mismatched stem cell transplantation and patients with chronic myelogenous leukemia. **Exp Hematol**, 37: (12): 1464-1471.

Silva, W.A., Jr., Covas, D.T., Panepucci, R.A., et al. (2003) The profile of gene expression of human marrow mesenchymal stem cells. **Stem Cells**, 21: (6): 661-669.

Simmons, P.J. and Torok-Storb, B. (1991) Identification of stromal cell precursors in human bone marrow by a novel monoclonal antibody, STRO-1. **Blood**, 78: (1): 55-62.

Sioud, M. (2011) New insights into mesenchymal stromal cell-mediated T-cell suppression through galectins. **Scand J Immunol**, 73: (2): 79-84.

Soleymaninejadian, E., Pramanik, K. and Samadian, E. (2012) Immunomodulatory properties of mesenchymal stem cells: cytokines and factors. **Am J Reprod Immunol**, 67: (1): 1-8.

Son, B.R., Marquez-Curtis, L.A., Kucia, M., et al. (2006) Migration of bone marrow and cord blood mesenchymal stem cells in vitro is regulated by stromal-derived factor-1-CXCR4 and hepatocyte growth factor-c-met axes and involves matrix metalloproteinases. **Stem Cells**, 24: (5): 1254-1264.

Song, J.S., Kang, C.M., Kang, H.H., et al. (2010) Inhibitory effect of CXC chemokine receptor 4 antagonist AMD3100 on bleomycin induced murine pulmonary fibrosis. **Exp Mol Med**, 42: (6): 465-472.

Sordi, V., Malosio, M.L., Marchesi, F., et al. (2005) Bone marrow mesenchymal stem cells express a restricted set of functionally active chemokine receptors capable of promoting migration to pancreatic islets. **Blood**, 106: (2): 419-427.

Sotiropoulou, P.A., Perez, S.A., Gritzapis, A.D., et al. (2006) Interactions between human mesenchymal stem cells and natural killer cells. **Stem Cells**, 24: (1): 74-85.

Spaggiari, G.M., Abdelrazik, H., Becchetti, F., et al. (2009) MSCs inhibit monocyte-derived DC maturation and function by selectively interfering with the generation of immature DCs: central role of MSC-derived prostaglandin E2. **Blood**, 113: (26): 6576-6583.

Spradling, A., Drummond-Barbosa, D. and Kai, T. (2001) Stem cells find their niche. **Nature**, 414: (6859): 98-104.

Steel, D.M. and Whitehead, A.S. (1994) The major acute phase reactants: C-reactive protein, serum amyloid P component and serum amyloid A protein. **Immunol Today**, 15: (2): 81-88.

Stramer, B.M., Mori, R. and Martin, P. (2007) The inflammation-fibrosis link? A Jekyll and Hyde role for blood cells during wound repair. **J Invest Dermatol**, 127: (5): 1009-1017.

Strieter, R.M., Keeley, E.C., Burdick, M.D., et al. (2009a) The role of circulating mesenchymal progenitor cells, fibrocytes, in promoting pulmonary fibrosis. **Trans Am Clin Climatol Assoc**, 120: 49-59.

Strieter, R.M., Keeley, E.C., Hughes, M.A., et al. (2009b) The role of circulating mesenchymal progenitor cells (fibrocytes) in the pathogenesis of pulmonary fibrosis. **J Leukoc Biol**, 86: (5): 1111-1118.

Su, G.L. (2002) Lipopolysaccharides in liver injury: molecular mechanisms of Kupffer cell activation. **Am J Physiol Gastrointest Liver Physiol**, 283: (2): G256-265.

Sun, L., Louie, M.C., Vannella, K.M., et al. (2011) New concepts of IL-10-induced lung fibrosis: fibrocyte recruitment and M2 activation in a CCL2/CCR2 axis. **Am J Physiol Lung Cell Mol Physiol**, 300: (3): L341-353.

Tao, X.R., Li, W.L., Su, J., et al. (2009) Clonal mesenchymal stem cells derived from human bone marrow can differentiate into hepatocyte-like cells in injured livers of SCID mice. **J Cell Biochem**, 108: (3): 693-704.

Taubenberger, A., Cisneros, D.A., Friedrichs, J., et al. (2007) Revealing early steps of alpha2beta1 integrin-mediated adhesion to collagen type I by using single-cell force spectroscopy. **Mol Biol Cell**, 18: (5): 1634-1644.

Tennent, G.A., Dziadzio, M., Triantafyllidou, E., et al. (2007) Normal circulating serum amyloid P component concentration in systemic sclerosis. **Arthritis Rheum**, 56: (6): 2013-2017.

Thankamony, S.P. and Sackstein, R. (2011) Enforced hematopoietic cell E- and L-selectin ligand (HCELL) expression primes transendothelial migration of human mesenchymal stem cells. **Proc Natl Acad Sci U S A**, 108: (6): 2258-2263.

Thelen, M. and Thelen, S. (2008) CXCR7, CXCR4 and CXCL12: an eccentric trio? **J Neuroimmunol**, 198: (1-2): 9-13.

Thompson, K., Maltby, J., Fallowfield, J., et al. (1998) Interleukin-10 expression and function in experimental murine liver inflammation and fibrosis. **Hepatology**, 28: (6): 1597-1606.

Titos, E., Claria, J., Planaguma, A., et al. (2003) Inhibition of 5-lipoxygenase induces cell growth arrest and apoptosis in rat Kupffer cells: implications for liver fibrosis. **FASEB J**, 17: (12): 1745-1747.

Tomchuck, S.L., Zvezdaryk, K.J., Coffelt, S.B., et al. (2008) Toll-like receptors on human mesenchymal stem cells drive their migration and immunomodulating responses. **Stem Cells**, 26: (1): 99-107.

Tourkina, E., Bonner, M., Oates, J., et al. (2011) Altered monocyte and fibrocyte phenotype and function in scleroderma interstitial lung disease: reversal by caveolin-1 scaffolding domain peptide. **Fibrogenesis Tissue Repair**, 4: (1): 15.

Tsukada, S., Parsons, C.J. and Rippe, R.A. (2006) Mechanisms of liver fibrosis. **Clin Chim Acta**, 364: (1-2): 33-60.

Uccelli, A., Moretta, L. and Pistoia, V. (2008) Mesenchymal stem cells in health and disease. **Nat Rev Immunol**, 8: (9): 726-736.

Uccelli, A. and Prockop, D.J. (2010) Why should mesenchymal stem cells (MSCs) cure autoimmune diseases? **Curr Opin Immunol**, 22: (6): 768-774.

van Deventer, H.W., Wu, Q.P., Bergstralh, D.T., et al. (2008) C-C chemokine receptor 5 on pulmonary fibrocytes facilitates migration and promotes metastasis via matrix metalloproteinase 9. **Am J Pathol**, 173: (1): 253-264.

Vannella, K.M., McMillan, T.R., Charbeneau, R.P., et al. (2007) Cysteinyl leukotrienes are autocrine and paracrine regulators of fibrocyte function. **J Immunol**, 179: (11): 7883-7890.

Varin, A., Mukhopadhyay, S., Herbein, G., et al. (2010) Alternative activation of macrophages by IL-4 impairs phagocytosis of pathogens but potentiates microbial-induced signalling and cytokine secretion. **Blood**, 115: (2): 353-362.

Vercammen, C. and Ceuppens, J.L. (1987) Prostaglandin E2 inhibits human T-cell proliferation after crosslinking of the CD3-Ti complex by directly affecting T cells at an early step of the activation process. **Cell Immunol**, 104: (1): 24-36.

Veyrat-Masson, R., Boiret-Dupre, N., Rapatel, C., et al. (2007) Mesenchymal content of fresh bone marrow: a proposed quality control method for cell therapy. **Br J Haematol**, 139: (2): 312-320.

Wada, T., Sakai, N., Matsushima, K., et al. (2007) Fibrocytes: a new insight into kidney fibrosis. **Kidney Int**, 72: (3): 269-273.

Wagner, W., Feldmann, R.E., Jr., Seckinger, A., et al. (2006) The heterogeneity of human mesenchymal stem cell preparations--evidence from simultaneous analysis of proteomes and transcriptomes. **Exp Hematol**, 34: (4): 536-548.

Wallace, K., Burt, A.D. and Wright, M.C. (2008) Liver fibrosis. **Biochem J**, 411: (1): 1-18.

Wang, D., Zhang, H., Liang, J., et al. (2011) Effect of allogeneic bone marrow-derived mesenchymal stem cells transplantation in a polyI:C-induced primary biliary cirrhosis mouse model. **Clin Exp Med**, 11: (1): 25-32.

Wang, J., Bian, C., Liao, L., et al. (2009a) Inhibition of hepatic stellate cells proliferation by mesenchymal stem cells and the possible mechanisms. **Hepatol Res**, 39: (12): 1219-1228.

Wang, J., Jiao, H., Stewart, T.L., et al. (2008) Increased severity of bleomycin-induced skin fibrosis in mice with leukocyte-specific protein 1 deficiency. **J Invest Dermatol**, 128: (12): 2767-2776.

Wang, Y., Zhang, A., Ye, Z., et al. (2009b) Bone marrow-derived mesenchymal stem cells inhibit acute rejection of rat liver allografts in association with regulatory T-cell expansion. **Transplant Proc**, 41: (10): 4352-4356.

Wasmuth, H.E., Lammert, F., Zaldivar, M.M., et al. (2009) Antifibrotic effects of CXCL9 and its receptor CXCR3 in livers of mice and humans. **Gastroenterology**, 137: (1): 309-319, 319 e301-303.

Weng, H.L., Liu, Y., Chen, J.L., et al. (2009) The etiology of liver damage imparts cytokines transforming growth factor beta1 or interleukin-13 as driving forces in fibrogenesis. **Hepatology**, 50: (1): 230-243.

Wilkins, B.S. and Jones, D.B. (1996) Contribution of monocyte/macrophage differentiation to the stromal layer in human long-term bone marrow cultures. **Biologicals**, 24: (4): 313-318.

Wong, K.L., Yeap, W.H., Tai, J.J., et al. (2012) The three human monocyte subsets: implications for health and disease. **Immunol Res**, 53: (1-3): 41-57.

Wu, Y., Wang, J., Scott, P.G., et al. (2007) Bone marrow-derived stem cells in wound healing: a review. **Wound Repair Regen**, 15 Suppl 1: S18-26.

Wu, Y. and Zhao, R.C. (2012) The role of chemokines in mesenchymal stem cell homing to myocardium. **Stem Cell Rev**, 8: (1): 243-250.

[www.britishlivertrust.org.uk](http://www.britishlivertrust.org.uk) (2008).

[www.osiris.com](http://www.osiris.com).

Wynn, R.F., Hart, C.A., Corradi-Perini, C., et al. (2004) A small proportion of mesenchymal stem cells strongly expresses functionally active CXCR4 receptor capable of promoting migration to bone marrow. **Blood**, 104: (9): 2643-2645.

Yagi, H., Parekkadan, B., Suganuma, K., et al. (2009) Long-term superior performance of a stem cell/hepatocyte device for the treatment of acute liver failure. **Tissue Eng Part A**, 15: (11): 3377-3388.

Yang, L., Cheng, F., Liu, T., et al. (2012) Comparison of mesenchymal stem cells released from poly(N-isopropylacrylamide) copolymer film and by trypsinization. **Biomed Mater**, 7: (3): 035003.

Yang, S.H., Park, M.J., Yoon, I.H., et al. (2009) Soluble mediators from mesenchymal stem cells suppress T cell proliferation by inducing IL-10. **Exp Mol Med**, 41: (5): 315-324.

- Yao, Y., Zhang, F., Wang, L., et al. (2009) Lipopolysaccharide preconditioning enhances the efficacy of mesenchymal stem cells transplantation in a rat model of acute myocardial infarction. **J Biomed Sci**, 16: 74.
- Ye, Z., Wang, Y., Xie, H.Y., et al. (2008) Immunosuppressive effects of rat mesenchymal stem cells: involvement of CD4+CD25+ regulatory T cells. **Hepatobiliary Pancreat Dis Int**, 7: (6): 608-614.
- Yoshida, D., Nomura, R. and Teramoto, A. (2009) Signalling pathway mediated by CXCR7, an alternative chemokine receptor for stromal-cell derived factor-1alpha, in AtT20 mouse adrenocorticotrophic hormone-secreting pituitary adenoma cells. **J Neuroendocrinol**, 21: (5): 481-488.
- Yourek, G., McCormick, S.M., Mao, J.J., et al. (2010) Shear stress induces osteogenic differentiation of human mesenchymal stem cells. **Regen Med**, 5: (5): 713-724.
- Yu, X., Cohen, D.M. and Chen, C.S. (2012) miR-125b is an adhesion-regulated microRNA that protects mesenchymal stem cells from anoikis. **Stem Cells**, 30: (5): 956-964.
- Yun, S.P., Ryu, J.M. and Han, H.J. (2011) Involvement of beta1-integrin via PIP complex and FAK/paxillin in dexamethasone-induced human mesenchymal stem cells migration. **J Cell Physiol**, 226: (3): 683-692.
- Zaldivar, M.M., Pauels, K., von Hundelshausen, P., et al. (2010) CXC chemokine ligand 4 (Cxcl4) is a platelet-derived mediator of experimental liver fibrosis. **Hepatology**, 51: (4): 1345-1353.
- Zhang, M., Xu, S., Han, Y., et al. (2011) Apoptotic cells attenuate fulminant hepatitis by priming Kupffer cells to produce interleukin-10 through membrane-bound TGF-beta. **Hepatology**, 53: (1): 306-316.
- Zhao, W., Li, J.J., Cao, D.Y., et al. (2012) Intravenous injection of mesenchymal stem cells is effective in treating liver fibrosis. **World J Gastroenterol**, 18: (10): 1048-1058.
- Zhou, H.P., Yi, D.H., Yu, S.Q., et al. (2006) Administration of donor-derived mesenchymal stem cells can prolong the survival of rat cardiac allograft. **Transplant Proc**, 38: (9): 3046-3051.
- Zhou, X., Hu, H., Balzar, S., et al. (2012) MAPK regulation of IL-4/IL-13 receptors contributes to the synergistic increase in CCL11/eotaxin-1 in response to TGF-beta1 and IL-13 in human airway fibroblasts. **J Immunol**, 188: (12): 6046-6054.